FNTG Research Society

第 57 回
フラーレン・ナノチューブ・グラフェン
総合シンポジウム

The 57th Fullerenes-Nanotubes-Graphene General Symposium

講演要旨集
Abstracts

2019 年 9 月 3 日（火） ～ 5 日（木）
名古屋大学　坂田・平田ホール
Nagoya　University, Sakata Hirata Hall

主催　フラーレン・ナノチューブ・グラフェン学会
The Fullerenes, Nanotubes and Graphene Research Society

共催 ・ 後援
日本化学会　The Chemical Society of Japan

協賛
日本物理学会　The Physical Society of Japan
応用物理学会　The Japan Society of Applied Physics
高分子学会　The Society of Polymer Science, Japan
電気化学会　The Electrochemical Society of Japan

Princeton Instruments

-100℃電子冷却型高感度CCDカメラ

BLAZE

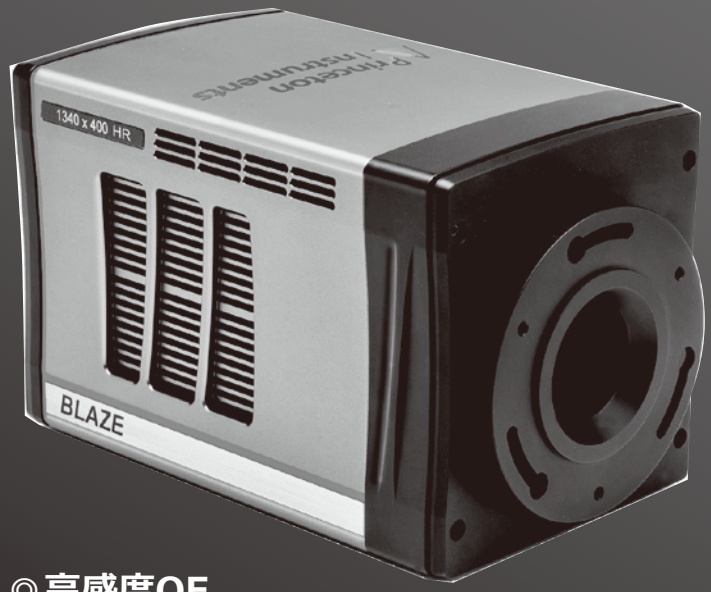

電子冷却 -100℃

極低ノイズ
0.0005 e-/pix/sec

高感度QE
波長1μm域で75%以上

高速読み出し@16MHz/AD

◎優れた冷却方式

20℃水冷により CCD が結露しません。

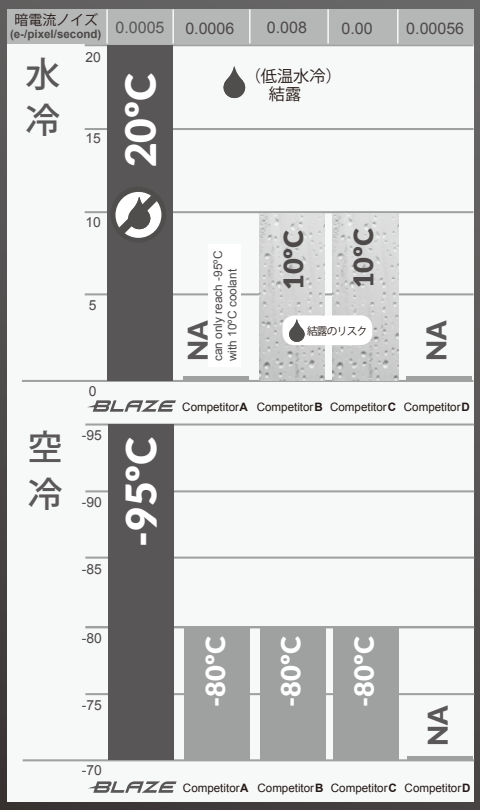

◎高感度QE

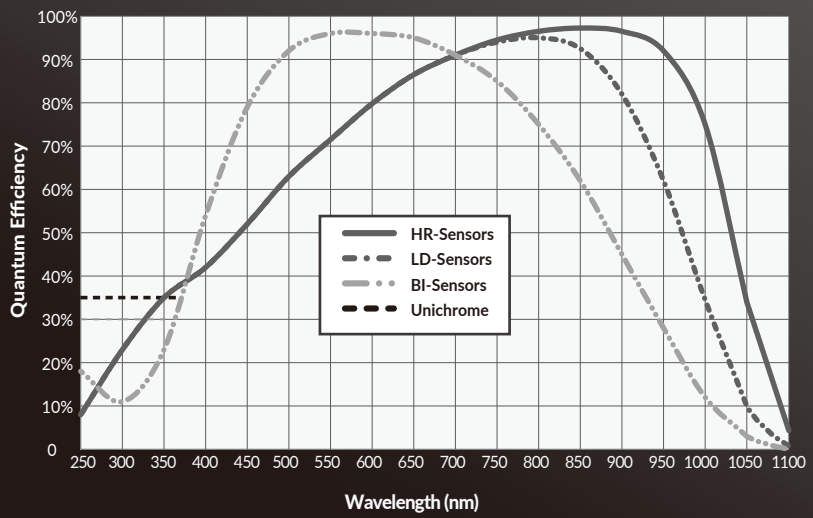

www.pi-j.jp

TELEDYNE PRINCETON INSTRUMENTS
Everywhereyoulook™
Part of the Teledyne Imaging Group

テレダイン・ジャパン株式会社
プリンストンインスツルメンツ
〒170-0013　東京都豊島区東池袋 3-4-3 池袋イースト13F
TEL 03-6709-0631　FAX 03-6709-0632

Abstract of
The 57th Fullerenes-Nanotubes-Graphene General Symposium

Sponsored by : The Fullerenes, Nanotubes and Graphene Research Society

Co-Sponsored by : The Chemical Society of Japan

Supported by : The Physical Society of Japan
The Japan Society of Applied Physics
The Society of Polymer Science, Japan
The Electrochemical Society of Japan

Date : September 3rd (Tue.) –5th (Thu.), 2019

Place : Sakata Hirata Hall, Nagoya University
Furo-cho, Chikusa-ku, Nagoya 464-8602, Japan

Presentation Time : Special Lecture (25 min presentation + 5min discussion)
Invited Lecture (10 min presentation + 5 min discussion)
Award Nominee Lecture (10 min presentation + 10 min discussion)
General Lecture (10 min presentation + 5min discussion)
Poster Preview (1 min presentation without discussion)

第 57 回フラーレン･ナノチューブ･グラフェン総合シンポジウム
講演要旨集

主催 ： フラーレン･ナノチューブ･グラフェン学会

共催･後援 ： 日本化学会

協賛 ： 日本物理学会、応用物理学会、高分子学会、電気化学会

日時 ： 令和元年 9 月 3 日(火)～9 月 5 日(木)

場所 ： 名古屋大学　坂田・平田ホール
〒464-8602 名古屋市千種区不老町

発表時間 ： 特別講演（発表　25 分 + 質疑応答　5 分）
招待講演（発表　10 分 + 質疑応答　5 分）
受賞対象者講演（発表　10 分 + 質疑応答　10 分）
一般講演（発表　10 分 + 質疑応答　5 分）
ポスタープレビュー（発表 1 分・質疑応答　なし）

展示団体御芳名 （五十音順、 敬称略）

（株）アントンパール・ジャパン

（株）セントラル科学貿易

テレダイン・ジャパン（株）

フィルジェン（株）

ミカサ（株）

（株）名城ナノカーボン

（株）リッチモアインターナショナル

広告掲載団体御芳名 （五十音順、 敬称略）

アイクストロン(株)

エクセルソフト(株)

工機ホールディングス(株)

（株）三洋商事

（株）セントラル科学貿易

ソーラボジャパン（株）

（株）ダルトン

テレダイン・ジャパン（株）

日本電子（株）

（株）堀場製作所

Contents

目次

プログラム早見表

9月3日 （火）

	受付開始 8:30～ 開会挨拶 8:55～
9:00	特別講演（湯村 守雄） 9:00–9:30
9:30	一般講演 4件 （ナノチューブの応用・ ナノチューブの生成と精製） 9:30–10:30
10:30	休憩 10:30–10:45
10:45	特別講演（齋藤 理一郎） 10:45–11:15
11:15	一般講演 1件 11:15–11:30 （グラフェンの物性）
11:30	ポスタープレビュー （ 1P–1 ～ 1P–30） 11:30–12:15
12:15	昼食 （幹事会） 12:15–13:30
13:30	ポスターセッション 13:30–14:00 若手奨励賞候補審査優先時間 【セミナー室】 13:30–15:00
15:00	特別講演（柚原 淳司） 15:00–15:30
15:30	一般講演 3件 （原子層） 15:30–16:15
16:15	休憩 16:15–16:30
16:30	特別講演（Lain-Jong Li） 16:30–17:00
17:00	特別講演（竹井 邦晴） 17:00–17:30
17:30	一般講演 2件 （原子層・グラフェンの応用）17:30–18:00
18:00	

9月4日 （水）

	受付開始 8:45～ 講演開始 9:00～
9:00	大澤賞・飯島賞 受賞対象者講演 4件 9:00–10:25
10:25	休憩 10:25–10:45
10:45	特別講演（千足 昇平） 10:45–11:15
11:15	一般講演 1件 11:15–11:30 （グラフェンの物性）
11:30	ポスタープレビュー （ 2P–1 ～ 2P–29 ） 11:30–12:15
12:15	昼食 12:15–13:30
13:30	ポスターセッション 13:30–14:00 若手奨励賞候補審査優先時間 【セミナー室】 13:30–15:00
15:00	授賞式 15:00–15:15
15:15	総会 15:15–15:45
15:45	特別講演（射場 英紀） 15:45–16:15
16:15	休憩 16:15–16:30
16:30	特別講演（宮内 雄平） 16:30–17:00
17:00	一般講演 4件 （原子層・グラフェン生成・ フラーレンの応用・フラーレンの化学） 17:00–18:00
18:00	移動
18:30	懇親会 【レストラン花の木】 18:30–20:30
20:30	

9月5日 （木）

	受付開始 8:45～ 講演開始 9:00～
9:00	特別講演（早水 裕平） 9:00–9:30
9:30	招待講演（Xuan Viet Nguyen）9:30–9:45
9:45	一般講演 3件 （バイオ・その他） 9:45–10:30
10:30	休憩 10:30–10:45
10:45	特別講演（越野 幹人） 10:45–11:15
11:15	一般講演 1件 11:15–11:30 （グラフェンの物性）
11:30	ポスタープレビュー （ 3P–1 ～ 3P–30 ） 11:30–12:15
12:15	昼食 12:15–13:30
13:30	ポスターセッション 13:30–14:00 若手奨励賞候補審査優先時間 【セミナー室】 13:30–15:00
15:00	一般講演 2件 15:00–15:30 （グラフェンの物性）
15:30	招待講演（Thomas Pichler）15:30–15:45
15:45	一般講演 3件 （ナノチューブの物性） 15:45–16:30
16:30	

講演会場 坂田・平田ホール

特別講演 発表25分・質疑5分
招待講演 発表10分・質疑5分
賞対象者講演 発表10分・質疑10分
一般講演 発表10分・質疑5分
ﾎﾟｽﾀｰﾌﾟﾚﾋﾞｭｰ 発表1分・質疑なし

Time table

September 3 (Tue.)

	Registration begins at 8:30 Opening greeting at 8:55
9:00	Special Lecture 9:00–9:30 (Motoo Yumura)
9:30	General Lectures [4] (Applications of nanotubes・ Formation and purification of nanotubes) 9:30–10:30
10:30	Coffee Break 10:30–10:45
10:45	Special Lecture 10:45–11:15 (Riichiro Saito)
11:15	General Lectures [1]11:15–11:30 (Properties of graphene)
11:30	Poster Preview (1P–1 through 1P–30) 11:30–12:15
12:15	Lunch (Administrative meeting) 12:15–13:30
13:30	Poster Session During 13:30–14:00, please give priority to selection of candidates for Young Scientist Poster Award 【 Seminar room 】 13:30–15:00
15:00	Special Lecture 15:00–15:30 (Junji Yuhara)
15:30	General Lectures [3] (Atomic Layers) 15:30–16:15
16:15	Coffee Break 16:15–16:30
16:30	Special Lecture 16:30–17:00 (Lain–Jong Li)
17:00	Special Lecture 17:00–17:30 (Kuniharu Takei)
17:30	General Lectures [2]17:30–18:00 (Atomic Layers・Applications of graphene)
18:00	

September 4 (Wed.)

	Registration begins at 8:45 Lectures begin at 9:00
9:00	Lectures of Osawa Award and Iijima Award Nominees 9:00–10:25
10:25	Coffee Break 10:25–10:45
10:45	Special Lecture 10:45–11:15 (Shohei Chiashi)
11:15	General Lectures [1]11:15–11:30 (Properties of graphene)
11:30	Poster Preview (2P–1 through 2P–29) 11:30–12:15
12:15	Lunch 12:15–13:30
13:30	Poster Session During 13:30–14:00, please give priority to selection of candidates for Young Scientist Poster Award 【 Seminar room 】 13:30–15:00
15:00	Awards Ceremony 15:00–15:15
15:15	General Meeting 15:15–15:45
15:45	Special Lecture 15:45–16:15 (Hideki Iba)
16:15	Coffee Break 16:15–16:30
16:30	Special Lecture 16:30–17:00 (Yuhei Miyauchi)
17:00	General Lectures [4] (Atomic Layers・Graphene synthesis・ Applications of fullerenes・Chemistry of fullerenes) 17:00–18:00
18:00	Moving
18:30	Banquet 【 Restaurant Hananoki 】 18:30–20:30
20:30	

September 5 (Thu.)

	Registration begins at 8:45 Lectures begin at 9:00
9:00	Special Lecture 9:00–9:30 (Yuhei hayamizu)
9:30	Invited Lecture(Xuan Viet Nguyen) 9:30–9:45
10:00	General Lectures [3]10:00–10:30 (Bio・Other topics)
10:30	Coffee Break 10:30–10:45
10:45	Special Lecture 10:45–11:15 (Mikito Koshino)
11:15	General Lectures [1]11:15–11:30 (Properties of graphene)
11:30	Poster Preview (3P–1 through 3P–30) 11:30–12:15
12:15	Lunch 12:15–13:30
13:30	Poster Session During 13:30–14:00, please give priority to selection of candidates for Young Scientist Poster Award 【 Seminar room 】 13:30–15:00
15:00	General Lectures [2]15:00–15:30 (Properties of graphene)
15:30	Invited Lecture(Thomas Pichler) 15:30–15:45
15:45	General Lectures [3] (Properties of nanotubes) 15:45–16:30
16:30	

Place : Sakata Hirata Hall
Special Lecture : 25 min (Presentation) + 5 min (Discussion)
Invited Lecture : 10 min (Presentation) + 5 min (Discussion)
Award Nominee Lecture : 10 min (Presentation) + 10 min (Discussion)
General Lecture : 10 min (Presentation) + 5 min (Discussion)
Poster Preview : 1 min (Presentation)

座長一覧 (Chairpersons)

9月3日（火） （敬称略）

セッション	時　　間	座　　長
特別講演(湯村 守雄)	9:00 ～9:30	岡崎 俊也
一般講演	9:30 ～10:30	千足 昇平
特別講演(齋藤 理一郎)	10:45 ～ 11:15	片浦 弘道
一般講演	11:15 ～ 11:30	
ポスタープレビュー	11:30 ～ 12:15	丸山 実那 中西 勇介
特別講演(柚原 淳司)	15:00 ～ 15:30	大野 雄高
一般講演	15:30 ～ 16:15	蒲 江
特別講演(Lain-Jong Li)	16:30 ～ 17:00	竹延 大志
特別講演(竹井 邦晴)	17:00 ～ 17:30	
一般講演	17:30 ～ 18:00	松田 一成

9月4日（水）

セッション	時　　間	座　　長
一般講演(受賞対象者)	9:00 ～ 10:25	斎藤 晋
特別講演(千足 昇平)	10:45 ～11:15	山本 貴博
一般講演	11:15 ～11:30	
ポスタープレビュー	11:30 ～ 12:15	蓬田 陽平 松永 正広
特別講演(射場 英紀)	15:45 ～ 16:15	松尾 豊
特別講演(宮内 雄平)	16:30 ～ 17:00	岡田 晋
一般講演	17:00～ 18:00	大町 遼

9月5日（木）

セッション	時　　間	座　　長
特別講演(早水 裕平)	9:00 ～ 9:30	吾郷 浩樹
招待講演(Xuan Viet Nguyen)	9:30 ～ 9:45	前田 優
一般講演	9:45 ～ 10:30	
特別講演(越野 幹人)	10:45～ 11:15	北浦 良
一般講演	11:15 ～ 11:30	
ポスタープレビュー	11:30 ～ 12:15	岡田 光博 西原 大志
一般講演	15:00 ～ 15:30	宮田 耕充
招待講演(Thomas Pichler)	15:30 ～ 15:45	
一般講演	15:45 ～ 16:30	廣谷 潤

9月 3日（火）

特別講演　　発表 25分 ・ 質疑応答 5分
一般講演　　発表 10分 ・ 質疑応答 5分
ポスタープレビュー　　発表 1分 ・ 質疑応答 なし

特別講演（ 9:00-9:30 ）

一般講演（ 9:30-10:30 ）
ナノチューブの応用 ・ ナノチューブの生成と精製

＞＞＞＞＞＞ 休憩（ 10:30-10:45 ）＜＜＜＜＜＜

特別講演（ 10:45-11:15 ）

一般講演（ 11:15-11:30 ）
グラフェンの物性

ポスタープレビュー（ 11:30-12:15 ）　（☆） 若手奨励賞候補
若手奨励賞候補

9月3日（火）

ナノチューブの物性

ナノチューブの生成と精製

9月3日（火）

9月3日（火）

＞＞＞＞＞＞＞ 昼食（ 12:15-13:30 ）＜＜＜＜＜＜＜

ポスターセッション（ 13:30-15:00 ）
13:30-14:00 若手奨励賞候補審査優先時間

特別講演（ 15:00-15:30 ）

一般講演（ 15:30-16:15 ）
原子層

＞＞＞＞＞＞＞ 休憩（ 16:15-16:30 ）＜＜＜＜＜＜＜

特別講演（ 16:30-17:30 ）

9月3日（火）

一般講演（ 17:30-18:00 ）

原子層 ・ グラフェンの応用

9月 4日（水）

特別講演　　発表 25分 ・ 質疑応答 5分
一般講演　　発表 10分 ・ 質疑応答 5分
大澤賞･飯島賞受賞対象者講演　　発表 10分 ・ 質疑応答 10分
ポスタープレビュー　　発表 1分 ・ 質疑応答 なし

一般講演（ 9:00-10:25 ）
大澤賞･飯島賞受賞対象者講演

＞＞＞＞＞＞＞ 休憩（ 10:25-10:45 ）＜＜＜＜＜＜＜

特別講演（ 10:45-11:15 ）

一般講演（ 11:15-11:30 ）
グラフェンの物性

ポスタープレビュー（ 11:30-12:15 ）　（☆） 若手奨励賞候補
若手奨励賞候補

9月 4日（水）

フラーレン

フラーレンの化学

ナノチューブの物性

9月 4日（水）

9月 4日（水）

原子層

＞＞＞＞＞＞＞ 昼食（ 12:15-13:30 ）＜＜＜＜＜＜＜

ポスターセッション（ 13:30-15:00 ）

13:30-14:00 若手奨励賞候補審査優先時間

授賞式（ 15:00-15:15 ）

総会（ 15:15-15:45 ）

特別講演（ 15:45-16:15 ）

＞＞＞＞＞＞＞ 休憩（ 16:15-16:30 ）＜＜＜＜＜＜＜

特別講演（ 16:30-17:00 ）

一般講演（ 17:00-18:00 ）

原子層 ・ グラフェン生成 ・ フラーレンの応用 ・ フラーレンの化学

移動

懇親会（ 18:30-20:30 ）

9月 5日（木）

特別講演　　発表 25分 ・ 質疑応答 5分
招待講演　　発表 10分 ・ 質疑応答 5分
一般講演　　発表 10分 ・ 質疑応答 5分
ポスタープレビュー　　発表 1分 ・ 質疑応答 なし

>>>>>>> 休憩（ 10:30-10:45 ）<<<<<<<

9月 5日（木）

9月 5日（木）

グラフェンの応用

原子層

>>>>>>> 昼食（ 12:15-13:30 ）<<<<<<<

ポスターセッション（ 13:30-15:00 ）

13:30-14:00 若手奨励賞候補審査優先時間

一般講演（ 15:00-15:30 ）

グラフェンの物性

招待講演（ 15:30-15:45 ）

一般講演（ 15:45-16:30 ）

ナノチューブの物性

September 3rd, Tue.

Special Lecture: 25min (Presentation) + 5min (Discussion)
General Lecture: 10min (Presentation) + 5min (Discussion)
Poster Preview: 1min (Presentation)

>>>>>>> Coffee Break (10:30-10:45) <<<<<<<

Properties of nanotubes

September 3rd, Tue.

Properties of graphene

Graphene synthesis

Applications of graphene

Atomic Layers

>>>>>>> Lunch Time (12:15-13:30) <<<<<<<

Poster Session (13:30-15:00)

During 13:30-14:00, please give priority to selection of candidates for Young Scientist Poster Award

Special Lecture (15:00-15:30)

General Lecture (15:30-16:15)

Atomic Layers

September 4th, Wed.

Special Lecture: 25min (Presentation) + 5min (Discussion)
Award Nominee Lecture: 10min (Presentation) + 10min (Discussion)
General Lecture: 10min (Presentation) + 5min (Discussion)
Poster Preview: 1min (Presentation)

General Lecture (9:00-10:25)
Lectures of Osawa Award and Iijima Award Nominees

>>>>>>> Coffee Break (10:25-10:45) <<<<<<<

Special Lecture (10:45-11:15)

General Lecture (11:15-11:30)
Properties of graphene

Poster Preview (11:30-12:15) (☆)Candidates for the Young Scientist Poster Award
Candidates for the Young Scientist Poster Award

Nanowires

Atomic Layers

>>>>>>> Lunch Time （12:15-13:30）<<<<<<<

Poster Session （13:30-15:00）

During 13:30-14:00, please give priority to selection of candidates for Young Scientist Poster Award

Awards Ceremony （15:00-15:15）

Genaral Meeting （15:15-15:45）

Special Lecture （15:45-16:15）

>>>>>>> Coffee Break （16:15-16:30）<<<<<<<

Special Lecture （16:30-17:00）

General Lecture （17:00-18:00）

Atomic Layers ・ Graphene synthesis ・ Applications of fullerenes ・ Chemistry of fullerenes

Moving

Banquet （ 18:30-20:30 ）

September 5th, Thu.

Special Lecture: 25min (Presentation) + 5min (Discussion)
Invited Lecture: 10min (Presentation) + 5min (Discussion)
General Lecture: 10min (Presentation) + 5min (Discussion)
Poster Preview: 1min (Presentation)

Applications of graphene

Atomic Layers

>>>>>>> Lunch Time （ 12:15-13:30 ）<<<<<<<

Poster Session （ 13:30-15:00 ）

During 13:30-14:00, please give priority to selection of candidates for Young Scientist Poster Award

General Lecture （15:00-15:30 ）

Properties of graphene

Invited Lecture （ 15:30-15:45 ）

General Lecture （ 15:45-16:30 ）

Properties of nanotubes

特別講演
Special Lecture

1S – 1 ～ 1S – 5
2S – 1 ～ 2S – 3
3S – 1 ～ 3S – 2

Putting Carbon Nanotubes to Use as Industrial Materials
-Research and Development of Carbon Nanotube at AIST since 1991

Motoo Yumura

CNT-Application Research Center, AIST (Japan)

1. Synthesis and Isolation of Multi Walled Carbon Nanotubes (MWCNT):(1991-2001)

First research on MWCNT was development of the isolation method of MWCNT from soot [1]. Then we started to develop Large Scale Synthesis method of MWCNT. We tried several methods i.e. Arc discharge, Laser CVD, Catalytic CVD. On the end of 2000, we established vapor phase flow method which capable to produce 200g/h MWCNT.

2. Single Walled Carbon Nanotube (SWCNT) Mass Production : (2002-2010)

Due to the high cost from low yield production, industrial use of SWCNTs has not yet been realized despite their excellent properties. Industrial mass production technology is being developed based on highly efficient "Super-Growth" (i.e. water-assisted chemical vapor deposition) method [2] by combining large area with continuous process. On February 2011, a pilot plant based was established (in AIST) with Nihon Zeon Corp. capable to produce 0.6 kg of SWCNT per day. Improvement of eDIPS (enhanced Direct Injection Pyrolytic Synthesis) method [3] was developed to control diameter of highly crystalline SWCNTs. As a result, the development of super-growth and eDIPS methods for mass production with low cost will promote the development of the industrial use of SWCNTs in the near future.

3. Development of SWCNT Application:(2010-)

In August 2010, the 'Innovative Carbon Nanotubes and Their Applications Project' was begun which aims to develop applications utilizing the excellent properties of carbon nanotubes. Research and development work of this project was assigned to Technology Research Association for Single Wall Carbon Nanotubes (TASC), a consortium of five companies (Sumitomo Precision Products Co., Ltd., TEIJIN Ltd., Toray Industries, Inc., ZEON Corporation, and NEC Corporation) and National Institute of Advanced Industrial Science (AIST). The goals of this project by 2017 are to promote the development of Single-Walled Carbon Nanotubes (SWCNT) technology. More specifically, we aim to develop innovative applications of SWCNTs synthesized by Super-Growth method and eDIPS methods, and to build up methods of separating [4] and dispersing SWCNTs. In addition, we are assessing the safety and the management of nanotube materials [5]. Moreover, we promote R&D on ultra-light, super-strength, high-performance materials for application development through the establishing a new industry on Carbon Nanotube (CNT) composite materials.

[1] M.Yumura, S.Ohshima, K.Uchida, F.Ikzakai., Mat.Res.Soc.Sympo.Proc. Vol.349. 231 (1994)

[2] K. Hata, D.Futaba et al., Science. 306, pp.1362 (2004)

[3] T. Saito et al., Journal of Nanoscience and Nanotechnology, vol.8, pp.6153 (2008)

[4] H. Kataura et al., Nano Lett. 9 pp.1497 (2009).

[5] J. Nakanishi et al., Executive Summaries of Interim Reports on Risk Assessments of Three Manufactured Nanomaterials, Carbon Nanotubes (CNTs) (issued on October 16, 2009)

Corresponding Author: M. Yumura

Tel: +81-29-861-9417, Fax: +81-29-861-4551,

E-mail: m.yumura@aist.go.jp

Optical properties of nanotubes and two-dimensional materials by using circularly polarized light

○Riichiro Saito

[1] *Department of physics, Tohoku University, Sendai 980-8578, Japan*

We overview our recent works on optical properties by using circularly polarized light in carbon nanotubes and two-dimensional materials. Electric field of circularly polarized light rotates as a function time, clockwise (left-handed, LH) or anti-clockwise (right-handed, RH) when we observe the rotation from the propagating axis. The freedom of LH and RH is a "spin" of a photon which can be applied for doubling the information in optical signal transmission or for interaction with the spin of electron. A photon of circularly polarized light has an angular momentum of $\pm\hbar$ which we call helicity of the phonon. First we report circular dichroism (CD) of carbon nanotubes. CD is defined by the difference of optical absorption for LH and RH circularly polarized light, which can be used for assignment of enantiomer of nanotubes. We will discuss how the CD is calculated [1] and observed [2] as a function of chirality of carbon nanotubes. CD generally appears in two-dimensional materials, too, which we discuss in connection with valley polarization or pseudo-spin polarization by using so-called Haldane model [3] or modified Haldane model [4] that covers the Hamiltonian of many two-dimensional materials such as graphene, h-BN etc. In the Raman spectroscopy, we will discuss the origin of helicity-changing Raman spectra [5] and the relevant conservation law of angular momentum [6]. Finally, we will discuss surface plasmon of two-dimensional materials which is coupled with circularly polarized light [7]. This work is supported JSPS KAKENHI No. JPB18H01810.

References:

[1] N. Sato, Y. Tatsumi, R. Saito, Phys. Rev. B. 95, 155436 (2017).

[2] X. Wei, T. Tanaka, Y. Yomogida, N. Sato, R. Saito, H. Kataura, Nat. Comm. 7, 12899 (2016).

[3] K. Ghalamkari, Y. Tatsumi, R. Saito, J. Phys. Soc. Jpn., 87, 063708 (2018).

[4] M. Villa, N. T. Hung, S. Roche, R. Saito, Phys. Rev. B, 99, 161404 (2019).

[5] Y. Tatsumi, R. Saito, Phys. Rev. B 97, 115407 (2018).

[6] Y. Tatsumi, T. Kaneko, R. Saito, Phys. Rev. B, 97, 195444 (2018).

[7] M. S. Ukhtary, M. Maruoka, R. Saito, unpublished.

Corresponding Author: Riichiro Saito
Tel: +81-22-795-7754, Fax: +81-22-795-6447,
Web: http://flex.phys.tohoku.ac.jp/
E-mail: rsaito@flex.phys.tohoku.ac.jp

Growth and structure of group 14 elemental 2D honeycomb structure

Junji Yuhara

Department of Energy Science and Engineering, Nagoya University, Nagoya 464-8601, Japan

The synthesis and characterization of post-graphene materials have been intensively studied with the aim of utilizing novel two-dimensional (2D) properties. Most studies adopted molecular beam epitaxy as a synthesis method of 2D materials grown on clean crystalline surfaces. In my talk, I will talk on the epitaxial growth of (1) germanene, (2) stanene, and (3) plumbene by segregation and deposition methods.

(1) **Germanene on Ag(111) thin film by segregation** [1]: On annealing the specimen of Ag(111) thin film grown on Ge(111) in an ultra-high vacuum chamber, germanene has been epitaxially prepared on the surface. Low-energy electron diffraction clearly shows incommensurate "(1.3×1.3)"R30° spots, corresponding to a lattice constant of 0.39 nm, in perfect accord with close-up scanning tunneling microscopy (STM) images, which clearly reveal an internal honeycomb arrangement with corresponding parameter and low buckling within 0.01 nm. From the STM images, two types of protrusions, named hexagon and line, form a $(7\sqrt{7}\times7\sqrt{7})$R19.1° supercell with respect to Ag(111) with a super large periodicity of 5.35 nm.

(2) **Stanene on Ag_2Sn surface alloy by deposition** [2]: The lattice parameters of Ag_2Sn surface alloy and free-standing stanene are close to each other. The Ag(111) easily react with Sn atoms on annealing, while the Ag_2Sn surface alloy is chemically inert against the Sn atoms. The Ag_2Sn surface alloy is physically and chemically ideal surface for epitaxial growth of stanene. We have successfully prepared large area planar stanene on Ag_2Sn surface alloy by Sn deposition, supported by thorough density functional calculations.

(3) **Plumbene on $Pd_{1-x}Pb_x$(111) alloy surface by deposition and segregation** [3]: The bulk Pb-Pd system exists in fcc solid solution with concentration x up to 10 ~ 17 % for $Pd_{1-x}Pb_x$ depending on the temperatures. No Pb atoms evaporate from the Pd(111) surface on annealing up to 1000 °C, examined by Rutherford backscattering spectrometry. Instead, the Pb atoms dissolve and segregate on the surface on annealing. Plumbene is epitaxially grown on $Pd_{1-x}Pb_x$(111) alloy surface. The surface exhibits in the STM images a unique morphology resembling the famous Weaire-Phelan bubble structure of the Olympic "WaterCube" in Beijing.

[1] J. Yuhara, Y. Fujii, K. Nishino, N. Isobe, M. Nakatake, L.Xian, A.Rubio, G. Le Lay, 2D Mater. **5** (2018) 025002.
[2] J. Yuhara, H. Shimazu, K. Ito, A. Ohta, M. Araidai, M. Kurosawa, M. Nakatake, G. Le Lay, ACS Nano **12** (2018) 11632.
[3] J. Yuhara, B. He, N. Matsunami, M. Nakatake, G. Le Lay, Adv. Mater. (2019) **31** (2019) 1901017.

Corresponding Author: J. Yuhara
Tel: +81-52-789-3792, Fax: +81-52-789-3779
Web: http://yuhara.nucl.nagoya-u.ac.jp
E-mail: j-yuhara@energy.nagoya-u.ac.jp

1S-4

Growth of Transition Metal Dichalcogenide 2D Layers for Electronics

Lain-Jong (Lance) Li
King Abdullah University of Science and Technology (Saudi Arabia)

Our recent demonstration on vapor phase growth of transition metal dichalcogenide (TMD) monolayers such as MoS_2 and WSe_2 has stimulated the related research areas. The growth mechanism and the orientation control of TMD 2D flakes will be first discussed. These 2D monolayer building blocks can form atomic scaled *p-n* junctions for modern electronics either through vertical stacking or lateral stitching. The electronic structures of the vertical stacks are dominated by the stacking orientation and interlayer coupling strength. While the lateral *p-n* junction exhibits diode properties and a large strain at the junction region offering tunability in electronic structures. The talk shall be ended by future research perspectives on the possibility of using 2D layers for future electronics.

Short Bio

Dr. Lain-Jong (Lance) Li now serves as a Research Director in Corporate Research at Taiwan Semiconductor Manufacturing Company (TSMC). He is also the adjunct professor at Univ. of New South Wales (Sydney) and King Abdullah University of Science and Technology (KAUST). He received his BSc and an MSc in chemistry at National Taiwan University. He obtained his PhD of condensed matter physics at Oxford University in 2006. He was an Assistant professor in Nanyang Technological University Singapore (2006-2009). Since 2010, he has become an Associate Professor at Academia Sinica Taiwan. He joined King Abdullah University of Science and Technology in 2014 and became a full professor in 2016. His main research interest focuses on fundamental studies of carbon and inorganic 2D materials, and large-scale growth of various 2D materials for electronic and energy applications. He is recognized as the 2018 highly cited scholar (Clarivate) in Physics and Universal Scientific Education and Research Network (USERN) 1% top scientist in 2017.

Nanocarbon-based flexible devices

○Kuniharu Takei[1,2]

[1] *Department of Physics and Electronics, Osaka Prefecture University, Sakai 599-8531, Japan*
[2] *JST PRESTO, Kawaguchi 332-0012, Japan*

Flexible and stretchable electronics are now widely studied for a next class of electric devices replaced from the silicon-based conventional inflexible devices. In particular, multi-functional sensor sheets can contribute to the applications for Internet of Things (IoT). For high performance and low power electronics, the method to form high quality active materials on soft substrates is important to develop because single crystalline substrate like Si wafer cannot be used for this flexible device.

To address this challenge, firstly, this talk introduces the transfer or deposition techniques of inorganic nanomaterials as the active components onto flexible films. In particular, carbon nanotube (CNT) networks and graphene are used to fabricate large-scale and high-performance transistors and sensors [1].

One of the main targets for the flexible electronics is to build the platform of wearable healthcare device applications. For healthcare application, multiple vital and molecule information such as pH, glucose levels are very important to monitor as well as activity information. Furthermore, simultaneous multiple condition monitoring of physical and chemical information is a next class of wearable devices for convenient and safe human life. To realize the multi-functional flexible sensor system, flexible physical and chemical sensor sheets will be discussed [2-3]. After understanding the fundamental properties and mechanism of the flexible transistors and sensors, integrated device applications with several sensors on a flexible film are demonstrated as proof-of-concepts for multi-functional sensor sheet platforms.

Although a lot of researches and developments are still required for practical application, these studies may help to open a door for the next step of flexible electronics. In the next step, the collaborative works between institute including university and industry are an important role to move forward to building a platform for flexible wearable healthcare applications. Furthermore, stability and reliability of sensors in terms of sensitivity and long-time measurements should be studied to break the barrier toward the practical applications from the academic research into the market.

[1] M. Shiomi *et al*., ACS Nano, **13**, 4771-4777 (2019).
[2] Y. Yamamoto *et al.,* Sci. Adv., **2**, e1601473 (2016).
[3] S. Nakata *et al.,* Nat. Electron., **1**, 596-603, (2018).

Corresponding Author: K. Takei
Tel: +81-72-254-9497,
Web: https://sites.google.com/site/kuniharutakeijp/
E-mail: takei@pe.osakafu-u.ac.jp

Templated synthesis of nanomaterials with single-walled carbon nanotubes and their properties

○Shohei Chiashi

Department of Mechanical Engineering, The University of Tokyo, Tokyo 113-8656, Japan

Single-walled carbon nanotubes (SWCNTs) are one of the nanomaterials that are structurally controlled in atomic scale. SWCNT structure, such as chirality, diameter, length etc. are diverse in nano-scale, and they can also be deformed in macro-scale due to high flexibility. As ideal SWCNTs consist of only six-membered rings of carbon atoms, they are mechanically strong and have chemically stable surfaces. Since the surface is chemically inactive even at high temperature, it is possible to synthesize new nano-materials whose structure is controlled in nano- and micro-scale by using SWCNTs as template.

We succeeded in synthesizing boron nitride nanotube (BN-NT), multi-walled carbon nanotube (MWCNT) and MoS_2 nanotube (MoS_2-NT) on the outer surface of SWCNTs[1]. By supplying the precursor molecules to SWCNTs at high temperature, these nanotubes were obtained as the additional layer through chemical vapor deposition process. It is thought that the precursor molecules and/or their decomposition products adsorbed on the outer surface of SWCNTs and then the tube structure grew up. Although the tube-structure itself was stable, their edge parts were unstable during the growth stage. While metal nano-particles are needed as catalysts in the case of SWCNT growth, SWCNT surface played an important role in the stable growth of these nanotubes. On the other hand, when water molecules were supplied to opened-SWCNTs at lower temperature, ice-nanotubes were obtained inside SWCNTs[2]. The inner space of SWCNT was the template in this case.

Here, with focusing the van der Waals interaction, the nanomaterial growth on SWCNTs and their physical properties are reported. Based on the growth on atomic layered materials on flat surface, such as MoS_2 flakes on h-BN, h-BN flakes on graphite, and so on, we will discuss the growth mechanism of the 1D and 2D nano-materials.

[1] R. Xiang et al., arXiv:1807.06154.
[2] S. Chiashi, *et al*., ACS Nano **19**, 1177 (2019).

Corresponding Author: S. Chiashi
Tel: +81-3-5841-6407, Fax: +81-3-5841-6408,
Web: http://www.photon.t.u-tokyo.ac.jp/~chiashi/
E-mail: chiashi@photon.t.u-tokyo.ac.jp

Nano carbon for sustainable mobility

○Hideki Iba

Battery Research Div., Toyota Motor Corporation, Shizuoka 410-1193, Japan

Electrification of cars is important to reduce carbon dioxide emission and in achievement of sustainable mobility (Fig.1). Improvement of batteries is the biggest challenge toward electrified vehicles. Innovative batteries such as all solid state battery or metal air battery are expected as a promising candidate for next generation energy storage (Fig.2). The recent progress and challenges of innovative batteries will be discussed. In addition, a few examples of the application of nano carbon technologies will be shown as technical basis for innovative batteries

Fig. 1 Plug in hybrid vehicle

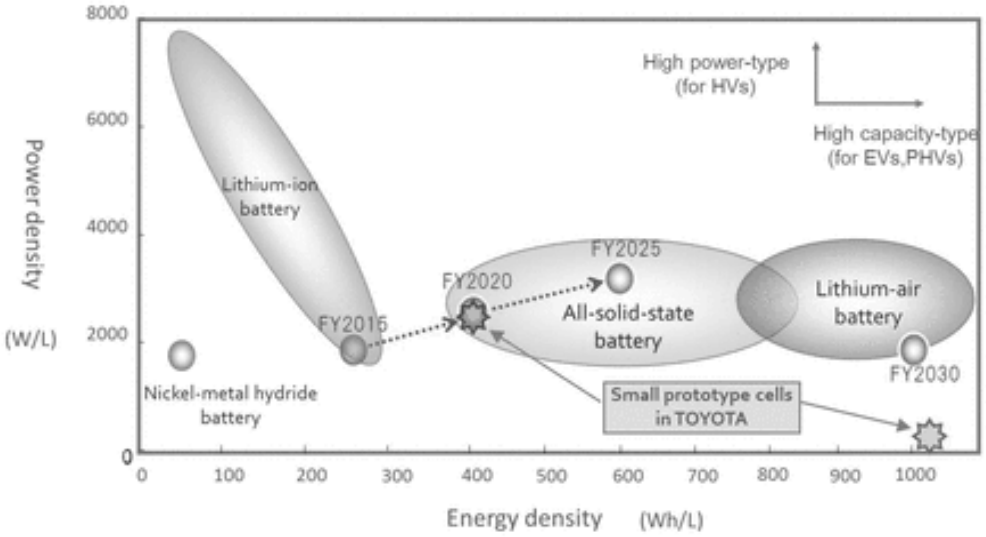

Fig. 2 Road map on innovative batteries

Tel: +81-55-997-9540, Fax: +81-55-997-7879,
E-mail: hideki_iba@mail.toyota.co.jp

Mechanical and thermal-optical properties of chirality-defined single-walled carbon nanotubes

○Yuhei Miyauchi [1,2]

[1] *Institute of Advanced Energy, Kyoto University, Kyoto 611-0011, Japan*
[2] *Graduate School of Science, Nagoya University, Chikusa, Nagoya 464-8602, Japan*

Since the discovery of carbon nanotubes [1], fabrication of macroscopic materials with exceptional physical properties using them has attracted much attention for more than a quarter century. In particular, their ultrahigh theoretical tensile strength (> ~100 GPa) and thermal conductivity (> ~2000 W/m·K) have inspired the realization of unprecedentedly strong structural materials and highly thermal conductive materials. Excitonic optical responses [2-7] of semiconducting single-walled carbon nanotubes (SWNTs) have also attracted great interest because of their potential applications in near-infrared photonics. However, these *dreams of carbon nanotubes* have not yet been realized as originally expected, mainly due to difficulties in keeping the excellent intrinsic properties of individual SWNTs in a macroscopic aggregation composed of them. We will report our recent experimental results on mechanical and thermal-optical properties of individual SWNTs with defined chirality, and will discuss how to make the best use of their intrinsic properties in macroscopic applications. First, we will discuss the measurements of the ultimate tensile strengths of chirality-defined individual SWNTs [8]. We found that the ultimate tensile strengths of SWNTs depend on their chiral structures, which clearly highlights the target nanotube structures that should be synthesized when attempting to fabricate the strongest structural materials [8]. Excitonic thermal radiation of SWNTs [9] will also be discussed. Because of their large binding energy, excitons in SWNTs are stable even at temperatures over 1000 K. This unique property enables thermal generation of excitons in semiconducting SWNTs. Thermal exciton radiation spectra of individual semiconducting SWNTs showed very narrow spectral bandwidth at 1000-2000 K [9]; this thermal-optical property is promising for their macroscopic application in heat-to-light energy conversion devices necessary for efficient thermophotovoltaics.

[1] S. Iijima, *Nature* **354**, 56 (1991).

[2] Y. Miyauchi*, *J. Mater. Chem. C* **1**, 6499 (2013).

[3] Y. Miyauchi*, M. Iwamura, S. Mouri, T. Kawazoe, M. Ohtsu, and K. Matsuda, *Nat. Photonics* **7**, 715 (2013).

[4] M. Iwamura, N. Akizuki, Y. Miyauchi*, K. Matsuda*, *et al*., *ACS Nano* **8**, 11254 (2014).

[5] N. Akizuki, S. Aota, S. Mouri, K. Matsuda, and Y. Miyauchi*, *Nat. Commun*. **6**, 8920 (2015).

[6] Y. Miyauchi*, T. Heinz*, *et al*., *Phys. Rev. B* **92**, 205407 (2015).

[7] Y. Miyauchi*, S. Konabe*, *et al*., *Nat. Commun.* **9**, 2598 (2018).

[8] A. Takakura, K. Beppu, T. Nishihara, A. Fukui, T. Kozeki, T. Namazu*, Y. Miyauchi*, and K. Itami*, *Nat. Commun.*, **10**, 3040 (2019).

[9] T. Nishihara, A. Takakura, Y. Miyauchi*, and K. Itami*, *Nat. Commun.* **9**, 3144 (2018).

Corresponding Author: Y. Miyauchi
Tel: +81-774-38-3463, E-mail: miyauchi@iae.kyoto-u.ac.jp

Bioelectronic interface controlled by self-assembled peptides on two-dimensional nanomaterials

○Yuhei Hayamizu[1]

[1] *Department of Materials Science and Engineering, School of Materials and Chemical Technology, Tokyo Institute of Technology, Tokyo 152-8550, Japan*

Developing elegant hybrid systems of biological molecules on two-dimensional nanomaterials, such as graphene, is a key in creating novel bio-nanoelectronic devices, where versatile biological functions are integrated with electronics of nanomaterials. Biomolecules self-assembling into organized structures on these nanomaterials offer a novel bottom-up approach, where biomolecular architectures spatially govern the electronics of nanomaterials. Despite the enormous potential in bridging nano- and bio-worlds at the molecular scale, no work has yet realized a way to control electronic and/or optical properties of nanomaterials by the biomolecular structures.

Our research target is the control of the interface between biotechnology and nanotechnology. More specifically, we employ solid binding peptides or artificially-designed peptides [1-5], which have specific binding affinities to 2D nanomaterials and an ability to form peptide nanostructures on atomically flat surfaces. These peptides spontaneously organize into coherent monolayer-thick nanostructures on surfaces of graphene and other 2D nanomaterials with a thickness of one layer of atoms. These peptides can work as a molecular scaffold for future biosensors using 2D nanomaterials [4]. Furthermore, the organization of peptides modify the electronic property of 2D nanomaterials spatially based on the nanostructures of self-assembled peptides [5]. On the other hand, the organization of peptides can be also tuned by applied electrochemical potential on the 2D nanomaterial [6]. In this talk, the details of peptide designing for molecular scaffold and its experimental characterizations will be discussed.

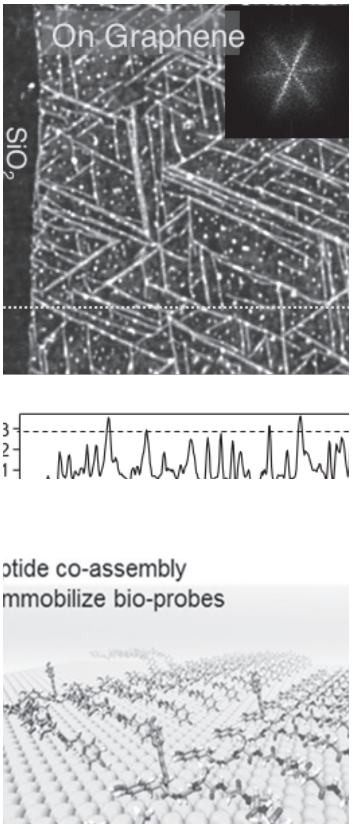

Fig. 1: Atomic force microscope image of self-assembled peptides on graphene (top), and molecular model of self-assembled peptides on graphene (left).

[1] C. R. So, Y. Hayamizu, H. Yazici, C. Gresswell, D. Khatayevich, C. Tamerler, and M. Sarikaya, *ACS Nano*, 6 (2) (2012) 1648-1656.
[2] D. Khatayevich, C. R. So, Y. Hayamizu, Carolyn Gresswell, and Mehmet Sarikaya, *Langmuir*, 28 (2012) 8589.
[3] D. Khatayevich, et al., *Small* 10.8 (2014): 1505-1513.
[4] P. Li, et.al., *ACS Applied Materials & Interfaces* 11, 20670 (2019).
[5] Y. Hayamizu, et.al., *Scientific Reports* 6, Article number: 33778 (2016).
[6] T. Seki, et.al., Langmuir 34(5), 1819-1826 (2018)

Corresponding Author: Y. Hayamizu
Tel and Fax: +81-03-5734-3651,
Web: http://www.op.titech.ac.jp/lab/hayamizu/index_e.html
E-mail: Hayamizu.y.aa@m.titech.ac.jp

Physics of twisted 2D materials

○Mikito Koshino[1]

[1] *Department of Physics, Osaka University, Osaka 560-0043, Japan*

When 2D materials having different periodicities are overlaid with each other, the interference pattern of the lattice mismatch often leads to unusual electronic properties. For instance, the twisted bilayer graphene (rotationally stacked graphene bilayer) exhibits dramatic phenomena such as the flat band formation and emergent superconductivity. In this talk, we introduce our recent theoretical works on incommensurate twisted bilayer systems and their interesting physical properties. First we will discuss the twisted bilayer graphene, where we introduce a theoretical framework to reduce its complex electronic structure into a simple effective model. We then discuss the lattice relaxation and the phonon vibrations in the twisted bilayer graphene. [2] There we show that the original linear dispersion of graphene's acoustic phonon is broken down into mini phonon bands separated by gaps, and the low-energy phonon modes are regarded as collective vibrations of the AB/BA domain wall network. Lastly we argue about the 30-degree twisted bilayer graphene, where the 12-fold quasicrystalline nature with nearly flat bands can be described in terms of the quasi-band picture.[3]

[1] M. Koshino, N. F. Q. Yuan, T. Koretsune, M. Ochi, K. Kuroki, L. Fu, Phys. Rev. X 8, 031087 (2018).
[2] M. Koshino and Y.-W. Son, arXiv:1905.09660 (2019), to be published in PRB.
[3] P. Moon, M. Koshino and Y.-W. Son, Phys. Rev. B 99, 165430 (2019).

Corresponding Author: Mikito Koshino
Tel: +81-6-6850-5742
Web: http://qp.phys.sci.osaka-u.ac.jp
E-mail: koshino@phys.sci.osaka-u.ac.jp

招待講演
Invited Lecture

3 I – 1 ～ 3 I – 2

Highly Uniform, Flexible Microelectrodes Based on the Clean Single-Walled Carbon Nanotube Thin Film with High Electrochemical Activity

○Nguyen Xuan Viet[1]

[1] *Department of Chemistry, VNU University of Science, Hanoi, 19 Le Thanh Tong, Hoan kiem district, Hanoi, Viet Nam.*

Electrochemical sensors based on carbon nanotubes (CNTs) have great potential for use in wearable or implantable biomedical sensor applications because of their excellent mechanical flexibility and biocompatibility. However, the main challenge associated with CNT-based sensors is their uniform and reproducible fabrication on the flexible plastic film. Here, we introduce and demonstrate a highly reliable technique to fabricate flexible CNT microelectrodes on a plastic film. The technique involves a process whereby the CNT film is formed by the dry transfer process based on the floating-catalyst chemical vapor deposition. An oxide protection layer, which is used to cover the CNT thin film during the fabrication process, minimizes contamination of the surface. The fabricated flexible CNT microelectrodes show almost ideal electrochemical characteristics for microelectrodes with the average value of the quartile potentials, $\Delta E = |E_{3/4} - E_{1/4}|$, being 60.4 ± 2.9 mV for the 28 electrodes, while the ideal value of ΔE = 56.4 mV. The CNT microelectrodes also showed enhanced resistance to surface fouling during dopamine oxidation in comparison to carbon fiber and gold microelectrodes; the degradation of the oxidation current after 10 consecutive cycles were 1.8, 8.3, and 13.9% for CNT, carbon fiber, and gold microelectrodes, respectively. The high-sensitivity detection of dopamine is also demonstrated with differential-pulse voltammetry, with a resulting limit of detection of ∼50 nM. The reliability, uniformity, and sensitivity of the present CNT microelectrodes provide a platform for flexible electrochemical sensors.

Corresponding Author: N.X Viet
Tel: +84-976-854-811
E-mail: vietnx@vnu.edu.vn

Position and momentum mapping of phonons and electronic excitations in graphene nanostructures in the electron microscope

○Thomas Pichler[1,2], Ryosuke Senga[2], Kazu Suenaga[2], Shigeyuki Morishita[3], Paolo Barone[4], Francesco Mauri[5]

[1] *Faculty of Physics, University of Vienna, Austria*
[2] *Nanomaterials Research Institute, AIST, Tsukuba, Japan.*
[3] *EM Research and Development Department, JEOL Ltd, Akishima, Japan*
[4] *SPIN-CNR, c/o Università G. D'Annunzio, Chieti, Italy.*
[5] *Dipartimento di Fisica, Università di Roma La Sapienza, Roma, Italy.*

Recent advances in improving the energy resolution in electron energy loss spectroscopy inside a transmission electron microscope enables the application in different energy scales ranging from the direct measurements of site selective core level spectroscopy, truly local and momentum resolved valence band excitations down to the energy of phonon spectroscopy. Here we ll present our new results on graphene nanostructures including (mono and few layer graphene, graphene nanoribbons and carbon nanotubes) combining high-resolution EELS with high-resolution TEM. Regarding core level excitations well separated peaks are obtained from a single freestanding nanotube with the local chiral index and unambiguously related to the van Hove singularities [1]. The local optical conductivity is directly determine the defect modulated gap transition in semiconducting nanotubes and correlate it to the optical conductivity. This allows for the first time to unravel the influence of an identified individual defect on the optical properties and directly probe e.g. their defect modulated exciton life time as crucial input for optoelectronic applications [2]. Regarding momentum resolved valence band excitations, we present new results on the interband plasmon dispersion of graphene monolayers. Last but not least, for phonon spectroscopy we show how to overcome the previous limitations of TEM-EELS to polar materials such as h-BN and regarding the momentum resolutiuon. Here, first examples on position and momentum mapping of phonons in apolar graphene nanostructures will be given [3]. This provides a new pathway to determine the phonon dispersions down to the scale of an individual freestanding graphene monolayer with nanometer size lateral resolution by mapping the distinct vibrational modes for a large momentum transfer. The measured scattering intensities are accurately reproduced and interpreted with density functional perturbation theory. Additionally, a nanometer-scale mapping of selected momentum resolved phonon modes using graphene nanoribbon structures allows to spatially disentangle bulk, edge and surface vibrations. Spatially resolved and momentum-resolved measurements will in the future enable us to fully disentangle different vibrational modes and their momenta, allowing phonon dispersion to be obtained even at interfaces and edges.

[1] R. Senga, T. Pichler, K. Suenaga, *Electron Spectroscopy of Single Quantum Objects To Directly Correlate the Local Structure to Their Electronic Transport and Optical Properties*, Nanoletters, 16, 3661 (2016)
[2] R. Senga, T. Pichler, Y. Yomogida, T. Tanaka, H. Kataura, K. Suenaga, *Direct Proof of a Defect-Modulated Gap Transition in Semiconducting Nanotubes*, Nanoletters, 18, 3920 (2018)
[3] R. Senga, K. Suenaga, P. Barone, S. Morishita, F. Mauri, T. Pichler. *Position and momentum mapping of vibrations in graphene nanostructures,* Nature, in press (2019).

Corresponding Author: T. Pichler

一般講演
General Lecture

1 – 1 ～ 1 – 10
2 – 1 ～ 2 – 9
3 – 1 ～ 3 – 9

Supercapacitors with no capacitance decay at -50 ℃ enabled by aligned CNT bundles connected with traversing CNTs

○Xiang Gao[1], Lingchang Li[1], Mengmeng Zhang[1], Don N. Futaba[2], and Ming Xu[1]*

[1] *State Key Laboratory of Materials Processing and Die & Mold Technology, School of Materials Science and Engineering, Huazhong University of Science and Technology (HUST), Wuhan 430074, China.*
[2] *CNT-Application Research Center, National Institute of Industrial Science and Technology (AIST), Tsukuba, 305-0044, Japan.*

. Aligned CNT is a promising material in supercapacitor due to the well-ordered and ultra-fast 1D electron transport. However, traditional aligned CNTs always encounter serious shrinking in electrolytes due to the high specific surface area (SSA) and overcrowding [1], greatly limiting the accessibility of ion which is urged for the ultrahigh rate and low temperature operation of supercapacitors [2-4]. To solve this problem, our strategy is to design the hybrid architecture to realize the structural stability in electrolyte. Here, we demonstrate supercapacitors where carbon nanotubes (CNTs) with aligned CNT bundles connected with traversing CNTs are designed to provide high accessibility of ions as well as exceptional structural stability. Traversing CNTs grow spontaneously with aligned CNTs, supporting the aligned CNTs and acting as the lateral frames of the whole structure, which is the key for their structural stability in electrolyte. Benefiting from the superiority of inter-tube structure, supercapacitors with high capacitance retention of 89% from 10 mV/s to 500 mV/s and no capacitance decay at -50 ℃ are realized. We finally obtain high power density of 40 kW/kg and high energy density of 43.1 Wh/kg at -50 ℃, surpassing most of the supercapacitors at low temperature. We believe that our design of the CNT architecture could provide a novel design principle for ultrahigh rate and low temperature supercapacitors.

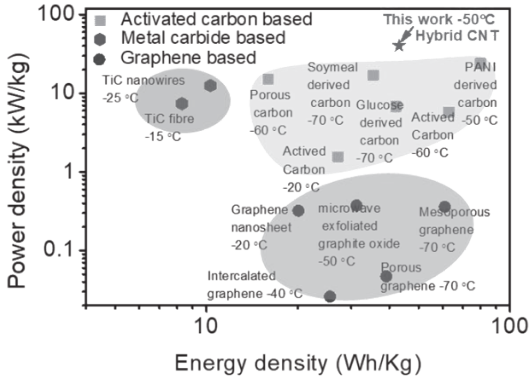

Fig. 1 Power density and energy density comparison of the supercapacitors at low temperature.

[1] Futaba, D.N. et al. Nat Mater 5, 987-994 (2006).
[2] Salanne, M. et al. Nat. Energy **1**, 16070 (2016).
[3] Lukatskaya, M.R. et al. Nat. Energy **2**, 17105 (2017).
[4] Xia, X. et al. Energy Environ. Sci. **8**, 1559-1568 (2015).

Corresponding Author: Ming Xu
Tel: +86-027-87557749
Web: https://www.nanocarbon-hust.cn/
E-mail: ming.xu@hust.edu.cn

Design of Carbon Nanotube-based Non-precious Metal Electrocatalysts with High Performance and Durability

Jin Nishida,[1] Jun Yang,[1] Shunsuke Uchimura,[2] Junko Matsuda,[3] Naotoshi Nakashima[1]

[1]International Institute for Carbon Neutral-Energy Research (WPI-I2CNER), Kyushu University, Fukuoka, Japan
[2]Graduate School of Engineering, Kyushu University, Fukuoka, Japan
[3]International Research Center for Hydrogen Energy, Kyushu University, Fukuoka, Japan
E-mail: nakashima.naotoshi.614@m.kyushu-u.ac.jp

In recent years, a sustainable and low-carbon emission energy chain has attracted much attention. Toward the goal, the development of non-precious metal electrocatalysts for fuel cells, water splitting and batteries with high performance, durablity, and scalability is a strong social demand for the next-generation eco-friendly energy society[1].

In this meeting, we summarize our recent studies on i) seven different nanocarbons /iron phthalocyanine (II) hybrids with well-defined nanostructures that show excellent efficiency and durability for oxygen reduction reaction[2,3], ii) decorating unoxidized-carbon nanotubes with homogeneous Ni-Co-spinel nanocrystals that show superior performance for oxygen evolution and oxygen reduction reactions[4], and iii) nanocarbon-Fe-Ni-based catalyst with high oxidation evolution reaction performance, in which we used several kinds of nanocarbon including multi-walled carbon nanotubes and carbon black as a carbon support and compared the performance of oxidation evolution reaction.

References

[1] N. Nakashima (Editor), "Nanocarbons for Energy Conversion-Supramolecular Approach-", Springer, **2018**, pp. 1-564.
[2] J. Yang, J. Tao, T. Isomura, H. Yanagi, I. Moriguchi, N. Nakashima, *Carbon*, **2019**, *145*, 565-571.
[3] J. Yang, F. Toshimitsu, T. Fujigaya, N. Nakashima, *J. Mater. Chem. A*, **2017**, *5*, 1184-1191
[4] J. Yang, T. Fujigaya, N. Nakashima, *Sci. Rep*., **2017**, *7*, art.no.45384.

Corresponding Author: N. Nakashima
Tel: +81-92-802-6745, Fax: Tel: +81-92-802-6745, E-mail:
nakashima.naotoshi.614@m.kyushu-u.ac.jp

1-3

Separation of carbon nanotubes using multiscale hydrophobic interaction

○Hiromichi Kataura, Mayumi Tsuzuki, Tomoko Sugita, Mariko Kubota, Guowei Wang, Takeshi Tanaka

Nanomaterials research Institute, AIST, Tsukuba 305-8565, Japan

Adsorption chromatography is very useful for large scale metal/semiconductor separation and structure sorting of single-wall carbon nanotubes (SWCNTs), where polysaccharide gels are used as stationary phase. However, adsorption and desorption mechanisms of SWCNTs have not been well understood to date. In this presentation, we will give a model of adsorption mechanism of SWCNTs on the polysaccharide polymer. We have fabricated seven different allyl dextran gels by changing dextran concentrations and measured their adsorption abilities. Power law dependence in the adsorption ability shows that effective adsorption site is not nanoscale but mesoscopic scale. This finding tells us that we have to consider the macroscopic hydrophobic interactions such as “wet-dry transition”. Wet-dry transition is the evacuation of water between two face to face placed hydrophobic plates dipped in water when the distance is short. In the case of SWCNT-gel system, the wet state means that SWCNT is covered with sufficient surfactants in water and dry state means that “bare” SWCNT is attached to polysaccharide polymer without surfactant molecules. Wet and dry states can be understood as metastable states where the total free energy of hydrogen bonding of surrounding water is minimized locally. Since the adsorption of surfactant is due to hydrophobic interaction in microscopic scale, the wet and dry states can be understood as multiscale hydrophobic interaction system. Therefore, hydrogen bonding system finally decides whether dry or wet states are more stable. Since the number of adsorbing sodium dodecyl sulfate to SWCNT is highly dependent on the band gap width of SWCNT due to its charge transfer nature, semiconducting SWCNTs are selectively adsorbed to the gels by the wet-dry transition. If we accept this adsorption model, furthermore, all the behavior based on hydrophobic interaction explains all of our experimental data and further contributed to automatic separation of 20 single chirality species, where the hydrophobicity of surfactant is the most important parameter for the chirality selective elution. Interestingly, we can separate SWCNTs based on the other parameter using the same adsorption mechanisms.

Corresponding Author: H. Kataura
Tel: +81-29-861-2551, Fax: +81-861-2786,
Web: https://staff.aist.go.jp/h-kataura/index.html
E-mail: hkataura@aist.go.jp

Aqueous two phase extraction of semiconducting single-wall carbon nanotubes with isomaltodextrin and thin-film-transistor applications

○Haruka Omachi[1,2], Tomohiko Komuro[1], Kaisei Matsumoto[1], Minako Nakajima[1], Hikaru Watanabe[5], Jun Hirotani[3], Yutaka Ohno[3,4], and Hisanori Shinohara[1]

[1] Department of Chemistry, Graduate School of Science, Nagoya University, Nagoya 464-8602, Japan

[2]Research Center for Materials Science, [3] Department of Electronics, Graduate School of Engineering, and [4] Institute of Materials and Systems for Sustainability, Nagoya University

[5] Hayashibara Co., Ltd.

Semiconducting single-wall carbon nanotubes (s-SWCNTs) are promising materials for electronic devices. However, because the conventional as-grown carbon nanotubes contain ca. 30 % metallic (m-) SWCNTs, separation is required to obtain high purity s-SWCNTs.

In this work, we developed a rapid and single-step aqueous two-phase (ATP) extraction of high-purity s-SWCNTs using isomaltodextrin (IMD), which is a cost-effective polysaccharide containing a much amount of α-1,6-glucosidic linkages [1]. The purity of s-SWCNT extract reached at >98%, confirmed by both optical absorption and Raman spectroscopies. We also succeeded to fabricate the high-dense and uniform film from the high-purity s-SWCNT extract directly. The fabricated TFTs exhibited excellent on/off ratios, carrier mobility, and current density.

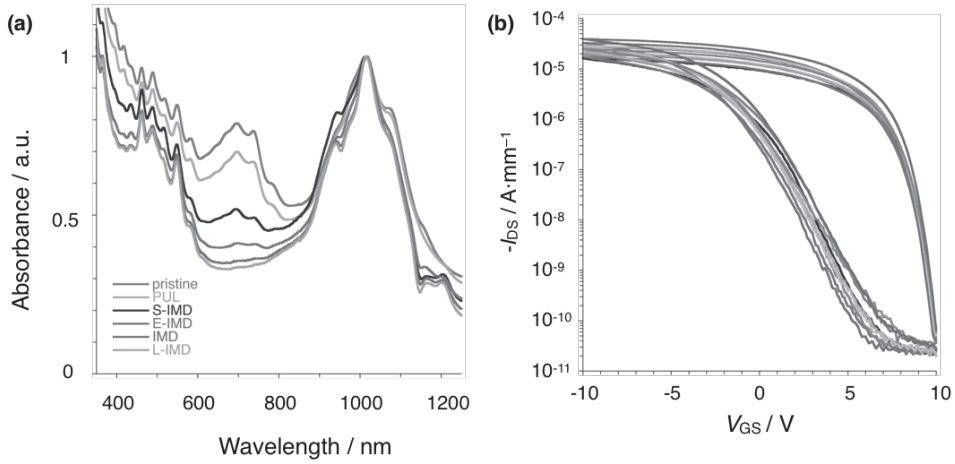

Fig.1 (a) Absorption spectra of pristine dispersion and ATP-extracts (b) Transfer characteristics of thin film transistors using extracted semiconducting CNT dispersion (channel length = 10 μm, V_{ds} = –0.5 V).

[1] H. Omachi *et al.*, Appl. Phys. Express *in press*.

Corresponding Author: Haruka Omachi, Hisanori Shinohara
Tel: +81-52-789-2482, Fax: +81-52-747-6442
E-mail: omachi@chem.nagoya-u.ac.jp, noris@nagoya-u.jp

Non-Zero Wavevector Electronic Excitation of Graphene induced by Localized Surface Plasmon

ZHANG Jinjiang[1]; ZHOU Ruifeng[1, 2], MINAMIMOTO Hiro[1]; ○MURAKOSHI Kei[1]

[1]*Department of Chemistry, Faculty of Science, Hokkaido University, Hokkaido 060-0810, Japan*
[2]*Institute for International Collaboration, Hokkaido University, Japan*

The fascinating electrical and optical properties of graphene render it wide application in photoelectronic devices. Its optical response and electronic interaction with substrate has been well investigated with Raman spectroscopy [1]. In the surface-enhanced Raman spectroscopy (SERS), band intensities are enhanced and new features may emerge due to the localized surface plasmon resonance (LSPR) of metal nanoparticles. In this work, the SERS spectra of monolayer graphene were investigated under electrochemical potential control. The influences of LSPR on the electronic excitation process in graphene were discussed.

Graphene was synthesized on Cu foil via chemical vapor deposition method and was transferred onto ITO glass (Gr/ITO glass) with poly(methyl methacrylate). The as-transferred graphene number of layer was confirmed to be single-layer and defect-free via the Raman spectroscopy [2]. Au nano-dimers were fabricated onto Gr/ITO glass (Au/Gr/ITO glass) via angle-resolved nano-sphere lithography method. The electrochemical Raman spectroscopy was carried out with a three-electrode system and 785 nm laser was used to excite the LSPR.

Around 1600 cm^{-1}, three sub-bands were observed in SERS of the single-layer defect-free graphene, in contrast to the single G band in the normal Raman spectrum. Electrochemical SERS showed that energy of one of the sub-bands shifts with potentials in a manner very similar to the G band, while the other two sub-bands were not sensitive to potential change. Thus, the three sub-bands can be assigned to the G band and two non-zero wavevector phonon modes, D' and D''. The visualization of the non-zero wavevector phonon modes in a defect-free graphene is ascribed to the plasmon-induced non-vertical electronic excitation . Furthermore, the SERS spectra differ from the normal Raman spectra of graphene at both low and high doping levels. At low doping level, the G phonon renormalization was suppressed (Figure); at high doping level, the quantum interference was smeared out. These findings demonstrate the modification of photoexcitation by LSPR. The new photoexcitation pathways not only change the optical response of graphene, but also alter the electrochemical potentials of hot electrons and holes.

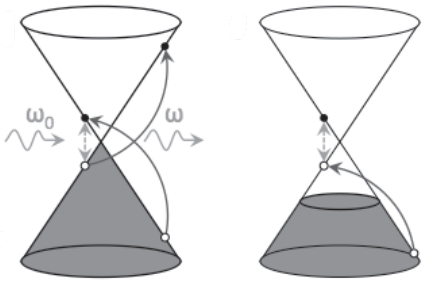

Figure. Scheme of G phonon renormalization at localized plasmon excitation under electrochemical potential control.

[1] R. Zhou *et al*. *ACS Omega,* **3**, 2322 (2018).
[2] S. Yasuda *et al*. *ACS Appl. Mater. Interfaces*, **9**, 38992 (2017).

Acknowledgements: This paper is resubmission as in the 55th FNTG symposium. The presentation was canceled due to the problem caused by Hokkaido earthquake on Sep . 6, 2018. All of the authors deeply appreciate very kind help and encouragement from the member of FNTG.

Corresponding Author: MURAKOSHI Kei
Tel: +81-(0)11-706-2704, Fax: +81-(0)11-706-4810,
Web: http://wwwchem.sci.hokudai.ac.jp/pc/
E-mail: kei@sci.hokudai.ac.jp

In-situ monitoring of monolayer WS_2 growth

○Tomoya Kameyama[1], Chao Li[1], Toshiro Kaneko[1], Toshiaki Kato[1, 2]

[1]*Graduate School of Engineering, Tohoku University, Sendai 980-8579, Japan*
[2] *JST-PRESTO*

Two dimensional (2D) materials have attracted intense attentions since they were discovered because of the ultrathin thickness, high mechanical flexibility, and topical optoelectronic properties [1, 2]. Nevertheless, graphene is difficult to be applied as practical applications for semiconductor devices due to its non-bandgap structure. Transition metal dichalcogenide (TMD) is known as another kind of 2D materials, which possess thin thickness as similar as graphene. TMD is expected to be applied on practical semiconductor devices because it has tunable bandgap structure by controlling layer number and kinds of elements consisting TMD. Furthermore, bright photoluminescence of TMD makes it promising candidate as critical materials for next generation optoelectrical applications such as flexible transparent solar cells [3]. To fabricate the high performance optoelectrical devices, it is greatly important to synthesize single crystal, monolayer, and large scale TMD [4]. Unfortunately, the uncertain growth mechanism of TMD makes it difficult to realize them.

In this study, to reveal the growth mechanism of monolayer WS_2 (kind of TMD), in-situ monitoring system has been developed, which can directly observe the time evolution of monolayer WS_2 growth (Fig. 1). The plot of crystal size as a function of growth time can be well-fitted by theoretical formula known as a growth equation. Through this fitting analysis, the important physical factors such as incubation time, growth rate, lifetime, and saturated crystal size can be obtained. It is found that the highest growth rate of monolayer TMD can be reached up to 15 μm/s, which is about ten times higher than that of multi-layer TMD. The effects of process parameters such as substrate temperatures and flow of carrier gas on those growth parameters are also investigated.

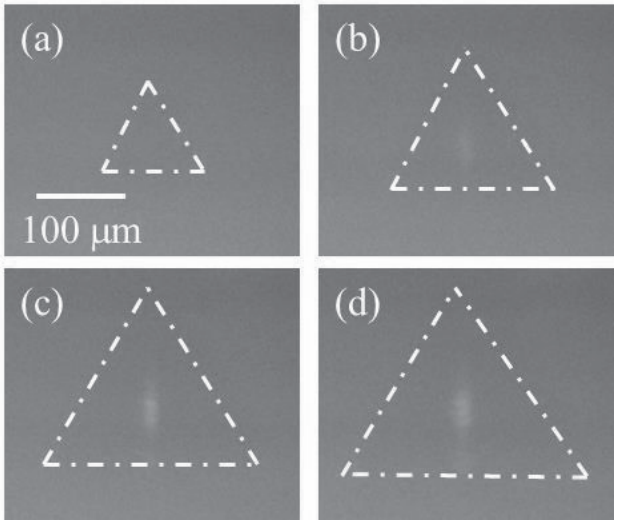

Fig. 1 Optical microscope images of monolayer WS_2 obtained by in-situ monitoring for growth time at (a) 20 s, (b) 50 s, (c) 80 s, and (d) 120 s.

[1] T. Kato and T. Kaneko: ACS Nano **8** (2014) 12777.
[2] T. Kato and T. Kaneko: ACS Nano **10** (2016) 9687.
[3] T. Akama, W. Okita, R. Nagai, C. Li, T. Kaneko, and T. Kato: Scientific Reports **7** (2017) 11967.
[4] C. Li, Y. Yamaguchi, T. Kaneko, and T. Kato: Applied Physics Express **10** (2017) 075201.

Corresponding Author: T. Kameyama
Tel: +81-22-795-7046, Fax: +81-22-263-9225,
http://www.plasma.ecei.tohoku.ac.jp/
E-mail: tomoya.kameyama.r1@dc.tohoku.ac.jp

Growth of pentagonal and diamond shaped h-BN crystals

○ Kamal P Sharma[1,2], Yuta Niimi[1], Aliza K. Sharma[1], Takahiro Maruyama[1,2]

[1] *Department of Applied Chemistry, Meijo University, Nagoya 468-8502, Japan*

[2] *Nanomaterials Research Center, Meijo University, Nagoya 468-8502, Japan*

Hexagonal boron nitride (h-BN), a structural analogue of graphene, is a wide band gap 2D insulating layered material, consisting of alternating sp^2–boned boron and nitrogen atoms [1]. It shows appealing properties such as thermally stable in air up to 800ºC, chemical inertness, stable thermal conductivity and superior elastic properties, and hence has drawn the significant attention as a promising material in frontier applications [2]. Although chemical vapor deposition (CVD) technique has developed as the most scalable process to synthesize h-BN on various transition metals, due to the complexity in growth mechanism, single domain h-BN is still limited to few micro meter scale [3, 4]. In this research, we study the growth kinetics of h-BN via morphological transition of triangular shaped into various polygonal shaped crystals.

For h-BN crystals synthesis, bare Cu foils were loaded into the horizontal growth furnace and heated at 26 ºC/min from room temperature to 1050 ºC with 100 sccm Ar. After annealing the Cu foil for 30 min with 100 sccm H_2 (Method-A) or 100sccm Ar (Method-B), ammonia borate (AB) was evaporated with 100:2 mixtures of Ar and H_2. 2 mg of AB was heated for various growth interval and are termed as Method- A_A, B_A, B_B, B_C, and B_D and the growth furnace was rapidly cooled down to room temperature within 30 min. As synthesized h-BN crystals were analyzed by optical microscopy (OM), Raman spectroscopy, FESEM, XPS, AFM.

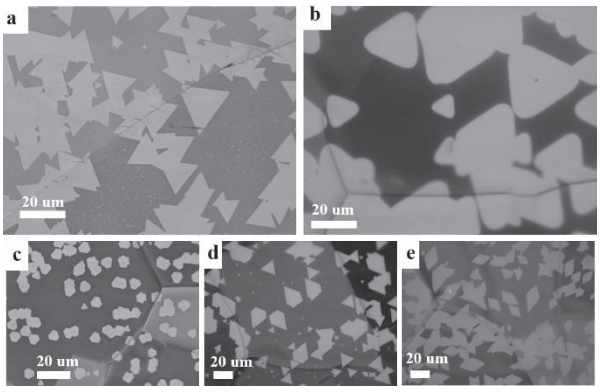

Fig. 1. OM images of h-BN crystals (white contrasted triangular structures) synthesized by (a) Method-A_A, (b) Method-B_A for 100 min, (c) Method-B_B, (d) Method-B_C, and (e) Method-B_D.

Regular triangular shaped h-BN crystals (Figure 1(a)) grown in Method-A_A changed into truncated triangles (Figure 1(b)) obtained in Method-B_A, it should be noted that only annealing of Cu in Ar was changed compared to former one. On decreasing the heating rate of AB, hexagonal, pentagonal and diamond shaped h-BN crystals were synthesized with elapsed growth time (Figure 1(c-e)) on decreasing the heating temperature of AB.

This work was supported in part by Private University Research Branding Project from the Ministry of Education, Culture, Sports, Science and Technology (MEXT), Japan.

[1] Kim, K. K. et al., Nano Lett., 12, 161 (2012).
[2] Sun, J. et al., Chem. Soc. Rev. 47, 4242 (2018).
[3] Tay, R. Y. et al. Nanoscale 8, 2434 (2016).
[4] Sharma, K.P. et al., CrysEngComm. 20, 550 (2018).

Corresponding Author: Takahiro Maruyama
Email:takamaru@maijo-u.ac.jp

Carrier accumulation in bilayer MoS_2 under a perpendicular electric field

○Mina Maruyama, Susumu Okada

Graduate School of Pure and Applied Sciences, University of Tsukuba, Tsukuba 305-8571, Japan

Transition metal dichalcogenides (TMDCs) are possible forms of atomic layer materials, which consist of an atomic layer of transition metals and those of chalcogens, resulting in the hexagonal network with the thickness of about 0.3 nm. The most of them are known to be semiconductors, so that they are regarded as the emerging materials of thin and flexible semiconducting devices. Because of their atomic layer structures, TMDCs can form van der Waals (vdW) heterostructures which exhibit interesting variations in their electronic structures depending on the electronic band structures of constituent layers. Accordingly, asymmetric carrier accumulation occurs in the vdW heterostructure of MoS_2 and WS_2 [1]. In the present work, we aim to investigate carrier accumulation in a bilayer MoS_2 under the perpendicular electric field for providing theoretical insight into the bilayer TMDC field-effect transistor (FET) with dual gate electrodes. All calculations are conducted using the density functional theory with the effective screening medium method. The bilayer MoS_2 is sandwiched by top and bottom gate electrodes simulated by effective screening medium.

Our calculation shows that the bilayer MoS_2 exhibits asymmetric carrier accumulation under the perpendicular electric field. Figure 1(a) shows charge density of the bilayer MoS_2 under the electric field of 1 V/nm without excess carriers. The perpendicular field induces polarization around the bottommost and the topmost atomic layers of the bilayer MoS_2. Then, by injecting the electron 10^{13} e/cm^2, the electron is primarily accommodated in the bottom layer of MoS_2 facing to the bottom gate electrode, while the hole is induced in the top layer, resulting in p-n junction between the layers, owing to the band offset between layers caused by the field [Fig. 1(b)]. With increasing the electron density up to 10^{14} e/cm^2, electron is injected into both layers of MoS_2 [Fig. 1(c)].

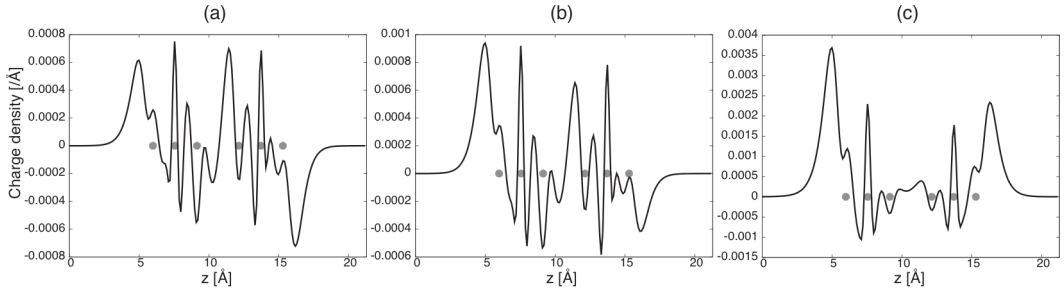

Figure 1: Accumulated carrier distribution in bilayer MoS_2 under the field of 1 V/nm with excess electron density of (a) 0, (b) 10^{13}, and (c) 10^{14} e/cm^2. Gray points denote the atomic position of MoS_2.

[1] M. Maruyama and S. Okada, Appl. Phys. Express, **12,** 075008 (2019).

Corresponding Author: M. Maruyama
Tel: +81-29-853-5921, Fax: +81-29-853-5924
E-mail: mmaruyama@comas.frsc.tsukuba.ac.jp

Room-Temperature Valley-Polarized Light-Emitting Devices *via* Strained Monolayer Semiconductors

○Jiang Pu[1], Hirofumi Matsuoka[1], Tomoyuki Yamada[1], Yu Koayashi[2], Yuhei Takaguchi[2]
Yasumitsu Miyata[2], and Taishi Takenobu[1]

[1] *Department of Applied Physics, Nagoya Univ., Nagoya 464-8603, Japan*
[2] *Department of Physics, Tokyo Metropolitan Univ., Tokyo 192-0397, Japan*

The valley contrasted electronic structure in monolayer transition metal dichalcogenides (TMDCs) provides unique optical functionalities, such us anomalous Hall effects and circularly polarized light emission [1]. In particular, the electrical control of circularly polarized light emission is one of the most desired device applications toward opto-valleytronics. Although several experimental demonstrations of chiral light-emitting devices have been reported, they have mostly realized at low temperatures and/or required high magnetic fields [2,3]. Therefore, the light-emitting devices that can control valley-polarized electroluminescence (EL) at room temperature are significant challenge. Interestingly, we recently found out that the local strains implanted inside CVD-grown TMDC monolayers might serve as a key role to generate circular polarized EL nearly room temperature. Moreover, the recent paper revealed the strain induced valley magnetizations in MoS_2, and that magnetization effects also obtained at room temperature [4]. On the basis of these observations, here, we try to realize the room-temperature valley-polarized light-emitting devices by combining electrolyte-based structures with strained monolayers.

The monolayer WS_2 and WSe_2 flakes were grown on sapphire substrate *via* CVD process, followed by transferring them onto PEN substrates using solution-based transfer process. After that, two Au electrodes were deposited on monolayer flakes, and then, the ion gels which are gelation of ionic liquids were spin-coated to construct two-terminal light-emitting structure (Fig 1a) [5]. The devices were set on the home-built bending stage with polarization-resolved optical set-up. Figs 1b and 1c show the PL mapping of channel regions with flat (Fig. 1b) and strained condition (Fig. 1c). We can notice obvious red-shifts were occurred in the strained devices, corresponding to 1 % uniaxial strain induced in monolayer flake. In the strained condition, we applied AC voltage to the devices to integrate EL intensity, and the chirality of EL (σ^+ and σ^-) was selectively detected by controlling quarter-wave plate (Fig. 1d). We observed EL polarizations ($P = [\sigma^+ - \sigma^-]/[\sigma^+ + \sigma^-]$) up to 20 % at room temperature. Importantly, we can also switch EL polarizations ($P \sim$ -6 %) through by inversing the current direction (Fig. 1d). These results demonstrated the electrical generation and control of room-temperature valley-polarized EL mediated by strains, offering a new way for achieving practical chiral light sources based on monolayer TMDCs.

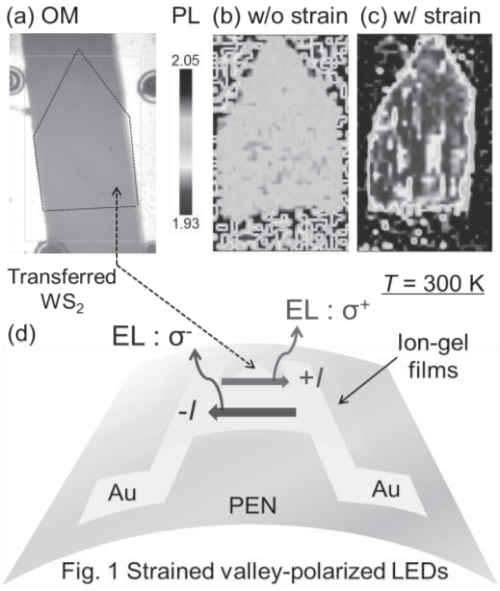

Fig. 1 Strained valley-polarized LEDs

[1] X. Xu, *et al*. *Nat. Phys.* **10**, 343 (2014)
[2] Y. J. Zhang, *et al*. *Science* **344**, 725 (2014)
[3] Y. Ye, *et al*. *Nat. Nanotechnol.* **11**, 598 (2016)
[4] J. Lee, *et al*. *Nat. Mater.* **16**, 887 (2017)
[5] J. Pu and T. Takenobu *Adv. Mater.* **30**, 1707627 (2018)
Corresponding Author: J. Pu, T. Takenobu
E-mail: jiang.pu@ngoya-u.jp, takenobu@nagoya-u.jp
Tel/Fax: +81-52-789-5165

Interface dependent photoresponsivity in graphene/GaN heterojunction

○Ajinkya K. Ranade[1]*, Rakesh Mahyavanshi[1], Pradeep Desai[1], Masaki Tanemura[1], Golap Kalita[1,2]*

[1]Department of Physical Science and Engineering, Nagoya Institute of Technology, Gokiso-cho, Showa-ku, Nagoya 466-8555, Japan.

[2]Frontier Research Institute for Material Science, Nagoya Institute of Technology, Nagoya, Japan

Two-dimensional (2D) graphene has been integrated with group III-nitride compound semiconductors notably gallium nitride (GaN), which is a wide band gap semiconductor (3.4 eV) to form a Schottky junction. Here, we report on the interface dependent photoresponsivity in graphene/GaN heterojunction. Graphene synthesized by low pressure chemical vapor deposition technique was transferred onto n-type GaN substrate by wet transfer procedure. The fabricated graphene/GaN heterojunction showed electrical hysteresis in dark condition which was enhanced in UV light illumination. A second device fabricated with much cleaner transferred graphene which was free from electrical hysteresis in no illumination condition (dark), showed hysteresis with the illumination of ultraviolet (UV) light. Moreover, the photoresponsivity of 1.4 A/W was obtained for this device which is much higher than other reported values for graphene/GaN heterojunctions. The residual impurities at the interface of junction and surface defects of GaN act as trap sites for photocarriers as a result interface dependent photoresponsivity is observed. Our findings can be significant in understanding the highly sensitive graphene/GaN and other 2D/3D heterojunction interfaces by characterization under UV illumination for developing high performance devices.

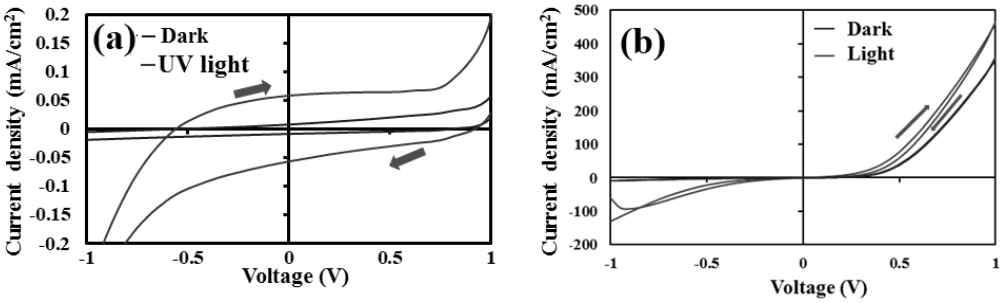

Figure 1. J-V characteristics (a) device with residual impurities showing electrical hysteresis in both dark conditions and UV illumination. (b) device showing electrical hysteresis only under UV light illumination.

[1] G. Kalita, M. D. Shaarin, B. Paudel, R. Mahyavanshi, M. Tanemura, Appl. Phys. Lett. 2017, 111, 013504.

Corresponding Author: Ajinkya K. Ranade, Golap Kalita
Tel: +81-527355216
E-mail: ajinkyaranade3@gmail.com , kalita.golap@nitech.ac.jp

Construction and solid-state dynamics of molecular bearings composed of finite carbon nanotube host and guest rotors

○Taisuke Matsuno[1], Yusuke Nakai[2], Yutaka Maniwa[2], Masahiro Fujita[3], Kengo Fukunaga[1], Sota Sato[1], Hiroyuki Isobe[1]

[1] *Department of Chemistry, The University of Tokyo and JST ERATO, Tokyo 113-0033, Japan*
[2] *Department of Physics, Tokyo Metropolitan University, Tokyo 980-8578, Japan*
[3] *Department of Chemistry, Tohoku University, Aoba-ku, Sendai 980-8577, Japan*

Dynamics of molecules in solid holds promise for connecting molecular behaviors with properties of bulk materials. However, controlling molecular motions in solid is challenging task due to the presence of severe friction between neighboring molecules. Recently, we have synthesized a chemically defined finite carbon nanotube, [4]cyclochrysenylene ([4]CC, Figure 1) [1], and found that [4]CC serves as a host for guest rotors to construct "molecular bearing", which is characterized by a set of contradictory properties: a tight binding and free rotation of rotors. In this study, we have constructed and revealed the dynamics of two molecular bearings (Figure 1). One is the "ball-in-tube" bearing possessing ball-shaped rotor C_{60}. The solid-state rotational dynamics of C_{60} in [4]CC was analyzed by solid-state ^{13}C NMR. Surprisingly, the rotation reaches the inertial regime at 335 K [2]. The second is "bowl-in-tube" bearing possessing a bowl-shaped rotor, corannulene (COR) [3]. ^{2}H NMR analysis revealed the fast single-axis rotation of the bowl-shaped rotors in solid. These unique dynamic supramolecular systems provided new design principles of the solid-state molecular machineries with smooth curved-π interfaces.

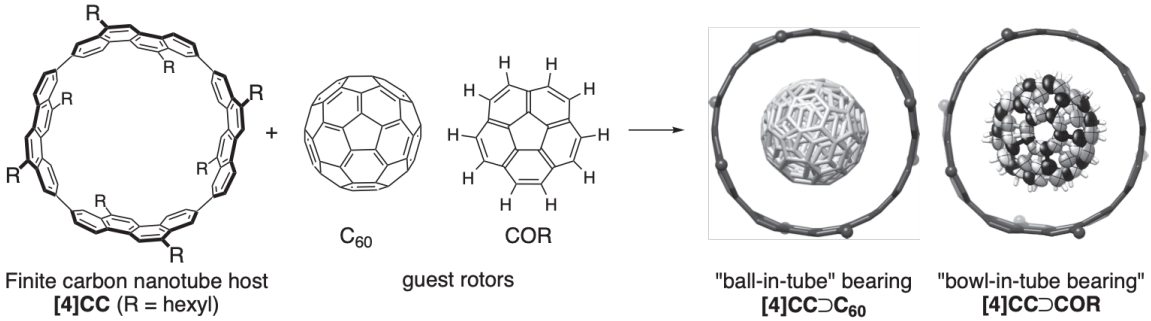

Fig 1. Construction of supramolecular hydrocarbon bearings [4]CC⊃C_{60} and [4]CC⊃COR.

[1] S. Hitosugi, W. Nakanishi, T. Yamasaki, H. Isobe, Nat. Commun. 2011, 2, 492.
[2] T, Matsuno, Y. Nakai, S. Sato, Y. Maniwa, H. Isobe, *Nat Commun.* **2018**, *9*, 1907.
[3] T. Matsuno, M. Fujita, K. Fukunaga, S. Sato, H. Isobe, *Nat. Commun.* **2018**, *9*, 3779.

Corresponding Author: H. Isobe
Tel: +81-(0)3-5481-4777, Fax: +81-(0)3-5841-4162
Web: http://www.chem.s.u-tokyo.ac.jp/users/physorg/
E-mail: isobe@chem.s.u-tokyo.ac.jp

Controlled Redox of Lithium-ion Endohedral Fullerene on Carbon Nanotubes for Efficient and Stable Metal-free Perovskite Solar Cells

○Il Jeon[1], Ahmed Shawky[1], Hiroshi Okada[1], Esko I. Kauppinen[2], Shigeo Maruyama[1,3], Yutaka Matsuo[1,4]

[1] *Department of Mechanical Engineering, The University of Tokyo, Tokyo 113-8656, Japan*
[2] *Department of Applied Physics, Aalto University School of Science*
[3] *Research Institute for Energy Conservation, AIST, Tsukuba 305-8565, Japan*
[4] *Institutes of Innovation for Future Society, Nagoya University, Nagoya 464-8603, Japan*

Perovskite solar cells (PSCs) have become an established photovoltaic technology owing to the exceptional power conversion efficiency (PCE). However, the low device stability poses a great challenge. There are two factors responsible for the low stability of PSCs: Li^+TFSI^- and metal electrodes. Use of hygroscopic Li^+TFSI^- in spiro-MeOTAD hole-transporting layer (HTL) results in an uncontrolled oxidation of spiro-MeOTAD as well as moisture-driven degradation. In the same vein, metal electrodes induce a metal ion-migration, which degrades the perovskite material, lowering the device stability.

We previously reported the use of lithium-ion containing [60]fullerene trifluoromethanesulfonylimide salt ($[Li^+@C_{60}]TFSI^-$) instead of Li^+TFSI^- in PSCs.[1] $[Li^+@C_{60}]TFSI^-$ induced an instant oxidation of spiro-MeOTAD and produced neutral $[Li^+@C_{60}]^{\bullet-}$ (= $Li@C_{60}$), which functioned as an antioxidant, protecting the device from intruding oxygen. With the instant generation of spiro-MeOTAD$^{\bullet+}TFSI^-$ and the anti-oxidation activity of $Li^+@C_{60}^{\bullet-}$, the stability of PSCs improved by 10-fold. However, the reported PCEs were relatively low due to the small amount of spiro-MeOTAD$^{\bullet+}TFSI^-$ and rough morphology of HTLs, caused by the low solubility of the endohedral fullerene species.

Replacing metal electrodes by carbon nanotubes has been reported to be one of the most effective ways to improve the PSC stability.[2] This is because the carbon electrodes prevent metal-ion migration and induce an encapsulation effect.

Combining those two technologies and controlling the redox reaction of $[Li^+@C_{60}]TFSI^-$ offer an outstanding synergic solution to the instability and low efficiency of PSCs. Because HTLs are typically spin-coated onto the CNT network in CNT-laminated PSCs, the CNT electrode functioned as a filter when the mixture of spiro-MeOTAD and $[Li^+@C_{60}]TFSI^-$ was applied, causing the undissolved $[Li^+@C_{60}]TFSI^-$ and $Li@C_{60}$ suspensions to stay on top of CNTs. This led to a more effective hole extraction by avoiding $[Li^+@C_{60}]TFSI^-$ aggregations in the charge pathways and an enhanced anti-oxidation activity by exposing $Li@C_{60}$ antioxidants to air. This meant that the reaction time control of the spiro-MeOTAD and $[Li^+@C_{60}]TFSI^-$ solution before the application to the CNT electrode was crucial. We found that a continuous stirring of the solution led to an increase in the spiro-MeOTAD$^{\bullet+}TFSI^-$ amount but a decrease in the $Li@C_{60}$ amount. 2 h of stirring time of the mixture gave the best PCE and device stability, as it produced the optimal amount of spiro-MeOTAD$^{\bullet+}TFSI^-$ and $Li@C_{60}$, which correspond to an initial PCE and anti-oxidation capability, respectively.

[1] I. Jeon *et al.* Angew. Chem. Int. Ed. **57**, 1 (2018). [2] I. Jeon *et al.* Adv. Energy Mater. **9**, 1801312 (2018).

Corresponding Author: Y. Matsuo
E-mail: matsuo@photon.t.u-tokyo.ac.jp

Observation and Spectral Assignment of Family of Hexagonal Boron Nitride Lattice Defects

○Daichi Kozawa[1], Ananth Govind Rajan[1], Jamie H. Warner[2], Daniel Blankschtein[1], Michael S. Strano[1]

[1] *Department of Chemical Engineering, Massachusetts Institute of Technology, Cambridge, Massachusetts 02139, United States*
[2] *Department of Materials, University of Oxford, Parks Road, Oxford, OX1 3PH, United Kingdom*

Atomic vacancy defects in single unit cell thick hexagonal boron nitride (Fig. 1) are of significant interest because of their photophysical properties, including single-photon emission, and promising applications in quantum communication and computation. The spectroscopic assignment of emission energies to specific atomic vacancies within the triangular lattice is confounded by the exponential scaling of defect candidates with the number of removed atoms. Herein, we collect more than 1000 spectra consisting of single, isolated zero-phonon lines between 1.69 and 2.25 eV, observing 6 quantized zero-phonon lines arising from hexagonal boron nitride vacancies. A newly developed computational framework for isomer cataloguing significantly narrows the number of candidate vacancies [1]. Direct lattice imaging of hexagonal boron nitride, electronic structure calculations, and subsequent boric acid etching are used to definitively assign the 6 features [2]. Systematic chemical etching supports the assignment by demonstrating the growth of larger from smaller vacancy centers, which include a single B vacancy and a 16-atom triangular defect. These features exhibit a range of emission lifetimes from 1 to 6 ns, and phonon sidebands offset by the dominant lattice phonon in hexagonal boron nitride near 1370 cm^{-1}. This assignment should significantly advance the solid-state chemistry and photophysics of such vacancy emitters.

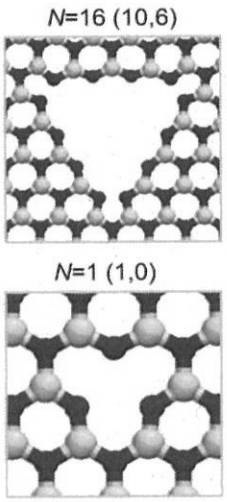

Fig. 1. Representative vacancy centers of hexagonal boron nitride, exhibiting visible to near IR single photon emission.

[1] A. Rajan *et al.* Nat. Mater, **18**, 129 (2019)
[2] D. Kozawa *et al.* Under Review (2019)

Corresponding Author: D. Kozawa
Tel: +81-48-462-1449
Web: http://orcid.org/0000-0002-0629-5589
E-mail: daichi.kozawa@riken.jp

Designing two-dimensional tetradymites with 20% thermoelectric efficiency

○ Nguyen T. Hung[1], Ahmad R. T. Nugraha[2], Riichiro Saito[2]

[1]*Frontier Research Institute for Interdisciplinary Sciences, Tohoku University, Sendai 980-8578, Japan*

[2]*Department of Physics, Tohoku University, Sendai 980-8578, Japan*

Thermoelectric (TE) research has been significantly activated during the past two decades by the quantum confinement effect, a characteristic of low-dimensional (1D & 2D) materials, thanks to the pioneering work by Hicks and Dresselhaus [1]. In particular, for two-dimensional (2D) material, the TE efficiency is enhanced only when the thickness of the material is smaller than the thermal de Broglie wavelength [2]. Monolayer semiconductors naturally satisfy such a condition so that they are a good candidate for thermoelectricity. However, the TE efficiency still smaller than 10% (or figure-of-merit ZT ~ 1), which needs to be improved for industrial applications. In this work, we theoretically investigate thermoelectric efficiency of the 2D tetradymites M_2X_3 (M=Bi, Sb; X=Te, Se, S). By using the density functional theory (DFT) to calculate transport properties with considering both electron-phonon and phonon-phonon interactions, we find that the nonparabolic Kane bands and large anharmonicity could lead to better thermoelectric performance of the 2D tetradymites [3]. Moreover, we show that ZT of 2D Bi_2Te_2Se can up to 2 at 500K, which is higher than that of bulk tetradymites [4]. In other words, we can archive the TE efficiency up to 20% in 2D tetradymites at near room temperature.

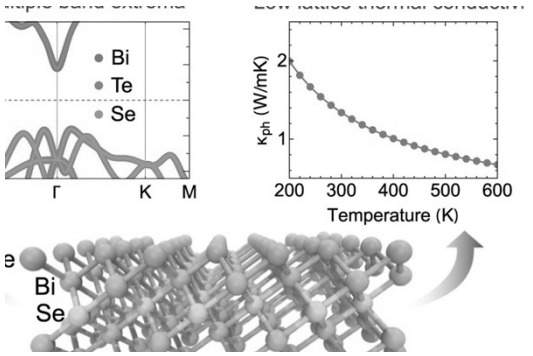

Figure 1: Two-dimensional tetradymites (Bi_2Te_2Se) with ZT = 2 at 500K.

[1] L. D. Hicks and M. S. Dresselhaus, Phys. Rev. B 47, 12727 and 16631(R) (1993).

[2] N. T. Hung et al., Phys. Rev. Lett. 117, 036602 (2016).

[3] N. T. Hung et al., Nano Energy 58, 743 (2019).

[4] J. P. Heremans et al., Nature Rev. Mater. 2, 17049 (2017).

Corresponding Author: Nguyen Tuan Hung
Tel: +81-22-795-6442, Fax: +81-22-795-6447, E-mail: nguyen@flex.phys.tohoku.ac.jp

Electronic Orbitals and Spin-Polarization at Graphene Edge Revealed by Field Emission and Field Ion Microscopy

○Yahachi Saito[1], Yuhdai Watanabe[2], Tohru Hoshino[2], Hitoshi Nakahara[2], Shigekazu Nagai[3], Hiromu Ikemizu[3], Kazuya Kunoh[3], Koichi Hata [3]

[1] Toyota Physical and Chemical Research Institute, Nagakute 480-1192, Japan
[2] Department of Applied Physics, Nagoya University, Nagoya 464-8603, Japan
[3] Department of Electrical & Electronic Engineering, Mie University, Tsu 514-8507, Japan

Electronic states at graphene edges exhibit peculiar properties, e.g., spin polarization at zigzag edge [1]. Field emission microscopy (FEM) of open graphene edges shows a striped pattern ("lip pattern"), reflecting the symmetry of π orbitals at a graphene edge [2]. Field ion microscopy (FIM), complementary to FEM, shows unoccupied π orbitals with higher spatial resolution. We also tried to measure spin-polarization of field-emitted electrons and obtained for the first time an evidence of the spin polarized states at edge of graphene.

Typical FEM and FIM images of a graphene emitter are shown in Figs. 1 (a) and (b), respectively. The FEM image (Fig. 1 (a)) exhibits a "lip pattern" characteristic to a graphene edge; an array of streaked double spots. The corresponding FIM image (Fig. 1 (b)), taken using Ne as imaging gas, reveals more detailed structures because of higher spatial resolution. Arrays of paired spots, being split on both side of a graphene plane, are observed as indicated by arrows. Based on our previous studies on FIM of carbon emitters [3], the spacing between adjacent streaks in FIM is presumed to correspond with interatomic distances at the graphene edge. Double spots are considered to be formed by Ne atoms ionized in proximate to an unoccupied π*-orbital at the edge.

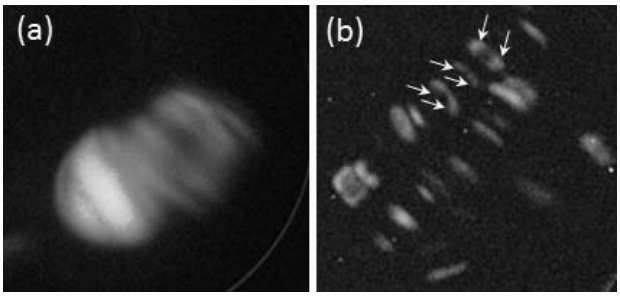

Fig. 1. (a) FEM and (b) FIM images of graphene.

Spin polarization measurements of field-emitted from graphene edges were measured by the Mott spin polarization analyzer [4]. The magnitude of spin polarization of 20 to 60%, depending on graphene emitters was obtained. The present result is the first demonstration of spin polarization of electrons at graphene edges by using field emission method. Abrupt changes in the spin polarization as a function of time, as shown in Fig. 2, may result from the adsorption of residual gas such as hydrogen in the UHV chamber.

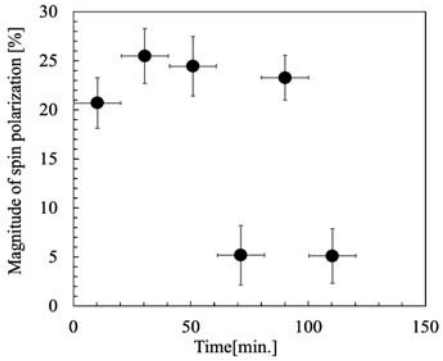

Fig.2. Spin polarizaton of field-emtted electrons from a graphene edge.

[1] M. Fujita, K. Wakabayashi, K. Nakada and K. Kusakabe, J. Phys. Soc. Jpn. **65** (1996) 1920. [2] N. Yokoyama et al., Surf. Interface Anal. **48** (2016) 1217. [3] Y. Saito, R. Mizushima and K. Hata, Surface Sci. Lett. **499**, (2002) L119. [4] S. Nagai, H. Sakakibara, K. Hata, M. Okada and H. Mimura, Ultramicroscopy **111** (2011) 405.

Corresponding Author: Y. Saito
Tel: +81- 561-57-9616, Fax: +81- 561-63-6302, E-mail: ysaito@toyotariken.jp

On-surface synthesis of conjugated polycyclic nanowires by copolymerization strategy

○Hironobu Hayashi, Hiroko Yamada

Division of Materials Science, Nara Institute of Science and Technology (NAIST), 8916-5, Takayama-cho, Ikoma, Nara 630-0192, Japan

Polycyclic aromatic hydrocarbons such as large acenes have gained great attention due to their potential as good building blocks for organic semiconductors. So far, by using a precursor method[1] and on-surface synthesis under ultrahigh vacuum (UHV) conditions, we have successfully synthesized heptacene and nonacene on Au(111) to provide experimental insight into the chemical and electronic structure.[2] In addition, we also reported the on-surface formation of heptacene organometallic complexes on Au(111) via a selective two-step activation of an α-diketone-type heptacene precursor.[3] However, due to the steric hindrance between the hydrogen atoms, further annealing did not give rise to aryl-aryl coupling between heptacene. Here, we have demonstrated a strategy for the aryl-aryl coupling of molecular building blocks unable to undergo homocoupling into extended architectures. Briefly, a copolymerization approach using suitable linkers allowed the on-surface synthesis of covalently linked chains with alternating building blocks, which were converted into fully conjugated polycyclic nanowires by further annealing (Figure 1).[4]

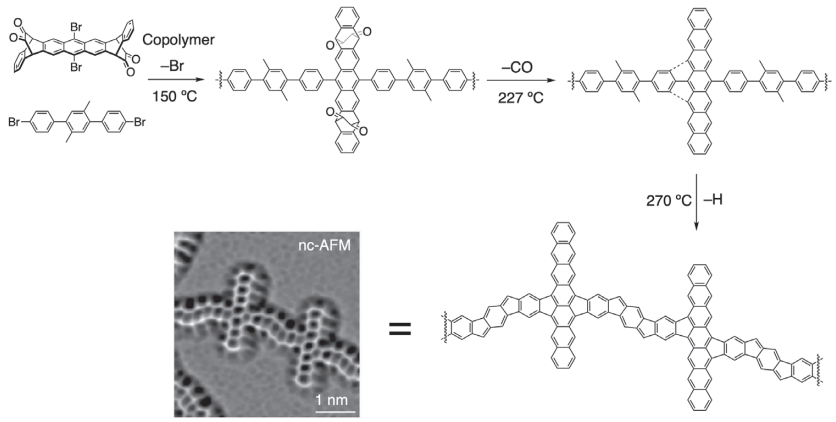

Figure 1. Reaction pathway of copolymerization and laplace-filtered constant-height frequency-shift nc-AFM image of an acene fused conjugated polycyclic nanowire. Acknowledgement: Dr. Urgel, J. I. and Prof. Fasel, R.@Empa.

[1] Yamada, H.; Yamashita, Y.; Kikuchi, M.; Watanabe, H.; Okujima, T.; Uno, H.; Ogawa, T.; Ohara, K.; Ono, N. *Chem.–Eur. J.* **2005***, 11,* 6212.

[2] Urgel, J. I.; Mishra, S.; Hayashi, H.; Wilhelm, J.; Pignedoli, C. A.; Giovannantonio, M. D.; Widmer, R.; Yamashita, M.; Hieda, N.; Ruffieux, P.; Yamada, H.; Fasel, R. *Nat. Commun.* **2019**, *10*, 861.

[3] Urgel, J. I.; Hayashi, H.; Giovannantonio, M. D.; Pignedoli, C. A.; Mishra, S.; Deniz, O.; Yamashita, M.; Dienel, T.; Ruffieux, P.; Yamada, H.; Roman, F. *J. Am. Chem. Soc.* **2017**, *139*, 11658.

[4] Giovannantonio, M. D.; Urgel, J. I.; Gandus, G.; Chen, Q.; Liu, X.; Hayashi, H.; Ruffieux, P.; Decurtins, S.; Narita, A.; Passerone, D.; Yamada, H.; Liu, S.; Müllen, K.; Pignedoli, C. A.; Fasel, R. *ChemPhysChem* **2019**, in press.

Corresponding Author: H. Hayashi
Tel: +81-743-72-6136, Fax: +81-743-72-6042,
Web: https://mswebs.naist.jp/LABs/env_photo_greenmat/
E-mail: hhayashi@ms.naist.jp

In Situ TEM study of catalytic property of Mo during graphene formation

°Subash Sharma, Golap Kalita, Masaki Tanemura
Department of Physical Science and Engineering, Nagoya Institute of Tech., Nagoya 464-8555, Japan

Graphene has been a topic of keen research interest due to its excellent electrical and material properties [1]. Cu and Ni are commonly used substrate for synthesis of high quality graphene. Among different metals, catalytic role of Mo during graphene formation is least studied. In this work, we study Joule heat induced graphene formation inside transmission electron microscope (TEM) with real time observation Mo-C interaction and change in electrical property during graphitization.

Mo included amorphous carbon nano-fiber (Mo-CNF) was used as starting material. Mo-CNF was fabricated using our previously reported method [2]. Bias voltage was applied to the tip of Mo-CNF. During application of voltage, joule heat comes in to play causing melting of embedded Mo and its voltage driven electromigration. During electromigration of Mo, amorphous CNF changes to graphitic form as shown in Figure 1(a-h). Figure 1(i-k) show that as synthesized graphene is crystalline with no presence of amorphous carbon. Simultaneous electrical measurement taken during transformation of CNF to graphene shows sudden increase in current during electromigration indicating graphene formation as shown in Figure 1(l). In summary, we demonstrated that Mo can act as an efficient catalyst for graphene synthesis and can be explored for large area graphene synthesis.

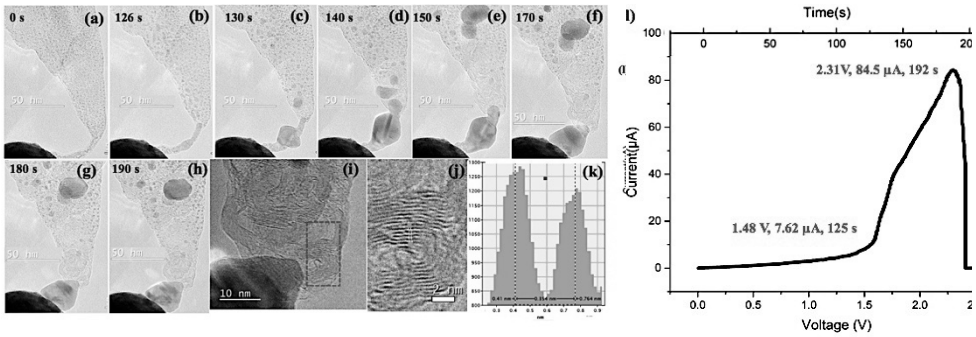

Figure 1. (a-k) Screenshots taken from in-situ TEM video showing transformation Mo-CNF to graphene under application of bias voltage at different time interval. (l) Corresponding IV curve showing change in electrical property of Mo-CNF during electromigration and graphitization of Mo-CNF.

[1] Novoselov et al. Science 306, no. 5696 (2004): 666-669.
[2] Sharma et al. Carbon 132 (2018): 165-171.

Corresponding Author: S. Sharma
Tel: +81-52-735-5379, Fax: +81-52-735-5379,
Web: http://tane-lab.web.nitech.ac.jp
E-mail: sharma.subash@nitech.ac.jp

Isomer effects of fullerene derivative acceptors on organic photovoltaic devices

○Tomokazu Umeyama[1], Hiroshi Imahori[1,2]

[1] *Department of Molecular Engineering, Graduate School of Engineering, Kyoto University, Kyoto 615-8510, Japan*
[2] *Institute for Integrated Cell-Material Sciences (WPI-iCeMS), Kyoto University, Kyoto 606-8501, Japan*

In recent years, [70]fullerene derivatives are preferentially employed in organic photovoltaic (OPV) devices compared with [60]fullerene derivatives. However, an important aspect of C_{70} derivatives, which is usually overlooked in photovoltaic applications, is that as-prepared C_{70} mono-adducts consist of regioisomers due to the lower symmetry of rugby-ball shaped C_{70} over spherical C_{60}. As contrasted with C_{60}, C_{70} has four distinct types of [6,6]-bonds (α-, β-, ε-, and κ-type bonds), and thereby [70]fullerene derivatives including [70]PCBM have been used as a regioisomer mixture in OPV devices.

In this study, by using a high-performance liquid chromatography (HPLC) suitable for the separation of fullerenes, we separated as-purchased [70]PCBM (denoted as mix-[70]PCBM) into isomerically pure ones and investigated the isomer separation effects on the photovoltaic properties (Figure 1) [1]. For instance, in combination with a high-performance conjugated polymer donor (PffBT4T-2OD), one of the diastereomers of the β-isomer (β_1-[70]PCBM) showed an extraordinary cohesion nature in the blend film, deteriorating the OPV device performance (0.4%). OPV devices based on the other isomers, i.e. α-[70]PCBM (8.4%) and β_2-[70]PCBM (8.4%), rival or slightly surpass the device with the as-synthesized isomer mixture (mix-[70]PCBM, 8.2%).

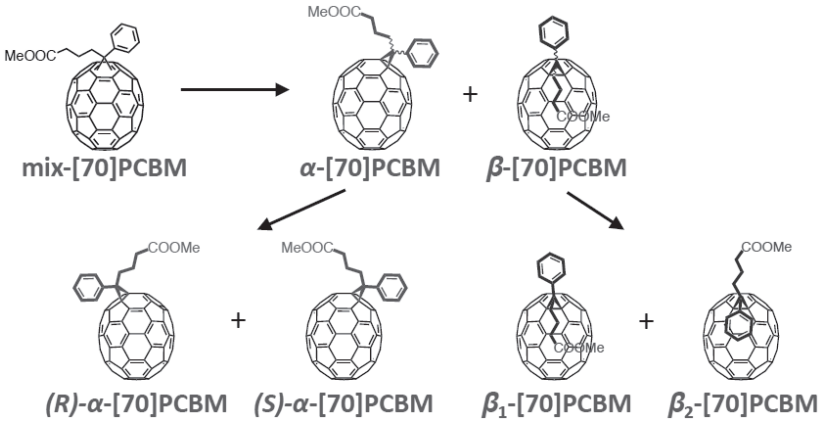

Figure 1. Isomer separations of [70]PCBM.

[1] *a*) Umeyama, T.; Imahori, H. *Acc. Chem. Res.* in press; *b*) Umeyama, T.; Miyata, T.; Jakowetz, A. C.; Shibata, S.; Kurotobi, K.; Higashino, T.; Koganezawa, T.; Tsujimoto, M.; Gelinas, S.; Matsuda, W.; Seki, S.; Friend, R. H.; Imahori, H. *Chem. Sci.* **2017**, *8*, 181; *c*) Umeyama, T.; Shibata, S.; Miyata, T.; Igarashi, K.; Koganezawa, T.; Imahori, H. *RSC Adv.* **2017**, *7*, 45967; *d*) Umeyama, T.; Shibata, S.; Igarashi, K.; Takahara, S.; Higashino, T.; Seki, S.; Imahori, H. *Chem. Lett.* **2017**, *46*, 1001; *e*) Umeyama, T.; Igarashi, K.; Sakamaki, D.; Seki, S.; Imahori, H. *Chem. Commun.* **2018**, *54*, 405.

Corresponding Author: T. Umeyama
Tel: +81-75-383-2568, Fax: +81-75-383-2571
Web: http://www.moleng.kyoto-u.ac.jp/~moleng_05/umeyama_e.html
E-mail: umeyama@scl.kyoto-u.ac.jp

Synthetic Usefulness and Device Application Studies of Cationic Fullerenes

○Yutaka Matsuo[1,2,3]

[1] *Institutes of Innovation for Future Society, Nagoya University, Nagoya 464-8603, Japan*
[2] *Department of Mechanical Engineering, The University of Tokyo, Tokyo 113-8656, Japan*
[3] *University of Science and Technology of China, Hefei 230026, China*

Normally, fullerene and fullerene derivatives have electron affinity to accept electrons. This is because of electrophilic surface of fullerenes derived from convex exterior shape giving lowered electron density in molecular orbital at the fullerenes surface. This nature makes fullerene anions stable after receiving electrons. Many fullerene functionalization reactions and electronic application researches have been developed and performed based on this electrophilic property. For example, synthesis of PCBM, Prato reactions, Bingel-Hirsch reactions, Grignard reagents addition, and so on take place starting from nucleophilic additions to fullerenes. Application studies of fullerenes as electron acceptors and electron transporting layers in organic thin-film solar cells and perovskite solar cells are also based on electron affinity of fullerenes.

On the other hand, removal of electrons from fullerenes, which provides cationic fullerenes, gives unique reactivity in fullerene modifications[1-3] and special ability in organic thin-film device applications.[4] An alternative method is inclusion of lithium ion into the fullerene cage to make it cationic (Figure 1). Obtained fullerene cation showed unique reactivity to produce new fullerene derivatives which are unavailable in conventional methods using anionic fullerene key intermediates. These unique reactivities are derived from much lower-lying LUMO levels of cationic fullerenes compared with neutral or anionic fullerenes after removal of electron or addition of positive charge. In other words, cationic fullerenes are more strongly electrophilic than neutral/anionic fullerenes, reacting with weak nucleophiles with high reaction rate and abstracting electron from electron rich compounds. These characters represent frontier of synthetic fullerene chemistry and create new organic electronic devices.

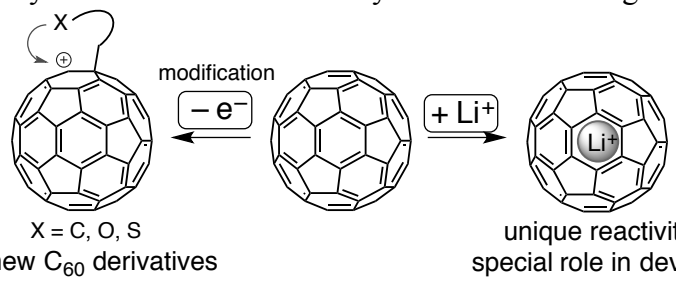

Figure 1. Formation of cationic fullerenes by removal of electrons and inclusion of lithium ion.

[1] H.-S. Lin, Y. Matsuo, *Chem. Commun.* **2018**, *54*, 11244–11259. (Feature article)
[2] Y. Matsuo, Y. Yu, X.-Y. Yang, H. Ueno, H. Okada, H. Shibuya, Y. S. Choi, Y. W. Jin, *J. Org. Chem.* **2019**, *84*, 6270–6277.
[3] H. Okada, H. Ueno, Y. Takabayashi, T. Nakagawa, M. Vrankić, J. Arvanitidis, T. Kusamoto, K. Prassides, Y. Matsuo, *Carbon* **2019**, *153*, 467–471.
[4] I. Jeon, H. Ueno, S. Seo, K. Aitola, R. Nishikubo, A. Saeki, H. Okada, G. Boschloo, S. Maruyama, Y. Matsuo, *Angew. Chem. Int. Ed.* **2018**, *57*, 4607–4611.

Corresponding Author: Y. Matsuo
Tel: +81-52-747-6722; Web: http://www.matsuo-lab.net; E-mail: yutaka.matsuo@chem.material.nagoya-u.ac.jp

Self-Assembled Peptides as a Molecular Scaffold on CVD Grown Monolayer MoS_2 Transistor towards Biosensing

○Hironaga Noguchi[1], Yuhei Hayamizu[1]

[1] *School of Materials and Chemical Technology Department of Materials Science and Engineering Tokyo Institute of Technology, 2-12-1 Ookayama, meguroku, Tokyo, Japan*

2D materials such as graphene have been investigated to be applied for biosensors due to their excellent electrical properties and high specific surface area. More recently, MoS_2 field-effect transistor (FET) has exhibited higher sensitivity than graphene FET due to its semiconducting nature [1]. There are some reported methods of probe immobilization on MoS_2 FET such as using dielectric layer and immobilizing via covalent bonds [1,2]. However these methods lead to decrease sensitivity and disturb intrinsic electrical properties. So we focus on self-assembled peptides to overcome these problems. These peptides on the surface of 2D materials form uniform and ordered structures arise from self-assembly with non-covalent integrations. These peptides are expected as a molecular scaffold for immobilizing probe molecules without degrading the electrical properties. Since the operation of the biosensor is carried out under wet condition, behavior of MoS_2 FET in solution is important. However, the response of MoS_2 FET to the absorbed peptides has not been reported yet. In this work, we observed the influence of the self-assembled peptides in buffer solution on the electrical characteristics of MoS_2 FET. We also immobilize bio-probe using self-assembled peptides to demonstrate target biomolecule through co-assembly process.

Y5Y (YGAGAGAGAGAY) peptide inspired by fibroin form uniform and oriented structure and can maintain ordered nanostructures even after rinsing with DI water [3]. In this work, we designed RY5, EY5, and QY5, in which positively charged arginine, negatively charged glutamic acid, and neutral glutamine were introduced at both ends of Y5Y. For the measurement, the source-drain current with respect to the gate voltage was measured with a platinum reference electrode in 10 mM phosphate buffer. After the formation of the peptide self-assembled structures, measurements were carried out in the same manner. The morphology of the self-assembled peptides on MoS_2 surface was also measured by Atomic force microscopy (AFM). We chose streptavidin (SA) as a detection molecule because specific interaction between biotin and SA is widely used to demonstrate biomolecule detection.

As results, we found that these three peptides form uniform and ordered structures on MoS_2 surface by AFM measurement. In the conductivity measurements, MoS_2-FET shows no shift of threshold voltage after forming peptide self-assembled structure on the surface and also no change in the transistor mobility. This result suggests that our peptides may be useful as a molecular scaffold for MoS_2 biosensor

[1] Sarkar, D.*et al. ACS Nano*, 2014, *8*(4), 3992-4003.

[2] Naylor, C. *et al. ACS Nano*, 2016, *10*(6), 6173-6179.

[3]Li, P. *et al. ACS Appl. Mater. Interfaces*, 2019, *11*, 20670–20677.

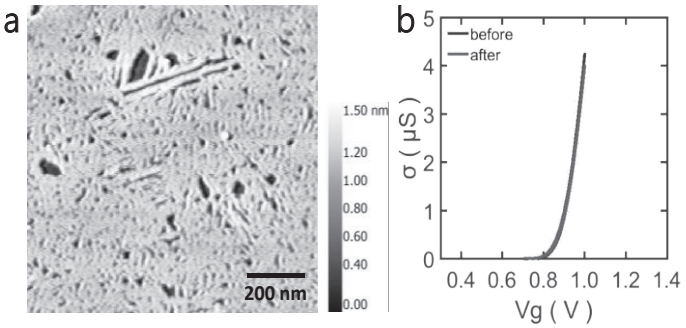

Figure1 (a) AFM image of self-assembled peptide structure on the MoS_2 surface. (b) Source-Drain conductivity *vs* applied Gate voltage of MoS_2-FET before and after the incubation of peptides.

High-resolution Measurement on Graphene Quantum Dots

○Toshiki Sugai, Fumiaki Uchiyama, Yuya Ooishi, Takanori Nakayasu, and Ryo Sasaki

Department of Chemistry, Toho University, Miyama 2-2-1 Funabashi, 274-8510, Japan

Ion mobility spectrometry (IMS) has revealed novel information on nano materials[1]. However, its resolution is low, which limit its role to a simple filter for mass spectrometry. To improve the resolution, IMS systems with trap functions have been developed by mainly extend the drift length of the system[2]. We also have been developing the ion trap ion mobility measurement system focusing on long cyclic and successive measurement on the same single nano particles. Even with trap functions, usual IMS systems are dedicated for mass spectrometry, which makes the cyclic measurement impossible. Here we present high-resolution measurement on graphene quantum dots (GQD) with successive measurements by an improved ion trap ion mobility system.

The system consists of several electrodes with a hole at the center, where an alternative current with high and low frequency were applied. Ionized GQD by laser desorption ionization by a YAG laser were trapped for around an hour and were moved reciprocally by 30 mm in nitrogen gas at ambient pressure. The distance was increased by an order of magnitude from that of the previous system of 3 mm.

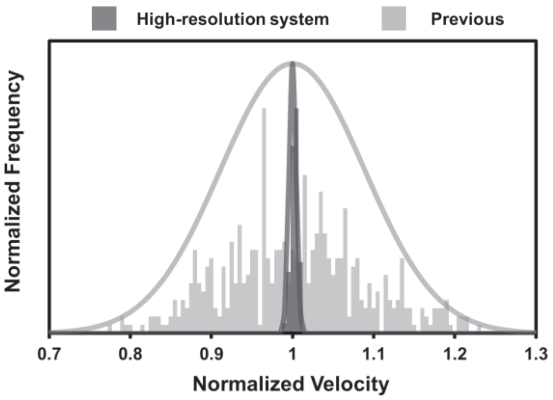

Fig. 1 Observed velocity distributions of GQD with the current and the previous system

Fig. 1 shows observed normalized mobility distribution of one particle of ionized GQD by the previous low-resolution and the present high-resolution systems. The resolution is enhanced from 5 of the previous system to 100 of the new system. Cyclic and successive measurement on a single GQD make it easy to evaluate the resolution precisely.

We will show other improvements on simultaneous measurement on optical response or charge together with mobility measurement for a single GQD molecule.

[1] T. Sugai *et al.*, *J. Am. Chem. Soc.* ***123***, 6427 (2001).

[2] F. Fernandez-Lima *et al.*, *J. Ion Mobil. Spec.* ***14***, 93 (2011)

TEL: +81-47-472-4406, E-mail: sugai@chem.sci.toho-u.ac.jp

A three-dimensional covalent network of fused pentagons: A hard carbon allotrope with negative Poisson's ratio

Y. Fujii[1], M. Maruyama[1], N. T. Cuong[1], and S. Okada[1]

[1]*Graduate School of Pure and Applied Sciences, University of Tsukuba, 1-1-1 Tennodai, Tsukuba, Ibaraki305-8571, Japan*

Carbon allotropes show interesting structural variations owing to three possible orbital hybridizations of constituent C atom. Carbon allotropes consisting of both sp^2 and sp^3 C atoms have been attracting much attention, because of their morphological diversity caused by the number of sp^2 and sp^3 C atoms and their mutual arrangements in networks. High-pressure and high-temperature treated C_{60} fullerenes are representative examples of such allotropes, being expected to the hard carbon allotropes with low mass density. The rapid quenching of amorphous carbon causes the sp^2 and sp^3 hybrid C allotrope, known as Q carbon, which has been reported to possess magnetism and remarkable hardness exceeding diamond. Recently, bottom-up synthesis technique realizes the novel carbon allotropes with significant mechanical and electronic properties.

In this work, we theoretically explore a three-dimensional carbon allotrope (pentadiamond) obtained by co-polymerization of spiro[4.4]nona-2,7-diene and [5.5.5.5]fenestratetraene, as a possible candidate for hard carbon allotropes with unusual mechanical properties (Fig. 1). Using the density functional theory with the generalized gradient approximation, we found that the pentadiamond has the high bulk modulus of 383 GPa and negative Poisson's ratio of -0.198 leading to the remarkable mechanical toughness against anisotropic structural deformations.

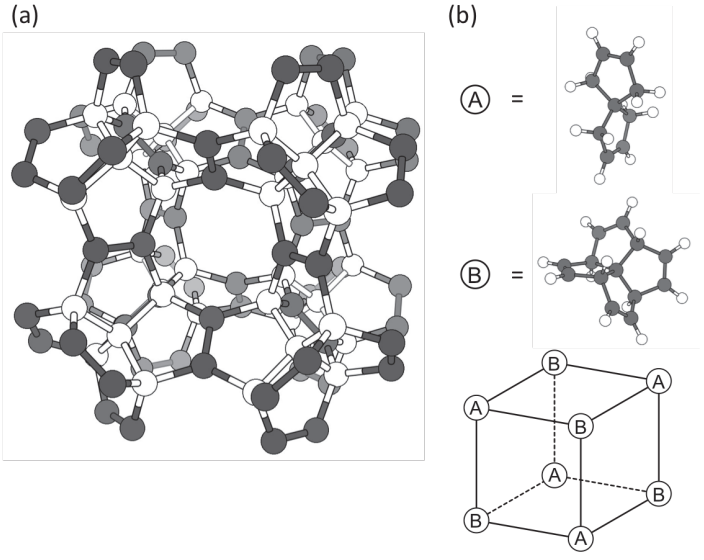

Fig. 1 (a) Optimized structures of pentadiamond. Gray and white spheres denote sp^2 and sp^3 C atoms, respectively. (b) Consistent units of pentadiamond, where A and B indicate spiro[4.4]nona-2,7-diene and [5.5.5.5]fenestratetraene, respectively. Gray and white spheres denote C and H atoms, respectively.

Corresponding author: Y. Fujii
(yfujii@comas.frsc.tsukuba.ac.jp)

Edge plasmon in graphene ribbon

M. Shoufie Ukhtary, Maruoka Masato, and Riichiro Saito
Department of Physics, Tohoku University, Sendai 980-8578, Japan

Surface plasmon is an oscillation of charge density that propagates as an electromagnetic (EM) wave on a surface. Surface plasmon has been an interesting platform to confine and control the light in sub-wavelength scale, since the EM fields of surface plasmon is spatially localized near the surface. In particular, we can control surface plasmon, since the charge density of graphene can be controlled by using gate voltage. As far as we consider graphene as an infinite two-dimensional (2D) material, the whole charges in graphene oscillates collectively, which forms a truly 2D plasmon. However, if we consider the region in the vicinity of edge, there will be an accumulation of charges near the edge. This accumulation of charges can also oscillate collectively and form so-called the edge plasmon with the EM fields localized near the edge [1]. The edge plasmon is a distinct mode from the 2D plasmon, since the frequency of edge plasmon is always lower than of the 2D plasmon and the EM fields is localized near the edge, not uniform across the surface [2].

In this work, we discuss the edge plasmon in graphene ribbon with a finite width by solving the electric potential analytically using the Lorentz gauge [3]. We show that the frequency of edge plasmon depends on the width and the Fermi energy of graphene. More importantly, we find that the electric field of edge plasmon on the surface of graphene rotates near the edge as a function of time. The reason of the rotation is that the localization of the induced electric fields near the edge induces phase difference between the electric fields in the direction parallel and perpendicular to the edge. In contrast to the out-of-plane rotation of electric field for 2D plasmon [4], the rotation of electric field is in-plane and the rotation direction (clockwise or anti-clockwise) depends on the direction of wavevector of the edge plasmon. As a result, the rotating electric field on the surface of graphene also induces rotating current, which generates scattered EM wave with elliptical polarization.

[1] A. L. Fetter. *PRB* **33**, 3717 (1986).

[2] J. Song et al. *PNAS* **113**, 4658 (2016)

[3] M. S. Ukhtary et al. in Preparation

[4] K. Y. Bliokh et al. *New J. Phys.* **19** 123014 (2017)

Electronic structure of hexagonal covalent networks with structural imperfections: Flat band engineering by atomic substitution and doping

Susumu Okada, Mina Maruyama, Tomonari Mizoguchi, and Yasuhiro Hatsugai

Graduate School of Pure and Applied Sciences, University of Tsukuba, Tsukuba 305-8571, Japan

Electronic structure of graphene is sensitive to structural imperfections introduced in honeycomb covalent networks. By imposing an open boundary condition, which is regarded as the line imperfection, with zigzag shapes, peculiar edge localized states emerges at the Fermi level and around the zone boundary known to be edge state. Atomic defects causes non-boding states at the Fermi level corresponding with the number of sublattice imbalance. In this work, we focus on graphitic network with monovacancies which are densely arranged in triangular manner (a Bishamon-kikko pattern: Fig. 1), and elucidate their electronic structure in terms of the on-site energy difference between two sublattices. Using the density functional theory and the tight-binding analysis, we found that the electronic structure of the network is highly modulated by introducing the on-site energy difference between two sublattices: the network without on-site energy difference has a Dirac cone and a flat band at the Fermi level, while the network with on-site energy difference possesses a Dirac cone and the kagome band around the Fermi level (Fig. 2). By analyzing the tight-binding Hamiltonian, the peculiar electronic structure is ascribed to the second-neighbor hopping, which form hexagonal and kagome networks for white and gray circles in Fig. 1, respectively, as the perturbation to the unperturbed Hamiltonian associated with the on-site energy. Compounds, C_2N_3, C_5N, C_5B, and C_6F, are possible materials those exhibit unusual electronic structures.

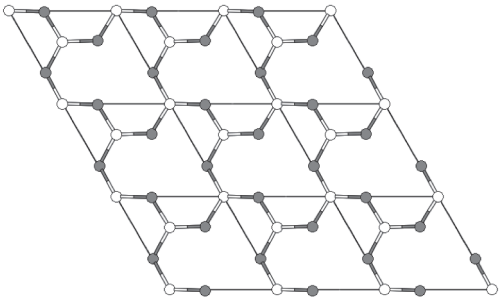

Figure 1: Geometric structure of a graphitic covalent network with monovacancies. Gray and white circles denote A and B sublattices, respectively.

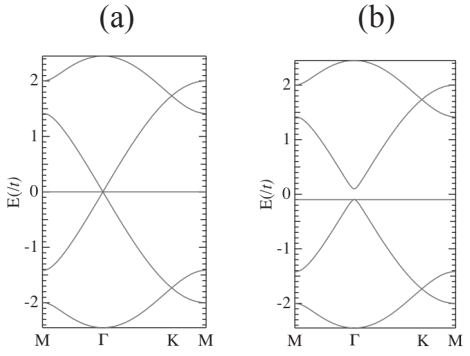

Figure 2: Electronic structures of graphitic network with monovacancies (a) without and (b) with onsite energy difference.

Corresponding Author: S. Okada
Tel: +81-29-8535921
E-mail: sokada@comas.frsc.tsukuba.ac.jp

Observation of third-harmonic generation in single-layer graphene using Maker fringe method

○Daiki Inukai[1], Takeshi Koyama[1], Kenji Kawahara[2], Hiroki Ago[2], and Hideo Kishida[1]

[1] *Department of Applied Physics, Nagoya University, Nagoya, Aichi 464-8603, Japan*
[2] *Global Innovation Center, Kyushu University, Kasuga, Fukuoka 816-8580, Japan*

Single-layer graphene shows distinctive optical responses which reflect the two dimensional honeycomb structure [1]. Single-layer graphene is expected to show strong nonlinear optical responses [2]. Single-layer graphene is desired to be utilized in optoelectronic applications such as optical switches and ultrafast optical detectors. Recently, there are several reports about third-harmonic generation (THG) in graphene [3,4]. The reported values of the third-order nonlinear optical susceptibility $\chi^{(3)}$ spread to more than six orders of magnitude [5]. Furthermore, the generation process was not elucidated until now.

In this research, we focus on THG in single-layer graphene and aim at the elucidation of the generation process on the basis of the magnitude of the third-order nonlinear susceptibility $\chi^{(3)}$ and its phase. In this experiment, we used a regenerative amplifier seeded by a mode-locked Ti-sapphire laser (1 kHz, 800 nm). The wavelength of the pulse laser is converted to be 2200 nm (idler beam) by an optical parametric amplifier (~150 fs). Single-layer graphene was transferred onto a SiO_2 substrate. THG was observed to use Maker fringe (MF) method. The intensity of third harmonic light was measured with change of optical length of the incident laser beam by rotating sample (Fig. 1). We compared the MF patterns of the graphene/SiO_2 sample with that of the SiO_2 substrate. As a result, we obtained the magnitude of the third-order nonlinear susceptibility $\chi^{(3)}$ of the graphene and its phase. The results of the analysis and the electronic process governing THG process in single-layer graphene will be discussed.

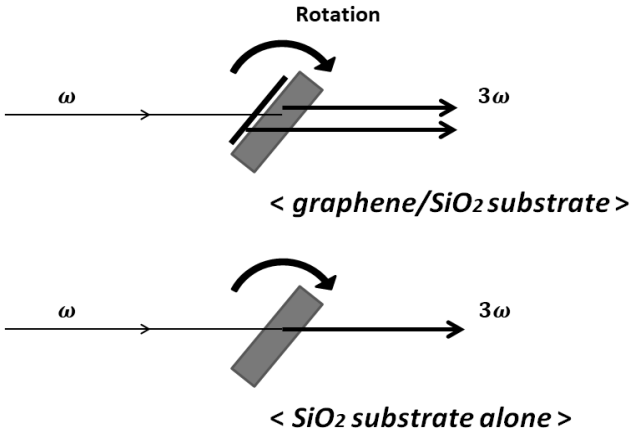

Fig. 1. Maker fringe method.

[1] F. Bonaccorso *et al*., Nat. Photonics **4**, 611-622 (2010).
[2] M. M. Glazov and S. D. Ganichev, Phys. Rep. **535**, 101-138 (2014).
[3] N. Kumar *et al*., Phys. Rev. B **87**, 121406 (2013).
[4] S.-Y. Hong *et al*., Phys. Rev. X **3**, 021014 (2013).
[5] T. Jiang *et al*., Nat. Photonics **12**, 430-436 (2018).

Corresponding Author: H. Kishida
Web: http://www.op.ap.pse.nagoya-u.ac.jp/
E-mail: kishida@nagoya-u.jp

Design and control of band gap of functionalized single-walled carbon nanotube quantum dots

○Yui Konno,[1] Yutaka Maeda[1], Kiyonori Kuroda[1], Haruto Tambo[1], Hiyori Murakoshi,[1] Michio Yamada,[1] Pei Zhao,[2] Xiang Zhao,[3] Shigeru Nagase,[4] Masahiro Ehara[2]

[1]Department of Chemistry, Tokyo Gakugei University, Tokyo 184-8501, Japan
[2]Research Center for Computational Science, Institute for Molecular Science, Okazaki, 444-8585, Japan
[3]Institute for Chemical Physics, Department of Chemistry, School of Science, State Key Laboratory of Electrical Insulation and Power Equipment, Xi'an Jiaotong University, Xi'an 710049, China
[4]Fukui Institute for Fundamental Chemistry (FIFC), Kyoto University, Kyoto 606-8103, Japan

Recently, it has been reported that the chemical functionalization of SWNTs, such as photooxidation and arylation, induces bright and red-shifted NIR PL peaks [1,2,3]. Wang et al. reported the observation of new PL peaks in the range of 1110–1148 nm from arylated (6,5) SWNTs depending on the substituents of the phenyl group [2]. A good correlation was found between this emission wavelength and Hammett's constant, which revealed that the electronic effect of the substituent is one of the factors in emission wavelength control. Recently, we have reported that dialkylation of (6,5) SWNTs using butyllithium and butyl bromide and their subsequent thermal treatment resulted in emergence of new strong PL peaks at around 1220 nm [4]. Additionally, (6,5) SWNTs functionalized using 1,2-bis(bromomethyl) benzene predominantly resulted in emergence of a PL peak at 1231 nm [5]. These results indicate that controlling the addition patterns of addenda are another factor that controls the emission wavelength. The contribution of the addition site carbons on the difunctionalized SWNTs has been confirmed theoretically [6]. In this work, we focus on bulkiness of addenda and local strain at the addition cites as another factor controlling the emission wavelength of functionalized SWNTs [7,8]. After functionalization using bromoalkanes, new red-shifted peaks were observed at ~1100 nm and/or ~1210 nm. The degree of functionalization of the SWNTs decreased with the increasing bulkiness of the reagents used. In addition, the PL efficiency was changed significantly with the increase of the bulkiness of reagents and PL peak at ~1100 nm was observed predominantly. On the other hand, after functionalization with dibromoalkanes, PL peaks were observed as a dominant peak in the range of 1215-1231 nm depending on the alkyl chain length of the dibromoalkane used. Density functional theory (DFT) and time-dependent DFT calculations of model compounds suggest that the bulkiness of the reagents and local strain induced by cycloaddition plays an important role in tuning the local band gap energies of functionalized SWNT quantum dots.

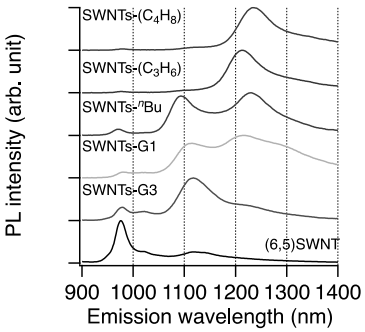

Fig.1 PL spectra of functionalized SWNTs.

[1] S. Ghosh *et al*. Science, **330**, 1656 (2010). [2] Y. Wang *et al*. Nat. Chem. **5**, 840 (2013). [3] Y. Maeda *et al*. J. Am. Chem. Soc., **135**, 6356 (2013). [4] Y. Maeda *et al*. Chem. Commun., **51**, 13462 (2015). [5] Y. Maeda *et al*. Nanoscale, **8**, 16916 (2016). [6] X. He *et al*. ACS Nano, **11**, 10785 (2017). [7] Y. Maeda *et al*. Nanoscale, **10**, 23012 (2018). [8] Y. Maeda *et al*. RSC Adv., **9**, 13998 (2019).

Corresponding Author: Y. Maeda Tel: +81-42-329-7512 E-mail: ymaeda@u-gakugei.ac.jp

Geometries and electronic properties of transition metal dichalcogenide nanotubes

○Shuntaro Oshima[1], Masayuki Toyoda[1], Susumu Saito[1, 2, 3]

[1] *Department of Physics, Tokyo Institute of Technology, Meguro, Tokyo 152-8551, Japan*
[2] *Advanced Research Center for Quantum Physics and Nanoscience, Tokyo Institute of Technology, Meguro, Tokyo 152-8551, Japan,*
[3] *Materials Research Center for Element Strategy, Tokyo Institute of Technology, Yokohama, Kanagawa 226-8503, Japan*

Group VI transition metal dichalcogenides (TMDs) are attracting growing attention. TMDs are composed of transition metal atoms (Mo, W, …) and chalcogen atoms (S, Se, …). Since monolayers of TMDs have direct energy gaps in the range of 1 to 2 eV, they are considered to be promising materials for optoelectronic devices. Because TMDs have high braking strength, the strain dependent electronic properties of TMDs have been vigorously studied.

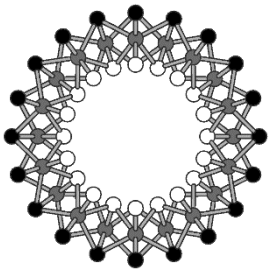

FIG. 1 Top view of (10,0) hybrid TMD nanotubes.

Recent development of experimental techniques has enabled us to synthesize single-walled TMD nanotubes [1], and hybrid TMD sheets containing two distinct chalcogens [2]. Because two chalcogen sides are asymmetric in hybrid TMD sheets, these mixed-chalcogen TMD layers prefer curved structures. Figure 1 illustrates the typical structures of these hybrid TMD nanotubes.

We study the geometries and the electronic properties of TMD nanotubes including these mixed-chalcogen TMD nanotubes under axial strains using local density approximation in the framework of density-functional theory (DFT). From the detailed analysis of the optimized geometries, we find a global strong correlation between fundamental gap values and some combined structural parameter (Fig. 2). This relationship will be useful to predict gap values in large TMD systems.

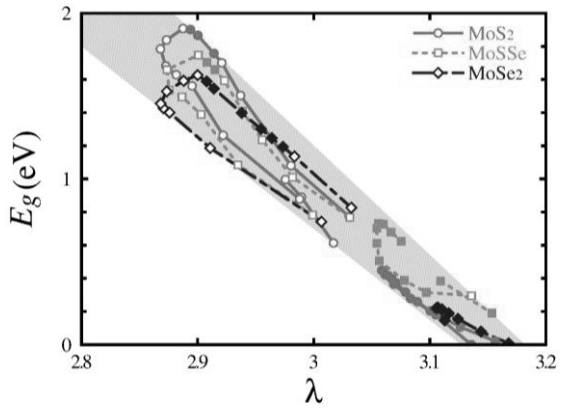

FIG. 2 Energy gap values of several TMD nanotubes and several TMD sheets versus geometrical parameter λ.

[1] R. Tenne and M. Redlich, Chem. Soc. Rev. **39**, 1423 (2010).
[2] A. Lu, H. Zhu, J. Xiao, C. Chuu, Y. Han, M. Chiu, C. Cheng, C. Yang, K. Wei, Y. Yang, Y. Wang, D. Sokaras, D. Nordlund, P. Yang, D. A. Muller, M. Chou, X. Zhang, and L. Li, Nature Nanotech. **12**, 744 (2017).

Corresponding Author: S. Oshima
Tel: +81-3-5734-2368, Fax: +81-3-5734-2739
E-mail: soshima@stat.phys.titech.ac.jp

Two-point modification for doped site creation of locally functionalized single-walled carbon nanotubes using bis-aryldiazonium salts

○Tomohiro Shiraki[1,2], Boda Yu[1], Yoshiaki Niidome[1], Tsuyohiko Fujigaya[1,2,3]

[1] *Department of Applied Chemistry, Kyushu University, Fukuoka 819-0395, Japan*
[2] *WPI-I2CNER, Kyushu University, Fukuoka 819-0395, Japan*
[3] *CMS, Kyushu University, Fukuoka 819-0395, Japan*

Photoluminescence (PL) of single-walled carbon nanotubes (SWNTs) appears in near infrared (NIR) regions, which is applicable to bioimaging and telecommunication devices. The NIR PL properties are governed by photogenerated excitons in the one-dimensional nanostructures. To enhance the contribution of the exctions to PL, defect doping to SWNTs by local chemical functionalization is gathering great attention. The locally functionalized SWNTs (lf-SWNTs) show additional PL (E_{11}*) with red-shifted wavelengths and enhanced quantum yields compared to original PL (E_{11}) of pristine SWNTs.[1-8] Therein, the doped sites work as emissive sites with narrower bandgaps and exciton trapping features. Interestingly, the functionalized molecules have been found to modulate PL of the lf-SWNTs. Here, we report two-point modification for longer wavelength NIR PL generation and its wavelength modulation based on molecular structures of the modifiers.

We synthesized bis-arydiazonium salts (bAs) that have two reactive aryldiazonium groups connected with a methylene linker. In order to achieve PL wavelength modulation, the linker effects were examined by changing the connected positons on the aryl groups (*p*bAs for para and *m*bAs for meta) and the length of methylene chains.[5,8]

For the local functionalization, SWNTs were solubilized in a micellar solution of sodium dodecyl sulfate (SDS), and then reacted with the synthesized bAs through diazonium chemistry. In PL spectra of the obtained lf-SWNTs (lf-SWNTs-*p*bA and lf-SWNTs-*m*bA), PL peaks appeared at 1245 nm and 1257 nm, respectively when the linker of five methylene units was used. Those were assigned to E_{11}^2* PL that were observed in longer wavelength regions than E_{11}* PL of mono-aryl functionalized lf-SWNTs (ca. 1140 nm). When the linker lengths of bAs were changed, the shorter linkers induced longer wavelength PL. Namely, the methylene chain length tunes the E_{11}^2* PL wavelengths. In addition, the lf-SWNTs-*m*bA showed larger spectral shifting behavior in the linker length-dependent E_{11}^2* wavelength compared to the lf-SWNTs-*p*bA.

Thus, the molecular design of the bis-aryldiazonoum modifiers achieves wavelength modulation of E_{11}^2* PL, which enables us to produce NIR PL nanomaterials with wider wavelength ranges of their emission.

[1] B. Weisman *et al.* Science, **330**, 1656 (2010). [2] Y. Miyauchi *et al.* Nat. Photon., **7**, 715 (2013). [3] Y. Wang *et al.* J. Am. Chem. Soc., **138**, 6878 (2016). [4] S. Doorn *et al.* Nat. Photon., **11**, 577 (2017). [5] T. Shiraki *et al.* Sci. Rep., **6**, 28393 (2016). [6] Y. Maeda *et al.* Nanoscale, **8**, 16916 (2016) [7] T. Shiraki *et al.* Chem. Commun., **53**, 12544 (2017). [8] T. Shiraki *et al.* Chem. Lett., **48**, 791 (2019).

Corresponding Author: T. Fujigaya
Tel: +81-92-802-2842, Fax: +81-92-802-2842
Web: http://www.chem.kyushu-u.ac.jp/~fifth/jp
E-mail: fujigaya.tsuyohiko.948@m.kyushu-u.ac.jp

ポスター発表
Poster Preview

1P – 1 ～ 1P – 30
2P – 1 ～ 2P – 29
3P – 1 ～ 3P – 30

Time-resolved photoluminescence spectroscopy of epitaxial bilayer graphene on SiC

○Kensuke Saito[1], Tomonari Koishi[1], Jianfeng Bao[2], Wataru Norimatsu[2], Michiko Kusunoki[3], Hideo Kishida[1], Takeshi Koyama[1]

[1] Department of Applied Physics, Nagoya University, Nagoya 464-8603, Japan
[2] Department of Chemical Systems Engineering, Nagoya University, Nagoya 464-8603, Japan
[3] Institute of Materials and Systems for Sustainability, Nagoya University, Nagoya 464-8603, Japan

Graphene has extremely high conductivity and unique optical properties, and many studies on device applications of graphene have been conducted until now [1]. In 2015, an article on thermal radiation of graphene was published [2]. For application of graphene in luminescence device, it is important to understand the origin of its luminescence. According to early studies on photoluminescence (PL) from monolayer graphene in the visible and infrared light regions [3-6], the origin of the PL from monolayer graphene is radiative recombination of free electron-hole pairs. For bilayer graphene, however, although infrared PL measurements were conducted [7], the origin of the PL from bilayer graphene has not been clarified.

Bilayer graphene has two advantages for application to luminescence device. Firstly, a bandgap can be induced by application of electric field for bilayer graphene [8], opening a possibility of control of excited-state relaxation. Secondly, bilayer graphene has more π-electrons related to optical transition than monolayer. In this study, we investigated the origin of the PL in epitaxial bilayer graphene by femtosecond time-resolved PL measurements.

The epitaxial bilayer graphene was prepared by thermal decomposition of 4H-SiC. The PL measurements were conducted based on the frequency up-conversion method. The light source was a mode-locked Ti:sapphire laser. The excitation photon energy and pulse duration were 1.55 eV and 90 fs, respectively. Figure 1 shows PL decay of the epitaxial bilayer graphene at a photon energy of 1.3 eV. The PL decay curve was analyzed by convolution method with a single-exponential function and an instrument response function (Gaussian shape with a full width at half-maximum of 130 fs). The obtained time constant is approximately 30 fs. We observed excitation density dependences of PL decay time and intensity. Based on the results, we discuss the origin of the PL from the bilayer graphene.

[1] K. S. Novoselov *et al*., Nature **490**, 192 (2012).
[2] Y. D. Kim *et al*., Nat. Nanotechnol. **10**, 676 (2015).
[3] C. H. Lui *et al*., Phys. Rev. Lett. **150**, 127404 (2010).
[4] W.-T. Liu *et al*., Phys. Rev. B **82**, 081408 (2010).
[5] T. Koyama *et al*., ACS Nano **7**, 2335 (2013).
[6] H. Imaeda *et al*., J. Phys. Chem. C **122**, 19273 (2018).
[7] H. Watanabe *et al*., Chem. Phys. Lett. **637**, 58 (2015).
[8] Y. Zhang *et al*., Nature **459**, 820 (2009).

Corresponding Author: T. Koyama
Tel: +81-52-789-4450, Fax: +81-52-789-4450,
E-mail: koyama@nuap.nagoya-u.ac.jp

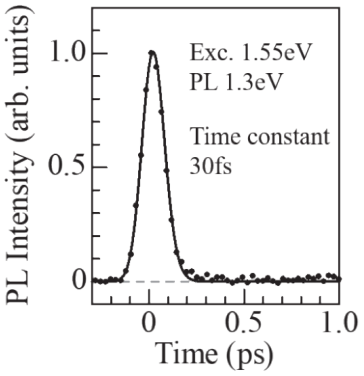

Fig. 1 Photoluminescence decay of epitaxial bilayer graphene on SiC at a photon energy of 1.3 eV.

Effects of CNT diameter on mechanical and electrical properties of aligned CNT/epoxy composites

○Yohei Tsuyuguchi, Kazuya Hosogi, Takayuki Nakano, Yoku Inoue

Department of Electronics and Materials Science, Shizuoka University, Hamamatsu 432-8561, Japan

Because of the high tensile properties of carbon nanotube (CNT), CNT/polymer composites have been studied as structural materials. We have been focusing on the mechanical and electrical properties of unidirectionally aligned multi-walled CNT /epoxy composite materials. In the CNT/resin composite, the outer layer is responsible for load and charge propagation, and the inner layer less contributes to it. Therefore, the larger the CNT diameter, the lower the mechanical and electrical properties in the composites. Thus, the dimension of CNT dramatically affects the features of the composite. In this work, we fabricated CNTs with different diameters and used them for composite materials. We evaluated its properties to understand the effects of CNT diameter on the mechanical and electrical properties of CNT/epoxy composites.

Spinnable MWCNT forests were synthesized by a chloride mediated chemical vapor deposition method and a floating catalyst CVD method. Then, CNT sheets were fabricated by stacking CNT webs drawn from the CNT forest. Then, CNT/epoxy composites were prepared by a hot melt method using the CNT sheet and an epoxy film. The volume fraction (V_f) of CNT in the composite was changed by changing the amount of CNT in composites. V_f was evaluated by thermogravimetric analysis. Tensile tests and electrical conductivity tests were performed to evaluate mechanical and electrical properties.

The average CNT diameters, used in this study, were 36.5 nm, 24.3 nm, 12.3 nm, and 8.3 nm. Figure1 shows the tensile strength of the composite as a function of V_f. With increasing V_f, tensile strength was monotonically increased. Comparing the tensile strength at V_f of 10 %, it increased from 80 MPa to 150 MPa with decreasing CNT diameter. Figure 2 shows the relationship between the electrical conductivity and V_f. As well as the tensile strength, the electrical conductivity was increased from 80 S/cm to 150 S/cm with decreasing CNT diameter among composites having V_f of 10 %. Through the tensile tests and electrical measurements, we found that composites, having CNT with smaller diameter, show higher tensile strength and electrical conductivity, and it is attributed to an increase in surface areas of CNT in composites resulting in effective propagation of load and charges.

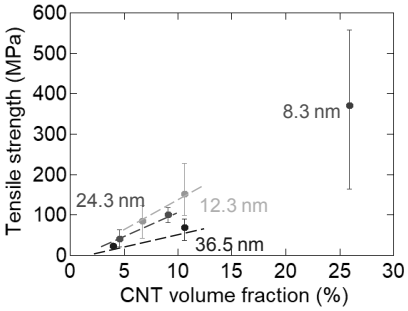

Fig.1 CNT diameter dependence of tensile strength

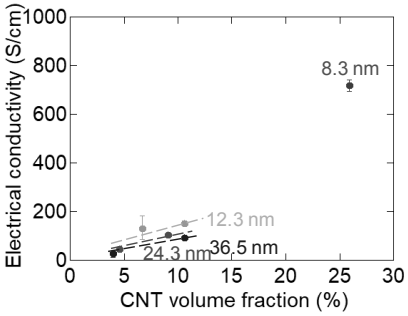

Fig.2 CNT diameter dependence of electrical conductivity

Corresponding Author: Yoku Inoue
Tel: +81-53-478-1356, Fax: +81-53-478-1356,
Web: http://cnt.eng.shizuoka.ac.jp/
E-mail: inoue.yoku@shizuoka.ac.jp

The effect of gas phase species on chirality selectivity between (6,4) and (6,5) single-walled carbon nanotubes

○Satoru Shiina[1], Takuya Shima[1], Bin Xu[1], Toshiro Kaneko[1], Toshiaki Kato[1,2]

[1] *Graduate School of Engineering, Tohoku University, Sendai 980-8579, Japan*
[2] *JST-PRESTO*

Single-walled carbon nanotubes (SWNTs) are promising candidate for high performance optoelectrical materials due to the unique 1-dimensional structure. Since physical properties of SWNTs strongly depend on the chirality, chirality selective synthesis is required for industrial application. In recent our study, (6,4) SWNTs has been grown with high purity (~57%) by controlling the oxidation degree of the Co catalyst surface [1]. To further increase the purity of (6,4) SWNTs, elucidation of the correlation between (6,4) SWNTs purity and plasma CVD conditions is an important subject.

Synthesis of SWNTs is carried out using a home-made diffusion type plasma CVD [2]. The gas phase species are directly monitored during plasma CVD synthesis by quadrupole mass analyzer (Q-mass). Gas phase condition is controlled by changing plasma generation power, gas pressure and power supply for plasma generation (CW or pulse). To elucidate the effects of gas phase species on chirality selectivity, correlations between these variations of gas phase conditions and purity of each chiralities are investigated.

Fig.1 is the plot of (6,4) SWNTs purity as a function of Δ16 and Δ26, which is the difference of Q-mass counts for specific mass (16 and 26) before and after plasma generation, respectively. Negative and positive value of Δ16 and Δ26 denotes the decomposition of CH_4 and generation of C_2H_2, respectively. As absolute value of Δ16 increases, (6,4) SWNTs purity increases (Fig. 1(a)). For Δ26, there is a suitable value to obtain the highest (6,4) SWNTs purity (Fig. 1(b)). (6,5) SWNTs purity has almost opposite tendency to that of (6,4) SWNTs. These indicate that the gas phase species strongly affect on the chirality selectivity between (6,4) and (6,5) SWNTs. This is the first result showing the direct contribution of gas phase precursors for the selective growth of specific chirality species.

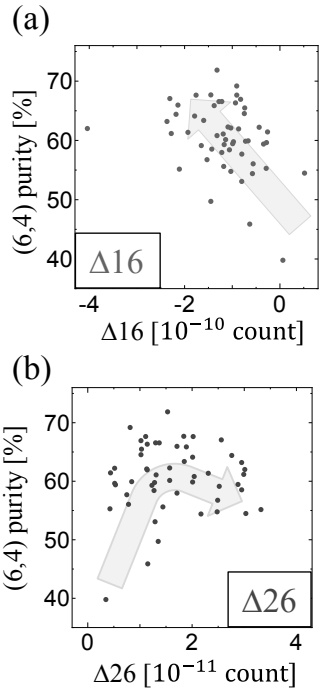

Fig.1 Purity of (6,4) SWNTs as a function of (a) Δ16 and (b) Δ26.

[1] B. Xu, T. Kaneko, Y. Shibuta and T. Kato: Sci. Rep. 7, 11149 (2017)

[2] T. Kato and R. Hatakeyama: Nat. Nanotechnol. 7, 651 (2012)

Corresponding Author: S. Shiina
Tel: +81-22-795-7046, Fax: +81-22-263-9225,
E-mail: satoru.shiina.s8@dc.tohoku.ac.jp

Wavelength modulation of near infrared photoluminescence from single-walled carbon nanotubes functionalized with diarylethene derivatives

○Yasuto Nakagawa[1], Tomohiro Shiraki[1,2], Tsuyohiko Fujigaya[1,2,3]

[1] *Department of Applied Chemistry, Kyushu University, Fukuoka 819-0395, Japan*
[2] *WPI-I²CNER, Kyushu University, Fukuoka 819-0395, Japan*
[3] *Center for Molecular Systems, Kyushu University, Fukuoka 819-0395, Japan*

Single-walled carbon nanotubes (SWNTs) with semiconducting features show photoluminescence (PL) in the near infrared region, which is applicable to a wide variety of optical applications including bioimaging and telecommunication devices. Locally functionalized SWNTs (lf-SWNTs), which are synthesized by a slight amount of chemical modification, produce red-shifted PL with enhanced quantum yields (E_{11}*) compared to the original PL (E_{11}) of pristine SWNTs[1]. The functionalized molecules on the lf-SWNTs have been found to determine and modulate the E_{11}* PL wavelength. In addition, the PL wavelength switching has been reported based on protonation (pH variation)[2] and molecular binding on the functionalized groups[3,4]. In this study, we examine PL property modulation of lf-SWNTs through functionalization with photochromic dyes of diarylethene derivatives (DEs) towards development of photoswitchable PL shifting systems[5].

The diazonium salt of DE was synthesized and reacted with solubilized SWNTs in a SDBS micellar solution for the synthesis of DE-modified lf-SWNTs (lf-SWNTs-DE). Fig.1 shows the PL spectra of pristine SWNTs and the lf-SWNTs-DE. The pristine SWNTs showed a PL peak at 980 nm assignable to E_{11} emission. For the lf-SWNTs-DE, an additional PL was observed at 1151 nm, which would be produced by local functionalization of DEs. When the solution of lf-SWNTs-DE was irradiated with ultraviolet (UV) or visible light, spectral changes were observed. Namely, UV/vis. absorption measurements showed absorbance changes relating to isomerization of DE and, accordingly, peak shifts of E_{11}* PL occurred for the lf-SWNTs-DE. The results indicate that a new photo-switching system for E_{11}* PL wavelength would be created by this approach.

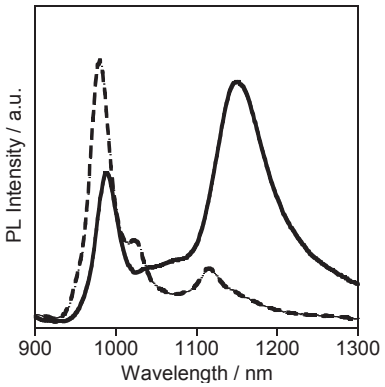

Fig. 1 PL spectra of pristine SWNTs (dashed line) and lf-SWNTs-DE (solid line).

[1] Y. Piao, B. Meany, L. R. Powell, N. Valley, H. Kwon, G. C. Schatz, Y. Wang, *Nat. Chem*. **2013**, *5*, 840.
[2] H. Kwon, M. Kim, B. Meany, Y. Piao, L. R. Powell, Y. Wang, *J. Phys. Chem.* **2015**, *119*, 3733.
[3] T. Shiraki, H. Onitsuka, T. Shiraishi, N. Nakashima, *Chem. Comm.* **2016**, *52*, 12972.
[4] T. Shiraki, T. Shiga, T. Shiraishi, H. Onitsuka, N. Nakashima, T. Fujigaya, *Chem. Eur. J*. **2018**, *24*, 19162.
[5] M. Irie, M. Mohri, *J. Org. Chem*. **1988**, *53*, 803.

Corresponding Author: T. Fujigaya
Tel/Fax: +81-92-802-2842,
Web: http://www.chem.kyushu-u.ac.jp/~fifth/jp/
E-mail: fujigaya.tsuyohiko.948@m.kyushu-u.ac.jp

Monolayer WS_2 Light-Emitting Devices with micro-cavity

○Tomohiro Ogura[1], Tomoyuki Yamada[1], Naoki Wada[2], Takahiko Endo[2], Kenichi Yamashita[3], Yasumitsu Miyata[2], Jiang Pu [1], Taishi Takenobu [1]

[1] *Department of Applied Physics, Nagoya Univ., Nagoya 464-8601, Japan*
[2] *Department of Physics, Tokyo Metropolitan Univ., Tokyo 192-0397, Japan*
[3] *Faculty of Electrical Engineering and Electronics, Kyoto Inst. of Tech., Kyoto 606-8585, Japan*

The interaction of tightly bounded excitons of monolayer transition metal dichalcogenides (TMDCs) in a micro-cavity offers a rich platform for exploring new optoelectronic devices. For example, when the excitons and the cavity photons are strongly interacted, a new quantum state, exciton-polariton is emerging in cavity-integrated TMDCs [1]. Exciton-polariton is expected to be applied to new optical devices such as very low threshold polariton lasers without population inversion. Although the exciton-polariton light emission was observed by photo-pumped measurements in TMDCs, the electrical generation of this optical signature has not yet been realized. Because the relevant TMDC light-emitting devices are difficult to assemble with micro-cavities due to their complicated structures [2], a simple device technique is necessary to achieve exciton-polariton light-emitting devices. Here, we combine electrolyte as an active medium to the Fabry-Perot-type micro-cavity. Owing to our proposed electrolyte-based structures [3], we can easily fabricate cavity-integrated TMDC light-emitting devices and try to realize exciton-polariton electroluminescence (EL).

The chemically grown WS_2 monolayer flakes are firstly transferred onto a Distributed Bragg Reflector (DBR as a bottom mirror), and then two gold electrodes are patterned. Finally, PMMA mixed with an ionic liquid are spin-coated followed by deposition of thin gold film on the PMMA surfaces as a top mirror (Fig. 1). Figure 2 shows the angle-resolved photoluminescence (PL) spectra for WS_2 in the micro-cavity. The results exhibit PL measured from 0 to 40 degrees at room temperature, and we can confirm obvious change of the peak shape and the peak energy depending on the angle. To further clarify the PL behaviors, Figure 3 presents a 2D color mapping of the angle-dependent PL. We performed spectrum analysis, and each fitted peak behaviors are also shown in Fig. 3. Since we can see the two distinct peak behaviors as a function of the angle, such peak behaviors indicate the observation of polariton dispersion; one is upper polariton (UP) for higher energy and the other is lower polariton (LP) band. In this device, when we apply voltages between two electrodes on WS_2 flakes, the ion distributions induce p-i-n junction to generate EL. Therefore, we can evaluate EL behaviors in same cavity, and we will also report the angle-resolved EL.

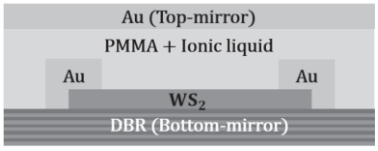

Fig.1 Device structure

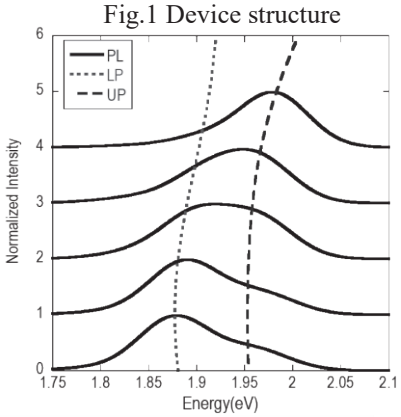

Fig.2 Angle-resolved PL spectra

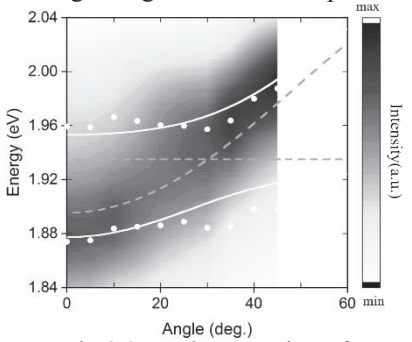

Fig.3 2D color mapping of PL

[1] N. Lundt *et al., Nat. Commun.* **7**. 13328 (2016)
[2] J. S. Ross *et al., Nat. Nanotechnol.* **9**, 268 (2014)
[3] J. Pu, *et al. Adv. Mater.* **29**, 1606918 (2017).

Corresponding Author: T. Takenobu, Tel/Fax: +81-52-789-5173, E-mail: takenobu@nagoya-u.jp

Restoring intrinsic optical properties of CVD-grown MoS_2 monolayers and their heterostructures

○Kana Kojima[1], Hong En Lim[1], Zheng Liu[2], Wenjin Zhang[3], Tetsuki Saito[1], Yusuke Nakanishi[1], Takahiko Endo[1], Yu Kobayashi[1], Kenji Watanabe[4], Takashi Taniguchi[4], Kazunari Matsuda[3], Yutaka Maniwa[1], Yuhei Miyauchi[3], Yasumitsu Miyata[1]

[1] *Department of Physics, Tokyo Metropolitan University, Hachioji, 192-0397, Japan*
[2] *Inorganic Functional Materials Research Institute, AIST, Nagoya, 463-8560, Japan*
[3] *Institute of Advanced Energy, Kyoto University, Uji, 611-0011, Japan*
[4] *National Institute for Materials Science, 1-1 Namiki, Tsukuba, Japan*

In this work, we have investigated the intrinsic optical properties of MoS_2 monolayers and MoS_2/WS_2 van der Waals (vdW) heterostructures, grown using chemical vapor deposition [1]. To understand the effect of growth substrate, the samples grown on SiO_2/Si surface were transferred and suspended onto a porous substrate (Fig.1a). This transfer resulted in a blue shift of the excitonic photoluminescence (PL) peak generated by MoS_2 monolayers, together with an intensity increase (Fig.1b). The blue shift and the intensity increase are attributed to the release of lattice strain and the elimination of substrate-induced non-radiative relaxation, respectively. This suspension technique also allowed observations of PL resulting from interlayer excitons in the MoS_2/WS_2 vdW heterostructures (Fig.1c). These results indicate that the suppression of lattice strain and non-radiative relaxation is essential to the formation of interlayer excitons, which in turn is crucial to understanding the intrinsic physical properties of vdW heterostructures.

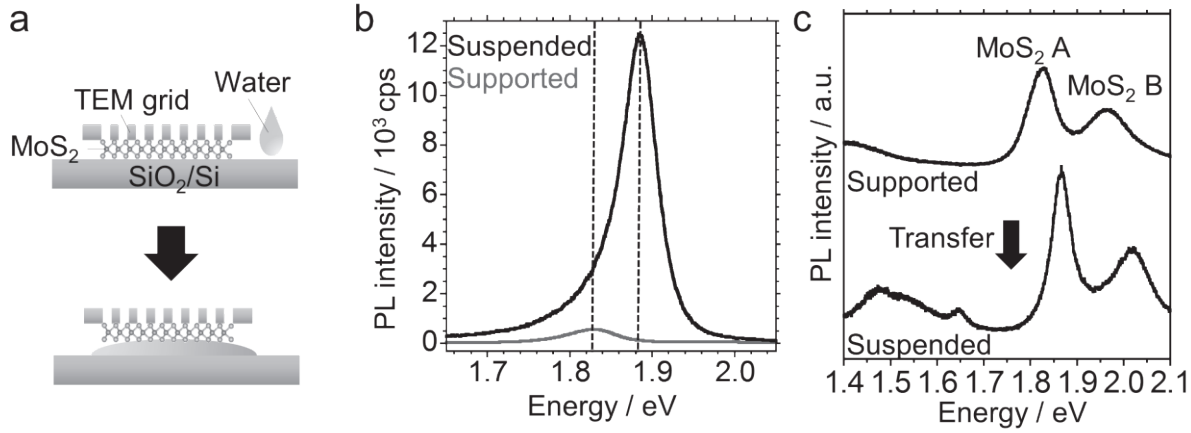

Fig. 1. (a) Schematic of a transfer process of samples on a porous substrate. (b) PL spectra of a MoS_2 monolayer suspended on a TEM grid and on a SiO_2/Si support. Broken lines indicate the primary peak position for each sample. (c) PL spectra of MoS_2/WS_2 vertical heterostructures grown on SiO_2 and after the transfer on a TEM grid.

[1] K. Kojima *et al.* Nanoscale, **11**, 12798-12803 (2019).
Corresponding Author: Y. Miyata, Tel: 042-677-2508, E-mail: ymiyata@tmu.ac.jp

Wide-range control of excitonic properties in monolayer WS_2 by dielectric screening effect

○Yuto Kajino, Kenichi Oto, and Yasuhiro Yamada

Department of physics, Chiba University, Inage, Chiba 263-8522, Japan

Monolayer Transition metal dichalcogenides (TMDCs), such as MoS_2, $MoSe_2$, WS_2, WSe_2, are ideal two-dimensional (2D) semiconductors with a direct bandgap in visible region, and their optical properties are strongly dominated by excitons because of large exciton binding energy. Recently, the flexible design for optoelectronic devices using stacking structures by van der Waals force, so-called vdW heterostructure, has also attracted much attention.

The screening effect by surrounding dielectric constant can dramatically change the optical properties in monolayer TMDCs through modifying the Coulomb interaction between an electron and a hole forming an exciton due to their atomically thin structures. This novel idea has been proposed as a Coulomb engineering [1]. Although several groups have reported the changes of the optical properties using organic solvents and layered materials such as graphene and h-BN [1,2], systematic changes on surrounding dielectric constant have not been demonstrated yet. It is also essential to accurately evaluate the dependence of the exciton resonance energy in monolayer TMDCs on modified effective dielectric constant. In this research, we investigated the changes of optical properties in monolayer WS_2 fabricated on various substrates with different dielectric constant, whose dielectric constant widely ranges from 2 to 5 at infrared frequency.

We fabricated the monolayer WS_2 on various substrates with different dielectric constant by mechanical exfoliation from a bulk crystal. The monolayer WS_2 at each substrate was then identified by optical microscopic observation, atomic force microscopy, and microscopic spectroscopy at room temperature. We performed the optical reflectance and PL spectroscopy at 10 K and compare the transition peak energies in monolayer WS_2 on different substrates.

The systematic shifts of A and B exciton peak energies depending on the dielectric constant of substrate were observed, and A maximum change of A-exciton resonance energy of 40 meV was achieved. These results clearly demonstrated the Coulomb engineering of monolayer TMDC by the dielectric substrate. Detailed analysis performed in combination with experimental results and theoretical calculation revealed that the bandgap energy as well as exciton binding energy is reduced by ~100 meV [3]. In the presentation, we will discuss the physical mechanism of the dielectric screening effect on the optical properties in monolayer TMDCs.

[1] A. Raja *et al*., Nat. Commun. **8**, 15251 (2017).
[2] Y. Lin *et al.*, Nano Lett. **14**, 5569 (2014).
[3] Y. Kajino *et al*., J. Phys. Chem. C **123**, 14097 (2019).

Corresponding Author: Y. Kajino
Tel: +81-043-290-2740
Web: http://physics.s.chiba-u.ac.jp/ssphoto/
E-mail: kajino@chiba-u.jp

Growth of Transition-metal-dichalcogenide-based two-dimensional superstructures with Cold-walled Metal-Organic CVD

○Satoshi Iida[1], Takato Hotta[1], Kenji Watanabe[2], Takashi Taniguchi[2], Hisanori Shinohara[1], and Ryo Kitaura[1]

[1]*Department of Chemistry, Nagoya University, Nagoya 464-8602, Japan*
[2] *National Institute for Materials Science, Tsukuba 305-0044, Japan*

Since the discovery of graphene, two-dimensional (2D) materials have been attracting considerable attention. Recent research on 2D heterostructures, including heterostacks and heterojunctions, has clearly demonstrated the possibility on emergence of novel properties in these heterostructures[1]. In this work, we have focused on growth of a new type of heterostructure, 2D superlattices (2D-SLs), where periodic junctions of different 2D materials form novel 2D superstructures. To fully explore the possibility of 2D-SLs, development of a highly-controllable crystal growth method is indispensable. For this purpose, we have focused on Metal-Organic Chemical Vaper deposition (MOCVD), in particular, a cold-wall type MOCVD. In this presentation, results on MOCVD growth of transition metal dichalcogenides (WS_2 and MoS_2) and 2D-SLs composed of WS_2 and MoS_2 are presented.

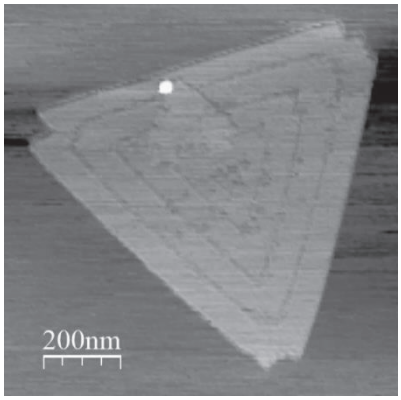

Fig. 1 An AFM image of a WS_2-MoS_2 superlattice

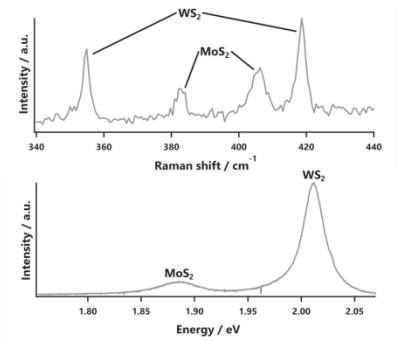

Fig. 2 A typical Raman and PL spectrum of a WS_2-MoS_2 superlattice measured at room temperature.

Figure 1 shows an AFM image of a 2D-SL composed of WS_2 and MoS_2. For the growth of 2D-SLs, we have developed an automatic valve control system that enables us to perform automatic switch of the source supply. The triangle contrasts correspond to a crystal of 2D-SL, and wide (narrow) contrasts seen in the crystal correspond to WS_2 (MoS_2) monolayers: widths of each WS_2 (MoS_2) region are 70 (10) nm. Figure 2 is typical Raman and PL spectrum of WS_2-MoS_2 2D-SLs, respectively. These spectra are consistent to the formation of 2D-SLs composed of monolayer WS_2 and MoS_2. We are, now, working on optimization of growth condition and investigation of atomic structure at interfaces of WS_2 and MoS_2. More details of growth condition and characterization will be shown in the poster.

[1] A. K. Geim. *et al.,* Nature **499**, 419-425 (2013).

Corresponding Author: R. Kitaura Tel: +81-52-789-2477, Fax: +81-52-747-6442, E-mail: r.kitaura@nagoya-u.jp

Thickness dependence of CVD-grown h-BN on PL emission and Raman of monolayer MoS_2

○Hiroki Honda,[1] Daichi Tanaka,[1] Yuki Uchida,[1] Kenji Kawahara,[2] Hiroki Ago[1,2,*]

[1] *Interdisciplinary Graduate School of Engineering Sciences, Kyushu University, Fukuoka 816-8580, Japan*

[2] *Global Innovation Center (GIC), Kyushu University, Fukuoka 816-8580, Japan*

Recently, hexagonal boron nitride (h–BN) has become a key material for observing intrinsic and/or exotic properties of various 2D materials and also for promoting their practical applications [1,2]. Although monolayer h-BN can be widely synthesized by CVD using Cu, it is not thick enough to screen out the influences of underlying SiO_2 substrate. We have recently demonstrated the CVD growth of multilayer h-BN using Ni-Fe catalyst [3], but influence of the h-BN thickness on 2D materials has not been clearly understood.

Here, we investigate the influence of thickness of CVD-grown multilayer h-BN on optical properties of monolayer MoS_2. Monolayer MoS_2 was grown by CVD as reported previously [4] and transferred onto a h-BN/SiO_2 substrate by a wet transfer method. Figure 1a shows the photoluminescence (PL) spectra of monolayer MoS_2 on bare SiO_2 and h-BN surfaces. For reliable study, we used one single MoS_2 grain deposited on h–BN with different thicknesses. We found that the PL spectrum of MoS_2 becomes sharper and more intense with increasing the thickness of multilayer h-BN. Moreover, the contribution of the low energy PL peak (~1.8 eV) corresponding to negative trions was significantly suppressed by multilayer h-BN, which can be explained by screening of charge impurities existing on the SiO_2 surface. Figure 1b displays the change of the Raman spectrum of the monolayer MoS_2. Both E^1_{2g} (386 cm^{-1}) and A_{1g} (403 cm^{-1}) peaks shifted to higher wavenumbers. Interestingly, these Raman peaks became very narrow even on 2 nm-thick h-BN. Therefore, our results indicate the contribution of multilayer h-BN on the PL and Raman spectra of MoS_2 can be different.

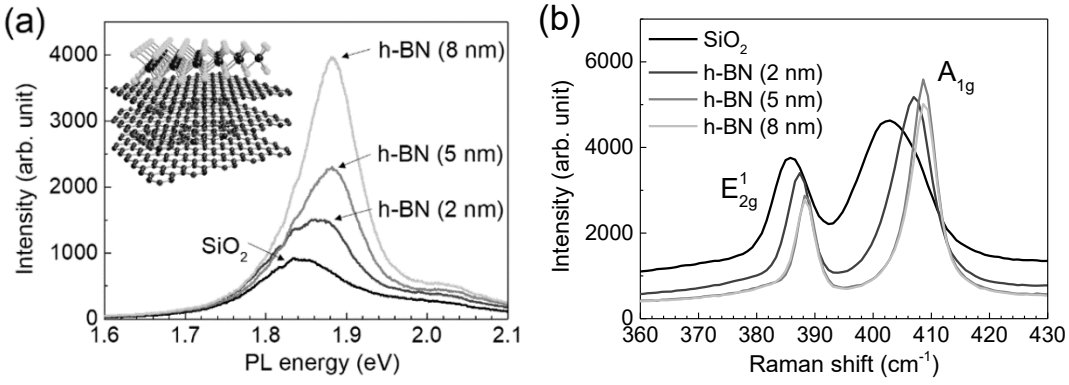

Figure 1. (a) PL and (b) Raman spectra of MoS_2 deposited on SiO_2 and h-BN with different thicknesses. Inset in (a) shows the atomic model of monolayer MoS_2 deposited on multilayer h-BN.

References

[1] C. R. Dean *et al.*, *Nat. Nanotechnol.*, **5**, 722 (2010). 10, 534. [2] Y. Cao *et al.*, *Nature*, **556**, 43 (2018). [3] Y. Uchida *et al.*, *ACS Nano*, **12**, 6236 (2018). [4] H. Ago *et al.*, *ACS Nano*, **10**, 3233 (2016).

Corresponding: H. Ago (E-mail: h-ago@gic.kyushu-u.ac.jp)

Charge-state investigation on metallic and semiconducting SWCNTs with various diameters

○Yuki Kuwahara and Takeshi Saito

Nanomaterials Research Institute (NMRI),
National Institute of Advanced Industrial Science and Technology (AIST),
Tsukuba 305-8565, Japan

The electric-field-induced layer formation (ELF) method, which can separate metallic (m-) and semiconducting (s-) SWCNTs by simply applying an electric field in the longitudinal direction to SWCNT dispersion, is one of the promising methods for the development of their industrial production process [1]. Recently, we revealed that s-SWCNTs are much more negatively charged than m-SWCNTs in the ELF separation by evaluating the charge states of m- and s-SWCNTs during the separation process. On the basis of this result, it was concluded that the ELF separation mechanism is attributed to the dynamic changing/balancing of the electrophoretic and electroosmotic forces acting on the SWCNTs [2]. One of the features on the ELF method is the relatively wide tube-diameter range of separable SWCNTs, from *ca*. 1.0 to 1.7 nm. In this study, we have investigated the charge states for m- and s-SWCNTs with various diameters in detail for examining the possibility of sorting in their tube diameter.

SWCNT samples with four different average tube-diameters, 1.0, 1.3, 1.7 and 2.0 nm, were synthesized using the eDIPS method [3], and were dispersed in the aqueous solutions of 1 wt% polyethylene (100) stearyl ether (Brij S100) by using ultrasonication. The obtained solutions were ultracentrifuged to eliminate bundled SWCNTs, and then the supernatant solutions were collected for the use of ELF separation. The charge state of SWCNTs was evaluated by the zeta potential measured under various conditions of pH and surfactant-concentration. As the result, the differences in the amount of negative charge between m- and s-SWCNTs were observed regardless of the average tube-diameters. On the other hand, the difference in the zeta potential among the tube-diameters remained obscure because of the data scattering, which suggests that the improvement of sample preparation procedures for measuring the zeta potential of SWCNTs would be needed in order to clarify the correlation between the tube-diameter and the zeta potential. In this presentation, the yield of m- and s-SWCNTs on the ELF separation for each SWCNT diameter will be also discussed.

[1] K. Ihara *et al*., *J. Phys. Chem. C*, 115, 22827 (2011).
[2] Y. Kuwahara *et al*., *J. Phys. Chem. C*, 123, 3829 (2019).
[3] T. Saito et al., *J. Nanosci. Nanotechnol*., 8, 6153 (2008).

Corresponding Author: T. Saito
Tel: +81-29-861-4863, Fax: +81-29-861-4413
E-mail: takeshi-saito@aist.go.jp

Fabrication of large-area aligned films of single-wall carbon nanotubes using artificially grooved membrane filters

○Atsuhiro Katagiri[1], Natsumi Komatsu[2], Junko Eda[1], Hitomi Okubo[1], Kanako Horiuchi[1], Kan Ueji[1], Yohei Yomogida[1], Weilu Gao[2], Junichiro Kono[2], and Kazuhiro Yanagi[1]

[1]*Department of physics, Tokyo Metropolitan University, Hachioji, Tokyo 192-0397, Japan*
[2]*Department of Electrical and Computer Engineering, Rice University, Houston, TX 77005, U.S.A.*

Precise control of alignment of single-wall carbon nanotubes (SWCNTs) is important for performance optimization of SWCNT thin film devices and for correct understanding of their physical properties. Recently, He *et al.* reported a technique to fabricate large-area aligned films of SWCNTs using filtration techniques [1]. However, in the method, the mechanism of SWCNT global alignment has not been clarified. Komatsu *et al.* pointed out that the presence of parallel grooves on the filter membrane, accidentally created through the filter production process, plays a key role in the formation of global one-direction alignment [2]. Therefore, in this study, we developed a technique to artificially fabricate grooves on the membrane filters, and investigated how the artificially formed groove structures influence the alignment of SWCNTs.

For preparation of artificially grooved membrane filters, first we prepared optical gratings with groove densities of 300 mm^{-1}, 600 mm^{-1} and 1800 mm^{-1} (25 mm width × 25 mm length). Then the groove structures of the gratings were transferred to the membrane filter using a technique similar to nano-imprinting. Figure 1(a) shows a typical AFM image of the detailed structure of a grooved membrane filter. As shown here, we succeeded in forming grooves at a pitch of about 1.66 μm with a height of about 60 nm when we use the 600 mm^{-1} grooved grating. Then we prepared SWCNT thin films with the controlled vacuum filtration technique developed by He *et al*. [1]. Figure 1(b) shows an AFM image of a SWCNT thin film prepared using the artificially grooved membrane filter. As shown here, SWCNTs were well aligned along the grooved structures. Thus, we found that artificially formed grooves can control the alignment of SWCNTs.

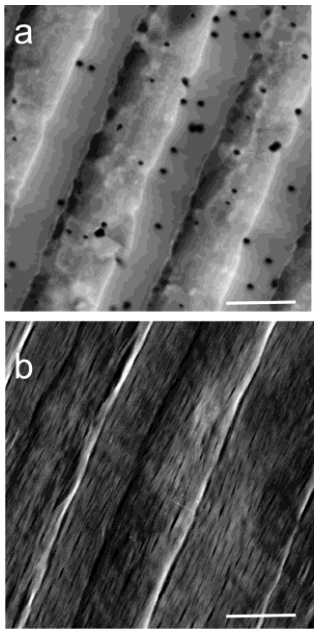

Figure 1 AFM images of (a) artificially grooved membrane filter and (b) SWCNT film prepared using the filter

References: [1] He *et al*. Nat. Nanotechnol. **11**, 1 (2016), [2] Komatsu et al., in preparation (2019)

Corresponding Author: K. Yanagi Tel: +81-42-677-2809 E-mail: yanagi-kazuhiro@tmu.ac.jp

Thermophysical property of single-wall carbon nanotube thin film on Au electrodes by a time-domain thermoreflectance method

○Yuya Matsuoka [1], Kan Ueji [1], Hiroyuki Matsuo [1], Yohei Yomogida [1],
Takashi Yagi [2], Kazuhiro Yanagi [1]

[1] *Department of Physics, Tokyo Metropolitan University, Hachioji, Tokyo 192-0397, Japan*
[2] *Department of Physics, National Institute of Advanced Industrial Science and Technology, Tsukuba, Ibaraki,305-8563, Japan*

Flexible materials such as carbon nanotubes and organic semiconductors have attracted attention as components for thin film devices. Not only their electrical properties but also their thermophysical properties are important to achieve optimal their device performances. However, evaluation of thermophysical properties of thin films is usually difficult. Time-domain thermoreflectance (TDTR) method is one of promising methods to clarify the thermal conductivity of thin films at the nanoscale [1]. TDTR method measures heat flow in a thin film through temporal changes in reflectance of a metal film after heating by irradiation of pump laser pulse, *i.e.* thermoreflectance signals. Usually, aluminum is used for TDTR measurements, because aluminum has large thermo-reflectance signals at 780 nm probe wavelength, which is the second harmonic of the pump laser pulse with wavelength of 1550 nm. For electronic device applications, however, gold is often used as a metal element for electrodes, not aluminum. Thus, understanding on thermophysical properties of thin-films on gold electrodes is required, but, the thermo-reflectance signals of gold at 780 nm are very small, thus we cannot use conventional TDTR setups for that purpose. Therefore, here, we are developed TDTR system which is suitable for detection of thermoreflectance signal of gold. We used probe laser pulse with wavelength of 520 nm because Au film has large thermoreflectance signals around this wavelength [2]. We investigated thermal conductivity of single-wall carbon nanotube (SWCNT) thin films on the Au electrode by TDTR method.

Fig.1, shows the difference of phase change between only Au and SWCNTs (MEIJO nano carbon ARCSO, 200 nm thickness)/Au. We observed a significant difference of temporal changes of thermo-reflectance signals between them, indicating that our system is applicable for evaluation thermal conductivity of SWCNTs on Au electrodes. In this presentation, the details will be discussed.

Ref: [1] Bruce M. Clemens *et al*. *Phys. Rev. B*, **37**, 1085 (1988).
[2] W. J. Scouler. *Phys. Rev. Lett*, **18**, 445 (1967).

Corresponding Author: K. Yanagi & K. Ueji,
Tel:＋81-42-677-2494, E-mail:yanagi-kazuhiro@tmu.ac.jp,
kueji@tmu.ac.jp

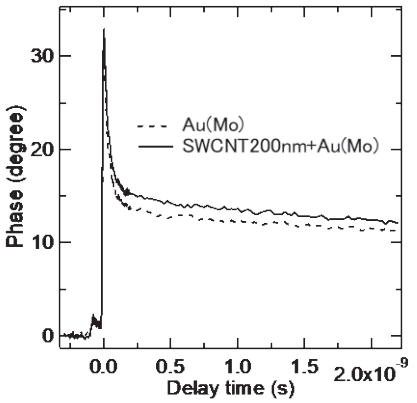

Fig. 1 : Phase changes in Au and SWCNTs/Au as a function of time.

Effect of palladium nanoparticle decoration on thermoelectric peeformance of carbon nanotubes with vacancy defects: first principles simulation

○Nayu Araki[1] and Takahiro Yamamoto[1,2]

[1] *Department of Electrical Engineering, Tokyo University of Science, Tokyo 125-8585, Japan*
[2] *Division of Nano carbon Research, RIST, Tokyo University of Science, Tokyo 125-8585, Japan*

Carbon nanotubes (CNTs) are expected to be thermoelectric materials because of their high thermoelectric power factor and mechanical flexibility [1]. As refined CNTs are however expensive, expectations for mass-produced inexpensive SG-CNTs (super-growth CNTs) are increasing for lowering the cost of CNT-based devices. Although SG-CNTs are inexpensive, they include many defects that influences the thermoelectric effects of SG-CNTs. As a new method to recover the thermoelectric performance of SG-CNTs, we now propose a palladium nanoparticle decorated method.

It has been experimentally reported that by applying chemical adsorption to defective CNTs by metal nanoclusters, the nanoparticles are selectively adsorbed on the defects of the CNTs and eventually the power factor (PF) recovers [2]. However, the detail of the effect has not been clarified yet. Thus, in this study, we theoretically investigate the effect of palladium adsorption to various defects existing in a CNT on PF using first principles calculation. In our first principles calculation, we adopted ATK 2017.2 software [3] based on the density functional theory combined with the non-equilibrium Green's function method. We calculated the conductivity, the Seebeck coefficient and PF of palladium-decollated CNTs with various shapes and densities of vacancy defect.

As a consequence, we clarify that the vacancy defects in a CNT cause electron scattering and eventually the electrical conductivity decreases and then PF decreases. In addition, palladium atoms are adsorbed to the vacancy defect sites, and the dangling bond is terminated by the palladium atoms, whereby the scattering is suppressed, the conductivity of the CNT is recovered, and consequently PF is improved. In the presentation, we would like to discuss the optimization of palladium adsorption that could improve PF most.

[1] Y. Nakai, K. Honda, K. Yanagi, *et al*., Appl. Phys. Express, **7**, 025103 (2014).
[2] N. Toshima, et al., 37th International and 16th European Conference on Thermoelectrics (ict2018:197517)
[3] https://www.synopsys.com/silicon/quantumatk.html

Corresponding Author: Takahiro Yamamoto
Tel: +81-3-5876-1492
Web: http://www.rs.tus.ac.jp/takahiro/
E-mail: takahiro@rs.tus.ac.jp

Production of Carbon Nano-Materials by the Bipolar-Pulsed Arc-Discharge Method

○Tetsu Mieno[1], Md Abul Kalam[1], Kazi Hanium Maria[2]

[1] Graduate School of Science & Technology, Shizuoka University, Shizuoka 422-8529, Japan
[2] Department of Physics, University of Dhaka, Dhaka-1000, Bangladesh

We have been studied to develop high-efficiency production of high-quality single-walled carbon nanotubes (SWNTs) and other carbon nano-clusters (fullerenes, metallo-fullerenes, metal-encapsulated carbon nano-particles (core-shell particles), magnetic particles by the arc discharge method.

In the usual arc-discharge method, about 50 % of carbon material re-deposits on a cathode, which is a large material-loss for the mass production. In the AC-arc discharge methods, the repetitive heating-cooling process makes large energy loss. To overcome these weak points, we have developed the bipolar-pulsed arc-discharge method (BPA method). [1 -3] Schematic of the reactor is shown in Fig.1. In this method, 4 electric relays are used to reverse the electric polarity. The time variation of the input electric power is almost constant, and the heating loss is suppressed. Figure 2 shows the Raman spectra of the sample. the D band is very small and the quality of SWNTs is good. We are now trying to produce high-quality carbon nano-particles (including magnetic nano-particles) by this method.

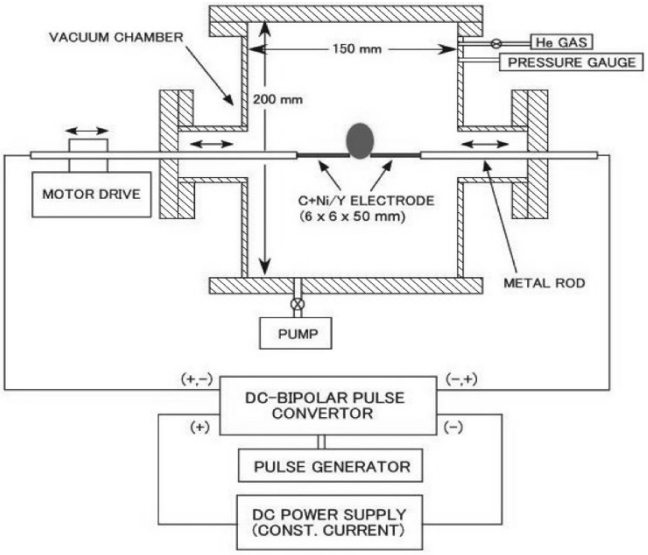

Fig. 1 Schematic of the bipolar pulsed arc discharge reactor. [1]

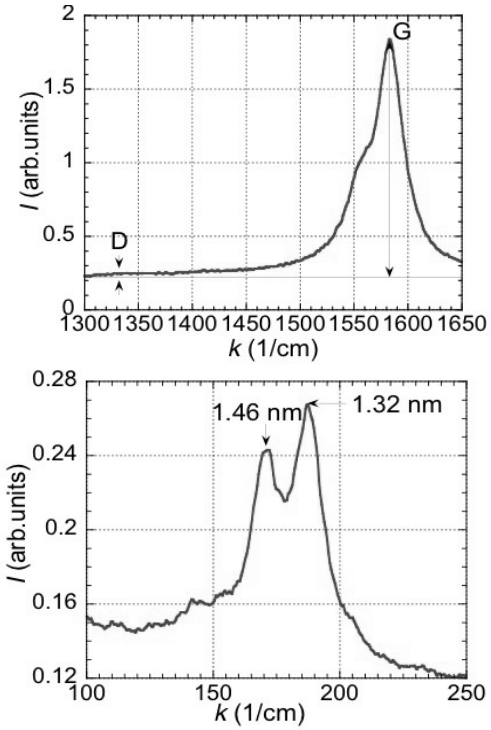

Fig. 2 Raman spectra of the sample (f= 0.050 Hz). G-band, G-band and RB-modes.

[1] K. H. Maria & T. Mieno, Vacuum, "Synthesis of single-walled carbon nanotubes by low-frequency bipolar pulsed arc discharge method", **113**, 11-18 (2015).
[2] Md. K. Kalam & T. Mieno, "Pressure and discharge current dependence of production rate of single-walled carbon nanotubes by the bipolar pulsed arc-discharge method", Fullerene, Nanotubes and Carbon Nanostructures, **26**, 458-464 (2018).
[3] T. Mieno, Jpn. Patent, 6386784, "The producer and the production method of carbon clusters", Aug. 17, 2018.

Corresponding Author: T. Mieno
Tel: +81-54-238-4750, Fax: +81-54-238-0993, E-mail: mieno.tetsu@shizuoka.ac.jp

Effect of ethanol gas flow on synthesis of single-walled carbon nanotube by a hot-wall chemical vapor deposition reactor using Ir catalysts

○Ai Misaki[1], Tomoko Suzuki[1], Takahiro Maruyama[1,2]

[1] *Nanomaterials Research Center, Meijo University, Nagoya 468-8502, Japan*
[2] *Department of Applied Chemistry, Meijo University, Nagoya 468-8502, Japan*

Single-walled carbon nanotubes (SWCNTs) have various unique properties and potential for applications to electronics devices in future. To realize CNT-FET, high-yield growth of small-diameter SWCNTs. At present, several groups have reported vertically aligned SWCNTs (VA-SWCNTs) via the chemical vapor deposition (CVD) method using Fe and Co catalysts. We also reported VA-SWCNTs by CVD using Co catalysts [1]. However, VA-SWCNTs grown from Fe or Co catalysts have diameters larger than 1 nm, and either Al_2O_3 buffer layer or cocatalyst is necessary to reduce the diameter. Recently, our groups reported growth of SWCNTs forests using cold-wall type CVD with Ir catalyst [2]. However, for scale-up of the growth, hot-wall CVD is desirable.

In this research, we attempted to grow VA-SWCNTs by alcohol catalytic CVD with an Ir catalyst using a hot-wall CVD reactor. The growth time was fixed at 10 min. Fig. 1 shows dependence of ethanol gas flow on Raman spectra of SWCNTs grown at 800ºC. The SWCNT yield reached its maximum at 200 sccm. Taking into account Raman shifts of RBM peaks in Raman spectra and "Kataura plot", the SWCNT diameters were estimated to be mainly distributed between 0.6 and 1.1 nm, irrespective of ethanol gas flow. FESEM showed growth of VA-SWCNT forests, when the ethanol gas flow was 200 sccm. We demonstrated that SWCNTs could be grown from an Ir catalyst using a hot-wall CVD.

This work was supported in part by Private University Research Branding Project from the Ministry of Education, Culture, Sports, Science and Technology (MEXT), Japan. Part of this work was conducted at the Institute for Molecular Science (IMS), supported by the "Nanotechnology Platform" of the Ministry of Education, Culture, Sports, Science and Technology (MEXT), Japan.

[1] A. Misaki et al. The 79th JSAP Autumn, 19a-224B-5 (2018)
[2] T.Okada et al. MRS Advances 4 (2019) 225.

Corresponding Author: T. Maruyama
Tel: +81-52-838-2386, Fax: +81-52-832-1179,
E-mail: takamaru@meijo-u.jp

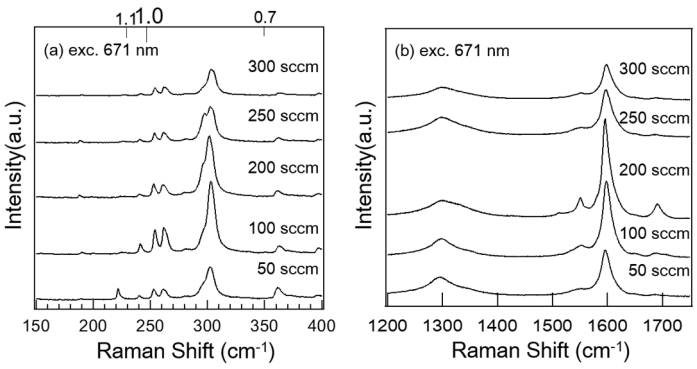

Fig.1 Raman spectra of SWCNTs grown at 800°C form Ir catalyst.

Growth of dense SWCNT from iron oxide nanoparticles for spin-capable forest

○Ryosuke Goto[1], Kento Tabata[1], Takayuki Nakano[1], Kazuhiko Takahashi[2], Yoku Inoue[1]

[1] *Department of Electronics and Materials Science, Shizuoka Univ., Hamamatsu 432-8561, Japan*
[2] *Toyota Motor Co., Toyota 471-8571, Japan*

In the conventional carbon nanotube (CNT) growth method, the catalyst thin film has been deposited on a substrate by sputtering and the catalyst thin film has been reduced under high temperature to form particles as CNT catalyst. Therefore, the method is difficult to independently control the catalyst density and size. In this study, CNT forest was synthesized using iron oxide nanoparticles synthesized by polyol method to control the size. We examined the effect of the assembly method of nanoparticles layer on the substrate and the process of CNT growth in order to achieve highly dense CNT forest.

A thermally oxidized Si wafer deposited with an Al_2O_3 thin film by sputtering was used as a substrate. Iron oxide nanoparticles were synthesized by the polyol method using iron acetylacetonate ($Fe(acac)_3$). The iron oxide nanoparticle dispersion solution was prepared using a mixed solution of hexane and toluene as a solvent. The concentration was 0.005 mg/ml. The iron oxide nanoparticles were dip-coated on the substrate. The substrate was immersed and stayed in the solution for 5 min, then the substrate was withdrawn with a speed of 10 μm/s. Then dried in air at room temperature. CNTs were grown by thermal CVD using acetylene, hydrogen and argon as a carbon source, a reducing agent for iron oxide nanoparticles and a carrier gas, respectively.

The average size of the iron oxide nanoparticles was 3.4 nm. Figure 1 shows the AFM image of iron oxide nanoparticles on the substrate. The iron oxide nanoparticles were dispersed on the entire surface of the substrate. Figure 2 shows an SEM image of the synthesized CNT forest. The length of the CNTs was about 70 μm. Figure 3 shows the result of Raman measurement of CNT. The intensity ratio of G band and D band was 8.9. Spin-capability of SWCNT forest will be discussed.

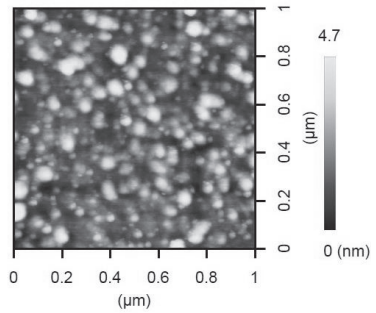

Fig.1 AFM image of iron oxide nanoparticles on substrate.

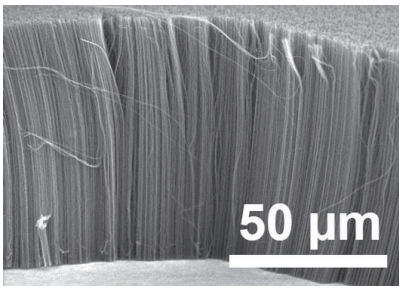

Fig.2 SEM image of CNT forest.

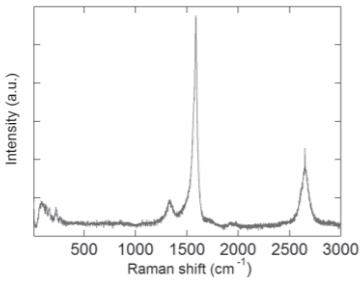

Fig.3 Raman spectrum of CNT.

Corresponding Author: Yoku Inoue
Tel: +81-53-478-1356, Fax: +81-53-478-1356,
Web: http://cnt.eng.shizuoka.ac.jp/
E-mail: inoue.yoku@shizuoka.ac.jp

Sub-nanometer diameter SWCNT Growth by Alcohol catalytic CVD

○ Kamal P Sharma[1,2], Daiki Yamamoto[1], Aliza K. Sharma[1], Takahiro Maruyama[1,2]

[1] *Department of Applied Chemistry, Meijo University, Nagoya 468-8502, Japan*

[2] *Nanomaterials Research Center, Meijo University, Nagoya 468-8502, Japan*

Single walled carbon nanotube (SWCNT) comprised of fore frontier application due to its superior chemical, electrical and optical properties [1]. Chirality controlled SWCNT synthesis is progressing very rapidly to surpass the post growth treatment process [2]. So synthesized SWCNTs had more than 1 nm diameter and with very low yield. Narrow diameter distributed SWCNTs possesses fewer chirality and synthesis of such tubes could be an alternative technique to solve the aforementioned problem. Here we challenge to address this issue by utilizing simultaneously deposited Co and W onto SiO_2 as a catalyst.

An ultrahigh vacuum (UHV) chemical vapor deposition (CVD) system with nozzle in the proximity of substrate though which ethanol is supplied as a chemical vapor was used as a growth chamber as reported elsewhere [3]. 0.2 nm Co and simultaneously deposited 0.2 nm Co and 0.4 nm W onto SiO_2/Si (referred as Method-A and Method-B respectively) were utilized as growth substrates. 10^{-1} Pa ethanol vapor over the 10^{-6} Pa base pressure was utilized for 60 min at elevated temperatures. As synthesized SWCNTs under our optimized condition were analyzed by Raman spectroscopy, FESEM, and XPS.

Figure 1 (a) and Figure 1 (b) show the Raman spectra of SWCNTs grown for 60 min at 600 ºC onto Method A and at 800ºC onto to Method B substrates respectively by keeping other conditions unchanged and were the optimal growth conditions. It is clearly observable in Figure 1 (b) that, from 250-500 cm-1 range, RBM peaks were observed indicating sub nanometer distributed SWCNT. Inset to Figure 1 (a) and (b) show the corresponding FESEM images.

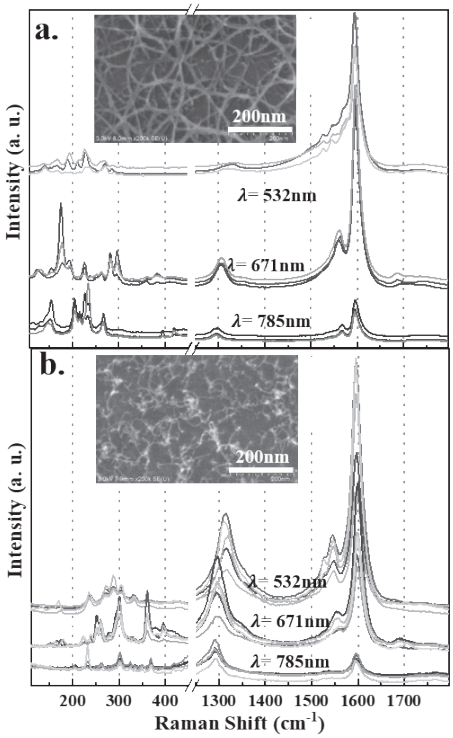

Figure 1. Raman spectrum of SWCNT grown onto SiO_2/Si by ACCVD technique at **(a)** 600ºC by utilizing 0.2 nm Co and **(b)** 800ºC using 0.4nm W/0.2nm Co. Inset show the corresponding FESEM images.

This work was supported in part by Private University Research Branding Project from the Ministry of Education, Culture, Sports, Science and Technology (MEXT), Japan.

[1] R. H. Baughman, et al. Science, 297, 787 (2002).
[2] F. Yang et al., Nature, 510, 522 (2014).
[3] T. Maruyama et al. Carbon 116, 128 (2017).

Corresponding Author: Takahiro Maruyama
E-mail: takamaru@meijo-u.ac.jp

Study of MWCNT/Cotton Composites and Development of Compact Load Cells

Md. Abdul Momin[1*], Mohammad Jellur Rahman[2] and Tetsu Mieno[1]

[1] *Graduate School of Science & Technology, Shizuoka University, Shizuoka 422-8529, Japan*
[2]*Department of Physics, Bangladesh University of Engineering and Technology, Dhaka-1000, Bangladesh.*

We have developed functionalized carbon nanotubes by citric acid assisted oxygen plasma treatment [1], by which the nanotube (NT) ink is easily prepared. By dipping cotton fibers into the NT ink for several times, MWCNT/cotton composites material is easily produced. Sandwiching the composites material between two electrodes, we could developed compact load cells [2]. The load cells have high sensibility, high durability, short response time and high reproducibility. It is conjectured that the mechanism of the load cell depends on the number of contacts among the MWCNT/cotton fibers at lower force region, and the contact areas among the deformed MWCNT coated cotton at higher force region. The load cells show high sensitivity of about 180–0.20 kPa^{-1} for a pressure of p= 8.84 Pa–884 kPa (F=1.0 mN–100 N), which is sufficient to precisely detect the basic movements of human and real-time sports performances. The MWCNT/cotton load cells show high reproducibility in different harsh environments. The efficiency of the sensors remains almost the same at low and high temperatures and under low- and high-humidity conditions. The load cell shows short response and relaxation times ($\tau_{1/2}$) of about 4.5 and 5 ms, respectively, and almost zero hysteresis is observed. The load cells can measure characteristic signals corresponding during walking, jogging, and standing conditions. An important application of the load cells is to measure locus of the center of gravity of a human foot during standing position, walking, and running, which can be used to monitor sick, old, or rehabilitating people. Therefore, the load cells have strong potential to be used as wearable force (or pressure)-monitoring devices, for healthcare tests, rehabilitation, real-time sports activities.

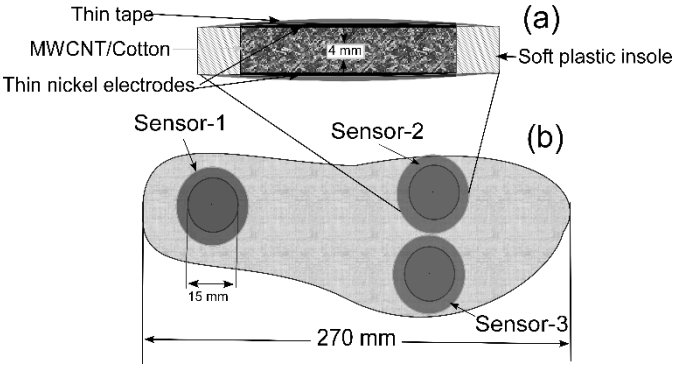

Fig.1: The three sensors are set in a shoe insole.

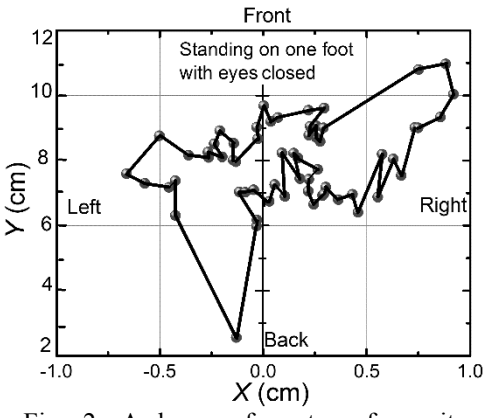

Fig. 2: A locus of center of gravity during standing. The measurement time is 10 s.

[1] M. J. Rahman, T. Mieno, J. Nanometer. **2014**, Article ID 508182, pp. 1–9 (2014).
[2] M. A. Momin, M. J. Rahman, J. Nanometer. **2019**, Article ID 7658437, pp. 1-15 (2019).

Corresponding Author: Md. Abdul Momin
Email: mamomin89bd@gmail.com
Mobile no: +8108051265887

Study of Ion Adsorption Properties of Single-Walled Carbon Nanotubes by Electrochemical Quartz Crystal Microbalance Method

○Mikako Takahashi, Masato Tsutsui, Yu Takeuchi,
Ayar Al-zubaidi, Yosuke Ishii, Shinji Kawasaki

Department of Life science and Applied Chemistry, Nagoya Institute of Technology, Nagoya 466-8555, Japan

Electric double-layer capacitors (EDLCs) store energy through reversible ion adsorption at the electrode−electrolyte interface. A major drawback of EDLCs is their lower energy density compared to that of the batteries. In order to increase the energy density of EDLCs, it is necessary to understand the ion adsorption mechanism in the electrode pore of EDLCs. In this study, I used single-walled carbon nanotubes (SWCNTs) as electrode material, because SWCNTs have simple and uniform nanostructure and work as good electrode model materials to study ion adsorption mechanism. Quartz Crystal Microbalance (QCM) was used as an analysis method of the mechanism of ion adsorption. QCM allows us to observe the mass change accompanied by ion adsorption, precipitation, desorption at the electrode with high sensitivity, so it is an effective method to understand the ion adsorption behavior in the nanopores of the electrode. [1]

So far, we have investigated the ion adsorption/desorption behavior at inner tube space of SWCNTs with different diameters (1-2.5 nm). Simultaneous measurements of cyclic voltammogram and QCM were performed using a three-electrode cell. In the measurements, self-supported SWCNTs sheets and activated carbon fiber wrapped in platinum mesh ware used as working and counter electrodes respectively. Triethylmethylammonium tetrafluoroborate ($TEMABF_4$) dissolved in propylene carbonate (PC) was used as an electrolyte.

It became clear that the ion adsorption behavior in $TEMABF_4$/PC differs depending on the tube diameter of SWCNTs. Furthermore, using metallic/semiconducting SWCNTs electrodes, we also examined how the electronic state of SWCNTs affects the ion storage behavior.

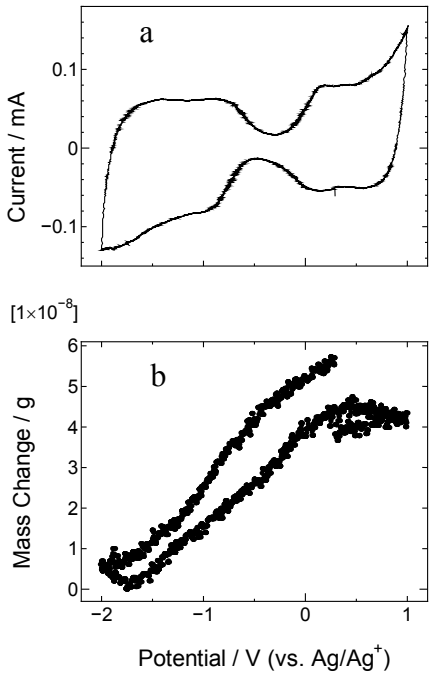

Fig. 1 (a) CV of semiconducting SWCNTs electrode (d = 1.5 nm) at a scan rate of 10 mV/s and (b) corresponding mass change obtained by QCM measurement.

[1] Mikhael Levi *et al*. Nature Mater. **8**, 872 (2009)

Corresponding Author: S. Kawasaki
E-mail: Kawasaki.shinji@nitech.ac.jp

High temperature capacitor electrode properties of nanocarbon materials in ionic liquid electrolytes

○Nanami Asai, Yosuke Ishii, Shinji Kawasaki

Department of Life Science and Applied Chemistry, Nagoya Institute of Technology, Nagoya 466-8555, Japan

Electric double layer capacitors (EDLCs) are attractive energy storage devices, due to their high speed and low cycle degradation. Organic solvents, such as propylene carbonate, are used for the electrolyte of conventional EDLCs. However, organic solvents have low boiling points and flash points, and are difficult to use at temperatures above 100°C. In order to develop EDLC which can be operated at high temperature above 100°C, it is necessary to search for electrolytes that work well even at higher temperatures.

In this study, ionic liquid was used as electrolyte, and the influence of temperature on EDLC characteristics of porous carbon electrode was investigated. Triethyl-(2-methoxyethyl)phosphonium bis(trifluoromethanesulfonyl)imide ($P_{222(2O1)}$-TFSI) was used as the electrolyte. As a porous carbon electrode, activated carbon, SWCNTs (1 - 5 nm in diameter), and reduced graphene oxide (rGO) were used. A symmetric two-electrode cell was constructed using these electrodes. Constant current charge/discharge measurement and electrochemical impedance measurement were performed in a temperature range of 25 - 250°C.

Fig. 1 shows the Nyquist plots for EDLC cell with (a) activated carbon electrodes, (b) SWCNT electrodes (d = 1.5 nm), and (c) rGO electrodes. As shown in Fig. 1, we observed different shapes of the Nyquist plots depending on nanocarbon electrodes. The difference was probably caused by ion diffusion in nanopores of the carbon electrodes.

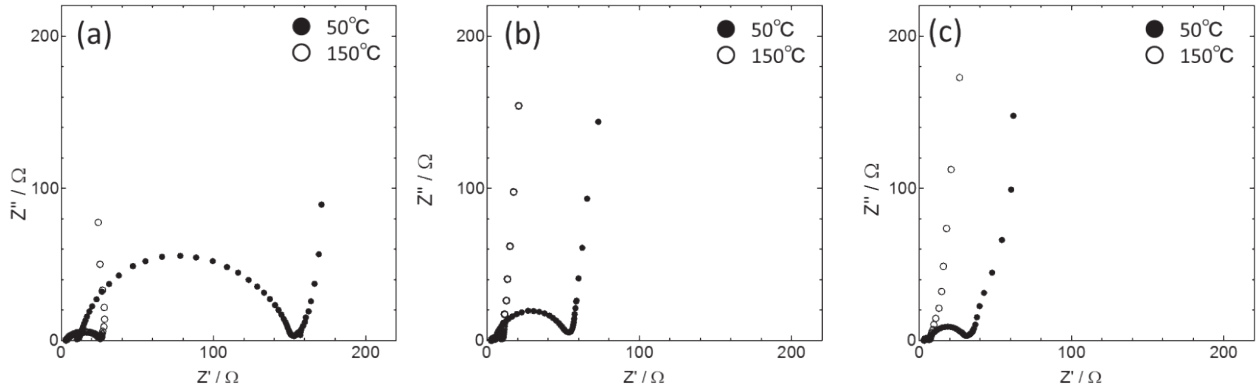

Fig. 1 Nyquist plots for symmetric EDLC cell with (a) activated carbon electrodes, (b) SWCNT electrodes (d = 1.5 nm), and (c) rGO electrodes.

[1] T. Sato *et al*. *Electrochem. Acta,* **49**, 3603 (2004).

[2] K. Tsunashima *et al. Electrochem. commun.,* **9**, 2353 (2007).

Corresponding Author: N. Asai

E-mail: 30411003@stn.nitech.ac.jp

1P-21

Catalytic properties of single-walled carbon nanotube /metal nanoparticles for CO_2 reduction reaction

○Sae Ishikawa, Shunya Inayama, Kohei Kondo, Yusuke Watanabe, Yosuke Ishi, Shinji Kawasaki

Department of Life science and Applied chemistry, Nagoya Institute of Technology, Nagoya 466-8555, Japan

With the development of industrial activities, environmental problems such as global warming due to the increase of CO_2 concentration and depletion of energy and carbon resources are getting serious. Therefore, research on photocatalysts capable of reducing CO_2 to carbon resources using solar energy has been actively conducted in the recent years. CO_2 reduction is performed using excitation electrons obtained by irradiating a photocatalyst with light. However, the conversion efficiency and selectivity of that approach are still low, and the practical application of such photocatalysts is therefore difficult.

In this study, we tried to develop an electrode capable of reducing CO_2 using solar energy more efficiently. It has been found that Cu functions effectively as a CO_2 reducing metal catalyst in electrochemical CO_2 reduction. Then we thought that TiO_2/ single-walled carbon nanotube (SWCNT)/Cu nanoparticle complex would be effective to achieve CO_2 reduction with light energy (Fig. 1). In this system, we expect efficient charge separation to be achieved due to the fact that TiO_2 absorbs light energy, while SWCNT sends excited electrons to Cu. In addition, a lot of Cu nanoparticles can be arranged by utilizing the high specific surface area of SWCNT. Furthermore, we expect Cu nanoparticles to improve the selectivity of the reduction process and the amount of the products.

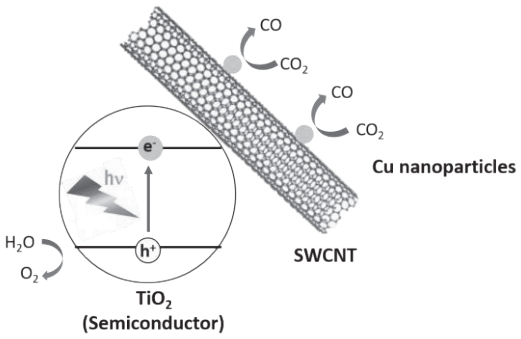

Fig.1 TiO_2/SWCNT/Cu complex as a photo-catalyst for CO_2 reduction

We first loaded Cu nanoparticles of various sizes on the surface of SWCNT, synthesized SWCNT/Cu nanoparticles complex, then examined the relationship between the size of Cu nanoparticles and the selectivity of CO_2 reduction process. Cu nanoparticles were synthesized using two methods: one is pulse electrodeposition, the other is vapor phase method (pyrolysis of Cu complex). We attempted to control the size of Cu nanoparticles in both methods. We used the resulting complex to evaluate the electrocatalytic activity using constant potential electrolysis. We carried out these experiments in 1 M aqueous solution of $KHCO_3$ (CO_2 sat.), and we analyzed the gaseous species generated by the catalytic reaction using gas chromatography (GC). We found that the vaper phase method allowed the synthesis of smaller nanoparticles than those synthesized in the pulse electrodeposition method, and had improved selectivity as well.

Corresponding Author: S. Kawasaki E-mail: kawasaki.shinji@nitech.ac.jp

Precise carrier density control of SWCNTs by controlled filling of donner and accepter molecules

○Guowei Wang, Takeshi Tanaka, Atsushi Hirano, and Hiromichi Kataura*

Nanomaterials Research Institute, National Institute of Advanced Industrial Science and Technology (AIST), Tsukuba, Ibaraki 305-8565, Japan

Electric power generation devices can be fabricated by moving an electrolyte droplet on a thin single-wall carbon nanotube (SWCNT) film. The carrier density of the SWCNT film should be controlled precisely for the optimization of the system. In this study, we report the controlled filling of electron donner and accepter molecules into SWCNTs [1]. The *N,N*'-bis(3-pentyl)perylene-3,4,9,10-bis(dicarboximide) (PBI) and 2,4-bis[4-(*N,N*-diphenyl amino)-2,6-dihydroxyphenyl]squaraine (DPSQ) were selected as donner and accepter molecules, respectively. PBI (or DPSQ) was mixed with coronene in a 1,4-dioxane, and the solution was refluxed with dispersed SWCNTs (EC1.5, Meijo Nano Carbon, unsorted). The SWCNTs were washed repeatedly to remove the residual chemicals on the surface and applied for optical absorption measurements. As shown in Fig. 1, the dopant molecule density inside the SWCNTs can be changed by simply adjusting the concentration ratio of dopant molecule to coronene. This method represents a new way to control the carrier density of SWCNTs precisely. We will show our recent results in the presentation.

This work was supported by JST CREST Grant Number JPMJCR16Q2, Japan.

Reference

[1] T. Takenobu et al. Nat. Mater. 2, 683 (2003).

Corresponding Author: H. Kataura
Tel: +81-29-861-2551, Fax: +81-29-861-2786,
E-mail: h-kataura@aist.go.jp

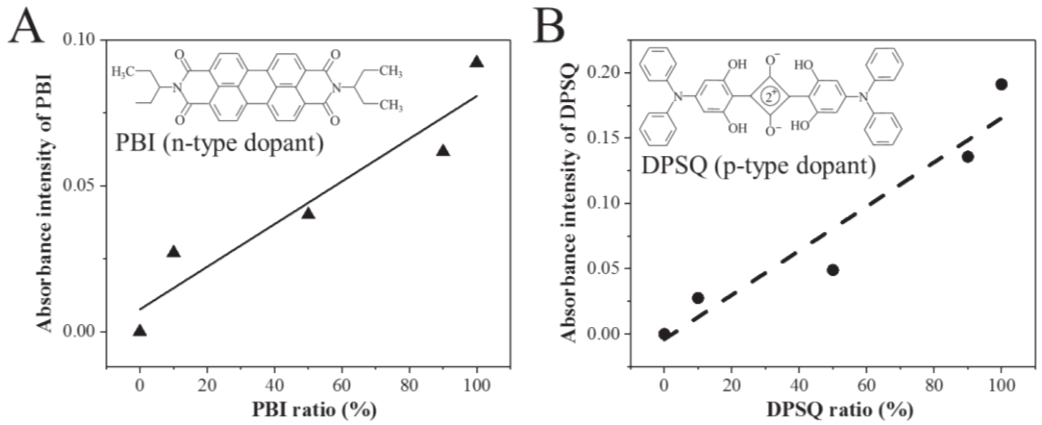

Fig. 1: The relationship of the optical absorbance intensity of encapsulated dopant molecules (PBI (A) and DPSQ (B)) with the dopant molecule ratio in the mixture of dopant and coronene molecules. Inset: the chemical structures of PBI (A) and DPSQ (B).

Novel Preparation Method of Carbon Nanobrushes using CO_2 Laser Ablation

○Ryota Yuge, Kiyohiko Toyama, Mayumi Kosaka, and Hideyuki Sato

System Platform Research Laboratories, NEC Corporation, Tsukuba 305-8501, Japan

Fibrous aggregates of single-walled carbon nanohorns, named as carbon nanobrushes (CNBs), were recently discovered [1-3]. The CNBs are receiving a lot of attention as electrode materials for various devices such as nanocarbon-polymer actuators, electric double-layer capacitors, and fuel cells since they have high electrical conductivity, high dispersibility in solutions, and large specific surface areas [1-3]. The CNBs are prepared by CO_2 laser ablation of an iron-containing carbon target under a nitrogen atmosphere at room temperature. For the large scale production of nanocarbons such as carbon nanohorns (CNHs), continuous laser ablation on spirally rotating target with a cylindrical form is very effective [4]. However, CNBs cannot be prepared continuously by this method since the catalyst containing in the vicinity of laser spots evaporates during laser ablation and the carbon in target also deteriorates. In this study, we succeeded in the continuous production of CNBs by using a novel method. The structures of obtained samples were also investigated in detail.

Cylindrical targets of 17 mm in diameter and 70 mm in length were ablated along the longitudinal direction of them by CO_2 laser at room temperature under ambient pressure. The CO_2 laser was operated at the power of 3.2 kW in the continuous-wave mode. The moving velocity of the target was controlled in the range of 0.13-0.47 cm/s. The gas pressure in the growth chamber was kept at 700-800 Torr by controlling the evacuation rate while the buffer gas of nitrogen was kept at a flow rate of 10 L/min. The carbon targets containing the iron (1, 3 at. %) were used.

The production rates of samples were 5-30 mg/s, which were larger than those of former preparation method [1-4]. From scanning electron microscopy and scanning transmission electron microscopy observations, CNBs were found to be prepared effectively when the moving velocity of target was slow. The CNB quantities prepared at 3 at. % of the iron concentration were much larger than those at 1 at. %. Therefore, CNB quantities strongly depend on the catalyst concentration. The details will be discussed in the presentation.

[1] R. Yuge *et al*. Adv. Mater. **28**, 7174 (2016).

[2] R. Yuge *et al*. Carbon **122**, 665 (2017).

[3] R. Yuge *et al*. Carbon **138**, 379 (2018).

[4] T. Azami *et al*. J. Phys. Chem. C **112**, 1330 (2008).

Corresponding Author: R. Yuge

Tel: +81-29-850-1566, Fax: +81-29-856-6137,

E-mail: r-yuge@bk.jp.nec.com

Topological phases in graphene nanoribbons

○Mari Ohfuchi[1]

[1]*Fujitsu Laboratories Ltd. & Fujitsu Limited, Atsugi 243-0197, Japan*

Graphene nanoribbons (GNRs) with atomic precision control of their edge and width have been synthesized from molecular precursors [1]. The topology of their electronic states has been paid attention, because it may lead to novel applications. When two insulators of different topological classes are joined, localized boundary states are produced in the band gap, which are so-called symmetry-protected topological (SPT) phases. Recently, it has been reported [2] that semiconducting GNRs of different width, edge, and end termination belong to different electronic topological classes. They have also shown that lateral junction geometry between two GNRs of distinct topology produces localized junction states. Cut termination is considered to be a junction with the vacuum. In this study, we investigate the SPT phases in cut terminated GNRs, i.e., the topological edge states, using density functional theory (DFT) calculations. When armchair graphen nanoribbons (N = 3, 3AGNR) are teminated as shown in Fig.1(a) (3AGNR-2(a)), the topological edge states appear in the band gap. Figure 2 shows that for 3AGNR-6(a), the anti-ferromagnetic (AF) state is slightly more stable than the ferromagnetic (FM) state. In the AF state, each spin state is localized at each edge of cut terminated AGNRs.

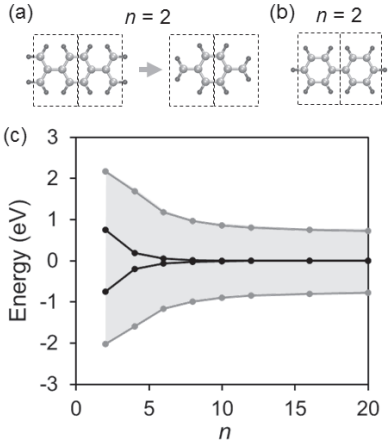

Fig. 1: (a) (b) Atomic geometries of 3AGNR-2(a) and -2(b). The gray and black spheres represent carbon and hydrogen atoms. (b) Electronic structures for 3AGNR-n(a). The black circles indicate the energy levels of the topological edge states in the band gap (gray area).

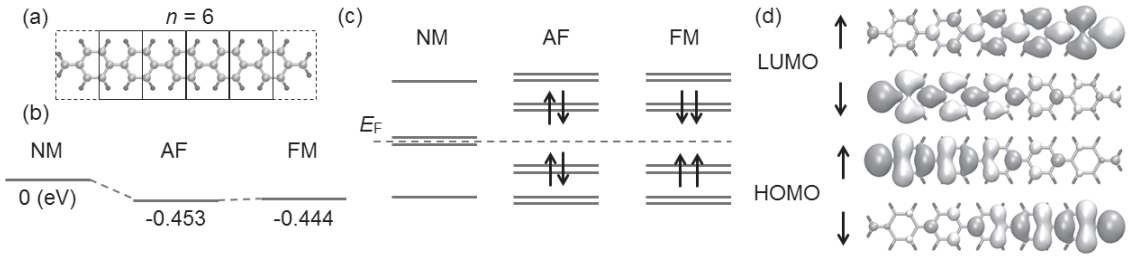

Fig. 2: (a) Atomic geometry of 3AGNR-6(a). (b) (c) Schematic diagrams of the total energies and the electronic structures for non-magnetic (NM), anti-ferromagnetic (AF), and ferromagnetic (FM) states. The arrows denote the spin orientations. (d) Molecular orbitals of the topological edge states for the AF state.

This work was partly supported by JST, CREST (No. JPMJCR15F1).

[1] J. Cai et al., Nature 466, 470 (2010).
[2] T. Cao et al., Phys. Rev. Lett. 119, 076401 (2017).

Corresponding Author: M. Ohfuchi, Tel: +81-46-250-8194, E-mail: mari.ohfuti@fujitsu.com

In situ XRD measurement of precipitation of multilayer graphene

○Jumpei Yamada[1], Yuki Ueda[1], Takahiro Maruyama[2], and Shigeya Naritsuka[1]

[1]*Department of Materials Science and Engineering, Meijo University, Nagoya 468-8502, Japan*
[2]*Department of Applied Chemistry, Meijo University, Nagoya 468-8502, Japan*

In the precipitation method, multilayer graphene is grown only by annealing a sample on which a solid carbon and catalyst are deposited. In order to obtain high quality multilayer graphene, it is necessary to understand the behavior of carbon atoms during annealing process. X-ray diffraction (XRD) measurement is one of excellent methods to analyze inside of the crystals. However, it is difficult to evaluate these carbons in an ordinary XRD equipment. Therefore, in this study, the precipitation method was in situ monitored using X-ray diffraction measurement (XRD) on BL11XU of SPring-8.

Amorphous carbon (a-C) (5 nm) and Ni (300 nm) layers were deposited on a sapphire (0001) substrate using electron-beam deposition. The sample was loaded in an ultra-vacuum chamber and annealed. The sample was pre-annealed at 300 ^{o}C, and the temperature was increased to 850 ^{o}C at a rapid rate. After the annealing for 2hr 20min, the temperature was cooled to 300 ^{o}C at a rapid rate. During the whole process, the sample was continuously monitored by using in situ XRD.

Fig.1 (a) shows an optical microscope image and the Raman spectrum of the sample. The detections of G and G' peaks indicate that multilayer graphene were successfully precipitated. Fig.1 (b) shows the intensity dependence of graphite (002) diffraction peak during the annealing. The intensity increased with two steps. First, precipitation of carbon through grain boundaries occurred at a low temperatures. Then, the graphene was further precipitated because carbon in Ni catalyst exceeded its saturation limit during the annealing at 850 ^{o}C. The peak intensity was also significantly increased during the cooling period. This corresponds to the precipitation of carbon dissolved in the Ni catalyst by cooling.

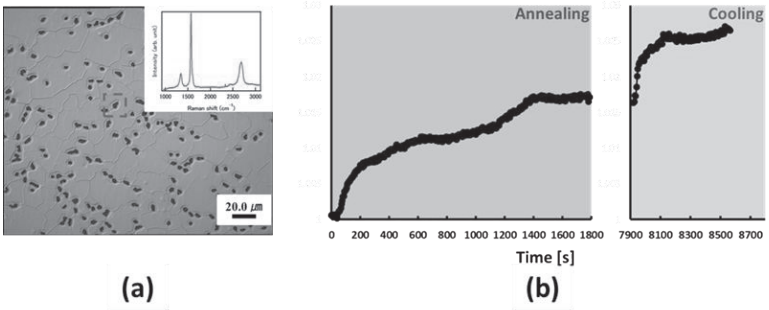

Fig. 1 (a) Optical microscope image and Raman spectrum of sample. (b) Intensity dependence of graphite (002) diffraction peak during direct precipitation of multilayer graphene.

Acknowledgement: This work was supported in part by JSPS KAKENHI Grant Numbers 2660089, 15H03558, 26105002, 25000011.

The X-ray diffraction measurements at SPring-8 were performed with the approval of the Japan Synchrotron Radiation Institute (Nos. 2016A1003, 2017B3584, 2018A3588, 2018B3588 and 2019A3589).

Corresponding Author: J.Yamada, E-mail: jjjjjjyyyyyy119@gmail.com

Direct growth of multilayer graphene on SiO_2 / Si substrate by precipitation method using nanodiamond ～Cooling rate dependence～

○Tatsuya Kashio[1], Asato Nakashima[1], Daichi Yamamoto[1],
Takahiro Maruyama[2], and Shigeya Naritsuka[1]

[1] *Department of Materials Science and Engineering, Meijo University Nagoya 468-8502, Japan*
[2] *Department of Applied Chemistry, Meijo University, Nagoya 468-8502, Japan*

Graphene is a promising material expected to be applied to various fields because of its excellent properties. In order to apply graphene to devices, it is necessary to grow graphene with good crystallinity even at low temperature. We have successfully grown graphene directly on the desired substrate at 400 °C by precipitation method using nanodiamond [1]. However, low-temperature-grown graphene is still with poor crystalline. So, in this research, we investigated the effect of the cooling rate on the precipitation of graphene using nanodiamond.

The Si substrate was annealed in air to form 300 nm thick SiO_2 on the surface. Further, Ni was deposited to a thickness of 100 nm using an electron beam deposition, and then nanodiamond was applied. The sample was annealed at 600 °C for 30 minutes in a vacuum. The cooling rate was changed among natural cooling, −10 °C/min, −5 °C/min, and −1 °C/min. Thereafter, the Ni layer was etched off using nitric acid to reveal the graphene on the SiO_2 / Si substrate.

Each Raman spectrum in Fig. 1 shows that multilayer graphene is successfully grown directly on SiO_2. From Fig. 2, the D/G ratio decreased as the cooling rate decreased. The crystallinity of graphene was improved with cooling rate decreased. This ascribes to the reduction of low quality three-dimensional nucleation observed in the naturally cooled sample. As a result, we succeeded in directly growth of high-quality multilayer graphene with D/G ratio of 0.36.

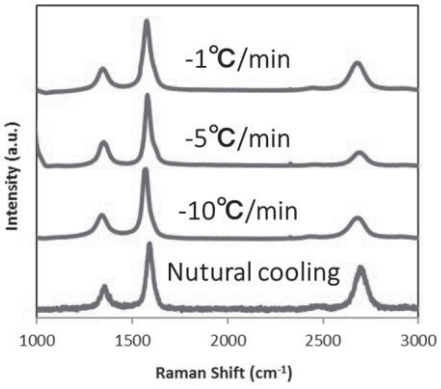

Fig. 1 Raman spectrum of multilayer graphene with growth temperature of 600 °C

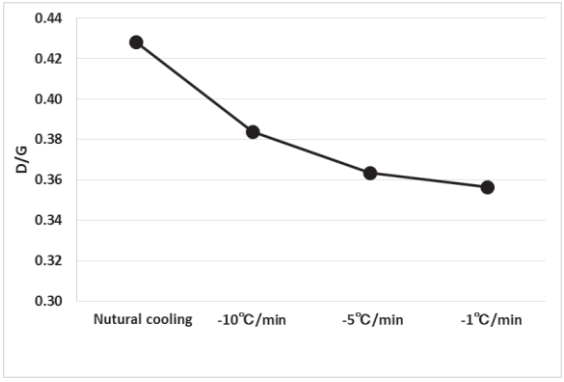

Fig. 2 D/G ratio vs cooling rate dependence

[1] Daichi Yamamoto et al. The 79th JSAP Autumn Meeting 19p-311-11

Acknowledgment: This work was supported in parts by JSPS KAKENHI Grant Numbers 2660089, 15H03558, 26105002, 25000011

Influence of the Au clusters at the graphene pore edge on the vibrational spectra of nucleotides translocating through the pore

○Tatiana Zolotoukhina[1], Momoko Yamada [1]

[1] *Department of Mechanical Engineering, University of Toyama, Toyama 930-8555, Japan*

Recently, surface-enhanced Raman scattering nanoprobes have shown tremendous potential in oncological imaging owing to the high sensitivity and specificity of their fingerprint-like spectra. As current Raman scanners rely on a slow, point-by-point spectrum acquisition, there is an unmet need for faster imaging to cover a clinically relevant area in real-time [1]. The gradual development of single-molecule resolution in the tip-enhanced and surface-enhanced Raman spectroscopy (TERS & SERS) promotes experimental work on DNA and protein identification by above methods and approaches a single oligomer resolution [2-3].

Therefore, studying vibrational spectra of the nucleotides in the dynamic interaction with the metallic nanoparticles (NP) located close to graphene nanopore can combine translocation localization and nucleotide interaction enhancement due to (1) graphene LJ interaction, (2) Au LJ interaction. The spectral maps of the nucleotides were studied by molecular dynamics (MD) simulation. Fourier transfer of the density of states (DOS) let us obtain the spectra of various bonds in reaction coordinates for DNA nucleotides during transport through the 1.5nm graphene nanopore and interaction with the Au NP at the edge of the pore. We test the nucleotide-graphene-NP system to understand whether the LJ interaction with Au NP at the translocation time can influence the changes in the vibrational spectra calculated by MD. The frequencies that can serve as markers of the corresponding Au – nucleotide interaction will be evaluated. Presence of the NP as plasmon enhances in the experimental SERS/TERS systems being in the LJ interaction with the measured molecule has a probability to influence the transient spectra. The size and shape of the NP were taken to be a stable configuration [4].

The Au_{20} and Ag_{20} nanoparticles were pyramid-shaped and optimized in ab initio DFT GGA calculations with the b3pw91 basis set. The obtained configuration was further relaxed by the MD calculation with the EAM potential and free boundary conditions during 3000step with Δt=0.1fs at T=300K to get stable nanoparticle samples that can be used on the top of the graphene sheet.

Fig1 Optimized by DFT GGA calculations Au20 and Ag20 nanoparticles

[1] S. Pal, A. Ray, C. Andreou, Y. Zhou, et al., *Nature Comm.*, 10, 1926 (2019)
[2] L.-J. Xu, Zh.-Ch. Lei, J. Li, et al., *JACS,* 137, 5149-5154 (2015).
[3] D.M. Sagar, L. E. Korhoj, K. B. Hanson, et al., *Small* 14, 1703165 (2018)
[4] J. Wang, G. Wang, J. Zhao, *Chem. Phys. Lett.,* 380, pp.716–720 (2003).

Corresponding Author: T. Zolotoukhina
Tel: +81-76-445-6739, Fax: +81-76-445-6739, E-mail: zolotu@eng.u-toyama.ac.jp

Co-Intercalation of Metal Chlorides in Large-Area Bilayer Graphene

○Amane Motoyama[1], Kenji Kawahara[2], Rika Matsumoto[3], and Hiroki Ago*[,1,2]

[1] IGSES, Kyushu University, Fukuoka, 816-8680, Japan, [2] Global Innovation Center (GIC), Kyushu University, Fukuoka, 816-8680, Japan, [3] Faculty of Engineering, Tokyo Polytechnic University, Kanagawa 243-0297, Japan

Bilayer graphene (BLG) has been attracting a significant interest, because it shows excellent properties, such as a tunable band gap [1] and angle-dependent superconductivity [2]. BLG has a well-defined unique 2D nanospace which can be used to intercalate molecules or ions to alter the physical properties. Several intercalants have been reported for BLG, such as metal chlorides ($FeCl_3$ [3] and $MoCl_5$ [4]), Ca and Li ions [5,6]. However, most of the previous works used small flakes of BLG, limiting the practical applications. In the case of graphite, co-intercalation was reported to give significant improvement in the electrical conductivity [7]. Here, we demonstrate the co-intercalation of two different metal chloride molecules into large area BLG produced by a CVD method.

Large-area BLG sheet was grown by CVD using a Cu-Ni(111) alloy thin films as catalyst [8]. The Raman spectroscopy analysis indicated the presence of both AB- and twist-stacked BLG, with a high bilayer coverage (>80%). After transferring the as-grown BLG onto a SiO_2 substrate, both $AlCl_3$ and $CuCl_2$ were simultaneously intercalated in the BLG sheet in vacuum. Figure 1a shows the Raman spectra of AB- and twist-stacked BLG before and after the intercalation process. Both the AB- and twist-stacked regions exhibited the upshift of the G-band to >1612 cm^{-1}, indicating effective intercalation. We found that the intercalation occurs more frequently in the twisted areas as compared with the AB-stacked areas. Under our experimental condition, around 70 % of the graphene area was intercalated with $AlCl_3$ and $CuCl_2$ (see Fig. 1b). This work presents a new strategy to tune the physical properties of BLG, which can be developed to various applications thanks to large-area availability of BLG sheets.

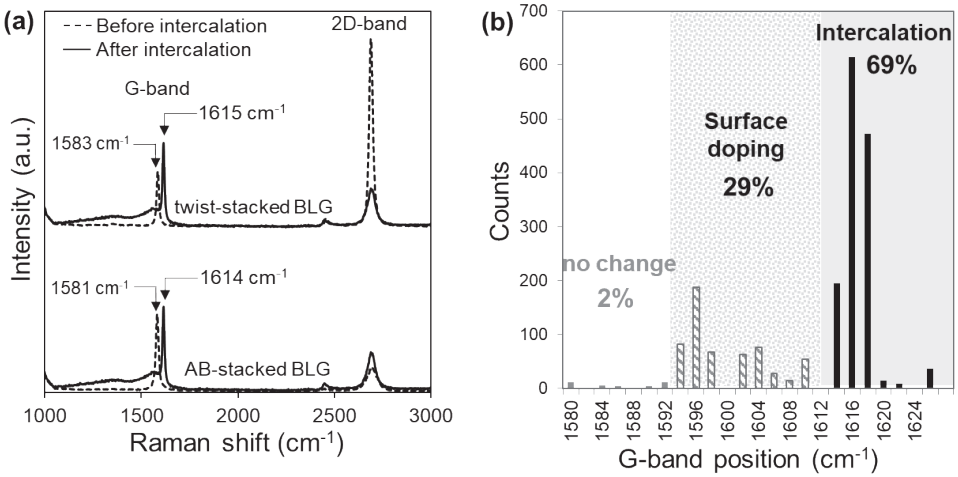

Fig. 1. (a) Raman spectra of AB- and twist-stacked BLG before and after the intercalation process with $AlCl_3$ and $CuCl_2$. (b) Histogram of the G-band position after the intercalation process.

References: [1] Y. Zhang *et al.*, *Nature*, **459**, 820 (2009). [2] Y. Cao *et al.*, *Nature*, **556**, 43 (2018). [3] I. Kharapach *et al.*, *Adv. Mater.*, **24**, 2844 (2012). [4] H. Kinoshita *et al.*, *Adv. Mater.*, **29**, 1702141 (2017). [5] S. Ichinokura *et al.*, *ACS Nano*, **10**, 2761 (2016). [6] M. Kühne *et al.*, *Nat. Nanotechnol.*, **12**, 895 (2017). [7] R. Matsumoto *et al.*, *Synth. Met.* **222**, 351 (2008). [8] Y. Takesaki *et al.*, *Chem. Mater.*, **28**, 4583 (2016).
Corresponding: H. Ago (Email: h-ago@gic.kyushu-u.ac.jp)

Role of the Hall conductivity in the optical absorption of circularly polarized light

F. R. Pratama, M. S. Ukhtary, R. Saito[1]
[1]Department of Physics, Tohoku University, Sendai 980-8578, Japan

Two-dimensional (2D) hexagonal materials, such as h-BN, silicene, & MoS_2 have promising applications in valleytronics and optical devices due to the occurrence of valley polarization (VP) and circular dichroism (CD). The electronic structure of the 2D materials can be generally expressed by the Haldane model [1], in which the inversion (I) and time-reversal (T) symmetries are broken. The broken I and T cause the band gap opening with different magnitude at the K and K' points.

Recently, Ghalamkari et al. [2] showed by the dipole approximation that VP as well as perfect CD occur *exclusively* in the material given by the Haldane Hamiltonian at the energy gap of the K and K' points. However, they did not discuss the absolute value of optical absorption probability as a function of laser excitation energy, which should be important for discussing the real materials. In this presentation, by using the Kubo formula [3], we calculate the longitudinal and the Hall optical conductivities of the Haldane model as a function of the photon energy. We found that the VP and perfect CD can be explained the Hall conductivities of the Haldane materials. We also found that the origin of the CD is the absence of the Joule heat for the left- or right-handed circularly polarized light that does not absorb the light, due to the cancellation of the longitudinal and the Hall current. We generalize our formula to include the absorption of elliptically polarized light and the depolarization effect in the materials, where the Hall conductivity enhances the depolarization effect.

[1] F. D. M. Haldane, Phys. Rev. Lett. 61, 2015 (1988).
[2] K. Ghalamkari et al. J. Phys. Soc. Jpn. 87, 063708 (2018).
[3] L. A. Valkovsky, A. A. Varlamov, Eur. Phys. J. 56, 281 (2007).

Corresponding author:
F. R. Pratama
E-mail: pratama@flex.phys.tohoku.ac.jp

Electrostatic properties of positively charged graphene edges terminated by functional groups

○Yanlin Gao, Susumu Okada

Graduate School of Pure and Applied Sciences, University of Tsukuba, Tsukuba, 305-8571, Japan

Field ion microscopy (FIM) is a simple microscopic technique providing the atomic-resolution image of the protruded surface of bulk materials and edges/tips of low dimensional materials. Rare gas atoms, which have been introduced to the sharp tips or edges of a material, are ionized and accelerated by the strong positive electric field, forming atomic-resolution images on the screen. These images reflect the atomic structure of surfaces, edges, or tips of matters. To give microscopic dynamics of the ionized rare gas atoms outside the graphene, it is mandatory to know the electrostatic properties of positively charged graphene edges. In our previous work, the field emission of electrons from graphene edges is sensitive to the edge shapes and terminations [1,2]. However, theoretical knowledge about the electrostatic properties of positively charged graphene edges in terms of their edge shapes and termination is absent to date. Thus, in this work, we aim to clarify the electrostatic properties of functionalized graphene edges under the positive electric field, using the density functional theory with the effective screening medium methods, to simulate the FIM of the functionalized edge of graphene. Fig. 1 shows the calculation model simulating the FIM of graphene edges terminated by various functional groups, where the holes are injected into the graphene edges by the counter electrode.

Our calculations showed that electrostatic properties of graphene edges under the positive electric field strongly depend on the edge shapes and terminations. The zigzag edges cause shallower potential and stronger electric field around the edge than the armchair edges under holes injection. Furthermore, we also calculated the distribution of the injected holes in graphene and found that accumulated hole also depends on the edge shape and termination. For zigzag edges, holes are primarily distributed at the terminated edges in accordance with the electrostatic potential and electric field. While, for armchair edges, the holes are not only accumulated in the functional edges, but also penetrated inside graphene.

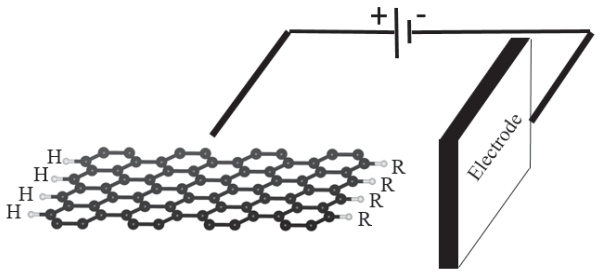

Fig.1 calculation model simulating the FIM of GNRs

Reference

[1] Y. Gao and S. Okada, *Appl. Phys. Lett.* **112**, 163105 (2018)
[2] Y. Gao and S. Okada, *Carbon* **142**, 190-195, (2019)

Corresponding Author: Y. Gao
TEL: +81-29-853-5921, FAX: +81-29-853-5924
E-mail: ylgao@comas.frsc.tsukuba.ac.jp

Influence of capacitance on field intensity in nano-scale filed emitters based on carbon nanotubes

○Keita Funayama[1, 2], Hiroya Tanaka[1], Jun Hirotani[2], Keiichi Shimaoka[1], Yutaka Ohno[2, 3], Yukihiro Tadokoro[1]

[1] *Toyota Central Research & Development Laboratory, Inc., Nagakute 480-1192, Japan*
[2] *Department of Electronics, Nagoya University, Nagoya 464-8603, Japan*
[3] *Institute of Materials and Systems for Sustainability, Nagoya University, Nagoya 464-8603, Japan*

Nano-mechanical electromagnetic receiver for sensing devices and wireless communication has investigated [1-3]. These innnovative systems translate the received electromagnetic signal into field emission (FE) current. This widely known physical phenomenon is described by Fowler-Nordheim theory i.e. $I = C_1\beta^2{\xi_{\mathrm{ex}}}^2\exp[-C_2/\beta\xi_{\mathrm{ex}}]$ where C_1 and C_2 are the constants. Enhancement factor, β, is a key parameter in designing of FE devices. This factor is traditionally discussed in terms of the shape of the emitter. Although the counter electrode is assumed as an infinite size of plate and its surface is considered as flat, the anode in nano-scale FE devices becomes narrow and thin electrode. Here, we investigate the influence of geometrical properties of the counter electrode on the enhancement factor.

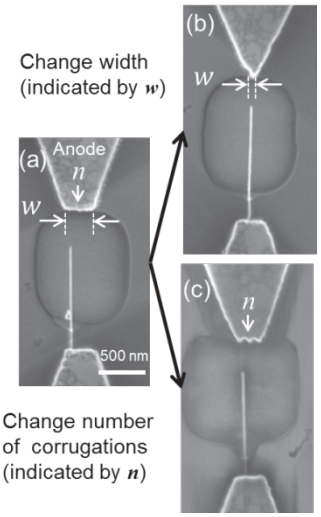

Fig. 1 SEM image of the nano-emitter made of CNT. (w, n) = (a)(300nm, 0) (b)(50nm, 0), and (c)(300nm, 3).

We fabricated the CNT emitters, whose counter electrode has different surface area, on a wafer. The surface area was varied by changing electrode width or number of corrugations as shown in Fig. 1. The nano-emitters were fabricated by electron-beam (EB) lithography, EB deposition, wet-etching and critical drying [3]. Our experimental results in Fig. 2 show that β increases as the surface area of the counter electrodes, S_{Anode}, increases. The reason is the increasing of the capacitance between the tip and the counter electrode, $C = Q/V$, where Q is the total induced charge on the tip of emitter. In the case of the corrugated counter electrode, the value of β, which was calculated theoretically from C, showed the same trend as obtained experimentally. The results indicate that the capacitance between the tip of emitter and counter electrode should be considered carefully as well as the shape of the emitter to evaluate total enhancement effect in nano-FE devices.

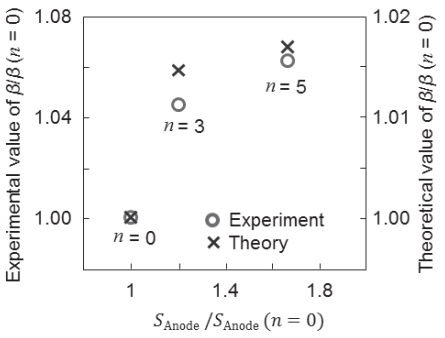

Fig. 2 The dependence of β on the surface area of counter electrode.

[1] K. Jensen, J. Weldon, H. Garcia, A. Zettl, 2007 *Nano Letters*, **7**, 11, 3508-3511.
[2] Y. Tadokoro, H. Tanaka, M. I. Dykman, 2018 *Scientific Reports*, **8** 11284.
[3] K. Funayama, H. Tanaka, J. Hirotani, K. Shimaoka, Y. Ohno, Y. Tadokoro, 2019 *IEEE Access* **7** 57820.

Corresponding Author: K. Funayama E-mail: funayama@mosk.tytlabs.co.jp

Growth of single-walled carbon nanotubes on chemically etched graphene layers by cold-wall CVD using Ir catalysts

Aliza Khaniya Sharma[1], Kamal P Sharma[2], Mayumi Saeki[1], Takahiro Saida[1,2], Shigeya Naritsuka[3], Takahiro Maruyama[1,2]

[1]*Department of Applied Chemistry, Meijo University, Japan*
[2]*Nanomaterials Research Center, Meijo University, Japan*
[3]*Department of Materials Science and Engineering, Meijo University, Japan*

1. Introduction

The widespread application of layered graphite as a promising nano-platform for biomedical, environmental and electronics have attracted much interest in the manufacturing of graphene and its derivatives. [1] The formation of graphene and carbon nanotube (CNT) hybrid structure is highly desirable for future nanoscale electrical and mechanical devices. Previously, our group succeed in synthesizing small diameter single-walled CNTs (SWCNTs) on the graphene layer by using Pt as a catalyst. [2]. However, the density of SWCNTs were not so high. In this study, to increase the density, we attempt to grow SWCNTs on graphene layers by alcohol catalytic chemical vapor deposition (ACCVD) using an Ir a catalyst.

2. Experimental procedure

A few graphene layers were peeled out from highly oriented pyrolytic graphite (HOPG) by mechanical exfoliation method and were transferred onto the Si/SiO_2 substrate. Graphene/SiO_2/Si substrate was then immerged in a mixed acid solution [(60%HNO_3:35%HCl) =1:3, v/v] for 20 min, followed by rinse with methanol, acetone and de-ionized water. Ir catalyst particles were deposited by a pulsed arc plasma gun. The nominal thickness of Ir was 0.2 nm. SWCNT growth was carried out at 800°C under an ethanol pressure of 40 Pa. The growth SWCNTs were characterized by Raman spectroscopy and FESEM.

3. Results and Discussion

Fig. 1 (a,b) show Raman Spectra of SWCNTs grown on chemically etched graphene layers. Radial breathing mode (RBM) peaks were observed, indicating that SWCNTs were grown on graphene layers. Fig1. (c) shows an FESEM image of the SWCNT grown under the same condition mentioned above. The image of SWCNTs grown on graphene is shown in inset. We will also discuss the density of grown SWCNTs.

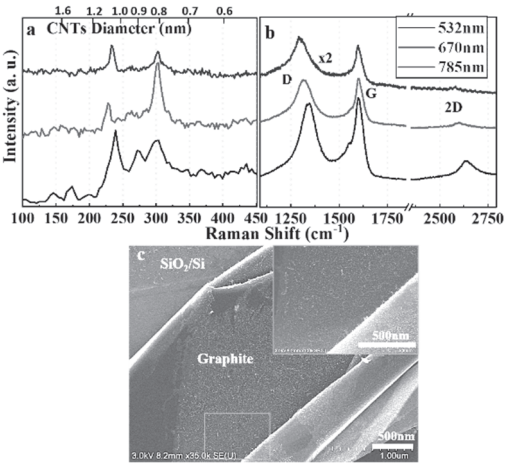

Fig. (a, b) Raman spectra of SWCNTs grown on chemically etched graphene layers. (c) FESEM image of SWCTs grown on chemically etched graphene layers.

This work was supported in part by Private University Research Branding Project from the MEXT, Japan.

[1] Y. Sang et.al. Nano 13 (2018)1850071.
[2] R. Ghosh et al. Chem. Commun. 51 (2015) 8974.

Corresponding Author: T. Maruyama
Phone: +81-52-838-2386, Fax: +81-52-832-1172
E-mail: takamaru@meijo-u.ac.jp

Control of high-harmonic generation in single-wall carbon nanotubes by gating

○Hiroyuki Nishidome[1], Kohei Nagai[2], Kent Uchida[2], Yota Ichinose[1], Kengo Fukuhara[1], Junko Eda[1], Hitomi Okubo[1], Yohei Yomogida[1], Koichiro Tanaka[2, 3], Kazuhiro Yanagi[1]

[1] *Department of Physics, Tokyo Metropolitan University, Tokyo 192-0397, Japan*
[2] *Department of Physics, Kyoto University, Kyoto 606-8502, Japan*
[3] *Institute for Integrated Cell-Material Sciences, Kyoto University, Kyoto 606-8501, Japan*

High-power laser sources in mid-infrared and terahertz (THz) region enable us to observe the extreme nonlinear optical phenomena in solid, such as high-harmonic generation (HHG) [1]. HHG is attracting a lot of interest for their uses of ultra-fast processing and short-wavelength light source. However, the generation mechanisms of the high harmonics in solid has not been elucidated yet. It is suggested that there are two dominant dynamics which generate high-harmonics in solid. One is carrier dynamics within a band (intraband dynamics) and the other is the dynamics between bands (interband dynamics) [2]. The amount of carrier in solid will strongly influence on HHG, but how the carrier density affects HHG is not simple. For example, increase of carrier density may enhance the HHG through intraband dynamics, but at the same time, it may suppress the HHG through interband dynamics by Pauli blocking process. Therefore, it is important to experimentally reveal relationships between the carrier density, electronic structure and HHG. Here this study investigated the Fermi-level dependence of HHG by using single-wall carbon nanotubes with a selected electronic structure.

We prepared a high-purity (6,5) thin film (bandgap E_g = 1.26 eV) and employed side-gating device using ionic liquid (TMPA-TFSI) as an electrolyte to tune Fermi level by shift of gate voltage, V_G.

Figure 1 shows the high-harmonic spectra with positive shift of V_G (electron injection). Interestingly, we found the increase and the decrease of harmonics as the increase of the amount of electron. We observed the enhancement of the 3rd harmonics, but the suppression of 5th and 7th harmonics. To understand the background precisely, we calculated HHG spectra by using the Liouville equation and succeeded to reproduce qualitatively the experimental results. We found that we can control the HHG by gating in both amplificative and reductive ways.

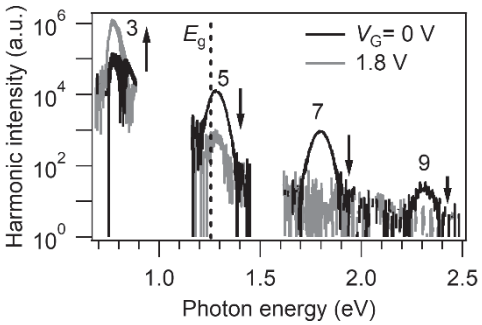

Fig. 1 High-harmonic spectra with Fermi-level (gate voltage (V_G)) shift.

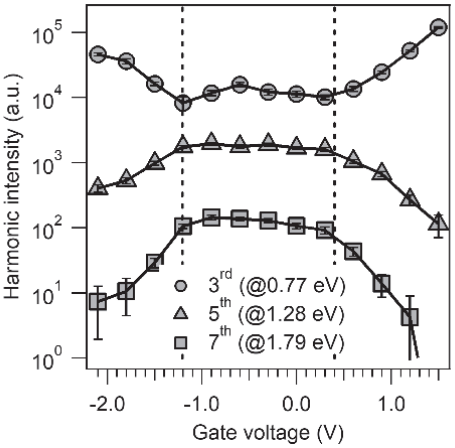

Fig. 2 Fermi-level dependence of high-harmonic intensity

[1] S. Ghimire *et al.*, Nat. Phys. **7**, 138 (2010)
[2] O. Schubert *et al.*, Nat. Photon., **8**, 119 (2014)

Corresponding Author: K. Yanagi
Tel: +81-42-677-2494,
Fax: +81-42-677-2483,
E-mail: yanagi-kazuhiro@tmu.ac.jp

Photoluminescence study of graphene quantum dots esterified with benzyl alcohol and their application to solar cells

○Suzuka Tachi, Toshiki Sugai, Shota Kuwahara

Department of Chemistry, Toho University, Chiba 274-8510, Japan

Graphene quantum dots (GQDs), nanometer-sized graphene fragments, have potential for the efficient photon conversion material due to their tunable optical and electronic properties, as well as upconversion optical characteristics [1, 2]. However, quantum yields (QYs) of GQDs are relatively low, which limits the general use of GQDs for application as luminescent materials. Herein, we report the enhancement of QY of GQDs by esterifying GQDs with benzyl alcohol, achieving the suppression of the flexibility arising from vibration and rotation of the surface functional groups on the edges of GQDs. Furthermore, GQDs esterified with benzyl alcohol (GQD-Bn) were utilized as the sensitizer of solid-state dye-sensitized solar cells (DSSCs), and GQD-sensitized solar cells (GQDSSCs) were successfully fabricated.

GQDs were prepared by using single-walled carbon nanotubes (CoMoCAT; Aldrich) via oxidation process in the mixture of concentrated H_2SO_4 and HNO_3. Then, the synthesized GQDs in water were refluxed with benzyl alcohol [3], resulting in replacing carboxyl groups on the GQDs with benzyl ester groups. After neutralization, we extracted organic soluble GQD-Bn into toluene, which was utilized for the sensitizer in GQDSSCs as previously reported [4]. GQDs esterified with 1-hexanol (GQD-Hex), aliphatic ester groups, were also used for the fabrication of GQDSSCs.

Fig. 1 shows photoluminescence excitation-emission-intensity map of GQD-Bn. The maximum emission wavelength was 432 nm, independent on the excitation wavelength and red-shifted by around 30 nm from an emission wavelength in GQD-Hex. The relative QYs of GQD-Bn and GQD-Hex were 67 and 10 %, respectively. Fig. 2 shows the current density-voltage (*J-V*) curves of GQDSSCs fabricated with GQD-Bn and GQD-Hex. All parameters, short-circuit current density, open-circuit voltage and fill factor, of GQDSSCs were improved by using GQD-Bn as the sensitizer.

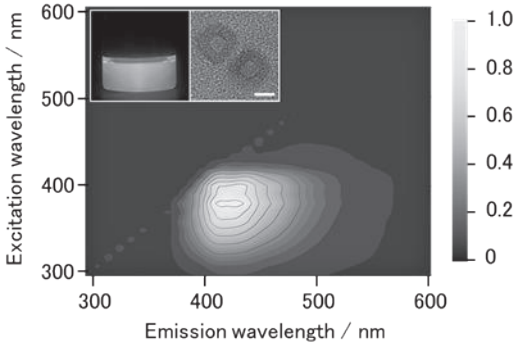

Fig. 1 Photoluminescence excitation-emission-intensity map of the GQD-Bn. Insets: photograph of GQD-Bn in toluene taken under UV illumination (λ = 410 nm) (left) and TEM image of GQD-Bn (scale bar: 10 nm) (right).

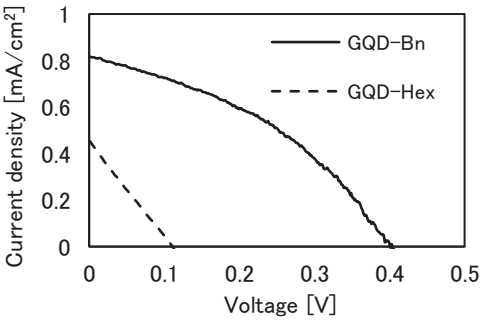

Fig. 2 *J*−*V* curves of GQDSSCs with GQD-Bn (solid line) and GQD-Hex (dashed line).

[1] S. Chen, *et al*., *J. Mater. Chem. C*, **6**, 6875 (2018). [2] S. Zhuo, *et al*., *ACS Nano*, **6**, 1059 (2012).

[3] S. Tachi, *et al.*, *submitted*.

[4] S. Tachi, *et al.*, *The 55th FNTG general symposium*, 3P12 (2018)

Corresponding Author: S. Kuwahara, Tel: +81-47-472-4442, E-mail: syouta.kuwahara@sci.toho-u.ac.jp

Interface electroluminescence from WS_2/WSe_2 in-plane heterostructures

○Naoki Wada[1], Jiang Pu[2], Wenjin Zhang[3], Zheng Liu[4], Hirofumi Matsuoka[2], Kazunari Matsuda[3], Yusuke Nakanishi[1], Yutaka Maniwa[1], Yuhei Miyauchi[3], Taishi Takenobu[2], Yasumitsu Miyata[1]

[1] *Department of Physics, Tokyo Metropolitan University, Hachioji 192-0397, Japan*
[2] *Department of Applied Physics, Nagoya University, Nagoya 464-8603, Japan*
[3] *Institute of Advanced Energy, Kyoto University, Uji, 611-0011, Japan*
[4] *Inorganic Functional Materials Research Institute, AIST, Nagoya, 463-8560, Japan*

Heterostructures of transition metal dichalcogenides (TMDCs) are an attractive system to realize high-performance devices such as light-emitting diodes and tunnel field-effect transistors. To realize such devices, it is important to understand the electrical and optical properties of TMDC-based heterointerface. Recently, electroluminescence (EL) has been observed for MoS_2/WSe_2 in-plane heterostructures by using electric-double layer technique [1]. In the previous study, the samples show EL peak only from monolayer MoS_2 due to strain-induced modulation of band alignment. However, less study has been conducted for such strain effect on the optical spectra of TMDC-based heterointrerface.

In this study, we report the characteristic EL from the strained heterointerface of WS_2/WSe_2 in-plane heterostructures. WS_2/WSe_2 in-plane heterostructures were grown on SiO_2/Si substrates by salt-assisted chemical vapor deposition (CVD). To observe EL, we have fabricated the EDLEDs with ion gel. The devices show linear light emission from the interface by applying voltage (Fig.1b). The EL spectra show two peaks, which can be assigned to exciton peaks of WS_2 and WSe_2. Interestingly, the PL peaks are shifted compared with these for PL spectra. These shifts can be explained by lattice strain in WS_2/WSe_2 lattice mismatched interface. Furthermore, valley polarization was also observed for WS_2 exciton peak even at room temperature probably due to valley magnetoelectric effect [2]. The present results indicate that TMDC-based heterointerfaces provide a unique system to control and use their unique electrical and optical properties.

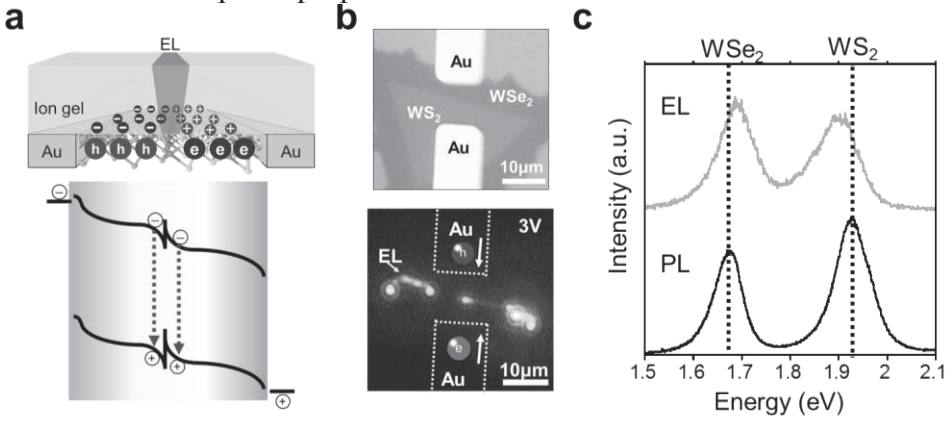

Fig.1 (a) Schematic of structure and energy band diagram of WS_2/WSe_2-based EDLED device after the formation of p-i-n junction by electric double layer doping. (b) Optical and electroluminescence (EL) images, and (c) EL and photoluminescence (PL) spectra of WS_2/WSe_2-based EDLED device.

[1] J. Pu *et al.,* ***Adv. Mater.,*** 29, 1606918 (2017). [2] J. Lee *et al*., ***Nat. Mater.***, 16, 887891 (2017).

Corresponding Author: Yasumitsu Miyata, Tel: 042-677-2508, E-mail: ymiyata@tmu.ac.jp

Simulating van der Waals Heteroepitaxy Using Classical Mechanical Approach

○Mitsuhiro Okada[1], Yosuke Uchiyama[2], Tetsuo Shimizu[1], Toshitaka Kubo[1], Ryo Kitaura[2]

[1] *Nanomaterials Research Institute, AIST, Tsukuba 305-8565, Japan*
[2] *Department of Chemistry, Nagoya University, Nagoya 464-8602, Japan*

Recent works on two-dimensional materials such as transition metal dichalcogenide (TMD) and hexagonal boron nitride (hBN) made van der Waals (vdW) heteroepitaxy regain the spotlight. vdW heteroepitaxy, i.e., "heteroepitaxial growth driven by interatomic force" has been observed on chemical vapor deposition growth on TMD onto hBN (TMD/hBN) system [1] (Figure 1). However, it is still unclear how the occurrence of vdW heteroepitaxy in the TMD/hBN system depends on the TMD cluster size.

In this work, we investigated how MoS_2 cluster size affected the vdW heteroepitaxy of MoS_2/hBN system by theoretical calculation. To calculate the total energy of optimal configuration of the MoS_2/hBN system, we used classical mechanics where the interlayer total energy can be described as a sum of the Lennard-Jones (LJ) potential and the Coulomb potential. This method allows us to treat a system containing large number of atoms (e.g., $Mo_{675}S_{1350}$ and $B_{10800}N_{10800}$), which cannot be treated on density functional theory (DFT). One of the models of the MoS_2/hBN system is shown in Figure 2. We found that considering only LJ potential is enough to simulate the MoS_2/hBN structure: the calculated interlayer distance is similar to that obtained from DFT (~0.472 and ~0.494 nm [2], respectively). Interestingly, the dependence of the calculated total energy as a function of the stacking angle and the cluster size (Figure 3) shows that structures with a stacking angle of 0 or 60 degree are strongly stabilized when the cluster size matches the lattice constant of MoS_2/hBN moiré superlattice (~four fold larger than that of the MoS_2 lattice constant. The stabilized clusters are marked with a circle in Figure 3). This indicates that moiré superlattice affects the heteroepitaxial growth at early stage.

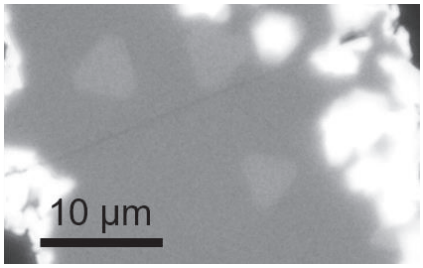

Figure 1. An optical microscope image of MoS_2 grown on hBN.

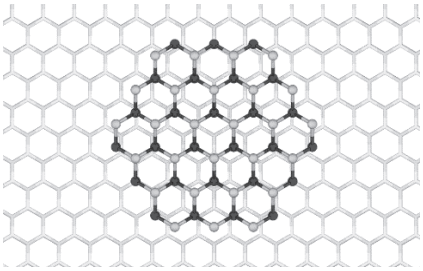

Figure 2. Structure model of MoS_2/hBN system.

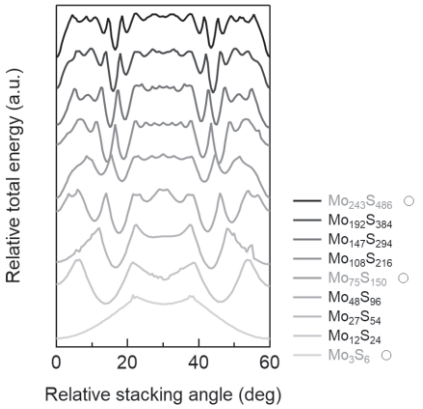

Figure 3. Total energy of MoS_2/hBN as a function of the stacking angle and its cluster size dependence.

[1] M. Okada *et al*. ACS Nano, **8**, 8273 (2014).
[2] A. P. Rooney *et al.*, Nano Lett., **17**, 5222, (2017).

Corresponding Author: M. Okada and R. Kitaura
Tel: +81-29-861-2880, +81-52-789-2477
Fax: +81-29-862-3550, + 81-52-747-6442
Web: https://unit.aist.go.jp/nmri/index.html
http://nano.chem.nagoya-u.ac.jp/japanese/
E-mail: mi.okada@aist.go.jp, r.kitaura@nagoya-u.jp

Molecular beam epitaxy growth of transition-metal-dichalcogenide based two-dimensional heterostructures

○ Yuya Murai[1], Nanami Ichinose[1], Satoshi Yasuda[2], and Ryo Kitaura[1]

[1] *Department of Chemistry, Nagoya University, Nagoya 464-8602, Japan*
[2] *Advanced Science Research Center, Tokai 319-1195, Japan*

The purpose of this study is to develop a new class of two-dimensional materials, two-dimensional superlattices (2D-SLs). The concept of "superlattices", periodic junctions of different materials, has been developed in research on compound semiconductors, leading to discoveries of novel phenomena such as negative resistance and Bloch oscillation[1]. The concept of “superlattices” can be extended to yield new type of 2D materials, 2D-SLs, which give a widespread platform to explore physics and chemistry at two-dimension. In this presentation, we focus on development of crystal growth method of 2D-SLs.

In this study, we used transition metal dichalcogenides (TMDs) as components of 2D-SLs. Various TMDs (more than 40 different TMDs are available) enable us to construct a wide variety of TMD-based 2D-SLs. For crystal growth of 2D-SLs, we employed the molecular beam epitaxy (MBE) method [2]. In the MBE method, source materials are supplied as highly directional molecular beams, and therefore, source supply can be instantaneously switched by the simple shutter operation. In this work, we have performed MBE growth of 2D-SLs composed of $MoSe_2$ and $NbSe_2$/WSe_2 by sequentially switching Mo supply to Nb/W supply under continuous supply of Se.

Figure 1 shows a dark field transmission electron microscope (DF-TEM) image of the 2D-SLs composed of $MoSe_2$ and $NbSe_2$. In this dark field image, the graphite substrate shows almost no contrast whereas 2D-SLs give strong image contrasts; the hexagonal white contrasts correspond to 2D-SLs composed of $NbSe_2$ and $MoSe_2$. The feed rates of Mo/Nb were 0.28 Å/s and 0.56 Å/s. First, $NbSe_2$ was grown for 7 minutes, and then, $MoSe_2$ and $NbSe_2$ were grown alternatively with interval of 1.5 minutes. As a result, it is considered that a 10 nm periodic superlattice is formed. Although periodic contrasts arising from the periodic lateral structure are not visible, we confirmed the existence of Nb and Mo atoms by energy dispersive X-ray analyses. The small difference in the image contrast arise from small difference in atomic numbers of Mo and Nb. For detailed structural characterization, we are working on scanning tunneling microscope observations of 2D-SLs.

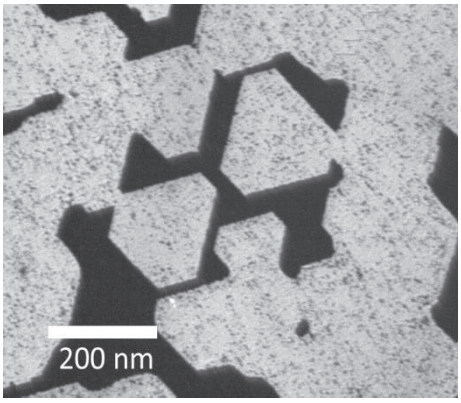

Fig.1 DF-TEM image fabricated heterostructure

[1] L. Esaki and R. Tsu, IBM J. Res. Dev. 14, 61 (1970).

[2] Hotta, T. et al., Appl. Phys. Lett., 109, 133101 (2016)

Corresponding Author: R. Kitaura
Tel: +81-52-789-2482, Fax: +81-52-747-6442
Web: http://nano.chem.nagoya-u.ac.jp/
E-mail: r.kitaura@nagoya-u.jp

Machine-learning approach for predicting low temperature valley polarization landscapes in 2D semiconductors

○Kenya Tanaka, Kengo Hachiya, Wenjin Zhang, Kazunari Matsuda, Yuhei Miyauchi

Institute of Advanced Energy, Kyoto University, Uji 611-0011, Japan,

Atomically thin two-dimensional (2D) semiconductors such as monolayer (1L) MoS_2 and WSe_2 (transition metal dichalcogenide) have attracted much attention, partially because of their potential applicability for valleytronics. Once a circularly polarized photons are absorbed by these materials, valley polarized excitons can be generated by virtue of their structures with broken inversion symmetry and large spin-orbit coupling [1-3]. The application of this phenomenon for opto-electronics, called opto-valleytronics, have also been of strong interest in the broad scientific community including condensed matter physics and more. In recent years, numbers of studies have been reported on the valley exciton properties in 2D semiconductors. The exciton valley polarization observed at low-temperature (LT) normally shows considerable spatial heterogeneity on the sample, mainly because the exciton characteristics are very sensitive to the local heterogeneity in the surrounding environment due to local defects, strain, carrier doping, and surface molecular adsorption. This heterogeneity is highly problematic for both fundamental scientific research and the future applications of these materials in valleytronic devices. However, the existence of this heterogeneity has been neglected in most of the previous studies, because a complex correlation among various local conditions and the resultant exciton valley polarization remain unclear, and there has been no established procedure to address this problem.

Here we demonstrate the applicability of employing machine-learning-based analysis to predict LT exciton valley polarization heterogeneity in 1L-WSe_2. We performed confocal photoluminescence (PL) mapping at 300 K (RT), and the exciton valley polarizations at each corresponding position (Fig. 1) were measured using circular polarization resolved PL spectroscopy at 15 K (LT). The data sets extracted from these observations were used as the input and output data to create regression forest for the machine-learning prediction using the Random Forest [4] algorithm. The created regression forest could well predict the spatial distribution of the LT exciton valley polarization in a 1L-WSe_2 that was not used for the learning of the regression forest, only from the RT PL data set of the sample. Furthermore, we numerically obtained the degree of importance of each input variable [5]. We will discuss that this procedure is quite helpful for examining the physics that shape the spatially heterogeneous valley polarization landscape of 1L-WSe_2.

[1] K. F. Mak *et al., Nat. Nanotechnol.* **7**, 494 (2012).
[2] Y. Miyauchi *et al., Nat. Commun.* **9**, 2598 (2018).
[3] K. Shinokita *et al., Adv. Funct. Mater.* 1900260 (2019).
[4] L. Breiman, *Mach. Learn*. **45**, 5 (2001).
[5] K. Tanaka *et al.,* submitted.

Corresponding Author: Y. Miyauchi
Tel: +81-774-38-3463
E-mail: miyauchi@iae.kyoto-u.ac.jp

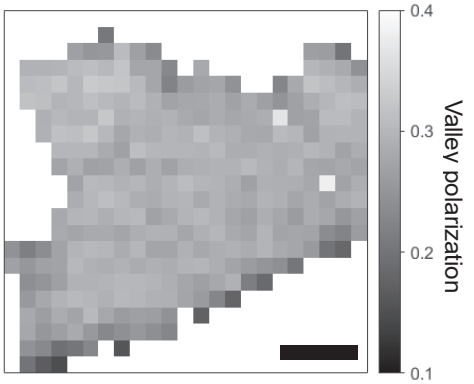

Fig.1 Exciton valley polarization map of a 1L-WSe_2 sample at 15 K. Scale bar indicates 3 μm.

Single-layer MoS_2 nanogenerator for harvesting clean electric energy from dynamic motion of liquid

○Adha Sukma Aji[1], Ryohei Nishi[1], Hiroki Ago[2], Yutaka Ohno[1]

[1] *Institute of Materials and Systems for Sustainability (IMaSS), Nagoya University, Nagoya 464-8601, Japan*
[2] *Global Innovation Center (GIC), Kyushu University, Fukuoka 816-8580, Japan*

Seeing the fact that energy demand in the world is always increasing, the researches on direct energy harvesting from the ambient environment are gaining a considerable amount of interest. As liquid kinetic energy is one of the most abundant clean energy sources, a method to directly convert liquid of motion into electricity is preferable. [1,2] Here, we demonstrate a novel MoS_2 nanogenerator to generate electricity from the liquid of movement.

In this work, the CVD grown large-area single-layer MoS_2 was used as active materials where the droplets glided on top of it. When droplets of 1 M NaCl were dropped on MoS_2 surface inclined at 45°, they automatically glided because of the hydrophobic nature of MoS_2 surface, as illustrated in Figure 1a. As the droplets glided, open-circuit voltages over 5 V were generated by MoS_2 surface, as shown in Figure 1b. This is the largest voltage generated by liquid motion on their surfaces compared with other 2D material-based nanogenerator reported so far. We also advanced our MoS_2 nanogenerator to harvest the energy of the sea wave. The experimental setup is shown in Figure 1c, where half of MoS_2 channel were submerged in simulated seawater (0.6 M NaCl). When the sequences of wave were generated, the height of seawater surface which contacted to MoS_2 surface was changed periodically. Figure 1d shows the capability of MoS_2 nanogenerator, which it could convert waving movement to electric energy up to 7.5 nW. The mechanism of the electric generation will be discussed in the presentation.

In summary, we have investigated the promising capability of MoS_2 as energy harvester from the liquid movement.

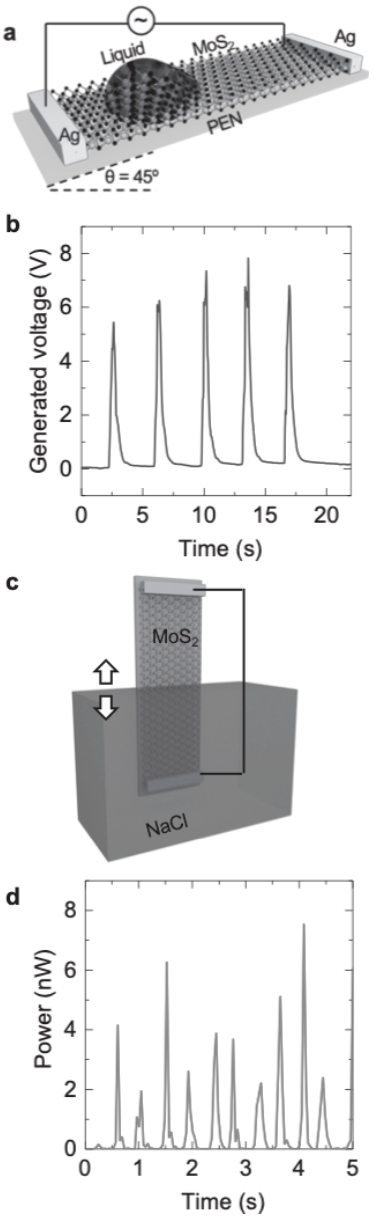

Fig. 1. (a) Schematic view of the device. (b) Generated voltage induced by liquid movement on MoS_2. (c) Schematic view of the experimental setup where the liquid surface moves up and down. (d) Generated power induced from liquid movement shown in (c)

[1] J. Yin *et al*., *Nat. Nanotechnol*. **9**, 378 (2014).
[2] S. Kwak *et al.*, *ACS Nano* **10**, 7297 (2016)

Corresponding Author: Y. Ohno
Tel & Fax: +81-52-789-5387
E-mail: yohno@nagoya-u.jp

Acknowledgment: JST/CREST (JPMJCR16Q2)

Infrared Spectral Simulation of Isotopically Manipulated C_{60}

○Tomonari Wakabayashi[1], Takamasa Momose[2], and Mario E. Fajardo[3]

[1]*Department of Chemistry, Kindai University, Higashi-Osaka 577-8502, Japan*
[2]*Department of Chemistry, University of British Columbia, Vancouver V6T 1Z1, Canada*
[3]*Munitions Directorate, US Air Force Research Laboratory, Eglin AFB, FL 32542-5910, USA*

High-resolution infrared (IR) absorption spectra of C_{60} were reported previously by our research group using solid para-H_2 matrices at 2 K [1]. Spectral features observed for four IR-active vibrational modes were analyzed by possible quantized rovibrational transitions with missing levels due to boson-exchange symmetry restrictions. In this work, we reanalyze the spectra by another idea of the mixture of a number of isotopomers present in the C_{60} sample. For the natural isotopic abundance of 1.1% ^{13}C, binomial fractions of the isotopologues are 51% for $^{12}C_{60}$, 34% for $^{13}C^{12}C_{59}$, 11% for $^{13}C_2{}^{12}C_{58}$, and 2.5% for $^{13}C_3{}^{12}C_{57}$. Molecular orbital calculations are performed for vibrational spectra of all possible isotpomers $^{13}C_n{}^{12}C_{60-n}$ up to n = 3, leading to a better agreement with the observed spectra. Molecular orbital (MO) calculations are performed for harmonic frequencies and IR absorption intensities at the B3LYP/6-31G(d) level of density functional theory (DFT). Target molecules are the icosahedral (I_h) $^{12}C_{60}$, the singly substituted $^{13}C^{12}C_{59}$ of C_s symmetry, 23 isotopomers of the doubly substituted $^{13}C_2{}^{12}C_{58}$, and 303 isotopomers of the triply substituted $^{13}C_3{}^{12}C_{57}$.

Figure 1 shows calculated IR absorption spectra of one of the four IR-active vibrational modes of C_{60}, namely $T_{1u}(3)$ observed at 1184 cm^{-1} [1,2]. For $^{12}C_{60}$, the transition is triply degenerate as T_{1u} in I_h symmetry, showing a single peak as the top trace in the inset. The degeneracy is lifted by substitution of ^{12}C by a heavier ^{13}C atom in $^{13}C^{12}C_{59}$, resulting in the split peaks toward lower frequencies as the second trace in the inset. For doubly and triply substituted molecules, split patterns are different for different substitutional sites in a molecule, resulting in multiple bands of peaks. Weighted sum spectra reproduce well the observed trend of increasing intensity of the low-frequency bands with increasing abundance of ^{13}C. The absolute IR emission band strength is discussed for the abundance of C_{60} in the planetary nebula [3].

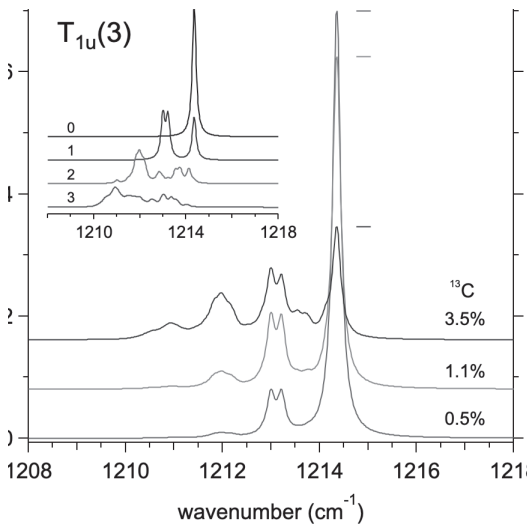

Fig. 1. Calculated IR absorption spectra of the $T_{1u}(3)$ mode of C_{60}. Inset shows spectra of isotopologues having n ^{13}C atoms, $^{13}C_n{}^{12}C_{60-n}$ of n = 0, 1, 2, and 3, containing 1, 1, 23, and 303 distinct isotopomers, respectively. Traces in the main panel are weighted sum of the inset spectra for three ^{13}C abundances.

[1] N. Sogoshi *et al*. JPCA **104**, 3733 (2000).
[2] W. Krätschmer *et al*. CPL **170**, 167 (1990).
[3] J. Cami *et al*. Science **329**, 1180 (2010).

Corresponding Author: T. Wakabayashi
Tel: +81-6-4307-3408, Fax: +81-6-6723-2721,
E-mail: wakaba@chem.kindai.ac.jp

Synthesis of Benzothieno[60]fullerenes Using Fullerenyl Cation Intermediates

○Yutaka Matsuo,[1,2,3] Yun Yu[3], Xiao-Yu Yang[3], Hiroshi Ueno[4], Hiroshi Okada[2]

[1] *Institutes of Innovation for Future Society, Nagoya University, Nagoya 464-8603, Japan*
[2] *Department of Mechanical Engineering, The University of Tokyo, Tokyo 113-8656, Japan*
[3] *University of Science and Technology of China, Hefei 230026, China*
[4] *Creative Interdisciplinary Research Division, The Frontier Research Institute for Interdisciplinary Sciences (FRIS), Tohoku University*

Benzothieno[60]fullerenes were synthesized using fullerenyl cations as key intermediates.[1] The reaction proceeded through a nucleophilic attack of the sulfur atom as a weak nucleophile to the fullerenyl cation electrophile (Figure 1).[2] A monoarylated fullerene, (2-methylthiophenyl)hydro[60]fullerene, $C_{60}ArH$ (Ar = C_6H_4-SMe-2, and so on; four derivatives) was subjected to deprotonation with KO^{t}Bu to form a fullerenyl anion ArC_{60}^-, followed by oxidation using I_2 to generate a fullerenyl cation ArC_{60}^+ leading to intramolecular demethylative cyclization via fullerene cation–S interaction to the product (Figure 2). Electrochemical and computational studies revealed slightly narrower band gap of this compound than usual fullerene derivatives because of the relatively high-lying HOMO of the fused thieno moiety.

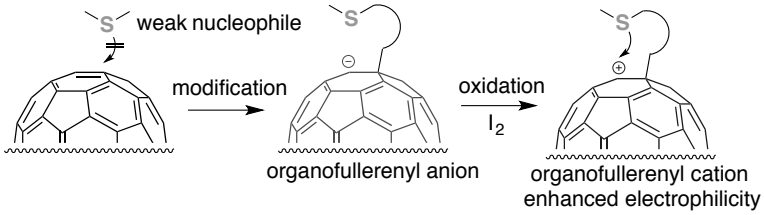

Figure 1. Concept of this study. The oxidized fullerene (fullerenyl cation) undergoes nucleophilic attack by the sulfur atom.

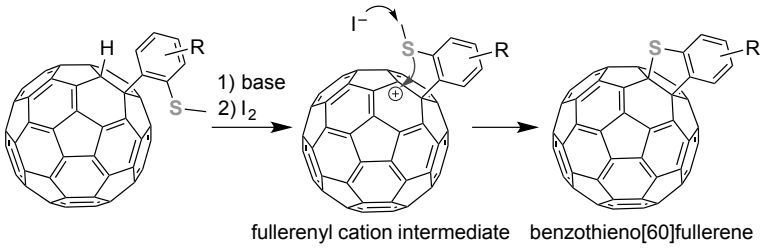

Figure 2. Synthesis of benzothieno[60]fullerenes.

[1] Y. Matsuo, Y. Yu, X.-Y. Yang, H. Ueno, H. Okada, H. Shibuya, Y. S. Choi, Y. W. Jin, *J. Org. Chem.* **2019**, *84*, 6270–6277.
[2] H.-S. Lin, Y. Matsuo, *Chem. Commun.* **2018**, *54*, 11244–11259. (Feature article)
[3] X.-Y. Yang, H.-S. Lin, I. Jeon, Y. Matsuo, *Org. Lett.* **2018**, *20*, 3372–3376

Corresponding Author: Y. Matsuo
Tel: +81-52-747-6722
Web: http://www.matsuo-lab.net
E-mail: yutaka.matsuo@chem.material.nagoya-u.ac.jp

Chirality dependence of the tensile strengths of carbon nanotubes

○Akira Takakura[1,2,3], Kou Beppu[4], Taishi Nishihara[1,2,3], Akihito Fukui[4], Takahiro Kozeki[5], Takahiro Namazu[4], Yuhei Miyauchi[1,2,3], Kenichiro Itami[1,2,6]

[1] *JST-ERATO, Itami Molecular Nanocarbon Project, Nagoya University, Chikusa, Nagoya 464-8602, Japan.*
[2] *Graduate School of Science, Nagoya University, Chikusa, Nagoya 464-8602, Japan.*
[3] *Institute of Advanced Energy, Kyoto University, Uji, Kyoto 611-0011, Japan.*
[4] *Department of Mechanical Engineering, Aichi Institute of Technology, Yakusa, Toyota, Aichi 470-0392, Japan.*
[5] *Graduate School of Mechanical Engineering, University of Hyogo, Himeji, Hyogo 671-2201, Japan.*
[6] *Institute of Transformative Bio-Molecules (WPI-ITbM), Nagoya University, Chikusa, Nagoya 464-8602, Japan.*

Single-walled carbon nanotubes (SWNTs) theoretically possess ultimate intrinsic tensile strengths of more than 100 GPa, among the highest in existing materials [1]. However, the experimentally reported values were always lower than the theoretical values, and even worse, they exhibited a considerable degree of scatter [2, 3]. Here we report the first direct measurements of the ultimate tensile strengths of individual chirality-defined SWNTs [4]. The strengths of 16 SWNTs measured in this study exhibited the strengths scattered in the range of 25-66 GPa (Figs. 1a and b). We found that the observed trend can be understood comprehensively via the intrinsic structure dependent inter-atomic stress, together with its concentration at structural defects existing in the real SWNTs (Fig. 1c). We developed empirical formula to predict the tensile strengths, and it highlights the target nanotube structures of selective synthesis, armchair or near-armchair species with relatively small diameters, to fabricate ultimately high-strength materials using SWNTs. In the presentation, we will discuss the fracture mechanism and derivation of an empirical formula to predict the ultimate tensile strength of real SWNTs.

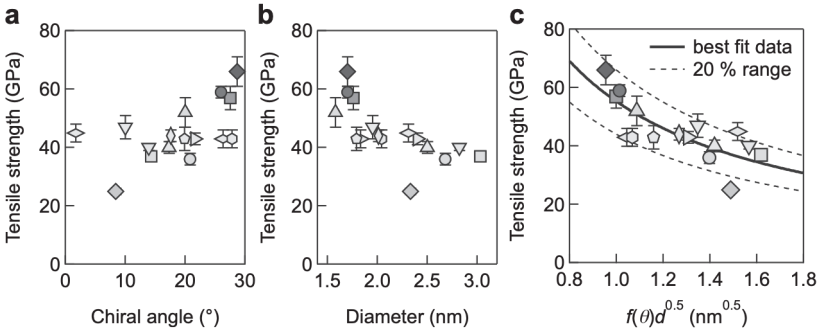

Fig. 1 The tensile strengths plotted as a function of the chiral angle (**a**), diameter (**b**) and $f(\theta)d^{0.5}$, where $f(\theta)$ is given by $(1/2)[(1-\nu)+(1+\nu)\cos 2\theta]$ ($\nu = 0.16$ is the Poisson ratio of graphite) (**c**).

[1] T. Dumitrica, M. Hua and B. I. Yakobson, *Proc. Natl. Acad. Sci. USA*, **103**, 6105 (2006).
[2] M. F. Yu *et al*., *Science*, **287**, 637 (2000).
[3] M. S. Wang, D. Golberg and Y. Bando, *Adv. Mater.*, **22**, 4071 (2010).
[4] A. Takakura *et al*., *Nat. Commun.*, **10**, 3040 (2019).

Corresponding Author: Y. Miyauchi
Tel: +81-774-38-3463
E-mail: miyauchi@iae.kyoto-u.ac.jp

In-plane and out-of-plane thermal conductivity of single wall carbon nanotube buckypapers with selected electronic structure

○Hiroyuki Matsuo [1], Kan Ueji[1], Yohei Yomogida [1], Takashi Yagi[2], Kazuhiro Yanagi [1]

[1] *Department of Physics, Tokyo Metropolitan University, Hachioji, Tokyo 192-0397, Japan*
[2] *Department of Physics, National Institute of Advanced Industrial Science and Technology, Tsukuba, Ibaraki,305-8563, Japan*

In recent years, understanding of the relationship between electrical conduction and thermal conduction in a material with flexibility is becoming of great importance to optimize the performance of flexible electronics and devices. For example, single-wall carbon nanotube (SWCNTs) have attracted a lot of interest as thermoelectric materials, and in order to maximize the thermoelectric performance, we need to prepare SWCNT thin films with large electrical conductivity and small thermal conductivity. Electrical conduction strongly depends on the electronic structure of the SWCNT and the location of the Fermi level. However, relationships among electronic structure, location of Femi-level, and thermal conductivity have not been elucidated yet. In addition, in the thin film form, it is important to understand the difference of in-plane and out-of-plane thermal conduction.

Here, in this study, we investigated the in-plane and out-of-plane directions of thermal conduction in SWCNT buckypapers with selected electronic structure. In the in-plane thermal conduction, both the conduction through long axis direction of the nanotube and the hopping interface contribute to the thermal conduction. However, in the out-of-plane conduction, the heat conduction through the hopping interface will play dominant role on the thermal conduction. Then we investigated how the electronic structure influences on the in-plane and out-of-plane thermal conductions.

Metallic and semiconducting buckypapers were prepared from SWCNT (MEIJO nano carbon ARCSO) through density gradient ultracentrifugation purifications. The thermal diffusivity was measured by periodic-heating method using a laser. We evaluated heat flow from through the phase delay of black-body radiation from the back surface of the sample. All the measurements were performed in a vacuum. Thermal conductivity is represented $\kappa = C_p \times \alpha \times \rho$ (C_p :specific heat ,α:thermal diffusivity, ρ : density). We measured thermal diffusivity in the in-plane, $\alpha_{\parallel}$, and the out-of-plane directions, $\alpha_{\perp}$, then, we evaluated the anisotropy ratio of thermal conductivity $\kappa_{\parallel} / \kappa_{\perp}$ by taking the ratio of thermal diffusivity ($\alpha_{\parallel}/\alpha_{\perp}$). Fig.1 shows the temperature dependence of the anisotropy ratio of three SWCNT free standing films (mixture, semiconductor, metal). As shown here, we found the anisotropy ratio depends on the electronic structures. The details of background will be discussed.

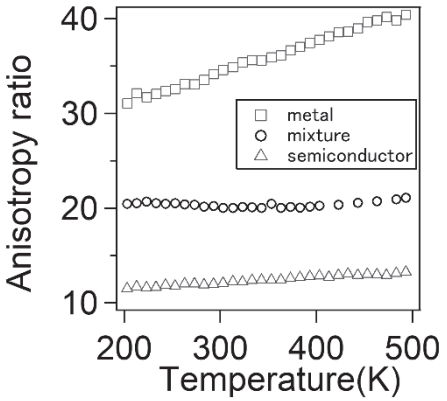

Figure1 ： Temperature dependence of the anisotropy ratio of three SWCNT free standing films (mixture, semiconductor, metal).

Corresponding Author: K. Yanagi, Tel: ＋81-42-677-2494, E-mail: yanagi-kazuhiro@tmu.ac.jp

Solving the Thermoelectric Trade-Off Problem with Metallic Carbon Nanotubes

○Yota Ichinose[1], Akari Yoshida[1], Kanako Horiuchi[1], Kengo Fukuhara[1], Natsumi Komatsu[2], Weilu Gao[2], Yohei Yomogida[1], Manaho Matsubara[3], Takahiro Yamamoto[3], Junichiro Kono[2,4,5] and Kazuhiro Yanagi[1]

[1]*Department of Physics, Tokyo Metropolitan University, Tokyo 192-0372, Japan*
[2]*Department of Electrical and Computer Engineering, Rice University, Houston, Texas 77005, USA*
[3]*Department of Liberal Arts, Tokyo University of Science, Katsushika, Tokyo 125-8585, Japan*
[4]*Department of Physics and Astronomy, Rice University, Houston, Texas 77005, USA*
[5]*Department of Material Science and NanoEngineering, Rice University, Houston, Texas 77005, USA*

One dimensional (1D) materials are predicted to exhibit the largest thermoelectric performance because of van Hove singularity (vHs) [1]. Particularly, semiconducting SWCNTs are paid attention to because of their much larger Seebeck coefficient *S*. However, it is widely recognized that there is a trade-off between electrical conductivity σ and *S*; increasing σ decreases *S* by shifting the Fermi level (E_F). And thus, this trade-off has hindered improving the power factor $P = S^2\sigma$. However, metallic SWCNTs also possess vHs. One should observe *P* enhancement if E_F is tuned with vHs because of the intrinsic large σ of metallic SWCNTs. Here, we investigated the σ, *S* and *P* of high-purity semiconducting and metallic SWCNTs as a function of E_F.

First, we prepared highly purified semiconducting SWCNTs (6,5) (>99%) and metallic SWCNTs (>99%). These samples were systematically mixed with ratios of 10:0 (#1), 9:1 (#2), 5:5 (#3) and 0:10 (#4), respectively (Fig. 1). In the thermoelectric measurement, we used electrolyte gating technique to shift E_F precisely [2].

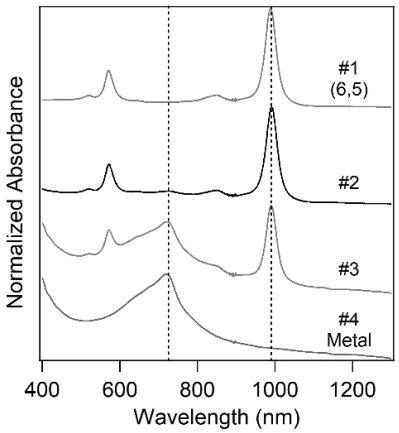

Fig. 1 Optical absorbance spectra.

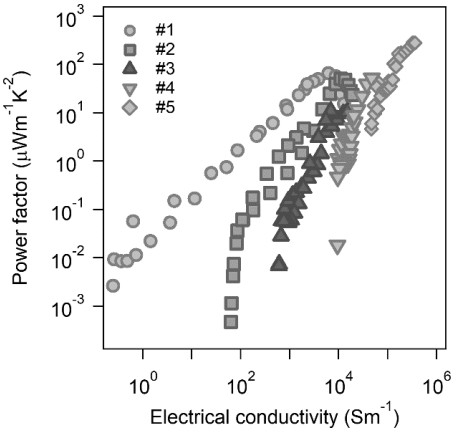

Fig. 2 Relationship between power factor and electrical conductivity.

As a result, in highly metallic sample (#4), simultaneous increase of σ and *S* was observed, while semiconducting sample (#1) showed the typical trade-off. The *P* of metallic sample (#4) almost reached that of semiconducting sample (#1) (~60 $\mu Wm^{-1}K^{-2}$) (Fig. 2). Moreover, when we aligned metallic SWCNTs (#5) to obtain higher σ [3], it exhibited the largest *P* (~300 $\mu Wm^{-1}K^{-2}$); exceeding the highest semiconducting purity sample (#1). We experimentally demonstrated that we can overcome the conventional trade-off using metallic SWCNTs.

[1] Hicks & Dresselhaus, *Phys. Rev. B* **47**, 16631 (1993). [2] K. Yanagi et al., *Nano letters* **14** (11), 6437 (2014). [3] X. He, et al., *Nat. Nanotechnol.* **11**, 633 (2016).

Corresponding Author: K. Yanagi Tel: +81-42-677-2494, Fax: +81-42-677-2483,
E-mail: yanagi-kazuhiro@tmu.ac.jp

Theoretical Study on Thermoelectric Properties of Nitrogen-Doped Carbon Nanotubes with Various Diameters

○Manaho Matsubara[1], Kenji Sasaoka[2], Takahiro Yamamoto[1,2]

[1] *Department of Electrical Engineering, Tokyo University of Science, Tokyo 125-8585, Japan*
[2] *W-FST Center RIST, Tokyo University of Science, Tokyo 125-8585, Japan*

Significant enhancement of thermoelectric performance is expected to be achieved by utilizing one-dimensional (1D) materials [1]. Single-walled carbon nanotubes (SWNTs) are potential candidates for 1D nanostructures with high thermoelectric performance as well as flexibility and lightweight. To achieve CNT-based thermoelectric devices, both n-type and p-type semiconducting CNTs are required. We focus on nitrogen-doped (N-substituted) SWNTs as a typical n-type semiconducting SWNTs, and we have investigated thermoelectric properties of N-substituted SWNTs with various diameters using Kubo-Lüttinger theory for thermoelectric effects [2-4]. For small-diameter SWNTs with large band gap, the N-substituted SWNTs exhibit high thermoelectric power factor at the room temperature originating from high-mobility carrier in the conduction band edge with sharp DOS due to van Hove singularity of 1D materials, which are excited from the impurity bands (i.e., N bands). On the other hands, for the large-diameter SWNTs with small gap, the thermally excited electrons in the conduction band from the valence band are not negligible even at room temperature. We found that the excitation affects the thermoelectric properties of N-substituted SWNTs. We explain these properties in the presentation.

[1] L. D. Hicks and M. S. Dresselhaus, Phys. Rev. B**47**, 16631 (1993).

[2] T. Yamamoto and H. Fukuyama, J. Phys. Soc. Jpn. **87**, 024707 (2018).

[3] T. Yamamoto and H. Fukuyama, J. Phys. Soc. Jpn. **87**, 114710 (2018).

[4] M. Ogata and H. Fukuyama, J. Phys. Soc. Jpn. **88**, 074703 (2019).

Corresponding Author: M. Matsubara
Tel: +81-3-5876-1492,
E-mail: mmatsubara@rs.tus.ac.jp

Towards high yield growth of single-walled carbon nanotubes by alcohol catalytic CVD using Pt catalyst

○Daiki Yamamoto[1], Kamal P Sharma[1], Takahiro Saida[1,2], Shigeya Naritsuka[3], Takahiro Maruyama[1,2]

[1]*Department of Applied Chemistry, Meijo University, Japan*
[2] *Nanomaterials Research Center, Meijo University, Japan*
[3]*Department of Materials Science and Engineering, Meijo University, Japan*

1. Introduction

Single walled carbon Nanotubes (SWCNTs) are one-dimensional materials, having various potential for future nanoelectronics. So far, we have reported SWCNT growth by alcohol catalytic CVD (ACCVD) using Pt catalysts and succeeded in growing small-diameter SWCNTs [1]. However, the yield of SWCNTs grown from Pt catalysts was not so high. In this study, we carried out SWCNT growth by ACCVD using Pt catalyst and succeeded in increasing the yield by optimizing the heating rate to the growth temperature.

2. Experimental procedure

Pt catalysts were deposited onto SiO_2/Si, which were used as growth substrate. The nominal thickness was 0.3 nm. An ultra-high vacuum (UHV) chemical vapor deposition (CVD) system was used for SWCNT growth. The substrates were heated to the growth temperature under H_2 atmosphere of 1×10^{-3} Pa. Then, ethanol gas was supplied through nozzle onto the substrates, as previously reported, to grow SWCNTs [1]. The heating rate was set to be higher than that in our previous report [1]. The grown SWCNTs were analyzed by Raman spectroscopy

3. Result and Discussion

Fig.1a is Raman spectra of SWCNTs grown from Pt catalysts at 800°C under an ethanol pressure at 1×10^{-1} Pa. The growth time was 10 min. Radial breathing mode (RBM) peaks were observed, indicating that the diameters of grown SWCNTs were distributed from 0.62 to 1.4 nm. Fig. 1b shows Raman spectra in the high-frequency region. Despite the short growth time, Raman spectra shows strong G band peaks. Considering that the intensity ratio of G band peak to Si phonon peak at 500 cm^{-1} (G/Si ratio) is 2.18, SWCNT yield was higher than that in our previous study about SWCNT growth from Pt catalysts. In addition, the G/D ratio is 7.7, indicating that the quality of SWCNTs were improved. By increasing the heating rate, we succeeded in increasing the growth amount of SWCNTs at 800°C. We will discuss the effect of growth condition on the property of grown SWCNTs.

This work was supported in part by Private University Research Branding Project from the Ministry of Education, Culture, Sports, Science and Technology (MEXT), Japan.

[1] T. Maruyama et al. carbon 96 (2016) 6.

Corresponding Author: T.Maruyama
Phone: +81-52-838-2386,
Fax: +81-52-832-1172
E-mail: takamaru@meijo-u.ac.jp

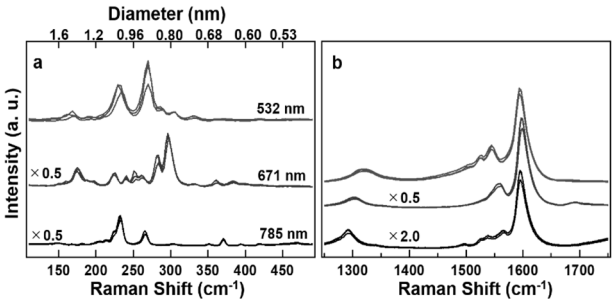

Fig. 1 Raman spectra of SWCNTs grown from Pt catalysts in a) the RBM region and b) high frequency region.

Synthesis of vertically aligned single walled carbon nanotube by conventional cold-wall CVD system using Ir catalysts

○Mayumi Saeki[1], Kamal P Sharma[1,2], Takahiro Saida[1,2], Shigeya Naritsuka[3], Takahiro Maruyama[1,2]

[1]*Department of Applied Chemistry, Meijo University, Japan*

[2] *Nanomaterials Research Center, Meijo University, Japan*

[3]*Department of Materials Science and Engineering, Meijo University, Japan*

1. Introduction

Single-walled carbon nanotubes (SWCNTs) have many unique properties and potential for various electronic device applications. At present, several groups have reported the growth of vertically aligned SWCNTs (VA-SWCNTs) via the chemical vapor deposition (CVD) using Fe and Co catalysts. Recently, our groups reported growth of VA-SWCNTs forests by alcohol gas source method from Ir catalysts [1]. However, the inplane uniformity of SWCNT length was not so good, because carbon source was supplied through a thin nozzle. In this study, we attempt to grow SWCNTs using conventional cold-wall type CVD system to improve the uniformity of SWCNT length.

2. Experimental Procedure

Ir catalyst was deposited on 3×14 mm SiO_2/Si substrates by a pulsed arc plasma gun. The SWCNT growth was performed by a conventional cold-wall type CVD system using ethanol as carbon source. The growth temperature was set to be 800℃. The grown VA-SWCNT was confirmed by using Raman Spectroscopy and FESEM.

3. Result and Discussion

Fig. 1(a) and (b) show the Raman spectra of the SWCNTs grown at 40 Pa ethanol pressure for 10 min. Fig.1 (c) shows the ethanol pressure dependence of G/Si intensity ratio in Raman spectra. The G/Si intensity became its maximum at an ethanol pressure of 40 Pa, indicating that this pressure was optimal. Fig. 1(d) Shows cross-sectional FESEM image of the VA-SWCNT grown under the optimal ethanol condition. We will also discuss the uniformity of SWCNT length.

This work was supported in part by Private University Research Branding Project from the Ministry of Education, Culture, Sports, Science and Technology (MEXT), Japan.

[1] T. Okada et al. MRS Advances, 4 (2019) 225.

Corresponding Author: T. Maruyama
Phone: +81-52-838-2386,
Fax: +81-52-832-1172
E-mail: takamaru@meijo-u.ac.jp

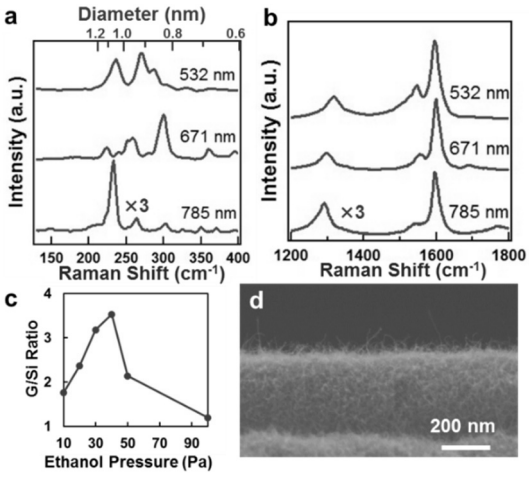

Fig.1(a,b) show the Raman spectra of SWCNTs, and **(c)** shows ethanol pressure dependence of the G/Si intensity ratio. **(d) C**ross-sectional FESEM image of a VA-SWCNT forest.

Interaction between defective carbon nanotubes and surfactant molecules

○Hideyuki Jippo[1], Mari Ohfuchi[1]

[1]*Fujitsu Laboratories Ltd. & Fujitsu Limited, Atsugi 243-0197, Japan*

We reported [1] how differently sodium dodecyl sulfate surfactants behave on metallic and semiconducting carbon nanotubes (CNTs) to reveal the mechanism of metal/semiconductor separation of CNTs. In this study, we investigate the adsorption of surfactant molecules, cholate and dodecyl sulfate ions, onto defective CNTs using ab initio methods. The semiconducting (6, 5) single-wall CNTs having one-atom hole with COO (COO-CNTs) are compared to pristine CNTs.

Figure 1 shows the obtained three optimized geometries of dissociated cholate and Sodium (Na) ions on COO-CNTs. Counter Na ions are put onto the opposite side of the CNTs as shown in Fig. 1. The dodecyl sulfate (DS) ions were also examined in the same configurations. The adsorption energies of cholate and DS ions onto pristine and COO-CNTs are summarized in Table 1. We found that the adsorption energies of DS ions are larger than those of cholate ions both for the pristine and COO-CNTs. The largest adsorption energy is obtained on the pristine CNTs for both of the cholate and DS ions. Among the COO-CNTs, the far adsorption site from the defect (COO-(c)) shows the largest adsorption energy. The adsorption energies are smaller on the sites close the defect or on the defect. Thus the ionized surfactants are less likely to adsorb defective CNTs. This result may explain experiments of the pristine/defective separation of the CNTs.

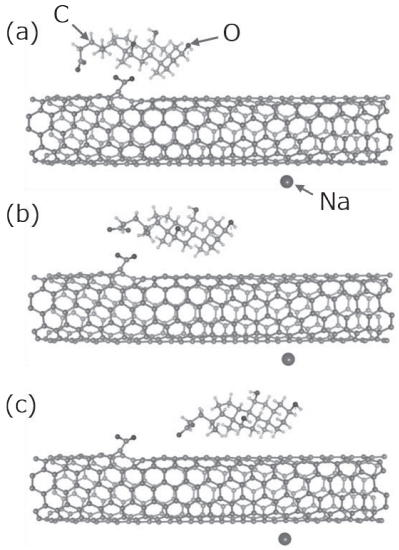

Fig. 1: Optimized geometries of dissociated cholate and Na ions on COO-CNTs per unit cell.

Table 1. Adsorption energies (kcal/mol) of Cholate and DS ions onto (6, 5) CNTs

	pristine	COO-(a)	COO-(b)	COO-(c)
Cholate	-36.90	-26.99	-20.99	-30.89
DS	-55.63	-31.37	-19.40	-44.79

This work was partly supported by JST, CREST (No. JPMJCR15F1).

[1] M. Ohfuchi, J. Phys. Chem. C 122, 4691 (2018).

Corresponding Author: H. Jippo, Tel: +81-46-250-8843, E-mail: jippo.hideyuki@fujitsu.com

Growth, etching, and regrowth of individual single-walled carbon nanotubes: Isotope labeling study

○Taiki Inoue[1], Bunsho Koyano[1], Shun Yamamoto[2], Keigo Otsuka[2,3], Rong Xiang[1], Shohei Chiashi[1], Shigeo Maruyama[1,4]

[1] Department of Mechanical Engineering, The University of Tokyo, Tokyo, 113-8656, Japan
[2] Quantum Optoelectronics Research Team, RIKEN Center for Advanced Photonics, Wako, 351-0198, Japan
[3] Nanoscale Quantum Photonics Laboratory, RIKEN Cluster for Pioneering Research, Wako, 351-0198, Japan
[4] Energy NanoEngineering Lab, National Institute of Advanced Industrial Science and Technology (AIST), Tsukuba, 305-8564, Japan

Toward broad applications of single-walled carbon nanotubes (SWCNTs), the growth efficiency of SWCNTs should be improved. For that, it is important to understand the effects of additive molecules on catalyst activity and growth rates of SWCNTs especially at the single nanotube level. In this study, we performed interrupted growth of SWCNTs by tentatively stopping ethanol supply and introducing only Ar, Ar/H_2, or Ar/H_2/H_2O. We analyzed the time evolution of individual SWCNT growth by an isotope labeling technique which we have recently proposed [1]. While all SWCNT terminated growth after interruption with Ar, the interruption with Ar/H_2 caused the regrowth of SWCNTs once ethanol was reintroduced. In the case of Ar/H_2/H_2O, SWCNTs were etched back with moving in the reverse direction of growth, followed by restarting growth (Fig. 1). We conducted analysis of radial breathing mode peaks of SWCNTs and found that the chirality was preserved even after etching and regrowth. While the growth rates of SWCNTs were unchanged by the interruption with Ar/H_2, they were increased after the interruption with Ar/H_2/H_2O. These result would suggest strategies to encourage the efficient growth of SWCNTs [2].

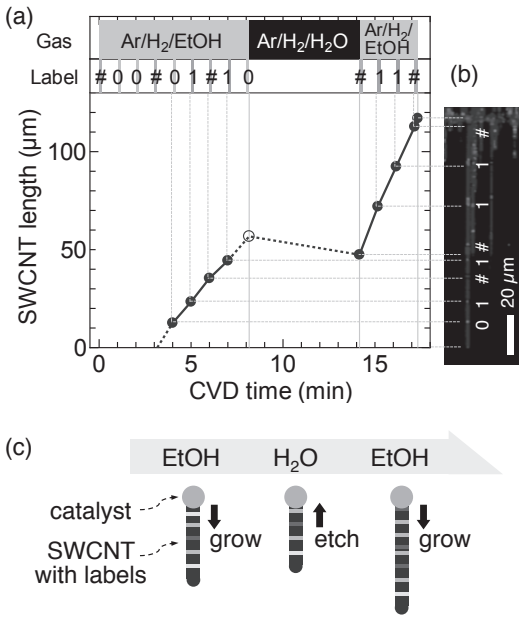

Fig. 1 (a) Growth curve of an SWCNT interrupted with Ar/H_2/H_2O. (b) Corresponding Raman G-band mapping image. (c) Schematic image of growth, etching, and regrowth of SWCNTs.

[1] K. Otsuka *et al.,* ACS Nano **12**, 3994 (2018).
[2] B. Koyano *et al.*, submitted.

Corresponding Author: S. Maruyama
Tel: +81-3-5841-6421, Fax: +81-3-5800-6983,
Web: http://www.photon.t.u-tokyo.ac.jp
E-mail: maruyama@photon.t.u-tokyo.ac.jp

Bright electroluminescence from air-suspended carbon nanotubes

○W. Terashima[1], H. Machiya[1,3], K. Otsuka[1], A. Ishii[1,2], and Y. K. Kato[1,2]

[1]*Nanoscale Quantum Photonics Laboratory, RIKEN Cluster for Pioneering Research, Saitama, 351-0198, Japan*
[2]*Quantum Optoelectronics Research Team, RIKEN Center for Advanced Photonics, Saitama, 351-0198, Japan*
[3]*Department of Electrical Engineering, The University of Tokyo, Tokyo, 113-8656, Japan*

Carbon nanotube light emitting diodes (CNT-LEDs) are expected to be useful for compact optical sources operating at telecommunication wavelengths. Previously, we have reported electroluminescence (EL) with narrow linewidth (~8 meV) comparable to photoluminescence (PL) from air-suspended CNTs within split-gate devices [1], but EL intensity is still low. The diffusion length of excitons in CNTs is estimated to be several hundred nanometers, which is very long compared to those of conventional bulk semiconductors [2]. It is therefore possible that EL intensity has been suppressed for the ~1-μm-long CNT in the device used in the previous report, where many of the generated excitons could have recombined nonradiatively at the point of contact with the substrate. In this study, we investigate nanotube length dependence on EL intensity to obtain insight for increasing EL intensity from air-suspended CNT-LED structures.

CNT-LED device structures are fabricated on silicon-on-insulator substrates with 0.7 to 3.7-μm-wide trenches. CNTs are synthesized by ethanol chemical vapor deposition at 800 ºC for 1 minute. PL and EL signals from CNT-LED structures are detected by an InGaAs photodiode array. All measurements are performed at room temperature in a nitrogen ambient.

Figure 1 shows gate voltage dependent integrated EL intensity and the spectra from an LED structure with a 4-μm-long CNT with chirality (9, 8) at a drain voltage of ~15 V. We observe sharp spectra where the intensity increases with the gate voltage. The maximum EL intensity in the best device reaches up to 30,000 counts/s, which is about 7.5 times higher than our previous work [1]. Details of the nanotube length dependence on EL intensity from air-suspended CNT-LED structures will be discussed.

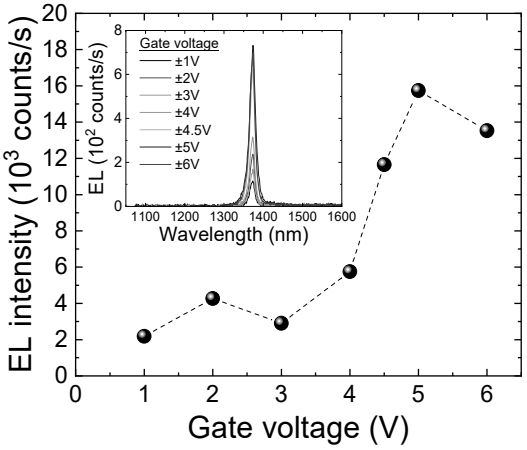

Figure 1: A Plot of integrated EL intensity as a function of gate voltage for an LED structure with a 4-μm-long (9,8) CNT. (Inset): Gate voltage dependent EL spectra at a drain voltage of 15 V.

Work supported by JSPS (KAKENHI JP16H0592, JP17H07359), MEXT (Nanotechnology Platform), and RIKEN (Incentive Research Project). H.M. acknowledges support by RIKEN Junior Research Associate Program and JSPS Research Fellowship. K.O. acknowledges support by JSPS Research Fellowship.

[1] N. Higashide, M. Yoshida, T. Uda, A. Ishii, Y. K. Kato, Appl. Phys. Lett. **110**, 191101 (2017).
[2] A. Ishii, M. Yoshida, Y. K. Kato, Phys. Rev. B **91**, 125427 (2015).

Corresponding Author: Yuichiro. K. Kato
Tel: +81-48-462-1111, Web: http://katogroup.riken.jp/, E-mail: yuichiro.kato@riken.jp

Effect of electrode configuration on formation and elongation of carbon nanotube filaments by gas discharge breakdown

○Masatoshi Hiromura, Soichiro Magata, Hideki Sato

Graduate School of Engineering, Mie University, Tsu 514-8507, Japan

We previously reported that gas discharge breakdown generated between planar electrodes, on which cathode electrode was coated with carbon nanotube (CNT) film, formed bridging of filament-like CNTs between them [1]. We consider that this phenomenon may be used as a method for spinning of CNTs. However, improvement of the CNT filament generation efficiency and development of an appropriate handling method of the CNT filaments are needed to fabricate the spinning CNT yarn using this method. We recently found that the CNT filaments were efficiently collected on an auxiliary electrode, which was additionally placed above the discharge electrodes (anode and cathode). In this study, we examined the formation characteristics of the CNT filaments on the auxiliary electrode.

A mat-shaped CNT sheet was applied on the stainless-steel plate of the cathode electrode by pressing. A tungsten wire (0.15 mm diam.) anode was placed horizontally to the CNT mat. The distance between the anode and the cathode was 1.0 mm. The auxiliary electrode made of tungsten was vertically positioned above the anode wire [Fig. 1(a)]. The auxiliary electrode was the same potential as the anode electrode. These electrodes were introduced to a discharge chamber. This chamber was filled with Ar gas at 10 kPa and then, DC voltage (800 V) was applied between anode and cathode to ignite the gas discharge breakdown. The formation behavior of the CNT filaments and those elongation behavior were observed.

The gas discharge was generated by applying DC voltage between anode and cathode [Fig.1(b)]. The discharge breakdown generated dust-like CNT bundles, which were peeled off from the CNT mat. These CNT bundles were attracted to the anode and auxiliary electrode. CNT filaments were formed around the electrodes. After that, the auxiliary electrode was moved away from the discharge area. This gave rises to elongation of the CNT filaments on the auxiliary electrode [Fig.1(c)]. This behavior indicates that the CNT bundles detached from the mat were attracted to the auxiliary electrode by electrostatic force and became adhered to it. These bundles attracted the other bundles, which were connected the end of CNT bundles adhered to the electrode. The repetition of this process elongated the CNT filaments. Further elongation of the filaments may be possible by optimizing the formation conditions (e.g., applying bias voltage to the auxiliary electrode).

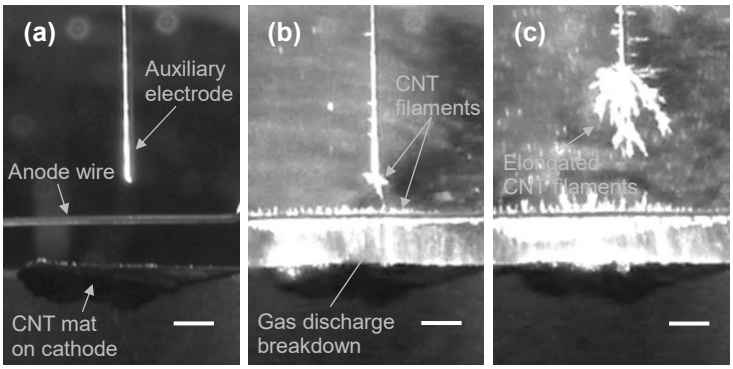

Fig. 1 (a) and (b) are photographs of electrodes before and (b) after ignition of gas discharge breakdown followed by formation of CNT filaments. (c) shows CNT filaments elongated by moving the auxiliary electrode upward. Scale bars are 1.0 mm.

This study was supported by JSPS KAKENHI Grant No. 19K05206.

[1] H. Sato *et al*., Appl. Phys. Lett., **110**, 033101 (2017).

Corresponding Author: H. Sato Tel: +81-59-231-9404, Fax: +81-59-231-9404, E-mail: sato@elec.mie-u.ac.jp

Encapsulation of $C_{60}F_x$ in SWCNTs and its properties

○Tsuyoshi Hasegawa, Shunsuke Kondo, Shun Manabe, Kohei Kondo,
Yosuke Ishii and Shinji Kawasaki

Department of Life Science and Applied Chemistry, Nagoya Institute of Technology,
Nagoya 466-8555, Japan

Single-walled carbon nanotubes (SWCNTs) can encapsulate several kinds of molecules. So far, we have inserted fullerenes (e.g. C_{60}, C_{70}), organic molecules (e.g. anthraquinone,) and elemental molecules (e.g. iodine, sulfur, phosphorus) into SWCNTs, and investigated the properties. One of the most classic and commonly known encapsulation-induced molecules, is the peapod, that is synthesized by inserting fullerene molecules inside SWCNTs. These fullerene molecules enjoy high reactivity that enables the synthesis of more advanced derivatives. One of the fullerene derivatives, fluorinated fullerene ($C_{60}F_x$), is a molecule in which fluorine atoms are bonded to a C_{60} (Fig.1 (a)). The crystal structure and physical properties of $C_{60}F_x$ are different from those of C_{60}. Since $C_{60}F_x$ works as an electron acceptor molecule, the electronic state of SWCNTs is expected to change by encapsulation of $C_{60}F_x$ into SWCNTs. However, such encapsulation of $C_{60}F_x$ into SWCNTs is difficult, because the molecule size of $C_{60}F_x$ is too large to the conventionally available SWCNTs having diameter less than 1.5 nm. Recently, larger diameter SECNTs become available. So, the encapsulation of $C_{60}F_x$ is now possible (Fig.1 (b)).

We prepared $C_{60}F_x$ encapsulated into SWCNTs using a gas phase method. We placed $C_{60}F_x$ and SWCNTs in a glass tube, and sealed the glass tube under vacuum. Then, we heated the glass tube to vaporize $C_{60}F_x$, allowing the $C_{60}F_x$ to be encapsulated into SWCNTs (Fig.1 (c)).

We confirmed using Seebeck coefficient measurement, that the surface of $C_{60}F_x$@SWCNTs was positively charged. We also confirmed the improvement of the performance to be an oxygen reduction reaction catalyst.

Acknowledgement

$C_{60}F_x$ samples were provided by Prof. Hattori (Shinshu Univ.).

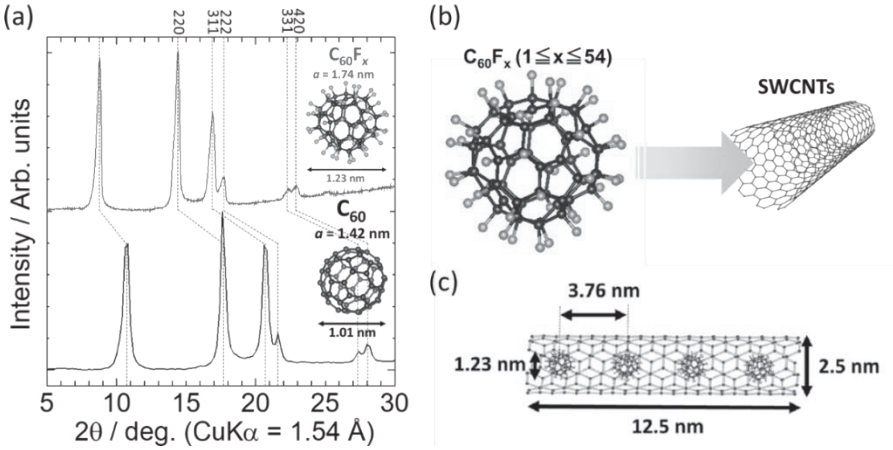

Fig.1 (a)XRD profile of $C_{60}Fx$ and C_{60}, it was confirmed that the structure was fcc. (b)Encapsulation of $C_{60}Fx$ into SWCNTs, (c)Expected model image of $C_{60}Fx$@SWCNTs

Corresponding Author: S. Kawasaki, Tel: +81-52-735-5221, E-mail: kawasaki.shinji@nitech.ac.jp

2P-23

Carbon nanobrushes-based gas sensor

○Mayumi Kosaka and Ryota Yuge

System Platform Research Laboratories, NEC Corporation, Tsukuba 305-8501, Japan

Monitoring of gas components is of increasing importance in many application fields for the safe and comfortable society, such as human health care, medical application, exhaled breath analysis, indoor air quality, fire detection, industrial safety, and global environmental protection. Especially, gas measurements for health conditions have come into the spotlight, since a number of gases have been recently reported to relate physical conditions or diseases. For instance, nonanal which is one of the volatile organic compounds (VOCs) is considered to be a marker for lung cancer [1], methyl mercaptan is reported to be produced by periodontitis and to be a marker for colon cancer or liver disease [2], acetone and isoprene are gaining attention as metabolic gases, and ammonia is supposed to relate hepatitis [3]. The gas sensor detecting these gases requires high sensitivity owing to the low target concentrations from ppb to ppm level, fast response time, low cost sensor system, and gas-selectivity.

Carbon nanobrush (CNB) which has fibrous aggregate structure of single-walled carbon nanohorns is a new member of the nanocarbons [4]. CNBs are expected to be good electrode material for the gas sensing devise, due to their unique characteristics including high dispersibility, large specific surface area and high electrical conductivity. However, yield of the CNBs prepared by CO_2 laser ablation is low and major products are spherical single-walled carbon nanohorn aggregates (CNHs) which are hard to remove from the CNB products.

In this study, we present the fabrication methods of the highly sensitive CNBs gas sensor. A casting film of the CNB products was prepared with the dispersion of CNBs products containing a large amount of CNHs. The particulate CNHs fill in the space between the fibrous CNBs in the film. The CNHs in the surface layer of the film block the gas diffusion path to the inner CNBs, then only the surface CNBs can contribute to the gas sensitivity, since not the CNHs but the CNBs with high conductivity respond to the gas adsorption. To expand the scope of the gas diffusion, we devised an original film fabrication method of the CNBs using a large pore size filter. Filtering the dispersion of CNBs products by a 5 micron pore size filter separates CNBs and CNHs partially in the filter. The CNBs get tangled in fibers of the filter surface and the CNHs accumulate in the deep part of the filter because the CNHs size is obviously smaller than the pore size of filter. Upon exposure to gaseous molecules, the CNBs with large spaces in the filter film respond efficiently to the gases and the electrical resistance dramatically increased for VOCs and ammonia gases. Furthermore, the CNBs-based gas sensor has demonstrated to have the highest sensitivity in the comparison with other nanocarbons-based them. Detail results of the gas sensors will be discussed in the presentation.

[1] P. Fuchs *et al*. Int. J. Cancer, **126**, 2663 (2010).
[2] A. Ishibe *et.al.* J. Clinical Oncology, **34**, 529 (2016)
[3] S. Ravi *et al.* Gastroenterology Report, **5**, 232 (2017)
[4] R. Yuge *et al.* Adv. Mater., **28**, 7174 (2016)

Corresponding Author: M. Kosaka
Tel: +81-29-850-1138, Fax: +81-29-856-6136
E-mail: m-kosaka@az.jp.nec.com

Fabrication of superhydrophobic and superoleophilic sponge using graphene oxide and carbon nanotubes

○Yuki Morikuni, Masanori Hara, Masamichi Yoshimura

Graduate School of Engineering, Toyota Technological Institute, Nagoya 468-8511, Japan

Oil spillage and industrial wastewater cause water pollution and damage to environment. The solid surface with superhydrophobic (water contact angle is higher than 150°) and super oleophilic (oil contact angle is lower than 10°) has attracted attention for oil/water separation [1]. In this paper, we fabricate hydrophobic and oleophilic sponge using graphene oxide (GO) combined with carbon nanotubes (CNT) and carboxylic acid functionalized CNT (f-CNT), and evaluate their hydrophobicity and oil absorption capacity.

GO were prepared from natural graphite by Hummers' method [2]. The specimens were fabricated by dipping commercial melamine sponge into the mixture of GO and CNT dispersion and by drying in vacuum oven. The GO coated on the sponges was reduced by ascorbic acid solution at 80 ℃. Then the sponges were dried in vacuum at 100 ℃ for 1 h.

Wettability of the sponges was measured by θ/2 method using a droplet of water or oil (1 μL) at room temperature. The morphology of the sponges was observed by scanning electron microscope (SEM) (S4700, HITACHI). GO and rGO were characterized by Raman spectroscopy and UV-visible spectroscopy.

Table 1. Water contact angle of coated sponges.

coating material	melamine sponge	rGO	rGO-f-CNT	rGO-CNT
contact Angle	—	127.3±3.2°	132.8±3.5°	135.5±2.1°

Water contact angle of each sponge is listed in Table 1. Melamine sponge easily absorbs water drop. On the other hand, rGO, rGO-f-CNT and rGO-CNT sponges show hydrophobicity.

Figure 1 shows SEM images of each sponge. Sheet-like rGO coats the surface of melamine sponge, as seen in Fig. 1 (b). The surface roughness of rGO-f-CNT and rGO-CNT increased as shown in Fig. 1 (c) and (d). We found that rough character induced by the attachment of CNT is responsible for the hydrophobicity.

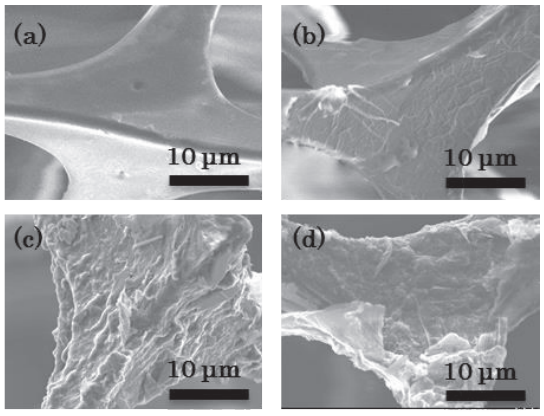

Fig. 1 SEM images of (a) pristine, (b) rGO coated, (c) rGO and f-CNT composite coated, (d) rGO and CNT composite coated melamine sponge.

[1] B. Wang, W. Liang, Z. G. Guo and W. Liu, Chem. Soc. Rev., 44 , 336 (2015)

[2] S. Abdolhosseinzadeh, H. Asgharzadeh and H. S. Kim, Sci. Rep. 5, 10160 (2015).

Corresponding Author: Masamichi Yoshimura

Tel: +81-52-809-1851

E-mail: yoshi@toyota-ti.ac.jp

Zinc Oxide Nanoparticle Decorated on Nitrogen-Doped Graphene Sheet as Advanced Supercapacitor Electrode

○Rohit Yadav, Masanori Hara, Prerna Joshi, Masamichi Yoshimura

Graduate School of Engineering, Toyota Technological Institute, 2-12-1 Hisakata, Tempaku, Nagoya 468-8511, Japan

Supercapacitor electrodes with large charge storage capacity are potential candidate in microelectronics and power storage. Transition metal oxides (MnO_2, RuO_2, etc.) and sulphides, conducting polymers (polyvinyl alcohol, polyaniline, etc.) and carbon-based materials (carbon nanotubes, graphene, etc.) have emerged as a unique class of active electrode material for supercapacitor applications. The present research work focuses on the investigation of a novel electrode material with the synergistic effect of metal oxide (ZnO) and carbon-based support material (nitrogen-doped reduced graphite oxide (N-rGO)) [1,2]. Low cost, non-toxicity, and environment-friendly nature of ZnO make it suitable for energy storage application, however, its limitation of low electrical conductivity can be overcome by its composite with N-rGO which will also provide mechanical support against volumetric change during charge-discharge.

For the synthesis of rGO and N-rGO, graphene oxide (GO) was synthesized using modified Hummers' method. Briefly, N-rGO was synthesized via pyrolysis of urea and GO at 800ºC for 1 hr in N_2 atmosphere. The ZnO/N-rGO composite was prepared by *in-situ* hydrothermal synthesis method using N-rGO, $Zn(NO_3)_26H_2O$ and NaOH as precursors at 150 ºC for 12 hrs. For comparison, ZnO and ZnO/rGO were also prepared using the same synthetic procedures. N-rGO, ZnO, ZnO/rGO and ZnO/N-rGO were characterized by XRD, FE-SEM, TEM, EDX and XPS, and Raman spectroscopy. Electrochemical measurement was performed using 3 electrode setup with Pt as a counter electrode, Ag/AgCl as a reference electrode in 1 M Na_2SO_4 solution.

XRD, XPS, FE-SEM and Raman spectroscopy confirm the characteristics of the synthesized support materials N-rGO, the formation of ZnO and its composites with rGO (ZnO/rGO) and N-rGO (ZnO/N-rGO). Fig. 1 shows HR-TEM micrographs with well crystalline ZnO NPs of size 1.6 ± 0.2 nm, homogeneously distributed on N-rGO sheets. The lattice spacing of 0.275 nm agrees with (100) plane of wurtzite HCP ZnO and 0.332 nm is consistent with (002) plane of N-rGO from XRD diffractogram. The electrochemical analysis demonstrates the ZnO/N-rGO composite as an advanced electrode material for supercapacitor performance.

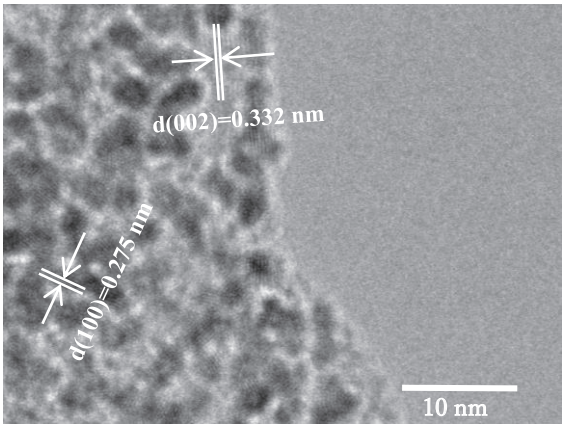

[1] C. K. Maity *et al.* Vacuum, **157**, 145 (2018).
[2] A. N. P. Madathil *et al.* Proc. SPIE 6639, Nanophotonic Materials IV, 66390J (2017).

Corresponding Author: Masamichi Yoshimura
Tel: +81-52-809-1851
Web: http://www.toyota-ti.ac.jp/surface
E-mail: yoshi@toyota-ti.ac.jp

Enhancement of electric field by surface plasmon on hollow cylinder

○Yuan Tian, Fenda Rizky Pratama, Muhammad Shoufie Ukhtary, Riichiro Saito

Department of Physics, Graduate School of Science, Tohoku University,

Sendai 980-8578, Japan

A metal cladded cylinder with dielectric core (Fig.1) can be a good model of tips used in tip enhanced Raman spectroscopy (TERS) [1] or probes used in scanning near-field optical microscopy (SNOP) [2]. In those experiments, a large enhancement of electric field near the probe is found when we shed the light to cylinder and it is considered to be the result of surface plasmon (SP). Such enhancement is important, since the enhancement of electric field provides better optical imaging of the sample below the diffraction limit. E. Devaux et.al observed the field enhancement on such hollow cylinder, they also theoretically predicted the existence of SP on such cylinder, and the relation of such SP with the enhancement they observed in experiment [3]. However, they did not calculate enhancement explicitly as a function of diameter or frequency. Such information may help to improve instrument for experiment.

In this work, we investigate the enhancement of electric field and absorption of light on metallic hollow cylinder. First we solve the electromagnetic field by the Helmholtz equation. We then calculate the energy dispersion relations of SP from the boundary conditions (Fig.2). In order to calculate the enhancement of several geometries, we include an incident light on the system. The absorption is also calculated since the peak of absorption corresponds the wave vector where SP modes were resonantly excited.

We find that the enhancement of electric field by SP excitation occurs only when dispersion of light intersects with that of SP, which corresponds to peak of optical absorption. We explain the optimum condition for the enhancement as a function of the thickness of cylinder wall.

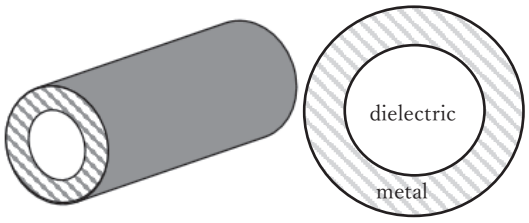

Fig.1 The layout of a hollow cylinder

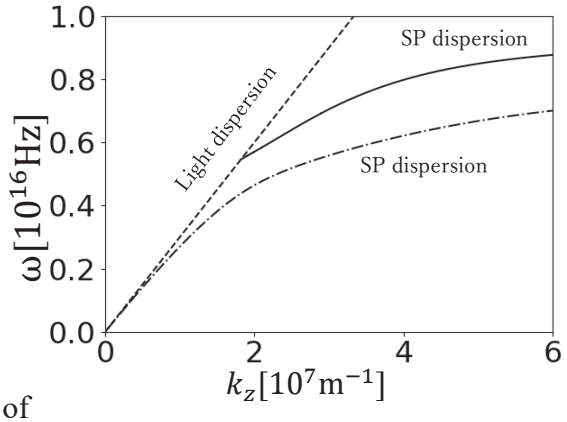

Fig.2 Energy dispersions of light and the two solutions of surface plasmon

Reference:
[1] Alexander S. McLeod *et.al.*, Phys. Rev. B 90, 085136 (2014).
[2] P. Wróbel *et.al.*, Journal of Applied Physics 112, 074304 (2012).
[3] U. Schröter, E. Devaux *et.al.*, Phys. Rev. B 64, 125420 (2001).

Synthesis of vertically aligned CNTs and evaluation of yarn spinnability

○Shinji Igimi[1], Morihiro Okada[1,2], Taiki Inoue[1], Shigeo Maruyama[1,3], Shohei Chiashi[1]

[1] *Department of Mechanical Engineering, The University of Tokyo, Tokyo 113-8656, Japan*
[2] *Department of Chemistry and Biochemistry, University of Maryland, Maryland 20742, United States*
[3] *Energy Nano Engineering Laboratory, National Institute of Advanced Industrial Science and Technology (AIST), Tsukuba 305-8564, Japan*

Carbon nanotube (CNT) yarns are highly expected toward macro-scale applications due to superior electrical and mechanical properties of CNTs. Researchers have studied how to make CNT yarns [1] and why CNT yarns can be spun by dry spinning from vertically aligned (VA) CNTs [2]. However, only VA-CNTs which are synthesized using iron catalyst under specific conditions can be spun, and the determining factors of spinnability have not been fully elucidated. In this study, we evaluated spinnability of VA-CNTs and its relationship with the weight of water molecules adsorbed on them. We synthesized VA-CNTs using cobalt catalyst and spun CNT yarns from them. We changed various synthesis conditions and grew VA-CNTs which can be spun into CNT yarns of up to about 1 cm (Fig. 1(a)). In addition, using thermogravimetric analysis (TGA), we evaluated the weight of CNTs and water adsorbed on CNTs (Fig. 1(b)), which provides the number of adsorbed water molecules per unit area of CNTs. We employed three types of samples: VA-CNTs which we synthesized with cobalt catalyst and two spinnable VA-CNTs provided from other groups [3,4]. The two spinnable samples adsorb water of 60 molecules/nm^2 and 14.5 molecules/nm^2, respectively. On the other hand, our samples adsorb water molecules of 3.0 molecules/nm^2. This result suggested that spinnable VA-CNTs adsorb more water than the VA-CNT synthesized using cobalt catalyst does

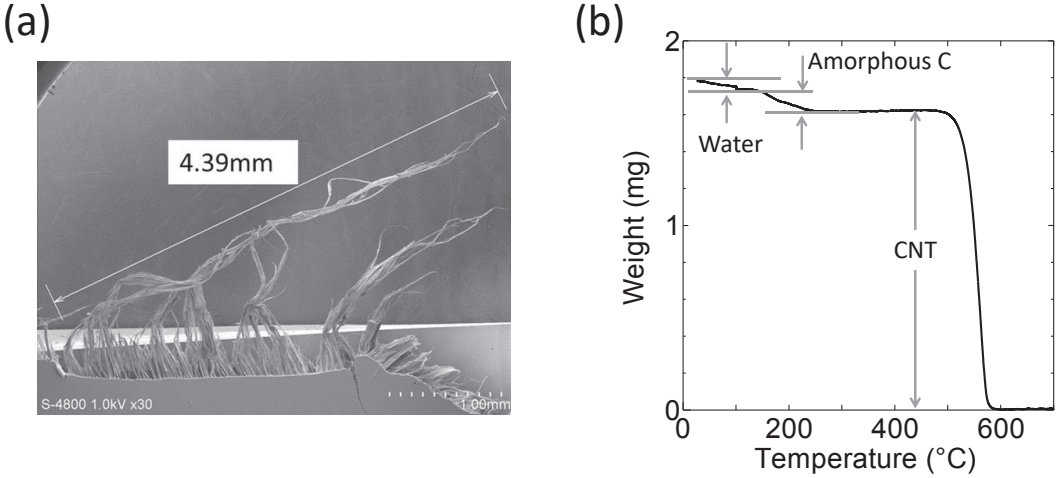

Fig. 1 (a) SEM image of a CNT yarn spun from VA-CNTs synthesized using cobalt catalyst. (b) TGA profile of CNTs, indicating the weight of CNTs, amorphous carbon, and adsorbed water.

[1] K. Jiang *et al*. Nature, **419**, 801 (2002).
[2] C. Zhu *et al*. Carbon, **49**, 4996 (2011).
[3] S. Kim *et al*. Science, **357,** 773 (2017).
[4] Y. Inoue *et al*. Appl Phys Lett, **92**, 90 (2008)

Corresponding Author: S. Chiashi
Tel: +81-3-5841-6407, Fax: +81-3-5841-6408, E-mail: chiashi@photon.t.u-tokyo.ac.jp

Laser-energy dependent helicity-changing Raman spectra of MoS_2

○Tong Wang[1], Nguyen T. Hung[2], Ahmad R.T. Nugraha[1], Riichiro Saito[1]

[1]Department of Physics, Tohoku University, Sendai 980-8578, Japan
[2]Frontier Research Institute for Interdisciplinary Sciences, Tohoku University, Sendai 980-8578, Japan

Recently, transition-metal dichalcogenides (TMDs) has attracted for many applications due to their unique properties. In particular, TMDs has been expected as good materials for valleytronics. For TMDs, valley-selective optical transition occurs by using circularly polarized light. In order to know the information of optical selection rule of TMDs with circular polarized light, we calculate the first-order Raman spectra of MoS_2 by using density functional theory (DFT) calculation [1].

In this study, we adapt circularly polarized light as the incident and scattered light to study helicity changing phenomenon in Raman spectra. Here, by using DFT with both electron-photon and electron-phonon interactions, we made our own program [3] to calculate the first-order helicity-changing Raman spectra. In Fig.1, we show the calculated results of the helicity-dependent Raman spectra as a function of laser energy. We found that E' mode shows the *helicity-changing* Raman spectra while the A1 mode shows the helicity-conserved Raman spectra. However, Miller et al. [2] showed that E' mode shows the *helicity-conserved* Raman spectra at laser energy of 1.95 eV, while it shows *helicity-changing* Raman spectra for other values of laser energy. We will discuss the origin of the phenomena based on the results by Miller's work.

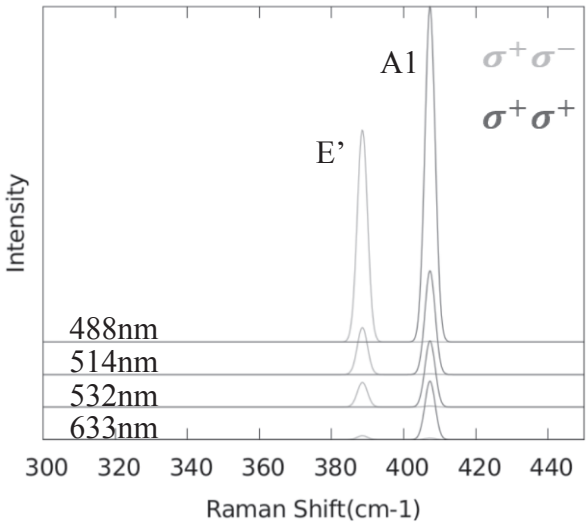

Fig.1 Helicity-changing Raman spectra of several energies of laser.

[1] Y. Tatsumi, R. Saito, Phys. Rev. B 94, 235408 (2016).
[2] B. Miller et al, Nature Communications 10, 807 (2019)
[3] Y. Tatsumi, R. Saito, Phys. Rev. B 97, 115407 (2018).

Corresponding Author: Tong Wang
E-mail: wang@flex.phys.tohoku.ac.jp

Edge plasmon in rectanglular antenna of grpahene

○ Masato Maruoka[1], Taisei Maeda[2], M. Shoufie Ukhtary[1], and Riichiro Saito[1]
[1]*Department of Physics, Tohoku University, Sendai 980-8578, Japan*
[2] *National Institute of Technology, Sendai College 989-3128, Japan*

When circularly polarized light comes into the chiral shape material such as S-shaped antenna, the absorption depends on the helicity of the incident light which is called circular dichroism [1]. We calculate the optical response of S-shaped antenna for circularly polarized light by finite-difference time-domain method (so called MEEP [2]) and we notice localized charge propagates along the edge. This behavior is similar to that of the plasmon in 2D material with edge [3]. In general, the electric field of the 2D plasmon is rotating out-of-plane if the 2D plasmon exist far from the edge. However, if the plasmon is near the edge, the charge is localized at the edge and electric field rotates in-plane. In other words, the current is rotating around the edge and thus we can discuss the phenomena by a response of rectangular disk with edge plasmon.

In this work, we investigate the relationship between circular dichroism and the edge plasmon. We calculate the edge plasmon in graphene nanoribbon by solving the Helmhotlz equation and by using MEEP. Both analytical and numerical solution show rotating current which is localized at the edges. Then we extend the analytical expression of the plasmon modes for the rectangular disk (4 edges). In order to discuss the optical absorption and emissions by exciting the plasmon, we include the incident light to the solution of the plasmon by the boundary condition of the Helmholtz equation. We will also discuss the circular dichroism of excited plasmon.

Corresponding Author: Masato Maruoka
Tel: +81-22-795-6442, Fax: +81-22-795-6447,
E-mail: maru@flex.phys.tohoku.ac.jp

[1] T. Narushima et al., J. Phys. Chem. C 2013, 117 (45).
[2] Oskooi, A. F. et al. Comp. Phys. Comm. 181, 687–702 (2010).
[3] A. L. Fetter. PRB 33, 3717 (1986).

Trion-based High-speed Electroluminescence Emitters with Carbon Nanotube Films

○Hidenori Takahashi[1], Yuji Suzuki[1], Norito Yoshida[1], Kenta Nakagawa[2] and Hideyuki Maki[1,3]

[1] *Department of Applied Physics and Physico-Informatics, Keio University, Yokohama 223-8522, Japan*
[2] *Kanagawa Institute of Industrial Science and Technology (KISTEC), Ebina 243-0435, Japan*
[3] *Center for Spintronics Research Network (CSRN), Keio University, Yokohama 223-8522, Japan*

Nanocarbon materials, such as carbon nanotubes (CNTs), are promising candidates for optoelectronic light sources, because they can be easily and directly formed on silicon substrate.[1-4] Here, as shown in Fig. 1, we fabricated several-GHz modulatable Electroluminescence (EL) emitters with high emission intensity and high fabrication yield by using semiconducting single-walled carbon nanotubes (SWNTs) films. The mechanisms of the EL emission from this emitter are elucidated by the emission spectrum as shown in Fig. 2 and p-type-like electric properties. The peaks of the EL emission, which correspond to each of the chiralities of the SWNTs, are about 0.15 eV red-shifted from the those of the absorption and PL emission. Such a red shift can be explained by the EL emission from the trion states. As shown in Fig. 4, rapid emission response was also observed. From the fitting by convolving the ideal EL response curve and simple relaxation curve given by $\exp(-t/\tau)$, 140-ps relaxation time, corresponding to ~ GHz modulation, is obtained.

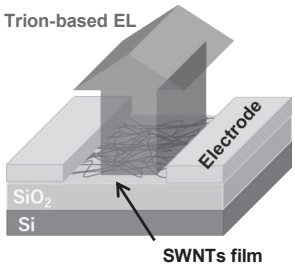

Fig. 1 A schematic illustration of a SWNTs film EL emitter.

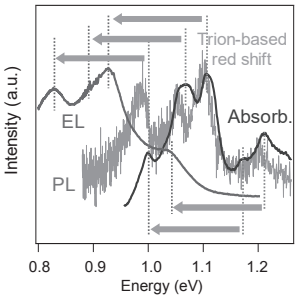

Fig. 2 Absorption spectrum (blue curve), PL spectrum (green curve), and EL spectrum (red curve) of the SWNTs thin film.

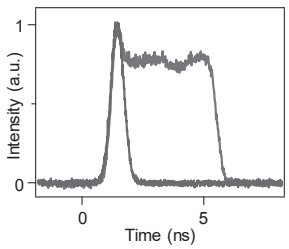

Fig. 3 Time-resolved emission intensities under a rectangular bias voltage.

[1] N. Hibino *et al.*, ACS Nano **5**, 1215-1222 (2011).
[2] M. Fujiwara *et al*, Appl. Phys. Lett. **103**, 143122 (2013).
[3] T. Mori *et al*, Nano Lett. **14**, 3277-3283 (2014).
[4] Y. Miyoshi *et al*, Nat. Commun. **9**, 1279 (2018).

Corresponding Author: H. Maki
Tel: +81-45-566-1643, Fax: +81-45-566-1587,
Web: http://www.az.appi.keio.ac.jp/maki/
E-mail: maki@az.appi.keio.ac.jp

Single-chirality separation of single-walled carbon nanotubes with a thermoresponsive polymer

○Eriko Shimura, Toshiki Sugai, Shota Kuwahara

Department of Chemistry, Toho University, Chiba 274-8510, Japan

The separation techniques for obtaining single-chirality of single-walled carbon nanotubes (SWCNTs) is crucial for application to electronic devices with SWCNTs. The difference in the hydrophobicity or surface charge of SWCNT micelles with surfactant molecules is reported to be a key factor to separate semiconducting and/or metallic SWCNTs with high purity. We have succeeded in separating semiconducting SWCNTs with poly(*N*-isopropylacrylamide) (PNIPAM), a well-known thermoresponsive polymer with reversible phase transition in aqueous solutions at the lower critical solution temperature (LCST) [1]. The difference in the hydrophobicity of SWCNTs is understood to be the origin of the selectivity in capturing SWCNTs with specific electronic structures inside globules, which are formed by PNIPAM aggregates above LCST, resulting in releasing semiconducting SWCNTs into the liquid phase after phase transition of PNIPAM. In this work, we investigated the dependence on PNIPAM concentration and additives for achieving single-chirality separation of SWCNTs, and found that the additives sensitively selected the chirality of the released SWCNTs into the liquid phase.

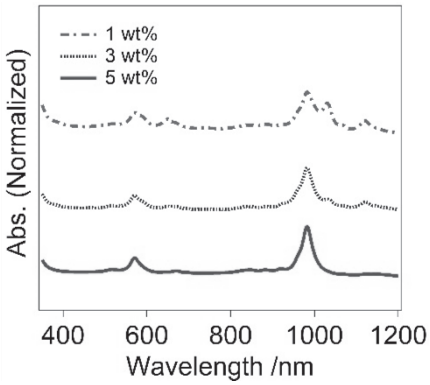

Fig. 1 Optical absorption spectra of the obtained liquid phase in the presence of NaClO with different concentrations of PNIPAM in solution.

A dispersion of SWCNTs in aqueous sodium cholate (SC) solution was prepared by using a probe tip ultrasonicator (TOMY, UR-20R), and added to PNIPAM solution with additive. Then, the mixed solution was heated to 45 °C above the LCST of PNIPAM and incubated for 15 minutes. The obtained liquid phase was collected, and characterized by UV-vis-NIR spectrophotometer (SHIMADZU, UV-3600).

As shown in Fig. 1, (6,5) SWCNT enriched sample was obtained in the existence of sodium hypochlorite (NaClO), additive for oxidant, and the purity of (6,5) SWCNTs depended on the concentration of PNIPAM. When tetraborate pH standard solution was used for the additive alternative to NaClO, (6,4) SWCNTs were selectively released to the liquid phase (Fig. 2). The separation mechanism seems to be explained by the dependence of chirality on the amount of SC and its orientation on the surface of a SWCNT, same as the commonly accepted explanation in the density gradient ultracentrifugation separation technique [2].

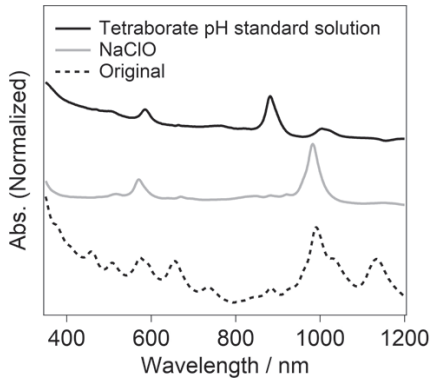

Fig. 2 Optical absorption spectra of the obtained liquid phase with different additives in solution.

[1] E. Shimura, *et al.*, *Chem. Commun.*, **54**, 3026 (2018).
[2] M. S. Arnold, *et al.*, *Nat. Nanotech.*, **1**, 60-65 (2006).
Corresponding Author: S. Kuwahara
Tel: +81-47-472-4442 E-mail: syouta.kuwahara@sci.toho-u.ac.jp

Optical Studies of Monolayer $MoSe_2$ on Strongly Correlated Manganese Oxide

○ Yan Zhang[1], Yutaka Moritomo[2], Keisuke Shinokita[1], Yuhei Miyauchi[1] and Kazunari Matsuda[1]

[1]*Institute of Advanced Energy, Kyoto University, Uji, Kyoto 611-0011, Japan*

[2]*Department of Physics, University of Tsukuba, Tsukuba, Ibaraki 305-8571, Japan*

Monolayer two-dimensional semiconducting transition metal dichlcogenides with coupled spin-valley degree of freedom have been attractive much attentions from the viewpoint of fundamental physics and application of valleytronics [1]. Recently, the artificial heterostructures based on monolayer transition metal dichlcogenides and various layered materials have been extensively studied. Among these layered materials, the strongly correlated manganese oxides exhibit unique carrier transport and magnetic properties [2]. Hence, it is interesting to explore excitonic and valley physics in the artificial heterostructure using manganese oxides.

In this study, we described novel optical properties of artificial heterostructure of monolayer $MoSe_2$ and $(La_{0.8}Nd_{0.2})_{1.2}Sr_{1.8}Mn_2O_7$ (Mn oxide). The manganese oxide shows paramagnetic-insulator to ferromagnetic-metal transition at ~80 K [2]. The temperature dependence of photoluminescence (PL) spectra of heterostructure ($MoSe_2$/Mn oxide) and $MoSe_2$ were measured. Figure 1(a) shows the two PL peaks due to the recombination of exciton (X) and trion (X^-) at 10 K. The temperature dependence of PL intensity ratio of X^- and X (I_{X^-}/I_X) in the heterostructure and monolayer $MoSe_2$ in Figure 1(b). We observed that significant difference of PL intensity ratio of X^- and X in the heterostructure and $MoSe_2$, which suggests that doped carrier density of $MoSe_2$ is much different between the heterstruture and reference. We discussed the excited state dynamics within the framework of an exciton and a trion in the heterostructure to analyze this difference [3]. Moreover, we will discuss the magneto-optical properties in the heterostructure under strong magnetic fields.

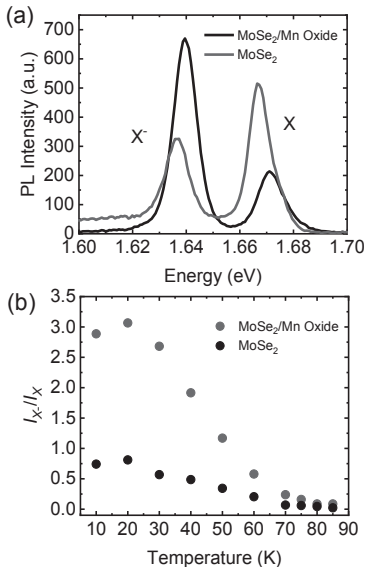

Fig.1 (a) PL spectra of $MoSe_2$/Mn oxide and $MoSe_2$ at 10 K. (b) PL intensity ratio of trion and exciton from 10 to 85 K.

[1] J. Ross, S. Wu, H. Yu. *et al. Nat. Commun.* **4**, 1473–1476 (2013).

[2] Y. Moritomo, Y. Maruyama, T. Akimoto. *et al*. *Phys. Rev. B*, **56**, R7057 (1997).

[3] S. Mouri, Y. Miyauchi, K. Matsuda. *Nano Lett.* **13**, 5944–5948 (2013).

Corresponding Author: K. Matsuda

Tel: +81-774-38-3460, Fax: +81-774-38-3460,

Web: http://www.iae.kyoto-u.ac.jp/conv/

E-mail: matsuda@iae.kyoto-u.ac.jp

Nearly Isotropic and Large Critical Field from Three-Dimensional Networks of Anisotropic Superconducting Flakes

○Chisato Ando[1], Yusuke Nakanishi[1], Jiang Pu[2], Togo Takahashi[2], Taishi Takenobu[2], and Yasumitsu Miyata[1]

[1] *Department of Physics, Tokyo Metropolitan University, Hachioji 192-0397, Japan*
[2] *Department of Applied Physics, Nagoya University, Nagoya 464-8603, Japan*

Two-dimensional (2D) superconductors have been recognized as ideal models for exploring superconductive phenomena at the 2D limit [1], as well as potential candidates for high-temperature superconductors [2]. Despite the growing interest in increasing T_c, less effort has been made to improve their anisotropy of upper critical field (H_{c2}). Most of layered 2D superconductors are not isotropically stable against magnetic fields due to their anisotropic structures. Definitely, their intrinsic anisotropy of H_{c2} is a crucial issue to be resolved for their future applications.

Here we demonstrate nearly isotropic and large H_{c2} in 3D networks of layered $NbSe_2$ with randomly aligned flakes. To fabricate the 3D structures, we have developed a selenization process to convert Nb layers into polycrystalline $NbSe_2$ films [3]. We find that $NbSe_2$ flakes are preferred to grow randomly with increasing thickness of initial Nb layers (**Figure 1**a, b), thereby resulting in the realization of nearly isotropic H_{c2} (**Figure 1**c). In addition, the H_{c2} for the present film is larger compared to the bulk layers (**Figure 1**d). The concept of building up with 2D superconductors would broaden the range of their applications.

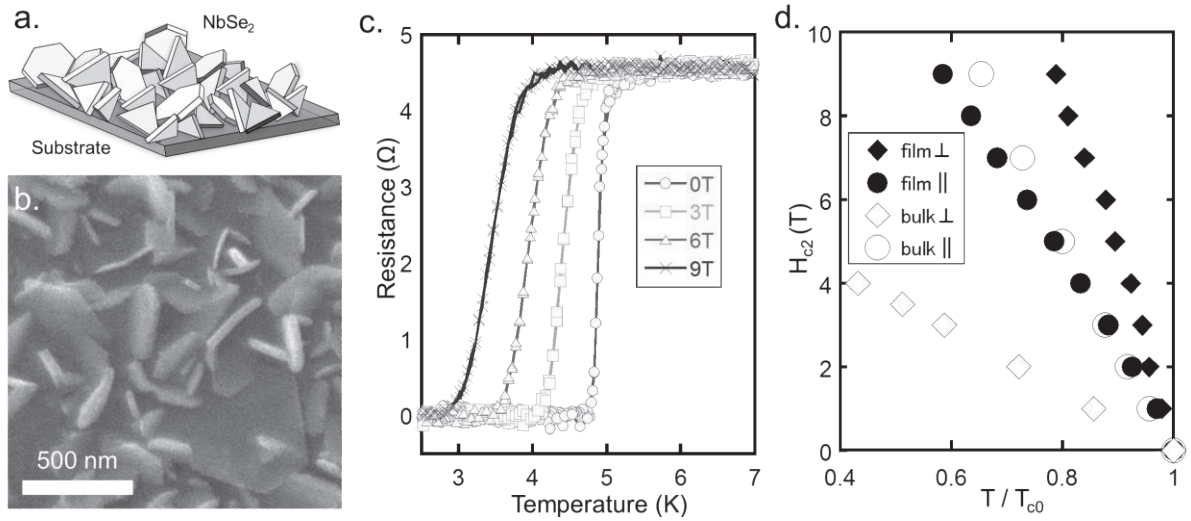

Fig. 1 (a) A schematic illustration of the $NbSe_2$ films converted from Nb layers via the selenization process. (b) A scanning electron micrograph image of the $NbSe_2$ film. (c) The superconducting transition of the prepared film under out-of-plane magnetic fields. (d) Temperature dependence of the H_{c2} for the present film and the bulk layers under out-of-plane and in-plane magnetic fields. The values of H_{c2} for the bulk are referred to ref [4].

[1] S. Qin *et al., Science* **324**, 1314 (2009).
[2] S. Tan *et al., Nat. Mater.* **12**, 632 (2013); J.-F. Ge, *et al., Nat. Mater.* **14**, 285 (2014)
[3] H. Lin *et al., Nat. Mater.* **18**, 602 (2019).
[4] X. Xi *et al., Nat. Phys.* **12**, 139 (2015).

Corresponding Author: Y. Nakanishi, Y. Miyata
Tel: 042-677-2508, E-mail: naka24ysk@tmu.ac.jp, ymiyata@tmu.ac.jp

Work function modulation of transparent electrode for fabrication of WS_2-based highly transparent solar cell

○X. He[1], Y. Yamaguchi[1], T. Kaneko[1], and T. Kato[1,2]

[1]*Graduate School of Engineering, Tohoku University, Sendai 980-8579, Japan*
[2] *JST-PRESTO*

Layered transition metal dichalcogenide (TMD) is known as a true 2D material with excellent semiconducting properties. TMD is one of the most attractive materials for future transparent and flexible optoelectrical devices due to their atomically thin structure, band gap in visible light range, and high optical transparency. Although the solar cell of TMD has been widely investigated by many groups, those are based on the pn junction type solar cell. Since complicated structures are required to form pn junction structures in TMD such as dual gate electrodes or position selective doping, the device size of pn junction solar cell with TMD is limited within very small region (few μm). In spite of the outstanding advantages of TMD, those merits of TMD have not been applied for transparent and flexible solar cell, which is attracted intense attention as a next-generation energy harvesting technology.

Recently, we have developed a new fabrication process of TMD-based solar cell [1]. In our process, Schottky type device configuration is utilized, which can be simply formed by asymmetrically contacting electrodes and TMD. The power conversion efficiency clearly depended on the work function difference between two electrodes (ΔWF), and a higher efficiency could be obtained with higher ΔWF (Pd-Ni). Based on the optimizations of electrodes and distance, the power conversion efficiency can be reached up to 0.7 %, which is the highest value for solar cell with similar TMD thickness [1].

In our previous study, we used conventional metals such as Ni and Pd to tune the Schottky barrier height between electrode and TMD, which suppress the transparency of whole device. Furthermore, the device size was limited within μm scale because of the size of exfoliated TMD.

To improve the transparency of whole device, we use indium tin oxide (ITO) as electrodes. The directly grown large area WS_2 films are also used to overcome the limited device size. The work function of transparent electrodes are controlled by inserting various thin metals between WS_2 and ITO (Fig. 1). After controlling the ΔWF of ITO electrodes and optimizing the synthesis method of WS_2, clear power generation can be observed with ITO/WS_2 based transparent solar cell in large scale (Fig. 1). Transparency of whole device reaches up to 80%, which is very important for realizing the industrial application of TMD as a transparent and flexible solar cell.

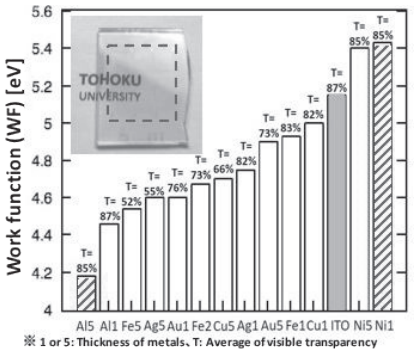

Fig. 1. Work function of different thin metal modified electrodes. Insertion is typical optical image of transparent solar cell fabricated with directly grown WS_2 crystal.

[1] T. Akama, W. Okita, R. Nagai, C. Li, T. Kaneko, and T. Kato, Sci. Reports **7**, 11967 (2017).

Corresponding Author: Xing He

Tel: +81-22-795-7046, Fax: +81-22-263-9225, E-mail: he.xing.q7@dc.tohoku.ac.jp

Fabrication and evaluation of hBN-encapsulated Monolayer $MoSe_2$ with CNT local gates

○Takato Hotta [1], Haruna Nakajima [1], Taiki Inoue [2], Shohei Chiashi [2], Keiji Ueno [3], Kenji Watanabe [4], Takashi Taniguchi [4], Shigeo Maruyama [2, 5] and Ryo Kitaura [1]

[1] *Department of Chemistry, & Institute for Advanced Research, Nagoya University, Nagoya 464-8602, Japan*
[2] *Departure of Mechanical Engineering, The University of Tokyo, Tokyo 113-8656, Japan*
[3] *Department of Chemistry, Saitama University, Saitama 338-8570, Japan*
[4] *National Institute of Materials Science, Tsukuba 305-0044, Japan*
[5] *Energy Nano Engineering Lab., National Institute of Advanced Industrial Science and Technology (AIST), Tsukuba 305-8564, Japan*

Confined excitons in two-dimensional (2D) semiconductors, such as transition metal dichalcogenides (TMDs), have provided fascinating opportunities for investigation of excitons at the 2D-limit. Recently, zero-dimensional (0D) confined excitons have been found in a $WSe_2/MoSe_2$ moiré superstructure, giving a playground to explore confined excitons at the 0D [1, 2]. In this work, we have focused on adding one more kind of confined excitons, excitons confined into one-dimensional space. For this purpose, we have fabricated hBN-encapsulated $MoSe_2$ devices with carbon nanotube (CNT) local gates.

We have fabricated two types of hBN-encapsulated monolayer $MoSe_2$ with CNT local gates by dry transfer method based on PC/PDMS stamps: hBN/$MoSe_2$/hBN with CNT top gates and CNT back gates. First, CNTs were grown on quartz substrates with chemical vapor deposition (CVD) method, and then, the CVD-grown CNTs were transferred to SiO_2/Si substrates with the wet transfer method. For fabrication of hBN/$MoSe_2$/hBN with CNT top gates, the CNTs transferred on SiO_2/Si were picked up with PC/PDMS stamps and transferred onto a hBN-encapsulated $MoSe_2$. Fig. 1 shows an optical microscope image of a fabricated hBN-encapsulated $MoSe_2$ with CNT top gates. Photoluminescence (PL) spectroscopy and imaging at cryogenic temperature has shown that PL intensity and PL spectra change according to gate voltage applied through CNT back gates. In the presentation, we will discuss the details of the sample preparation and PL measurement.

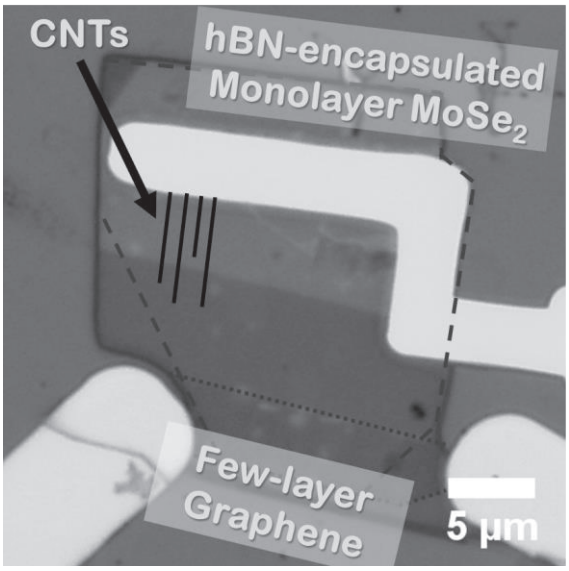

Fig. 1 An optical microscope image of the fabricated hBN/G/$MoSe_2$/hBN with CNT top gates. Positions of CNTs are indicated by solid lines.

[1] K. L. Seyler, et. al., Nature 567, 66-70 (2019).

[2] K. Tran, et. al., Nature 567, 71-75 (2019).

Corresponding Author: R. Kitaura
Tel: +81-52-789-3660, Fax: +81-52-747-6442,
E-mail: r.kitaura@nagoya-u.jp

Detection of odor molecule with graphene biosensor

Chishu Honma[1)], Hironaga Noguchi[1)], Yoshiaki Sugizaki[2)],
Atsunobu Isobayashi[2)], Yuhei Hayamizu[1)]

1) School of Materials and Chemical Technology Department of Materials Science and Engineering, Tokyo Institute of Technology, 2-12-1 Ookayama, meguroku, Tokyo, Japan
2) Corporate Research & Development Center, Toshiba Corporation, 1, Komukai-Toshiba-cho, Saiwai-ku, Kawasaki 212-8583, Japan

E-mail: honma.c.aa@m.titech.ac.jp

Graphene biosensor attracts wide attentions due to its unique properties [1]. The applications are not limited only in the medical field, but also in the environmental field. The functionalization of the surface of graphene is a key to be act as a sensor. However, immobilization of bio-probe molecules using covalent bonds can cause a degradation of the intrinsic electronic properties. Furthermore, it is crucial to control the orientation of probe molecules for sustaining its activity. In this work, we address these problems by using self-assembled peptides that self-assemble on the graphene surface, resulting in non-covalent immobilization of bio-probes [2]. These peptides can form uniform and ordered structures on graphene spontaneously. Using the self-assembled peptides, we aim to create an odor biosensor that detects limonene (citrus odor molecule) as a model molecule. We designed two kinds of peptides: (1) molecular scaffold and (2) bio-probe. By co-assembling these peptides, we formed a uniform thin film of peptides on the surface of graphene, and succeeded to biofunctionalized it with a good sensitivity to limonene. Figure 1 shows images of atomic force microscope of the self-assembled membrane of peptides with various mixing ratio of the two kinds of peptides. In the presentation, we will introduce electrical characteristics of the biosensor. This work was supported by the Cabinet Office (CAO), Cross-ministerial Strategic Innovation Promotion Program (SIP), "An intelligent knowledge processing infrastructure, integrating physical and virtual domains" (funding agency: NEDO).

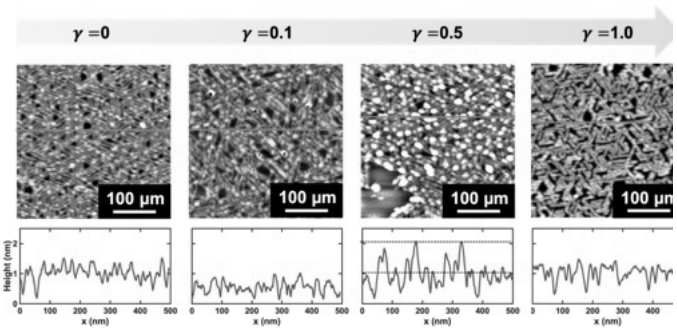

Figure 1. Images of assembled peptide on graphene surface observed by atomic force microscope, and their height profiles.

Reference

[1] Ohno,Yasuhide ,et al.; J. Am. Chem. Soc., 2010, 132 (51), 18012–18013

[2] Khatayevich, Dmitriy, et al. Langmuir 28.23 (2012): 8589-8593.

Efficient Production and Characterization of 1D Transition Metal Monochalcogenides Inside Carbon Nanotubes

○Naoyuki Kanda[1], Yusuke Nakanishi[2], Dan Liu[3], Zheng Liu[4], Kazu Suenaga[4], David Tomanek[3], and Hisanori Shinohara[1]

[1] *Department of Chemistry, Nagoya University, Nagoya 464-8602, Japan*
[2] *Department of physics, Tokyo Metropolitan University, Hachioji 192-0397, Japan*
[3] *Department of physics and Astronomy, Michigan State University, East Lansing, MI 48824-6455, USA*
[4] *National Institute of Advanced Industrial Science and Technology (AIST), Nagoya 463-8560, Japan*

The idea that single units of van der Waals (vdW)-bonded materials might show exotic properties distinct from their bulk counterparts has been verified by the successful isolation of 2D vdW-layered materials such as graphene and transition metal dichalcogenides (TMDs). Similarly, isolated 1D vdW-wired materials like transition-metal monochalcogenides (TMMs) could exhibit superlative properties being significantly absent in their bundles [1, 2]. Recently, our group has successfully isolated MoTe nanowires (NWs) inside carbon nanotubes (CNTs), and observed their unusual torsional dynamics [3]. On the encapsulation of TMM-NWs, transport characteristics of CNTs are also expected to vary drastically due to their interaction. However, the current method for the synthesis of MoTeNWs from MoTe2 produces the NWs in low yield, which makes it difficult to perform detailed studies of their properties.

Here we report high-yield synthesis of MoTeNWs inside CNTs from molybdenum oxides and "naked" terullium. We found that MoTeNWs can be efficiently self-assembled from these precursors (Fig. 1a, b). Furthermore, this method was applied to a new member of TMM-NWs, WTeNWs. The efficient synthesis method allows for the studies of twist-induced properties of TMM-NWs as well as transport characteristics of the hybrid CNT materials. Detailed discussion will be presented in the conference.

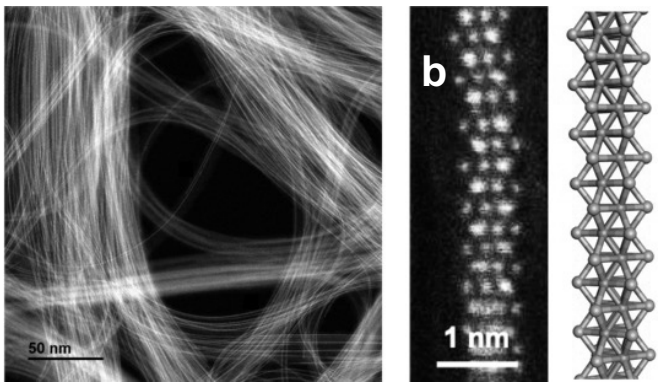

Fig. 1a, b. HAADF-STEM image of MoTeNWs

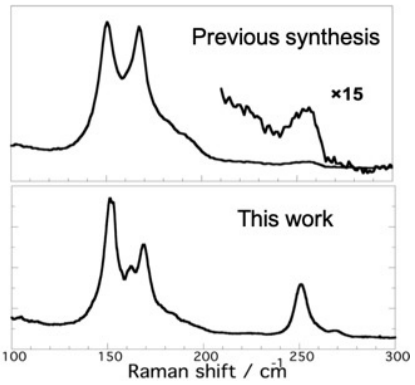

Fig. 2. Raman spectrum of MoTeNWs@CNTs

[1] H. Zhu, Q et al., Adv. Mater. 29, 1606264 (2017).
[2] I. Popov, S et al., Nano Lett. 8, 12 (2008).
[3] M. Nagata et al., Nano Lett., in press.

Corresponding Author: Y. Nakanishi
Tel: +81-42-677-1111
Web: http://naka24ysk.jp/wp/
E-mail: naka24ysk@tmu.ac.jp

Supramolecule of $Li^+@C_{60}$ and fluorinated tetraphenylporphyrin

○ Kazuhira Miwa[1], Shinobu Aoyagi[1], Hiroshi Ueno[2,3], Hiroshi Okada[4,5,6], Kazuhiko Kawachi[4], Yasuhiko Kasama[4]

[1]*Dept. of Information and Basic Science, Nagoya City Univ., Nagoya, 467-8501, Japan*
[2]*Frontier Research Institute for Interdisciplinary Sciences, Creative Interdisciplinary Research Division, Tohoku Univ., Sendai, 980-8578, Japan*
[3]*Dept. of Chemistry, Graduate School of Science, Tohoku Univ., Sendai, 980-8578, Japan*
[4]*Idea International Co., Ltd. Sendai, 981-0922, Japan*
[5]*Fukamatsugumi Co., Ltd. Sendai, 981-0931, Japan*
[6]*Center for Fundamental and Applied Research of Novel Nanocarbon Derivatives, Center for Key Interdisciplinary Research, Tohoku Univ., Sendai, 980-8578, Japan*

Lithium ion endohedral fullerene ($Li^+@C_{60}$) has a unique structure encapsulating Li^+ inside the π–conjugated spherical C_{60} cage. The cationic $Li^+@C_{60}$ crystallizes with weakly coordinated anions such as $SbCl_6^-$ [1], PF_6^- [2], and bis(trifluoromethanesulfonyl)imide anion ($TFSI^-$) [3]. $Li^+@C_{60}$ also forms a guest–host type supramolecule with [10]cycloparaphenylene ([10]CPP) [4] and π–π stacked supramolecules with porphyrins. A supramolecule of $Li^+@C_{60}$ and 5,10,15,20-tetrakis(4–sulfonatophenyl)porphyrin zinc (ZnTPPS), [$Li^+@C_{60}$ – $ZnTPPS^{4-}$] shows a long–lived electron charge separation state by photoinduced electron transfer [5]. The optical property and intermolecular interaction can be applied to photovoltaic cells [6] and tuned by chemical modification of porphyrins. Fluorinated porphyrin, tetrakis(pentafluorophenyl)porphyrin (TPFPP) shows additional intermolecular interaction with C_{60} via C–F···C (fullerene) contacts [7][8]. It is interesting to investigate intermolecular interactions between cationic $Li^+@C_{60}$ and fluorinated porphyrin.

In order to reveal properties and intermolecular interactions of supramolecule of $Li^+@C_{60}$ and fluorinated tetraphenylporphyrin, we investigate crystal structure of co–crystals of $Li^+@C_{60}$ ($TFSI^-$) and fluorinated porphyrins. 5,10,15,20-tetrakis(2,3,5,6-tetrafluorophenyl)porphyrin (TTFPP) was prepared according to the Lindsey method. $Li^+@C_{60}$ ($TFSI^-$)/TTFPP co–crystals were grown from solution of $Li^+@C_{60}$ ($TFSI^-$) and TTFPP by diffusion method. The co–crystal structure was determined by X-ray diffraction measurement at SPring-8. Although the crystal system is different, coordinated structure around $Li^+@C_{60}$ in the $Li^+@C_{60}$ ($TFSI^-$)/TTFPP co–crystal is similar to that around C_{60} in the C_{60}/TPFPP co–crystal. C–F···C (fullerene) distances in $Li^+@C_{60}$ ($TFSI^-$)/TTFPP are 2.953 – 3.489 Å which are comparable with that in C_{60}/TPFPP.

References

[1] S. Aoyagi *et al.* Nature Chem. **2**, 678–683 (2010).
[2] S. Aoyagi *et al.* Angew. Chem. Int. Ed. **51**, 3377–3381 (2012).
[3] S. Aoyagi *et al.* R Soc Open Sci. **5**, 180337 (2018).
[4] H. Ueno *et al*. Angew. Chem. Int. Ed. **54**, 3707–3711 (2015).
[5] K. Ohkubo *et al.* Chem. Commun., **48**, 4314–4316 (2012).
[6] K. Ohkubo *et al.* Chem. Commun. **49**, 4474–4476, (2013).
[7] A. Hosseini *et al.* Crystal Growth & Design. **6**, 397–403, (2006).
[8] M. Olmstead *et al.* Crystal Growth & Design. **6**, 109–113, (2006).

Corresponding Author: S. Aoyagi
E-mail: aoyagi@nsc.nagoya-cu.ac.jp

Catalytic activity for reduction of 4-nitroaniline with nickel oxide nanoparticle-[C_{60}]fullerene nanowhisker composites

○Jeong Won Ko[1], Sugyeong Jeon[2], Weon Bae Ko[1,2,3]

[1] Nanomaterials Research Institute, [2]Department of Convergence Science, Graduate School, [3]Department of Chemistry, Sahmyook University, 815, Hwarang-ro, Nowon-gu, Seoul 01795, Republic of Korea

Nickel nitrate hexahydrate ($Ni(NO_3)_2 \cdot 6H_2O$) and sodium hydroxide(NaOH) were dissolved in to distilled water and then stirring for 30 min. The green precipitate($Ni(OH)_2$) was heated to obtain nickel(II) oxide nanoparticle in an electric furnace under Ar gas at 700 ºC for 45 min [1]. Nickel(II) oxide nanoparticle-[C_{60}]fullerene nanowhisker composites were prepared by using nickel(II) oxide nanoparticle solution, C_{60}-saturated toluene, and isopropyl alcohol by liquid-liquid interfacial precipitation (LLIP) method [2]. The resulting product of nickel(II) oxide nanoparticle-[C_{60}]fullerene nanowhisker composites was characterized by X-ray diffraction, scanning electron microscopy, Raman spectroscopy, and transmission electron microscopy. The catalytic activity of nickel(II) oxide nanoparticle-[C_{60}]fullerene nanowhisker composites was confirmed in the reduction of 4-nitroaniline by UV-vis spectroscopy.

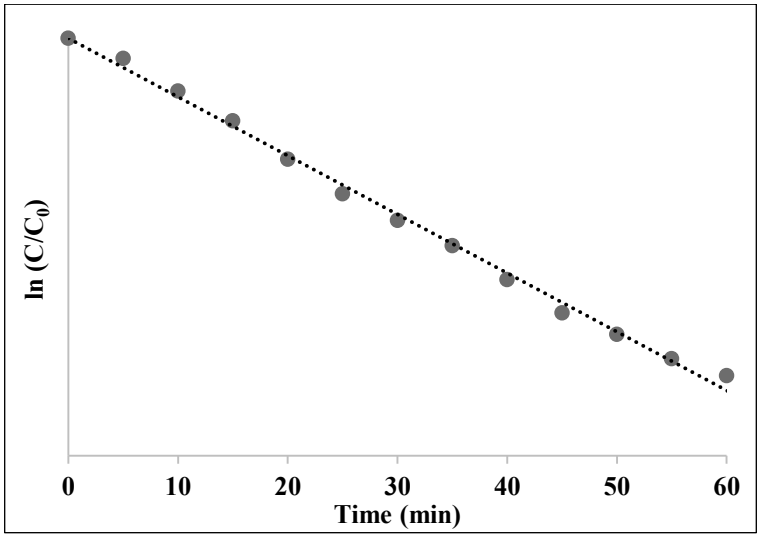

Fig.1 Kinetic study for reduction of 4-nitroaniline with nickel(II) oxide nanoparticle-[C_{60}]fullerene nanowhisker composites

[1] K. Karthik *et al*. J. Alloys. Compd., **509**(1), 181 (2011).

[2] K. Miyazawa *et al*. Surf. Eng. doi.org/10.1080/02670844.2017.1396779 (2017).

Corresponding Author: W. B. Ko

Tel: +82-2-3399-1700, Fax:, +82-2-979-5318,

E-mail: kowb@syu.ac.kr

Thermal transport study of molybdenum disulfide nanotubes by molecular dynamics simulations

○Kaoru Hisama[1], Takuma Shiga[1], Susumu Okada[2], Shohei Chiashi[1] and Shigeo Maruyama[1,3]

[1] *Department of Mechanical Engineering, The University of Tokyo, Tokyo 113-8656, Japan*

[2] *Graduate School of Pure and Applied Sciences, University of Tsukuba, Tsukuba 305-8571, Japan*

[3] *Energy NanoEngineering Lab., National Institute of Advanced Industrial Science and Technology (AIST), Ibaraki 305-8564, Japan*

One-dimensional, single-walled structures of transition metal dichalcogenide nanotubes (TMDNTs), have recently been synthesized from templates of carbon nanotube (CNT) [1] and these TMDNTs were previously predicted to show different electronic and optical properties from their two-dimensional counterparts [2]. However, little is known about thermal properties of TMDNTs, such as diameter, chirality or length dependence of thermal conductivity unlike that of CNT, which are investigated by many literature [3]. For the future design of electronic devices with TMDNTs, it is important to understand these thermal transport properties in detail.

Thus, here we investigated the heat conduction of molybdenum disulfide nanotube (MoS_2NT) by combining non-equilibrium molecular dynamics (NEMD) and lattice dynamics (LD) [4, 5]. We employed the modified Stillinger-Weber (SW) potential parameters [6] for describing the interatomic interactions.

Dispersions of MoS_2NT in the range of 3-10 nm were calculated by LD, as is shown in Fig.1 (a). NEMD was executed for an end-fixed MoS_2NT with length about 10 nm shown in Fig. 1(a). Although a previous study [7] showed that thermal conductivity of MoS_2NT with diameter D > 7 nm did not have significant diameter dependence, our result suggested that there was a gradual tendency of increase of the thermal conductivity as a function of diameter with the same range as our LD, as is shown in Fig 1(c).

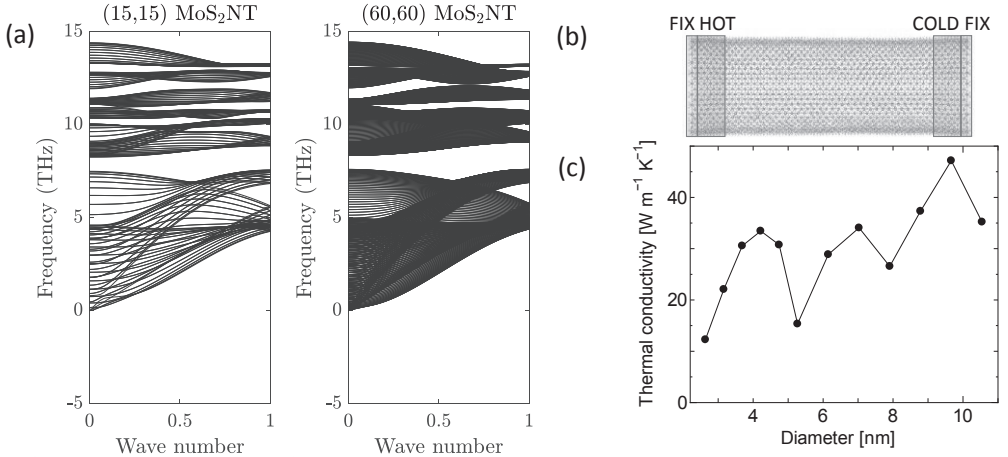

Figure 1 (a) Phonon dispersion of MoS_2NT (15,15) and (60,60). (b) Schematics of MoS_2NT (27,27) and NEMD settings. (c) Thermal conductivity of armchair MoS_2NT as a function of diameter.

[1] R. Xiang *et al*., arXiv:1807.06154 (2018). [2] Seifert *et al., Phys. Rev. Lett.*, **85**, 146 (2000).
[3] P. Wang and S. Maruyama, *Advances in Heat Transfer*, **50**, 43 (2018). [4] LAMMPS: S. Plinpton, *J. Comp. Phys*, **117**, 1 (1995). [5] GULP: J. Gale, and A. Rohl. *Molecular Simulation* **29**, 291 (2003).
[6] J-W. Jiang *et al., J. Appl. Phys*., **114**, 064307 (2013). [7] H. Meng *et al*., arXiv:1906.05495 (2019).
Corresponding Author: Shigeo Maruyama E-mail: maruyama@photon.t.u-tokyo.ac.jp

Hall Effect on Aligned Metallic Single-Wall Carbon Nanotube Thin Films

○Kanako Horiuchi[1], Ryotaro Okada[1], Hideki Kawai[1], Kan Ueji[1], Yohei Yomogida[1], Weilu Gao[2], Junichiro Kono[2], Kazuhiro Yanagi[1]

[1] *Department of Physics, Tokyo Metropolitan University, Tokyo 192-0397, Japan*
[2] *Department of Electrical and Computer Engineering, Rice University, Texas 77005, USA*

Hall effect measurements are important for understanding the charge transport mechanisms and intrinsic carrier mobility. However, in hopping conduction systems, it is not possible to correctly evaluate carrier density through the hall effect measurements, because hopping carriers only respond to the electric force, not to the Lorentz force.[1] Transport mechanisms in most of single-wall carbon nanotube networks are hopping conductions, thus it has been considered that hall effect cannot be correctly observed in SWCNT systems. However, in the metallic SWCNT networks, weak localization conduction has been observed, and in such conduction, it may be possible that the hall effect can be observed. Previously, we tried to measure the hall effect on metallic SWCNT thin film where the nanotubes were randomly distributed, but we could not identify correct hall signal. In this study, we investigated the hall effect in aligned metallic SWCNT systems because aligned structure may reduce the localized hopping conduction.

We prepared thin films of aligned metallic SWCNTs using a method reported by He et al. [2]. The aligned SWCNT thin film was transferred to the SiO_2 substrate deposited electrodes, and we injected carrier by using side gating techniques using electrolyte gating.

First, we checked the transport characteristics, and we confirmed ambipolar conduction. Then, we investigated the hall voltage at hole and electron conductions. We observed that the hall voltage becomes negative as increase of magnetic field at the electron conduction region, but, the hall voltage becomes positive as the increase of magnetic field at the hole conduction region (Figure 1). The sign of the hall voltage changed according to the types of conduction carriers. These results suggest that the hall effect was detected in the aligned metallic thin film system.

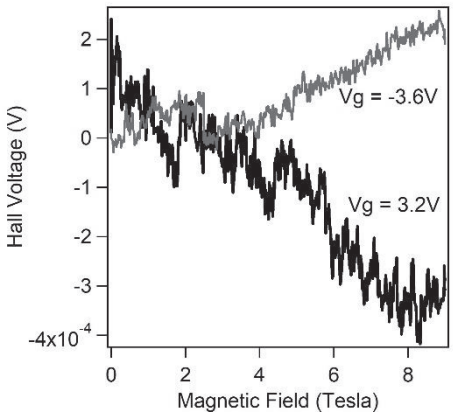

Figure 1: Hall voltage as a function of magnetic field at Vg of -3.6 V (hole conduction) and 3.2 V (electron conduction).

References: [1] Yi et al., Sci. Rep. 6 23650 (2016) [2] He et al, Nat. Nanotech. 11, 633 (2016)
Corresponding to Kazuhiro Yanagi, yanagi-kazuhiro@tmu.ac.jp

Transition from Metallic to Semiconducting behaviors in Seebeck coefficients of Semiconducting Single-Wall Carbon Nanotube film.

○Akari Yoshida, Yota Ichinose, Kengo Fukuhara,
Kan Ueji, Yohei Yomogida and Kazuhiro Yanagi

Department of Physics, Tokyo Metropolitan University, Tokyo 192- 0397, Japan

In metallic materials, the decrease of temperature induces the increase of conductivity and the decrease of Seebeck coefficient. In semiconducting materials, the decrease of temperature induces the decrease of conductivity and the increase of Seebeck coefficient. However, in a variable range hopping (VRH) conduction system, we sometimes observe contradictive behaviors among these temperature dependences of conductivity and Seebeck coefficients, i.e. decrease of both the conductivity and the Seebeck coefficient as the decrease of temperature. Usually, single-wall carbon nanotubes (SWCNTs) thin films exhibit VRH conductions. Thus as far as we know, the absolute value of the Seebeck coefficient decreases as the decrease of temperature although the conductivity also becomes small, reflecting hopping conduction. However, recently, theoretical calculation suggests when the Fermi-level is precisely tuned around the band-edge of the semiconducting van hove singularities, it is possible to change the temperature dependence of the Seebeck coefficient from the metallic to the semiconducting behaviors.[1] Therefore, in this study, in order to understand the background of the thermoelectric properties of hopping systems, we investigated whether it is possible to change the metallic and semiconductor behaviors of the Seebeck coefficient by tuning carrier injections in semiconducting SWCNTs.

We fabricated an electric double layer transistor (EDLT) devices using an ion gel for the semiconductor SWCNTs thin film with a diameter of 1.4 nm, which was purified through density gradient ultracentrifugation. By changing the gate voltage (V_G), the carrier injection amount of the sample is changed to control the location of the Fermi level. And we have investigated the temperature dependence of the Seebeck coefficient.

Fig. 1 shows temperature dependence of the Seebeck coefficient in semiconducting SWCNTs thin films in with controlled Fermi level. When the Fermi level is in the energy band (V_G = -0.8 V, In-Band region), the Seebeck coefficient decreases as the decrease of the temperature, which is conventional behavior in VRH hopping systems. On the other hand, when the Fermi level is located in the energy gap (V_G = -1.0 V, In-Gap region), we observed the increase of the Seebeck coefficient as the decrease of the temperature. We observed the transition in temperature dependence of the Seebeck coefficient from metallic to semiconducting types.

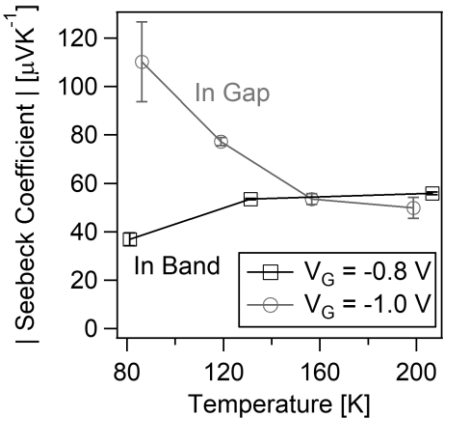

Fig. 1 Temperature dependence of Seebeck coefficient in semiconducting SWCNTs thin films.

[1] Yamamoto&Fukuyama, JPSJ 87, 114710 (2018)

Corresponding Author: K. Yanagi
Tel: +81-42-677-2494, Fax: +81-42-677-2483
E-mail: yanagi-kazuhiro@tmu.ac.jp

Theoretical Study on Thermoelectric Properties of Local Distorted Carbon Nanotube

○Keiichiro Matsumoto[1], Takahiro Yamamoto[1,2]

[1] *Department of Electrical Engineering, Tokyo University of Science, Tokyo 125-8585, Japan*
[2] *RIST, Tokyo University of Science, Tokyo 125-8585, Japan*

Thermoelectric generation is expected to use for the self-sustaining sources, which are required to realize IoT society. As a material used for the thermoelectric generation devices, a carbon nanotube (CNT) is a potential candidate for flexible devices. In the CNT film, some of the CNTs are considered to be locally distorted and/or bent. In fact, the previous experimental studies confirmed the existence of bent CNTs and showed that the thermoelectric properties vary when the CNT film is deformed by external forces [1,2,3]. However, the detailed influence of such mechanical deformation on thermoelectric properties of CNTs has not been clarified thus far.

In the present study, we have theoretically investigated thermoelectric properties of a locally distorted semi-conducting CNT using the non-equilibrium Green's function method combined with the tight-binding method. We show that the Seebeck coefficient, the electrical conductivity and the power factor of semiconducting CNTs are almost independent with the local distortion when it is less than ~30%. On the other hand, when the local distortion is larger than ~30%, the electrical conductivity increases with increasing the local distortion, whereas the both Seebeck coefficient and the power factor decrease.

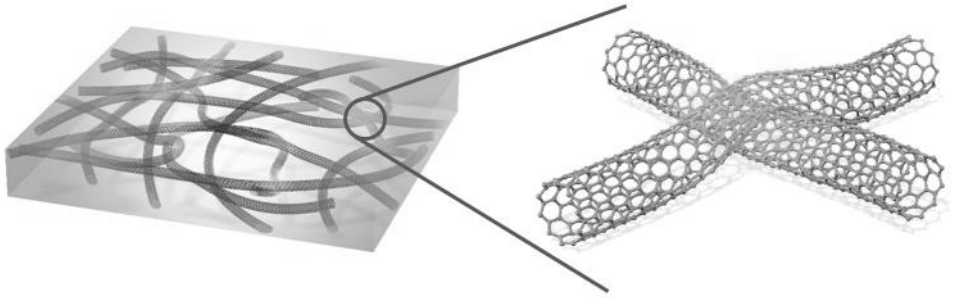

Fig. 1 Schematic illustration of CNTs which are locally distorted by contact between CNTs in the CNT film

[1] J. Bernholc *et al*. Annu. Rev. Mater. Res. **32**, 347 (2002).
[2] H. E. Romeo *et al*. Phys. Rev. B. **65**, 205410 (2002).
[3] C. H. Hu *et al*. Appl. Phys. Lett. **93**, 033108 (2008).

Corresponding Author: T. Yamamoto
Tel: +81-3-5876-1486,
Web: https://www.rs.tus.ac.jp/takahiro/
E-mail: takahiro@rs.tus.ac.jp

3P-15

Long-term measurement of sheet conductance of CNT ink on papers

○Nanami Yamazaki, Yoichiro Hashizume, Takahiro Yamamoto

Department of Electronics, Tokyo University of Science, Katsushika Tokyo 125-8585, Japan

Although poor biodegradable plastics are used as conventional substrates for flexible devices, a large amount of consumption of plastic contributes to global problems, such as oil exhaustion and micro plastics problems. These problems correspond to Goal 12 (Responsible Consumption & Production) and Goal 14 (Life below Water) of SDGs (Sustainable Development Goals). Therefore, it is required to develop new materials replacing plastic substrates. One of potential candidates for biodegradable substrates is a paper consisting of cellulose that is the most abundant carbohydrate on the earth. Electronics using paper substrate is referred to as “paper electronics” and it is expected to be utilized in a wide range of industries related to a paper. Ag ink has been mainly used in as the conductive ink thus far. However, Ag ink shows low resistance only for exclusive papers, but it has extremely high resistance for regular papers.

In this study, we propose water-soluble carbon nanotube (CNT) ink as a versatile ink for various types of papers. We measured four-terminal sheet resistance of water-soluble single-wall CNT (SWCNT) ink and multi-wall CNT (MWCNT) ink applied to three types of papers: a calligraphy paper, a drawing paper and a copy paper. In particular, we focus on the temporal change, temperature dependence and humidity dependence of sheet resistance. We found the sheet conductance of both SWCNT and MWCNT inks depends strongly on humidity, not on temperature. Interestingly, the humidity dependence of sheet conductance of SWCNT ink is inversely correlated with that of MWCNT ink independently of paper types.

Corresponding Author: Takahiro Yamamoto
Tel: +81-3-5876-1492
Web: https://www.rs.tus.ac.jp/takahiro/
E-mail: takahiro@rs.tus.ac.jp

Effect of nickel/aluminum bilayer film on growth and magnetic properties of carbon nanotubes filled with iron nanowire

○Masayoshi Oka, Hideki Sato, Yuji Fujiwara

Graduate School of Engineering, Mie University, Tsu 514-8507, Japan

Carbon nanotubes encapsulating iron nanowires (Fe@CNTs) show remarkably high coercivity to those tube axis directions owing to those magnetic shape anisotropies originating in high aspect ratio shape of nanowires [1]. Because of these reasons, it is expected that Fe@CNTs can be used in many application areas such as flexible magnets, magnetic recording media, electromagnetic interference shielding and so on. However, further improvement of coercivity in Fe@CNTs is required to realize these applications. We have examined that metal catalyst films, which was deposited on the substrates used for the Fe@CNT growths by chemical vapor deposition (CVD) influence those growth and magnetic properties. Here we confirmed that Fe@CNTs grown on Ni thin film shows higher coercivity than those grown on the other metals such as Fe [2]. Furthermore, we have found that Ni film under which Al underlayer was formed further enhanced the magnetic properties. In this study, we investigated growth and magnetic properties of Fe@CNTs that were grown on Ni/Al bilayer catalyst film.

Silicon (100) substrate with thermal oxide layer (300 nm) was used for Fe@CNTs growth. Al underlayer (0.3-2.0 nm) and Ni top catalyst layer (0.3-2.0 nm) were vacuum-deposited sequentially with the same thickness on the substrates. The substrates were introduced to a CVD reactor. The reactor was evacuated by a vacuum pump and Ar gas was introduced into the reactor to atmospheric pressure. The rector was then heated to 725℃ and sublimated ferrocene was introduced into it for 10 min to carry out the Fe@CNT growth.

Fig. 1 shows the cross-sectional SEM image of Fe@CNTs grown by CVD. Fe@CNTs were vertically grown to the substrate. The magnetic characteristics were examined by a vibrating sample magnetometer. The magnetization curves of Fe@CNTs grown of Ni(0.5 nm)/Al(0.5 nm) film is shown Fig. 2. The solid and dashed lines show the hysteresis loop of the perpendicular and parallel directions to the substrate, respectively. The coercivity of the perpendicular direction is higher than that of the parallel direction. Fig. 3 shows the perpendicular coercivities of the Fe@CNTs plotted as a function of Ni and Al total film thickness. 1.0 nm of the thickness gives the maximum coercivity of 2.08 kOe. This indicates that the Ni/Al bilayer film is effective for the enhancement of coercivities of Fe@CNTs.

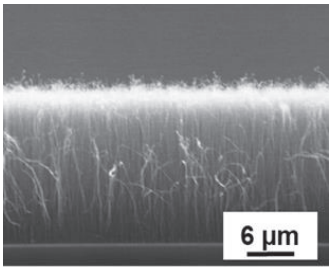

Fig. 1 Cross sectional SEM image of Fe@CNTs films grown on substrate.

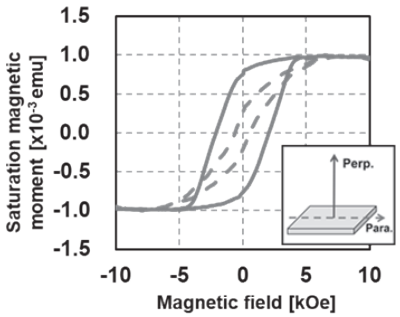

Fig. 2 Magnetic hysteresis loops of Fe@CNTs grown on films of Ni 0.5 nm/Al 0.5 nm.

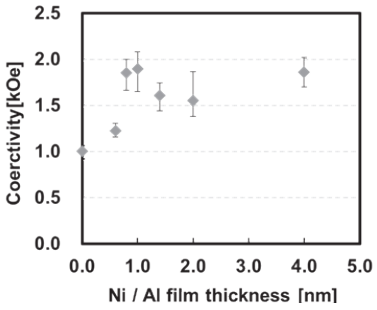

Fig. 3 Dependence of coercivity on Ni/Al film thickness. The thicknesses show total thicknesses of Ni and Al.

This study was supported by JSPS KAKENHI Grant Number 19K05206.

[1] H. Sato *et al*, Jpn. J. Appl. Phys. 52, 11NL03 (2013).

[2] E. Tamaki, H. Sato, Y. Fujiwara, J. Vac. Sci. Technol. A, 34 02D105 (2016).

Corresponding Author: H. Sato Tel/FAX: +81-59-231-9404, E-mail: sato@elec.mie-u.ac.jp

Carbon nanotube growth on discontinuous alumina buffer layer

○Taishi Yamashita [1,2] , Hiromichi Watanabe [2], Takaya Akashi [3]

[1]*Graduate School of Science and Engineering, Hosei University, Koganei 184-8584, Japan*
[2]*Research Institute for Material and Chemical Measurement, National Institute of Advanced Industrial Science and Technology (AIST), AIST Tsukuba Central 3, 1-1-1*
[3]*Faculty of Bioscience and Applied Chemistry, Hosei University, Koganei 184-8584, Japan*

Carbon nanotubes (CNTs) can be applied as an optical / thermal absorption media for black-body radiation sources and optical baffles, because of their extremely high emissivity. In the CNT growth process based on a floating catalytic chemical vapor deposition (FCCVD) method, CNTs are grown on substrates by thermally decomposing a kind of hydrocarbon species with the assistance of metal fine particles used as the CNT catalyst. If CNTs have to be grown on metallic substrates, an oxide layer, which can act as the catalyst-support one, has to be generally formed on the substrates by physical vapor deposition (PVD) methods such as an electron beam vacuum evaporation. However, the application of PVD is an obstacle to applying CNTs as a blackbody radiation light sources or light shielding materials, because it is too expensive and time-consuming to form a thin film on the surface of a three-dimensional object by PVD methods. In the previous study, we have demonstrated that alumina thin films deposited on the surfaces of W and Si substrates by alumina sand-blasting (SB) [1] can act as a supporting layer equivalent to alumina thin film by electron beam vacuum deposition in the following growth of multi-walled CNTs on the sand-blasted substrates by FCCVD method [2]. Although a continuous film is formed by PVD methods, a discontinuous film is formed by SB, which would result in any substrate effects on the CNT growth. In addition, there have been few works on the CNT growth on metallic substrates in contrast to silicon or ceramics substrates.

In this work, we compare the structure and characteristics of the alumina buffer layers formed on various metal substrates by electron beam evaporation and SB, respectively, and evaluate the effects of the buffer layer morphology (continuous / discontinuous film) and a face of the present substrates of W, Ti, Cu, Mo, Al, and a stainless steel was divided into four sections, one of which was air-blasted with alumina fine particles with a particle size of about 50 μm for 30 seconds to form a discontinuous alumina buffer layer and one of which is kept as-received. The remaining two sections were covered with continuous alumina films with a thickness of 20 nm by electron beam vacuum evaporation using Al and α-$A1_2O_3$ as evaporation sources, respectively. Then, CNTs were grown on each substrate at three temperatures (700, 800, and 900 ℃) by FCCVD using ferrocene and C_2H_2 as catalyst precursor and carbon source, respectively. As results, CNTs are fully grown on Ti and Al substrates irrespective of the growth temperature, though the amount of CNTs grown on the other investigated substrates decreases as the growth temperature increases. This discrepancy indicates that Ti and Al substrates themselves can promote the growth of CNT especially at high temperatures compared to the other investigated metallic substrates.

[1] H. Watanabe, J. Ishii, and K. Ota: *Nanotechnology* 27 (2016) 335605.
[2] T. Yamashita, et al., *The 56th fullerenes-nanotubes-graphene general symposium*, 3P-20 (2018)
Corresponding Author: H. Watanabe
Tel: 042-387-6257, Fax: 042-387-7002,
E-mail: taishi.yamashita.8i@stu.hosei.ac.jp

Synthesis of WSe_2 nanotubes by selenization of tungsten oxide nanowires

○Yohei Yomogida, Yoshiki Kainuma, Takahiko Endo, Yasumitsu Miyata, and Kazuhiro Yanagi

Department of Physics, Tokyo Metropolitan University, Tokyo 192-0397, Japan

Transition-metal dichalcogenides (MX_2, M = Mo, W; X = S, Se) can form tubular structures of rolled MX_2 sheets, namely MX_2 nanotubes. They are semiconducting regardless of how they are rolled and have advantages in semiconductor applications such as field effect transistors [1], compared to carbon nanotubes, because carbon nanotubes contain metallic nanotubes that cause bottleneck for the applications. MX_2 nanotubes have various combinations of transition metal and chalcogen, but typically-investigated ones are just WS_2 nanotubes. In the case of two-dimensional MX_2, WSe_2 has attracted more attentions than WS_2 because of the higher carrier mobility of WSe_2. Thus, WSe_2 nanotubes can be more powerful tools to achieve high-performance applications. Here, we develop the method to prepare WSe_2 nanotubes by utilizing the previous synthesis method of WS_2 nanotubes [2]. This process takes place by replacing O atoms of tungsten oxide nanowire precursor by S atoms and can be applicable to synthesis of WSe_2 nanotubes by using Se precursor.

Tungsten oxide nanowire precursor was synthesized via solvothermal reaction of WCl_6 in ethanol at 180°C for 24 h. The obtained nanowire precursor was reacted with Se precursor for 1 h in Ar flow. The selenization was optimized by changing temperature and concentration of H_2 in Ar flow, which is known as a promotor of sulfurization.

Fig. 1 shows typical TEM image of the sample selenized with H_2. We successfully synthesized WSe_2 nanotubes with 20 nm in diameter, which structure is similar to that of the previous WS_2 nanotubes [2]. On the other hand, the sample selenized without H_2 has no tubular structure. Considering Raman spectra shown in Fig. 2, the sample selenized with H_2 shows a clear peak of WSe_2, while the sample selenized without H_2 shows peaks of only tungsten oxides. This result indicates that H_2 is necessary to form WSe2 nanotubes and the synthetic condition of WSe_2 nanotubes is not the same as that of WS_2 nanotubes that can be synthesized without H_2. In the poster, we will discuss carrier transport properties of WSe_2 nanotubes compared to those of WS_2 nanotubes.

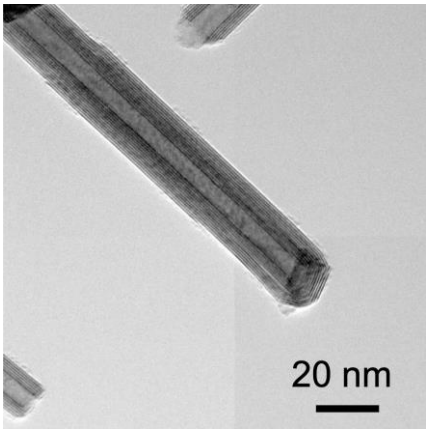

Fig. 1 TEM image of WSe_2 nanotubes selenized with H_2.

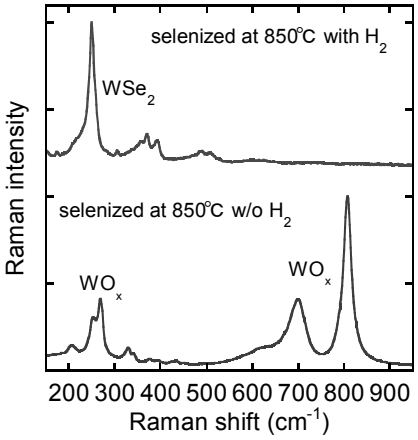

Fig. 2 Raman spectra of the samples selenized with H_2 and without H_2.

[1] M. Sugahara et al, Appl. Phys. Express 9, 075001 (2016)
[2] Y. Yomogida et al, Appl. Phys. Express 12, 085001 (2019)

Aqueous electrolyte secondary batteries using organic molecules encapsulated in Single-walled carbon nano tubes (SWCNTs)

○○Itta Yamada, Remi Date, Kento Hosoe, Kousuke Tashiro, Yosuke Ishii, Shinji Kawasaki

Department of Chemistry, Nagoya Institute of Technology, Nagoya 466-8555, Japan

Because they have high energy densities, Li ion batteries (LIBs) have been widely used. However, LIBs have (1) flammability, (2) high cost, (3) long charging time problems. Therefore, next generation batteries conquering these problems have been highly demanded. We have developed such a new battery by combining alkali metal halide aqueous electrolytes and single-walled carbon nanotube (SWCNT) electrodes. In our batteries, anions and cations are simultaneously adsorbed in anode and cathode electrodes for charging just like electric double layer capacitors. Quinone molecules encapsulated in SWCNTs and empty SWCNTs are used as anode and cathode electrodes, respectively. We reported that quinone molecules encapsulated in SWCNTs can work as Li and Na ion battery electrodes. On the other hand, we also reported that empty SWCNT electrode can store iodine molecules in its hollow core after oxidizing iodide ions. In this work, we fabricated new aqueous electrolyte batteries by combining these two SWCNT electrodes. Several kinds of alkali metal halides including LiI, NaI, LiBr, NaBr, MgI_2 and ZnI_2 were used as electrolytes. Two kinds of quinone molecules: 9,10-anthraquinone (AQ) and 9,10-phenanthrenequinone (PhQ) molecules were introduced into SWCNTs by subliming the molecules and transferring them into SWCNTs having mean tube diameters of 1.0-5.0 nm in evacuated glass tubes. We'll discuss charge-discharge properties of the aqueous electrolyte batteries.

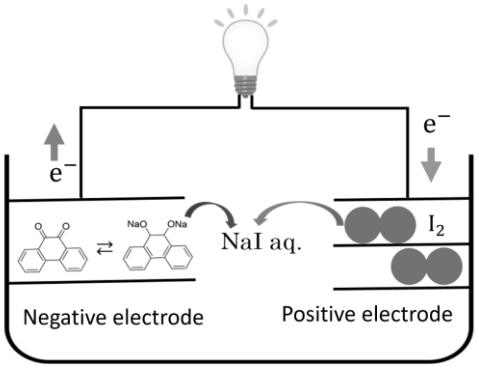

Fig. 1 Schematic picture of a newly proposed aqueous secondary battery using SWCNTs

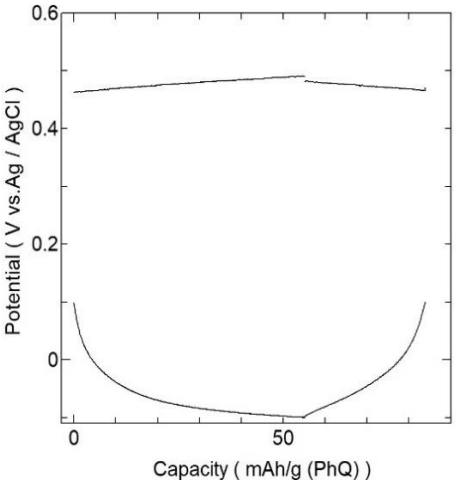

Fig. 2 Charge and discharge curves observed for PhQ-I_2 battery

Corresponding Author: S. Kawasaki
E-mail: Kawasaki.shinji@nitech.ac.jp

Effect of single-walled carbon nanotubes on electrochemical properties of platinum-based electrocatalyst for fuel cells

○Kazuki Kishida[1], Toru Harigai[1], Hirofumi Takikawa[1], Takeshi Hashimoto[2]

[1] *Department of Electrical and Electronic Information Engineering, Toyohashi University of Technology, Toyohashi 441-8580, Japan*
[2] *Meijo Nano Carbon Co., Ltd., Nagoya 463-003, Japan*

Platinum-based (Pt-based) catalysts are often used as electrocatalysts in fuel cells. In our previous study, it was indicated that the addition of high-crystalline single-walled carbon nanotubes (SWCNTs) to Pt-based electrocatalyst leaded to increase the electrochemical surface area (ECSA) [1]. However, the mechanism that the addition of SWCNTs in Pt-based electrocatalyst increase the ECSA of the Pt-based electrocatalyst has not been clear. In this study, the effect of SWCNTs on the electrochemical properties of Pt-based electrocatalyst are investigated by cyclic voltammetry (CV) under different scanning rates.

SWCNT-added Pt-based electrocatalyst was prepared as follows. Pt-based electrocatalyst used was Pt/Vulcan XC-72 catalyst (50 wt.%$_{\text{-Pt}}$, TEC10V50E, TANAKA KIKINZOKU KOGYO K.K.) and SWCNT additive used was SWCNT aqueous dispersion composed of SWCNTs of 200 mg in water of 100 ml without dispersing agents (Meijo Nano Carbon Co. Ltd.). Pt-based electrocatalyst and SWCNT aqueous dispersion were mixed with auto pestle for 5 min. Then nafion and methanol were added and mixed by ultrasonication for 30 min. The experimental parameter was the amount of SWCNTs; 5, 10, 15, and 20 mg for Pt-based electrocatalysts of 200 mg.

The catalytic performance was evaluated by the charge (Q_H) which contributed to hydrogen reduction reaction and ECSA based on CV. The CV were conducted in H_2SO_4 solution of 0.5 M well-degassed by Ar at 25°C under the condition of the scanning rate of 10 or 50 mV/s, and the potential scanning rage from -0.25 to 1.00 V. The Ag/AgCl electrode, Pt-wire electrode with 0.5 mm in diameter and 57 mm length, and glassy carbon electrode with 10 mm in diameter and 55 mm length were used as a reference electrode, counter electrode, and working electrode, respectively. The loading amount of Pt on the working electrode was 130 μg.

The Q_H and ECSA of Pt/Vulcan XC-72 catalysts with and without SWCNTs were summarized in Table. 1. It was found that the addition of SWCNTs leaded to increase the Q_H and ECSA at the scanning rates of 10 and 50 mV/s. Especially, the Pt/Vulcan XC-72 catalyst with SWCNTs of 15 mg showed the highest Q_H and ECSA in the prepared catalysts. Compared to Pt/Vulcan XC-72 catalysts without SWCNTs, the Q_H and ECSA of Pt/Vulcan XC-72 catalyst with SWCNTs of 15 mg was approximately 1.3 times higher at the scanning rate of 10 mV/s.

Table 1. Q_H and ECSA of Pt-based electrocatalysts with and without SWCNTs.

V_s (mV/s)	10		50	
Pt/Vulcan XC-72 : SWCNTs (wt.)	Q_H (C)	ECSA (m^2/g)	Q_H (C)	ECSA (m^2/g)
200 : 0	18.3	66.9	7.6	27.7
200 : 5	18.5	67.7	11.5	42.3
200 : 10	23.6	86.5	15.9	58.2
200 : 15	24.3	89.1	16.6	60.6
200 : 20	21.0	77.1	16.1	58.9

[1] K. Kishida, *et al*.: The 56th Fullerenes-Nanotubes-Graphene General Symposium, 2P-4 (2019).

Corresponding Author: K. Kishida, Tel: +81-532-44-1228, E-mail: kishida.kazuki@pes.ee.tut.ac.jp

Self-powered wireless optical transmitter based on triboelectric generator with carbon nanotube thin film

○Masahiro Matsunaga[1], Jun Hirotani[2], Shigeru Kishimoto[2], Yutaka Ohno[1,2]

[1]*Institute of Materials and Systems for Sustainability, Nagoya University, Nagoya 464-8603, Japan*
[2]*Department of Electronics, Nagoya University, Nagoya 464-8603, Japan*

With the rapid growth of the field of the internet-of-things, the demand for sensor devices has been predicted explosive increase [1]. The growing demand will lead to being a difficult problem that is huge amounts of the time-consuming work for replacing the batteries. To solve the issue, self-powered electronics have been attracted considerable attention in both the scientific and industrial communities. Energy harvesting, which converts small ambient energy to the electricity, is a key to realize the self-powered system. Previously, we reported the highly transparent and stretchable triboelectric generator (TEG) using carbon nanotube thin film. The TEG is a kind of mechanical energy harvester based on the triboelectrification [2]. We obtained high output power up to ~8 W/m^2, which is enough to drive several tenses of LED chips [3].

Here, we constructed the self-powered signal transmitting system based on the TEG and demonstrated the optical signal transmitting by the combination of different color LED chips. The system can operate intuitively such as “tap” and “swipe”.

The transmitter was fabricated based on the TEG. The TEG was composed of a carbon nanotube thin film sandwiched with polydimethylsiloxane (PDMS) layers. After spin-coating PDMS onto a plastic substrate, the CNT transparent electrodes and connections were patterned on the PDMS surface by the spray coating of CNT ink (Meijo Nano Carbon, eDIPS ink) with a shadow mask as shown in Fig. 1. After connecting LED chips with the silver paste, the top PDMS was spin-coated to cover the CNT electrode. To enhance the performance, we then applied CF_4 plasma to modify the PDMS surface. The detail of the transmitter and operation will be discussed in the poster.

Acknowledgment: This work was supported by JST/CREST (JPMJCR16Q2).

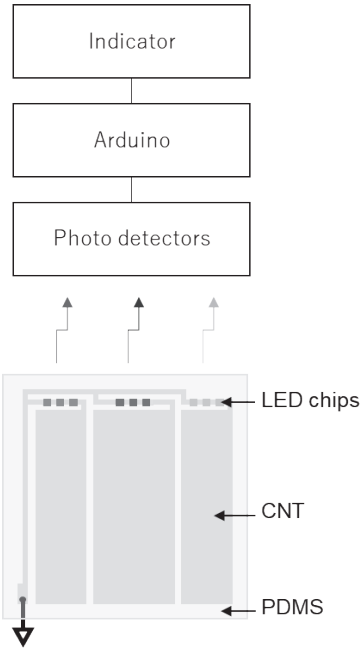

Fig. 1 Schematic of the diagram and the signal transmitter.

[1] Roadmap for the Trillion Sensor Universe (2013).
[2] Z. L. Wang, Mater. Today **20**, 74 (2017).
[3] M. Matsunaga *et al*., The 55th FNTG symposium, 1P-8 (2018).

Corresponding Author: Y. Ohno
Tel & Fax: +81-52-789-5387,
E-mail: yohno@nagoya-u.jp

Effect of surface oxidation of carbon nanotube electrodes in streaming potential-based generators

°Yuzuki Ando[1], Ryohei Nishi[1], Shigeru Kishimoto[1], and Yutaka Ohno[1,2]

[1]*Department of Electronics, Nagoya University, Nagoya 464-8603, Japan*
[2] *Institute of Materials and Systems for Sustainability, Nagoya University, 464-8601, Japan*

The voltage generation phenomenon called streaming potential occurs when a fluid is driven by a pressure gradient along a charged surface. The streaming potential is potentially useful for energy harvesting from fluid energy [1] as well as flow sensors [2, 3]. For these applications, the enhancement in electrochemical activity at the electrode/fluid interface is essential. In this work, we introduce the carbon nanotube (CNT) thin film, which are often used as electrodes of electrochemical sensors because of the excellent electrochemical properties, as the electrode of voltage generator. The effect of the surface functionalization is also investigated to further enhance the electrochemical activity.

Fig. 1(a) shows a schematic structure of a generator device consisting of CNT electrodes on a polyethylenenaphthalate (PEN) substrate. The generator device was inserted into a silicone tube, and a load resistance of 1 to 200 MΩ was connected. The output voltage was measured by a semiconductor device parameter analyzer as shown in Fig. 1(b). Since a power-driven pump could be a noise source, the fluid was driven by the gravity. Deionized water was used as the fluid and the flow velocity was ~70 cm/s. We also carried out the electrochemical functionalization of the CNT surface in 2M H_2SO_4 to enhance the electron transfer rate [4]. Fig. 2 shows the output power of the voltage generators with as-fabricated and functionalized CNTs as a function of load resistance, respectively. The maximum output power was enhanced to be 53 pW by the functionalization from 6 pW for as-fabricated CNT electrodes. In addition, the load resistance at which the maximum power was obtained was reduced by the functionalization. These results suggest that the resistance at the electrode/fluid interface was reduced by the functionalization probably due to the enhancement in the electron transfer rate.

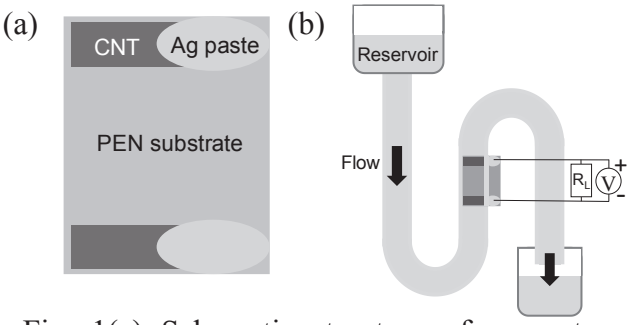

Fig. 1(a) Schematic structure of generator device, (b) experimental setup.

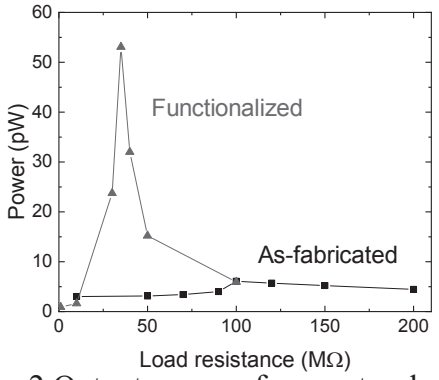

Fig. 2 Output power of generator devices.

Acknowledgment: This study was partially supported by JST/CREST (JPMJCR16Q2).

[1] R. Zhang *et. al.*, Adv. Mater. 27, 6482 (2015).
[2] B. Bourlon *et. al.*, Nat. Nanotechnol. 2, 104 (2007).
[3] R. X. He *et. al.*, Nano Lett. 12, 1404 (2012).
[4] K. Nishimura *et al*., Electrochim. Acta **295,** 157 (2019).

Corresponding Author: Y. Ohno
Phone & Fax: +81-52-789-5387
E-mail: yohno@nagoya-u.jp

Study on one-dimensional stacking structure of polycyclic aromatic hydrocarbon molecules encapsulated in single-walled carbon nanotubes by molecular dynamics simulations(Ⅱ)

○Ryo Nagai[1], Yosuke Kataoka[3] and Hironori Ogata [1,2]
[1]*Graduate School of Sci. and Engin., Hosei University, Koganei, 184-8584, Japan*
[2]*Research Center for Micro-Nano Technology, Hosei University, Koganei, 184-0003, Japan*
[3]*Research Center for Computing and Multimedia Studies, Hosei University, Koganei, 184-8584, Japan*

Single-walled carbon nanotubes (SWNTs) have hollow spaces of about several nm in diameter. Various functional molecules such as fullerenes can be encapsulated in the hollow space, and it is expected that new functions will be developed by capsulation. It has been reported that columnar layered polycyclic aromatic hydrocarbon (PAH) molecules such as coronene encapsulated in SWNTs can exhibit unique luminescence properties depending on their molecular orientations. We have been investigated the local structures and properties of various kinds of PAH molecules encapsulated in SWNTs systematically and have clarified that the difference of the chiral vector of SWNT can affect the stacking structure of PAH molecules. Figure 1 shows the snapshots of coronene molecules encapusulated in SWNT of different chiral vector with almost the same diameter ((a) coronene@(16,4)SWNT and (b)coronene@(18,1)SWNT). It is suggested that the difference in elastic modulus of SWNT in the direction perpendicular to the long axis of SWNT may affect the stacked structure of encapsulated PAH molecules. In this study, the elastic moduli of SWNT with different chiral vector are calculated by molecular dynamics simulation and the correlation between the stacking structure of encapsulated PAH molecules (perylene, corannulene, or coronene) and the elastic modulus of SWNT were investigated.

Detailed results will be discussed at the conference.

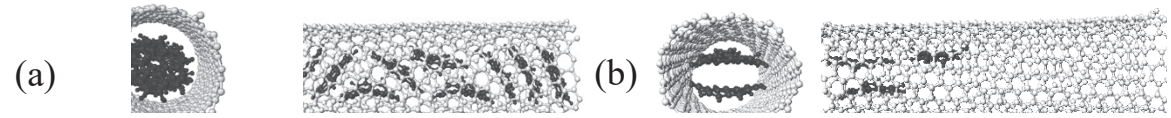

Figure 1. Snapshots of (a) coronene@(16,4)SWNT and (b)coronene@(18,1)SWNT at 300 K.

References:

[1] Miho Fujihara, *et al*., *J. Phys. Chem.* C **116**(2012)15141−15145.

[2] Alexander I. Chernov *et al., Phys. Status Solidi* B **251**(2014)2372–2377.

[3] Y. Sakane, *et al., AIP ADVANCES* **5** (2015)117113.

[4] Y.Joko, *et al., Phys. Chem. Chem. Phys*.**19**(2017)27704-27715.

[5] T.Koyama, *et al., J.Phys. Chem. C* **122**(2018)5805-5812.

Corresponding Author: H. Ogata
Tel: +81-42-387−6229, Fax: +81-42−387−6229, E-mail: hogata@hosei.ac.jp

Brighter Near-IR Emission of Single-Walled Carbon Nanotubes Modified with a Cross-Linked Polymer Coating

○Yukiko Nagai[1], Masako Yudasaka[2], Hiromichi Kataura[2], Tsuyohiko Fujigaya[1,3,4]

[1]Department of Applied Chemistry, Graduate School of Engineering, Kyushu University, 744 Motooka, Fukuoka 819-0395, Japan. [2]Nanomaterials Research Institute, National Institute of Advanced Industrial Science and Technology (AIST), Higashi 1-1-1, Tsukuba, Ibaraki 305-8565, Japan. [3]WPI I[2]CNER, Kyushu University. [4]Center for Molecular Systems, Kyushu University.

Single-walled carbon nanotubes (SWNTs) have unique near-infrared (NIR) absorption and photoluminescence (PL) properties, and expected as a next-generation NIR emission imaging probes. However, in a hydrophilic environment such as *in vivo*, it is difficult to maintain strong PL intensity because it is quenched by energy transfer due to aggregation of SWNTs and approach of water to the SWNT surface.Therefore, a smart functionalization strategy to realize both strong NIR emission and stable dispersion at the same time is strongly required.

Recently, we have reported a unique method, denoted as carbon nanotube micelle polymerization, to functionalize SWNTs with cross-linked polymer gel [1]. In this study, the various monomers were tested to fabricate gel-coated SWNT hybrid to design more hydrophobic SWNT/gel interface for brighter NIR emission (***Fig. 1***).

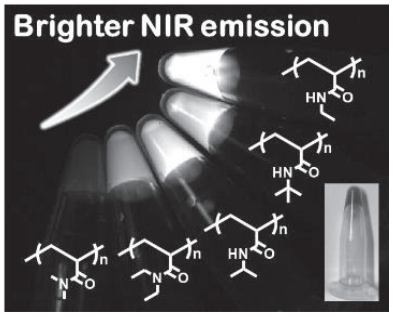

Fig. 1. NIR emission image of gel-coated SWNT dispersion [2].

The PL intensity normalized by the absorption intensity of the gel-coated SWNT hybrids is plotted as a function of the absorption peak wavelength in ***Fig. 2***. It is known that a more hydrophobic environment induces a blue shift of the absorption owing to reduction of the dielectric constant. Therefore, the good linearity in ***Fig. 2*** strongly indicates that the hydrophobicity of the SWNT environment can be controlled by changing the chemical structure of the monomer, and a more hydrophobic environment results in brighter PL emission of the SWNTs [2]. As a result, gel-coated SWNT hybrid achieved about 1.5 times stronger PL intensity than that of the PEG phospholipid (PLPEG)/SWNT complex that was used for vascular imaging [2].

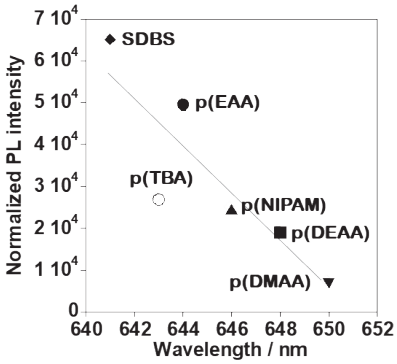

Fig. 2. Plot of the normalized PL intensity of gel-coated SWNT as a function of absorption wavelength.

[1] T. Fujigaya *et al.*, *RSC. Adv.* **2014**, *4*, 6318.
[2] Y. Nagai and T. Fujigaya *et al.*, *Chem. Commun.* **2019**, *55*, 6854.

Corresponding Author: T. Fujigaya
Tel: +81-92-802-2842, Fax: +81-92-802-2842, E-mail: fujigaya.tsuyohiko.948@m.kyushu-u.ac.jp

3P-25

Dependence of surface roughness of Cu foil on the growth of pristine and boron doped graphene

Mariko Shamoto, ○Shunji Bandow

Department of Applied Chemistry, Meijo University, Nagoya 468-8502, Japan

A well-flattened /or single crystalline Cu substrate is generally used for graphene growth by thermal CVD. In order to improve a flatness of Cu surface, we carried out to anneal Cu foil in a low pressure hydrogen flow (3 kPa, 20 sccm) at 1000 °C for 6 hours. By using such Cu foil, although several layered graphene film certainly grew, reproduceability was somewhat low; that is, faint /or no Raman signal was often observed. By the SEM observation, graphene was usually grown on the edge of the copper domain or around somewhat bumpy rough surface area, and maybe atomically defective parts.

For the purpose of making conductive transparent film, large area and several layered graphene films are needed instead of a single /or a few layered crystalline small size graphene. In the present study, we focus to make several layered graphene which is uniformly covered on the Cu substrate. Furthermore, it is necessary to improve reproduceability of the growth and applicable to heteroatom doping (at the present we selected B-dope). As noted in the former paragraph, graphene islands are usually grown at some irregular points. Hence we intend to make some irregularities on the surface of Cu (4N, 0.05 mm thick) by blasting diamond powder.

Blasting was conducted by following way: we sank Cu foil in water including diamond powder (TOMEI DIAMOND, IRV 120 /or IRM 40), and carried out high power sonication using an ultrasonicator of Nanoruptor, NR-350. By using such a blasted Cu foil, thermal CVD of methane as carbon source /or in case of B-dope we add a vapor of pheneylboronic acid/ was carried out at depressurized condition of 20 kPa. Brief results examined by Raman scattering were shown in Fig. 1, in which one can see that multilayered graphene was well-grown on the Cu blasted by diamond powder rather than un-blasted one. Experimental and detailed results including boron doping studied by XPS will be opened.

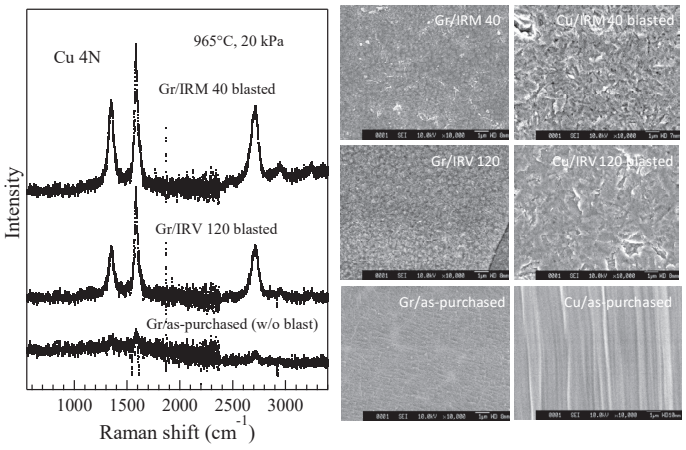

Fig. 1. Raman spectra of graphene on diamond powder blasted Cu foil and their SEM Images.

Corresponding Author: S. Bandow, E-mail: bandow@meijo-u.ac.jp, Tel: +81-52-838-2404

Highly uniform single-layer graphene CVD on 2-inch r-plane sapphire

○Yuki Ueda[1], Jumpei Yamada[1], Takahiro Maruyama[2], and Shigeya Naritsuka[1]

[1] *Department of Materials Science and Engineering, Meijo University, Nagoya 468-8502, Japan*
[2] *Department of Applied Chemistry, Meijo University, Nagoya 468-8502, Japan*

Large-size single-layer graphene is usually obtained on copper-based catalyst by chemical vapor deposition (CVD). However, the transfer process, which is mandatory for the device fabrication, largely deteriorates the grown graphene. Direct growth of graphene on a dielectric substrate is the best answer to solve the problem. We found that the growth rate of graphene on r-plane sapphire is faster than c-plane or a-plane sapphire [1]. The r-plane sapphire has a strong catalytic effect and enables to decompose the source materials. In this study, we attempted that direct growth of highly uniform single-layer graphene on 2-inch r-plane sapphire by low-pressure CVD without a metal catalyst.

Graphene was directly grown on r-plane sapphire at 1210 ºC by low-pressure CVD without metal catalyst. Mixture gas of nitrogen, hydrogen, and diethylacetylene (C_6H_{10}: 3-Hexyne) was flown to a reactor for the growth of graphene. Growth time was changed between 7 and 180 min.

Figure 1 shows (a) surface photograph of directly-grown graphene and (b) their corresponding Raman signals. Almost the same Raman signals at each measurement point indicate that highly-uniform graphene was grown on all over the 2-inch r-plane sapphire. The graphene was estimated to be single-layer by AFM height analysis of the islands grown in a short time. Figure 2 shows growth time dependence of Raman spectra. The Raman spectra were not changed for the growth time above 60 min. It was observed by AFM that the sapphire surface was covered with graphene with growth time of 60 min. These results show that graphene growth terminated when the whole surface of sapphire was covered with single-layer graphene. It is because the decomposition of source materials is decreased when the catalytic effect of r-plane sapphire was covered with graphene. Therefore, highly-uniform single-layer graphene was obtained on the whole surface of 2-inch r-plane sapphire.

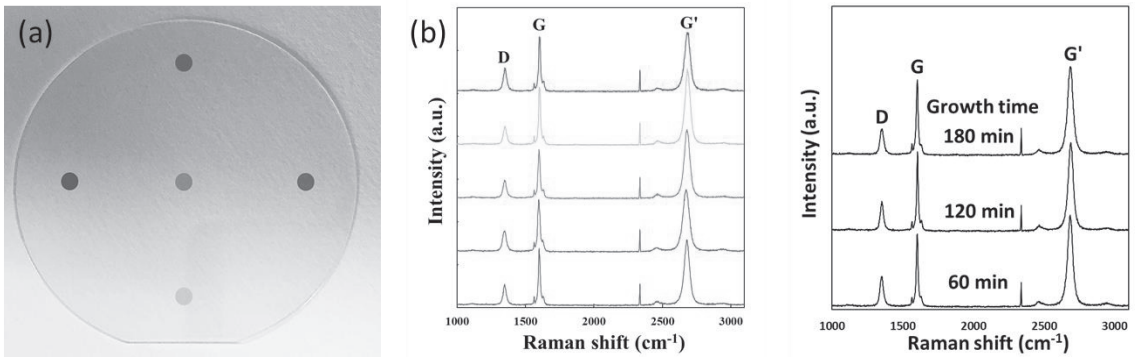

Fig. 1 (a) Surface photograph of directly-grown graphene and (b) their corresponding Raman signals.

Fig. 2 Growth time dependence of Raman spectra.

Acknowledgement: This work was supported in part by JSPS KAKENHI Grant Numbers 15H03558, 26105002.

[1] Y. Ueda et al., Appl. Phys. Lett. 115, 013103 (2019).

Corresponding Author: Y. Ueda, Tel: +81-52-838-2387, E-mail: 173441501@ccalumni.meijo-u.ac.jp

Preparation of IrO_2 nanoparticles on CVD graphene by hydrothermal method

○Shuhei Ogawa, Seiya Suzuki, Masanori Hara, Masamichi Yoshimura

Graduate School of Engineering, Toyota Technological Institute, Nagoya 468-8511, Japan

Water electrolysis is a promising technology to store energy as hydrogen gas due to the passage of an electric current. Iridium dioxide (IrO_2) works as the catalyst for oxygen evolution reaction (OER) at the cathode in water electrolysis. The high overpotential and small specific surface area of IrO_2 limit the practical use. In a previous report, reduced graphene oxide (RGO) as a supporting material (IrO_2/RGO) increases catalytic activity of IrO_2 by nanoparticle (NP) formation [1]. It is also claimed that the size of metal NPs, which is important for catalytic activity, depends on the type or density of defects in carbon-based supporting materials in density functional theory (DFT) studies [2]. To clarify this relationship experimentally, we use a graphene with few defects grown by chemical vapor deposition as a supporting material. Defects are introduced by ozone treatment. We examine the relationship between the size of IrO_2 and the density of defects in CVD graphene.

The preparation process of IrO_2/graphene/SiO_2/Si is summarized in Fig. 1. A graphene was grown on copper substrates by CVD [3]. The graphene was transferred onto a SiO_2/Si substrate by a bubble transfer method [4], then defects were introduced by ozone treatment. IrO_2 NPs were synthesized on it in alcohol/water solution through the following two steps; (1) hydrolysis of iridium precursor ($IrCl_6^{2-}$) at 80 ºC, and (2) crystallization of IrO_2 on graphene by hydrothermal method at 150 ºC. Surface morphology of IrO_2/graphene was observed by scanning electron microscopy (SEM) and atomic force microscopy (AFM).

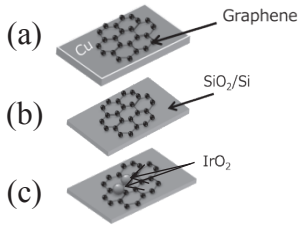

Fig.1. Schematic illustration of (a) graphene grown by CVD, (b) transferred graphene and (c) IrO_2/graphene deposited by hydrothermal method.

SEM image shows the formation of NPs on the graphene. NPs were dispersed only on the graphene covered areas. Fig. 2(a) shows an AFM image of the IrO_2 NP on graphene. Fig. 2(b) shows the crosssection of the NP. The size of NP is ~ 8.8 nm, which is larger than that in the case of RGO (~ 1.6 nm [1]). The present study suggests that the size of IrO_2 NPs can be controlled by the density of defects in the supporting graphene.

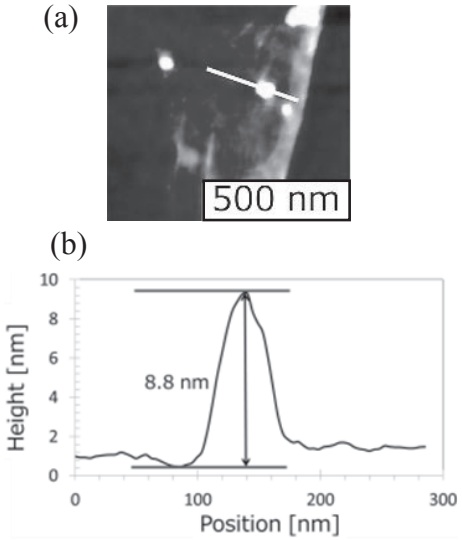

Fig. 2. (a) AFM image of the IrO_2/graphene/SiO_2/Si. (b) height profile along the line in (a).

[1] D. Fan *et al*., Int. J. Hydrogen Energy, **38,** 9217 (2013).
[2] M. Matsutsu *et al.,* Phys. Chem. Chem. Phys., **18,** 25693 (2016)
[3] S. Suzuki *et al*., Coatings, **7,** 206 (2017).
[4] J. Lee *et al*., Coatings, **7,** 218 (2017).

Corresponding Author: Masamichi Yoshimura
Tel: +81-52-809-1852
E-mail: yoshi@toyota-ti.ac.jp

B, N-codoped Reduced Graphene Oxide as a Support for IrO_2 as Active OER Electrocatalyst

○Prerna Joshi, Rohit Yadav, Yuki Matsuoka, Masanori Hara, Masamichi Yoshimura

Surface Science Laboratory, Toyota Technological Institute, Nagoya, 468-8511, Japan

A great amount of efforts has been devoted to tailor the band gap of graphene, rendering graphene suitable for application in energy devices. One such approach is doping of graphene with heteroatoms [1]. Often doped with boron (B) and nitrogen (N), modification of graphene alters its electronic structure and changes its semi-metal nature to semi-conductor. In our group, such modified graphene is used as metal oxide catalyst support for electrochemical water splitting in water electrolyzers (WEs) for hydrogen production. Practically, water splitting is limited by oxygen evolution reaction (OER) at the anode due to its complex reaction kinetics and high over-potential for which metal oxides catalysts such as IrO_2 come to rescue [2]. However, high cost and low natural abundance of IrO_2 limit its extensive use. Hence, using an economical support with modified electronic structure like heteroatom-doped graphene appears to be one potential solution. Present research aims to study the effect of the codoping of B and N on the activity of IrO_2 towards OER.

Boric anhydride, urea and graphene oxide (prepared by synthetic graphite via modified Hummers' method) were used to prepare B, N-codoped reduced graphene oxide (BN-rGO) via pyrolysis in N_2 atmosphere at 1000 ºC for 60 min. Further, IrO_2 nanoparticles (nps) were decorated onto doped rGO by hydrothermal synthesis at 150 ºC for 4 h using H_2IrCl_6 as the precursor (IrO_2-BN-rGO). Prepared catalysts were characterized by X-ray photoelectron spectroscopy (XPS), transmission electron microscopy (TEM), energy dispersive X-ray spectroscopy (EDX) and evaluated for their electrochemical activity towards OER by cyclic voltammetry (CV) and linear sweep voltammetry (LSV).

XPS analysis of IrO_2-BN-rGO revealed the formation of B-N bond along with the presence of C-C bond (rGO). Further, EDX analysis confirmed the existence of B and N in 9.4 and 11.5 wt. %, respectively. EDX and TEM confirmed the uniform dispersion of IrO_2 over BN-rGO sheets with an average particle diameter of 1.8 nm (Fig. 1). Electrochemical analysis was carried out for the prepared catalysts by LSV with rotating disk electrode (RDE) system in 0.5 M H_2SO_4 solution and showed high durability for ~3000 cycles with a retention in current.

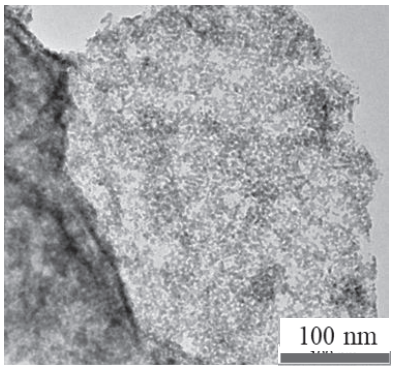

Fig. 1. TEM image of IrO_2 nps decorated on BN-rGO sheet.

[1] M. Alattas *et al*. Scientific Reports, **8**, 17689 (2018).
[2] T. Reier *et al*. ACS Catalysis, **2**, 1765 (2012).

Corresponding Author: Dr. Prerna Joshi
Tel: +81-52-809-1852, Fax: +81-52-809-1851
Web: https://www.toyota-ti.ac.jp /surface/
E-mail: joshiprerna2011@toyota-ti.ac.jp

Growth of single-crystalline MoS_2 on 1D and 2D boron nitride systems

○Taikou Murakami[1], Hayato Arai[1], Yongjia Zheng[1], Yang Qian[1],
Taiki Inoue[1], Rong Xiang[1], Shohei Chiashi[1], Shigeo Maruyama[1,2]

[1] *Department of Mechanical Engineering, The University of Tokyo, Tokyo 113-8656, Japan*
[2] *Energy Nano Engineering Laboratory, National Institute of Advanced Industrial Science and Technology (AIST), Tsukuba 305-8564, Japan*

Transition metal dichalcogenides (TMDs) have attracted great attention as a two-dimensional (2D) material. In addition, a 1D counterpart of TMD layers, which is known as TMD nanotubes (NTs), has the potential to be used as electronic [1], thermoelectric [2], and photovoltaic devices [3]. However, conventional growth methods only provide TMDNTs with large layer numbers and diameters (> 50 nm). We have recently reported the growth of a single-walled MoS_2NT with 5 nm-diameter by using heterostructure of boron nitride (BN) and a SWCNT (BN/SWCNT) as a template (Fig. 1a) [4]. BN is considered as a favorable platform for TMDs due to its large bandgap and atomic smoothness. To realize long and single-crystalline TMDNTs required for applications, the crystal size of TMDs needs to be increased. In this study, we performed comparative growth of MoS_2 on both 1D BN/SWCNTs and exfoliated 2D BN layers. We synthesized suspended SWCNTs over trenches, followed by growing BN coaxially on them. Then, MoS_2 was grown by using MoO_3 and S as precursors. The SEM (Fig. 1b) and Raman mapping images (Fig. 1c,d) indicate growth of MoS_2NTs along the templates. We also synthesized MoS_2 on exfoliated BN (Fig. 1e). SEM image (Fig. 1f) shows triangle-shaped MoS_2 flakes on BN. By tuning growth conditions, the flake size of MoS_2 was increased. Feedback of this result to the 1D system is expected to realize long MoS_2NTs.

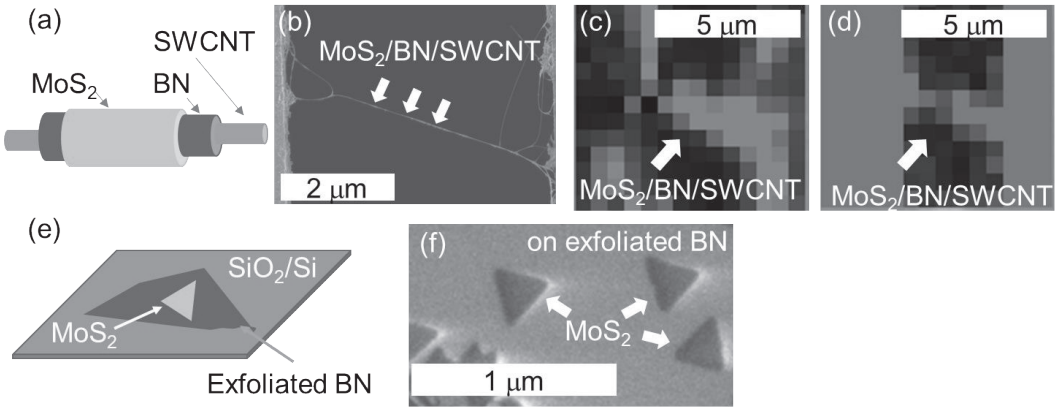

Fig. 1 (a) Schematic image, (b) SEM image, and (c,d) Raman mapping images of suspended MoS_2/BN/SWCNT. The intensity of (c) G-band of SWCNT and (d) A_{1g} peak of MoS_2 is denoted in the images. (e) Schematic image and (f) SEM image of MoS_2 grown on exfoliated BN.

[1] R. Levi *et al.*, Nano Lett., **13**, 3376 (2013). [2] H. Kawai *et al.*, Appl. Phys. Express., **10**, 015001 (2017).
[3] Y.J. Zhang et al., Nature, **570**, 349 (2019). [4] R. Xiang *et al.*, arXiv :1807.06154.
Corresponding Author: S. Maruyama, Tel: +81-3-5841-6421, Fax: +81-3-5800-6983,
E-mail: maruyama@photon.t.u-tokyo.ac.jp

Deposition of MoS_2 layer on GaN semiconductor for photoresponsive device application

○Pradeep Desai[1], Ajinkya K. Ranade[1], Mandar Shinde[1], Bhagyashri Todankar[1], Masaki Tanemura[1], Golap Kalita[1, 2]

[1] *Department of Physical Science and Engineering, Nagoya Institute of Technology, Nagoya 466-8555, Japan*
[2] *Frontier Research Institute for Material Science, Nagoya Institute of Technology, Nagoya 466-8555, Japan*

Lattice mismatch between molybdenum disulfide (MoS_2) and gallium nitride (GaN) is only 0.8%, hence it is feasible to develop an epitaxial heterostructure for novel device application. In our study, epitaxial oriented growth of MoS_2 on GaN substrate were synthesized to study its photoresponsive device application. A thin film of MoS_2 was deposited on GaN substrate by the sulfurization process of molybdenum oxide (MoO_3).

The method of synthesis of MoS_2 involves two stage. Firstly a thin film of MoO_3 was deposited on GaN substrate using Thermal Evaporation Technique at 40 A of current under ~ 1×10^{-4} Pa vacuum condition for 3 minutes. Subsequently MoS_2 was synthesized by sulfurization process at 750° C and in the Ar+H_2 atmosphere using a quartz tube having a length 85 cm. On top of ceramic boat the MoO_3 deposited GaN substrates was kept facing downwards. Sulphur (nearly 1g) was kept in Low Temperature Furnace (LTF). Fig. 1 shows the ball and stick diagram of MoS_2 on top of GaN substrate. Fig. 2 shows the raman spectra of the MoS_2-GaN heterostructure. The peaks corresponding to E_2(High) and A_1(LO) of GaN layer were observed at 570.2 and 749.2 cm^{-1}, respectively. Additional small intensity peaks were observed at lower wavenumber as shown in the inset which corresponds to the E_{2g} and A_{1g} peaks of MoS_2 layer at 385 and 412 cm^{-1}, respectively. The spectroscopy analysis confirmed the formation of MoS_2 layers on GaN and their heterostructure.

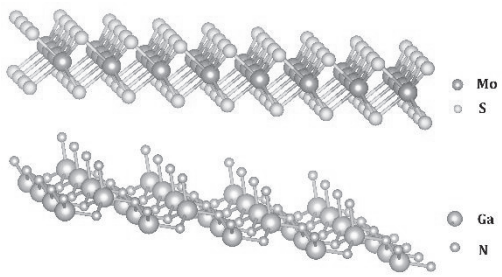

Fig 1: Ball and stick diagram of the heterostructure of MoS_2 on GaN

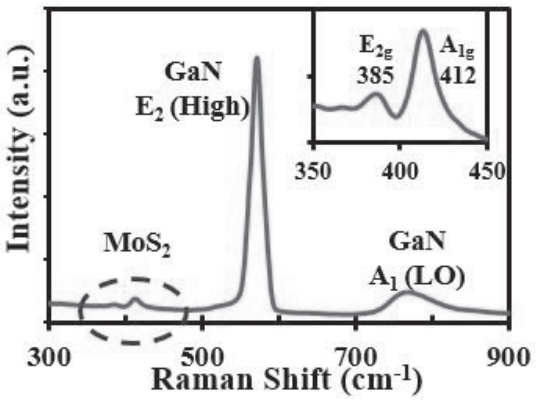

Figure 2: Raman Spectra of MoS_2 on GaN heterostructure

Corresponding Author: Pradeep Desai
Tel: +81-52-735-5216, Fax: +81-52-735-5216,
Web: http://www.nitech.ac.jp/
E-mail: desai.pradeep@zoho.com

発表索引
Author Index

Author Index

2019 年 9 月 3 日発行

第 57 回フラーレン・ナノチューブ・グラフェン総合シンポジウム
講演要旨集

≪フラーレン・ナノチューブ・グラフェン学会≫
〒113-8656 東京都文京区本郷 7-3-1
東京大学大学院工学系研究科　機械工学専攻
丸山研究室内
Phone/Fax：03-3830-4848
E-mail：fntg@photon.t.u-tokyo.ac.jp
URL：http://fullerene-jp.org
印刷　/　製本　名古屋大学消費生活協同組合　印刷部

POWERED BY Neo Engine

JEM-ARM200F NEOARM

原子分解能分析電子顕微鏡

“NEOARM”は、当社独自の技術で開発された
冷陰極電界放出形電子銃(Cold-FEG)と
高次の収差まで補正可能な
新型球面収差補正装置(ASCOR)を標準搭載し、
200 kVの高加速電圧だけでなく
30 kVの低加速電圧においても
原子分解能での観察を実現しました。

JEOL 日本電子株式会社

本社・昭島製作所　〒196-8558　東京都昭島市武蔵野3-1-2　TEL:(042)543-1111(大代表)　FAX:(042)546-3353
www.jeol.co.jp　ISO 9001・ISO 14001 認証取得

JEOLグループは、「理科学・計測機器」「産業機器」「医用機器」の3つの事業ドメインにより事業を行っております。
「理科学・計測機器事業」電子光学機器・分析機器・計測検査機器　**「産業機器事業」**半導体関連機器・産業機器　**「医用機器事業」**医用機器

ご注文品は最短で翌日納品

倉庫面積を大幅拡張。国内在庫がさらに充実し、ますます多くの製品が当日出荷可能*となりました。お客様の急なニーズにも迅速に対応いたします。

■ 当日出荷が可能な製品の一例です。

* 弊社に直接ご注文をいただいた場合の出荷予定日です。ご注文の時間帯によっては、翌営業日の出荷となる場合がございます。また出荷予定日は在庫状況に応じて変わる可能性がありますのでご了承ください。

見積・注文のご依頼はウェブサイトから

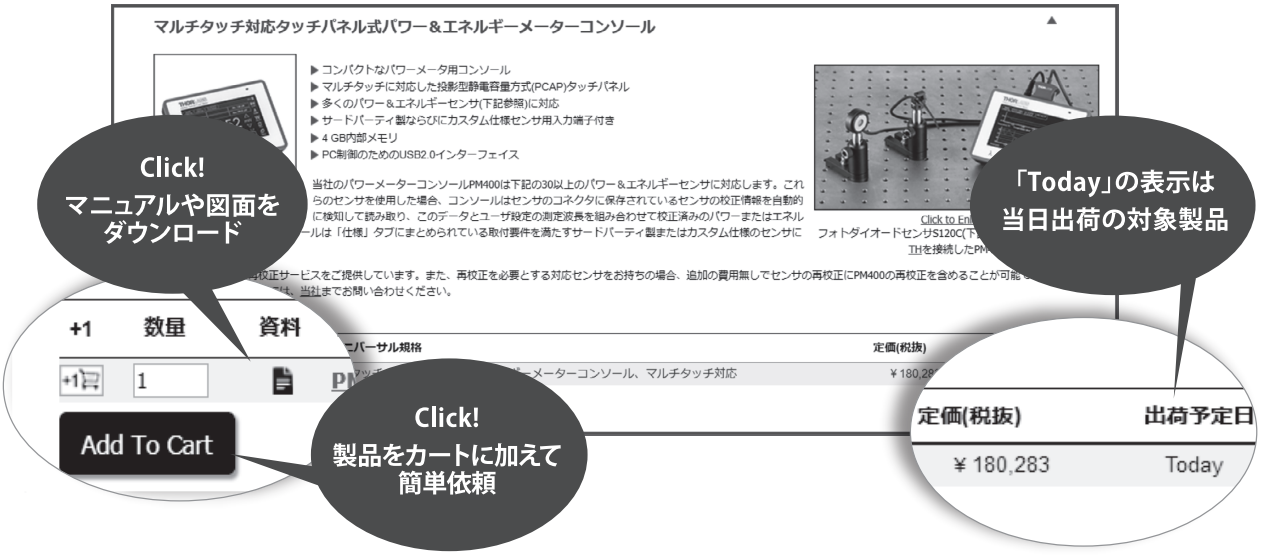

定価や出荷予定日、製品仕様・図面等の詳細はウェブサイトでご確認いただけます。

www.thorlabs.co.jp **E-mail: sales@thorlabs.jp**

THORLABS ソーラボジャパン株式会社
〒179-0081 東京都練馬区北町3-6-3 TEL：03-6915-7701 FAX：03-6915-7716

モデルチェンジ　～スマートなデザインに簡単操作～

BRANSON 超音波ホモジナイザー

長くご愛顧いただいておりますBRANSON超音波ホモジナイザーで新たなモデルが誕生しました。

主な特長

1.電気エネルギーから超音波振動への変換効率が95%以上
→ 無駄なエネルギーロスが小さく、安定した振幅が得られる。

2.通常では、液体の種類によって振幅が安定し難い。
→ 条件を変えても一定の振幅を保つ機能がついている。

3.ジュール（watt×sec）による発振制御が可能
→ Total何ジュールでこの処理が完了するという情報が論文に掲載できる。

20kHz超音波ホモジナイザー
BRANSON SONIFIER SFX250,550

40kHz超音波ホモジナイザー
BRANSON SONIFIER SFX150HH

主なアプリケーション

分散

カーボンナノチューブ　有機顔料　無機顔料　セラミック　セメント　感光体　記録材料
磁性粉　粉末冶金　酸化鉄　金属酸化物　シリカ　アルミナ　カーボンブラック
ポリマー　ラテックス　製紙　ファンデーション
研磨剤　電池　フィラー　光触媒　触媒　ワクチン　体外診断薬　歯磨き粉　シャンプー
半導体　電子基盤　液晶　貴金属　金属　宝石　タイヤ　発酵菌類　その他

乳化

エマルジョン製剤　農薬　トナー　ラテックス　界面活性剤　クリーム　乳液　その他

日本国内販売総代理店　株式会社 セントラル科学貿易

東京本社:　〒136-0071 東京都江東区亀戸1-28-6 タニビル3F　TEL 03-5627-8150 FAX 03-5627-8151
技術物流センター:〒272-0146 千葉県市川市広尾2-1-9　TEL 047-701-6100 FAX 047-701-6116
大阪支店:　〒533-0031 大阪府大阪市東淀川区西淡路1-1-36 新大阪ビル　TEL 06-6325-3171 FAX 03-6325-5180
福岡営業所:　〒812-0016 福岡県福岡市博多区博多駅南1-2-15 事務機ビル　TEL 092-482-4000 FAX 092-482-3797
札幌出張所:　〒001-0911 北海道札幌市北区新琴似11条13-7-13-2　TEL 011-764-3611 FAX 011-764-3612
https://www.cscjp.co.jp

himac 超遠心機シリーズ！

CNTの
分離精製に！

小形超遠心機

小形超遠心機　**バイオ&マテリアルサイエンスの強い味方**

himac 床置タイプ
CS-FNX Series

himac 卓上タイプ
CS150NX
世界トップクラスの高性能！

▼ローターは全て載せるだけ！

▼カラー液晶タッチパネル

▼USB ポート（CS150FNXとCS150NXのみ標準装備）

特長

- 世界最大*遠心加速度 1,050,000×g
  （CS150FNX とS140AT ローターの組み合わせにて）
- サンプルのバランス取りは目分量でOK（液面差5mm 以内、全ローター本数分対応）
- クラス最静音45dB（A）*　●世界最小*コンパクトサイズ　●エコ対応省エネモデル
- スイングローターではクラス最大*処理容量の7mL×4本（S50ST）が回せます
- 世界標準の安全規格CEマーキング適合の安全性

*2019年6月現在当社調べ（小形超遠心機比）

遠心機形名	CS150FNX	CS120FNX	CS100FNX	CS150NX
最高回転速度（rpm）	150,000	120,000	100,000	150,000
最大遠心加速度（×g）	1,050,000	771,000	571,000	1,050,000
画面表示・操作部	カラー液晶タッチパネル （日本語／英語切替可能）			
温度設定可能範囲（℃）／冷却方式	0～40／サーモモジュール冷却（フロンレス）			
サイズ（W×D×Hmm）／質量（kg）	440×520×910／105			590×582×408 ／ 97
電源	AC100V ±10%　50/60Hz 15A			
標準価格（税別）	￥5,700,000	￥5,000,000	￥4,500,000	￥6,200,000

CS-FNX シリーズ＆CS150NX 用 ローター形名	S140AT	S110AT	S58A	S55A2	S50A	S50ST
外観						
最高回転速度（rpm）	140,000	110,000	58,000	55,000	50,000	50,000
最大遠心加速度（×g）	1,050,000	691,000	289,000	201,000	210,000	253,000
標準チューブ呼称容量（mL×本）　（注記1）	1.0×10	4.0×8	10.0×8	1.5×12	25.0×6	7.0×4
最大チューブ容量（mL×本）　（注記2）	2.0×10	5.0×8	13.5×8	1.5×12	30.0×6	7.0×4
K ファクタ	5	15	50	40	61	77
標準価格（税別）	￥1,290,000	￥1,100,000	￥1,000,000	￥750,000	￥950,000	￥1,500,000

注記1：標準チューブ呼称容量とは、ローターに標準付属しているチューブの呼称容量です。　注記2：S140AT、S110AT、S58Aは、シールチューブを使用した場合に最大容量となります。
注記3：S55A2は、市販マイクロチューブは使用できません。

超遠心機

超遠心機
himac **CP-NX** Series
バイオ&マテリアルサイエンスのスタンダード

遠心分離のための機能を満載！

特長

- クラス最大*遠心加速度 803,000×g
  （CP100NX とP100AT2 ローターの組み合わせにて）
- ローター寿命自動管理と寿命延長機能搭載（RLM アダプタ付ローター）
- サンプルのバランス取りは目分量でOK（液面差5mm 以内）**
- 省電力エコ設定機能搭載（省エネ）
- 世界標準の安全規格CE マーキング適合の安全性
- 離れていても運転状況がわかるLED インジケータ搭載
- ユーザー支援ソフト「 himac *ASSIST* 」標準装備
- 他社ローターが使用可能（オプション）
- バイオハザード対応可能（真空ラインにマイクロフィルタ）（オプション）

▼ローターは全て載せるだけ！

▼光るLED インジケータ

▼カラー液晶タッチパネル

▼USB およびLAN ポート
標準装備

*2019年6月現在当社調べ
**一部のローターを除く

遠心機形名	CP100NX	CP90NX	CP80NX
最高回転速度（rpm）	100,000	90,000	80,000
最大遠心加速度（×g）	803,000	700,000	615,000
画面表示・操作部	カラー液晶タッチパネル（表示は11ヶ国語対応）		
温度設定可能範囲（℃）／冷却方式	0～40 ／ サーモモジュール冷却（フロンレス）		
サイズ（W×D×Hmm）／質量（kg）	790×690×880（最大H：ドアハンドルまで925、最大D：セイフティカバ取付時890）／ 390		
電源	AC 単相200V ±10% 50/60Hz 最大20A（通常8A）		
標準価格（税別）	￥11,000,000	￥9,500,000	￥8,500,000

CP-NX シリーズ用 ローター形名	P100AT2	P80AT	R70AT	P50AT2	P45AT	P21A2	P40ST	P32ST	P32ST2
外観									
最高回転速度（rpm）	100,000	80,000	70,000	50,000	45,000	21,000	40,000	32,000	32,000
最大遠心加速度（×g）	803,000	615,000	505,000	303,000	235,000	71,000	284,000	180,000	193,000
呼称容量（mL）×本数（本）	6.5×8	12×8	40×8	40×12	94×6	230×6	13×6	40×6	16×6
K ファクタ	18	27	44	70	130	486	139	198	216
質量（kg）	3.7	6.0	10.2	13.0	13.2	11.4	6.9	7.1	7.2
標準価格（税別）	￥2,250,000	￥2,300,000	￥2,200,000	￥2,200,000	￥2,350,000	￥1,800,000	￥2,490,000	￥2,480,000	￥2,480,000

【製造・販売・保守】 工機ホールディングス株式会社 C&P事業本部

himac 遠心機お客様相談センター 0120-024125
受付時間 9:00～12:00 / 13:00～17:00（土・日・祝日・弊社休業日除く）

東日本地区　03-6738-0860　　西日本地区　0798-23-4125

URL https://www.himac-science.jp ▶

- 製品の仕様、外観および価格は、予告なく変更する場合があります。
- 印刷の都合上、実際の色と異なる場合があります。
- 標準価格は仕様や構成により異なります。
- 製品写真は、特に断りがない限り標準仕様です。
- 安全のために使用環境、使用条件、据付条件が制限される場合があります。
- 全て税別価格となります。

日立工機株式会社は、2018年6月「工機ホールディングス株式会社」に社名変更致しました。

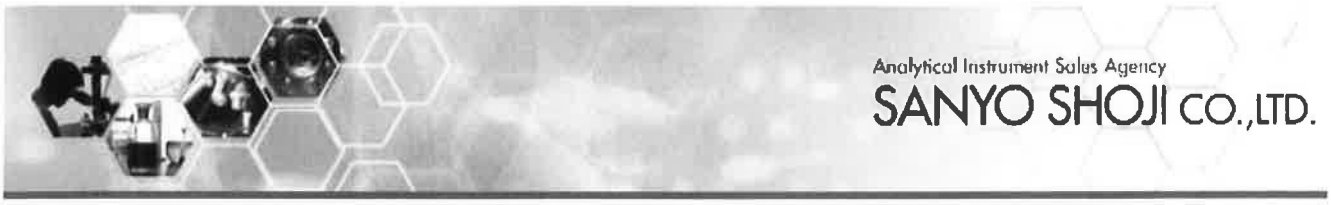

Analytical Instrument Sales Agency
SANYO SHOJI CO.,LTD.

株式会社 三洋商事は
分析・試験装置のエキスパートです。

お客様の研究開発、品質管理、製造工程等、色々な分野におけるご要望に対し、
総合的なご提案が出来るように努めております。
そして、新しい技術や内外の幅広い商品に関する知識情報を生かし、
皆様の発展に貢献出来る事を希望しております。

●企業活動の基本方針

弊社の方針と致しまして“企業のコンプライアンスの遵守”
“地球環境に配慮した経営の推進”“地域社会に貢献し相互繁栄を考えた施策”
などを重視してまいります。

●お客様の満足度を第一に考えた営業活動

装置の導入目的、技術評価、コスト、納期、アフターサービス等
のお客様のニーズに貢献できるよう、迅速な対応に努力し、
お客様との信頼関係を大切に致します。

●取扱商品の充実

新しい技術や内外の幅広い商品に関する情報収集と
共に知識の向上に努め、お客様の立場に立ったご相談相手として
お役に立てる事を目標にしております。

取扱品目

分析測定器 ・試験検査器 ・バイオ機器
理化学機器 ・実験用器具 ・実験室設備
環境計測測定機器 ・粉粒体測定装置
真空機器 ・その他専用機器

株式会社 三洋商事

〒451-0045名古屋市西区名駅二丁目27番8号

TEL 052-583-7070 FAX 052-583-7110

E-mail : nago@sanyo-shoji.co.jp

http : //www.sanyo-shoji.co.jp

株式会社ダルトン ITOKI GROUP　http://www.dalton.co.jp | info@dalton.co.jp

東　京　〒104-0045　東京都中央区築地5-6-10 浜離宮パークサイドプレイス
TEL 03-3549-6810　FAX 03-3549-6851

北海道　〒060-0808　北海道札幌市北区北八条西5-1 サイエンスビル
TEL 011-758-3131　FAX 011-758-3151

仙　台　〒980-0811　宮城県仙台市青葉区一番町4-6-1 仙台第一生命タワービル
TEL 022-217-7266　FAX 022-217-7261

名古屋　〒460-0002　愛知県名古屋市中区丸の内1-16-4 BPR プレイス名古屋丸の内
TEL 052-209-6631　FAX 052-209-6642

大　阪　〒541-0053　大阪府大阪市中央区本町1-8-12 オーク堺筋本町ビル
TEL 06-6268-8610　FAX 06-6268-8560

中四国　〒732-0824　広島県広島市南区的場町1-2-21 広島第一生命OSビルディング
TEL 082-568-4501　FAX 082-261-7170

九　州　〒812-0011　福岡県福岡市博多区博多駅前3-19-5 博多石川ビル
TEL 092-411-2826　FAX 092-431-6580

HORIBA Scientific

ナノ材料イメージング装置
HORIBA NanoRaman

AFM-Raman ＋ TERS・SNOM

NanoRaman 特長

- ✔ ラマン光に干渉しない IR AFM ダイオード
- ✔ チップ交換時にヘッドの移動が不要
- ✔ カンチレバーのオートアライメント
- ✔ TERS 用 高 NA 対物レンズ（0.7 NA）

NanoRaman 用途

✔ AFM/ ラマン同一領域測定

ラマン
有機物、無機化合物、結晶性などの化学情報

AFM
形状、電気・磁気的性質、機械特性、熱特性などの可視化

✔ TERS（Tip Enhanced Raman Spectroscopy）分析

▶ 回折限界を超える測定空間分解能（数十nm~）によるラマン測定

アプリケーション例

✔ TERS hyperspectral imaging

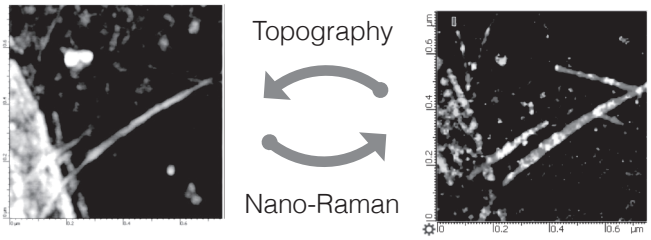

✔ Gap mode TERS response of 1-D patterns

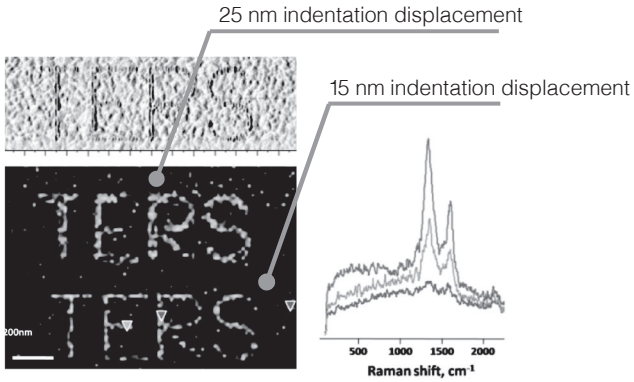

測定例）金基板上カーボンナノチューブ・グラフェンの TERS

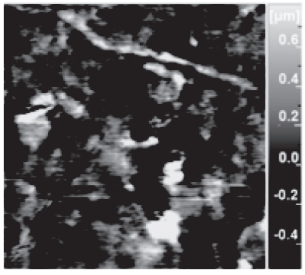

（a）AFMイメージ

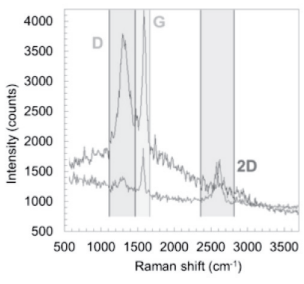

（b）TERSスペクトル

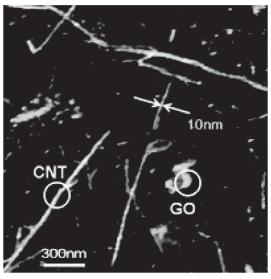

（c）TERSスペクトルイメージ

200 YEARS 1819-2019
HORIBA JOBIN YVON
HORIBA JOBIN YVON の分光技術は
今年で創業200 周年を迎えました

株式会社 堀場製作所
本社 〒601-8510京都市南区吉祥院宮の東町2番地　TEL（075）313-8121 http://www.horiba.com/jp/scientific/
●東京（03）6206-4717 ●名古屋（052）936-5781 ●大阪（06）6390-8011 ●福岡（092）292-3593

グラフェンの量産化に向けて…

Neutron

▼概要▼
Roll-to-Roll (R2R)
ロール状に巻いた金属ホイルを、巻き取りながら連続的にグラフェンを成長可能な量産用装置

◆特徴◆
- 連続成長
- 生産能力 20,000 m^2 / year
- Cuホイル及びSteelホイルの両方に対応
- 大気環境で成長可能で、真空チャンバ不要
- 生産コストの大幅削減

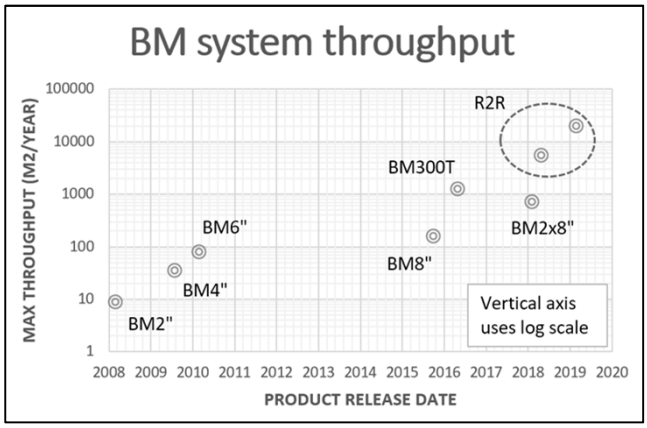

CCS 2D & NOVO

▼概要▼
2D材料及びグラフェンの成長装置

◆特徴◆
- Closed Coupled Showerhead(CCS) 技術を適用
- 成長温度は1400℃まで昇温可能
- 基板に直接2D材料またはグラフェンを成長可能
- プラズマ機能装備
- 多種原料を搭載可能(hBN, MoS2, WSe2)

BM300T

▼概要▼
ウェハ基板上CNT及びグラフェン成長装置

◆特徴◆
- 12”及び8” wafer 自動搬送対応
- プラズマ機能装備
- High 2D/G > 2.5の高品質を達成

アイクストロン株式会社 www.aixtron.com
〒140-0001 東京都品川区北品川1-8-11 Daiwa品川Northビル9F
E-mail: japaninfo@aixtron.com Phone: 03-5781-0931 Fax: 03-5781-0940

AIXTRON
Our technology. YOUR FUTURE

計算処理を高速化
インテル®
Parallel Studio XE

インテル® Parallel Studio XE は、C/C++、Fortran や Python* が使用されたソフトウェアの計算処理の高速化を支援します。近年、増加を続けるプロセッサーの全てのコアや、インテル® アドバンスト・ベクトル・エクステンション 512 (インテル® AVX-512) を有効活用できる機能を提供します。

並列コードの構築

C/C++ と Fortran コードをインテル® コンパイラーでコンパイルし、最適化されたバイナリーを生成します。必要に応じて、OpenMP* などのプログラミング手法や同梱されるライブラリーを適用することで、より高いパフォーマンスを発揮させることが可能です。

Process / Function / Thread / Call Stack	Serial CPU Time	CPU Time Effective Time by Utilization ▼ Idle Poor Ok Ideal Over
TargetApp	100.0%	100.0%
CalcApproximatePI	0.0%	39.6%
myMatmul::matmul	99.9%	31.8%
NumberOfPrimes	0.0%	28.4%
OMP Worker Thread #3 (	0.0%	12.3%
OMP Worker Thread #2 (	0.0%	8.6%
OMP Worker Thread #1 (	0.0%	5.5%
OMP Master Thread #0 (	0.0%	2.0%

インテル® VTune™ Amplifier によるスレッド解析の結果。アプリケーション TargetApp の処理時間の内訳で、特に関数 myMatmul::matmul が Serial CPU Time (単一コアのみの実行時間) のほとんどを占めていた。

インテル® C++/Fortran コンパイラー
- 第 2 世代 インテル® Xeon® スケーラブル・プロセッサーを含むインテル® プロセッサー向けの最適化
- OpenMP* 4.5 と 5.0 (ドラフト仕様) による汎用的なスレッド並列と SIMD 並列のプログラミング

高速な Python* 実行環境
"インテル® Distribution for Python*"

パフォーマンス・ライブラリー
数値計算、画像 / 信号処理、並列化テンプレート、データ解析

並列コードの解析

ソフトウェアの現状のパフォーマンスを分析し、問題点を調べます。(※) かかった処理時間について、CPU 使用率、FLOPS、メモリー帯域幅といった様々なハードウェアの要素と、プロセス / スレッド、関数 / ループ、ソースコード行といったソフトウェアの要素に分類および対応付けて把握することで、高速化のために取り組むべき問題を明確にすることが可能です。

※ インテル® Parallel Studio XE Professional Edition または Cluster Edition でのみ利用可能

製品の詳細に関するお問い合わせ先：

XLSOFT エクセルソフト株式会社

Tel: 03-5440-7875 Fax: 03-5440-7876 E-mail: intel@xlsoft.com
お問い合わせフォーム : www.xlsoft.com/jp/qa

製品詳細はこちらから
www.xlsoft.com/intel/fntg